**Naval Research Laboratory**

**Washington, DC 20375-5320**

**NRL/MR/6170--05-8890**

# Replacement of Chromium Electroplating on Gas Turbine Engine Components Using Thermal Spray Coatings

BRUCE D. SARTWELL
*Surface Chemistry Branch*
*Chemistry Division*

KEITH O. LEGG
*Rowan Technology Group*
*Libertyville, IL*

JERRY SCHELL
*GE Aircraft Engines*
*Cincinnati, OH*

BOB BONDARUK AND CHARLES ALFORD
*Propulsion Environmental Working Group (PEWG)*
*Wright-Patterson AFB, OH*

PAUL NATISHAN AND STEVEN LAWRENCE
*Center for Corrosion Science and Engineering*
*Chemistry Division*

GARY SHUBERT
*Pratt & Whitney*
*East Hartford, CT*

PHILIP BRETZ
*Metcut Research Inc.*
*Cincinnati, OH*

ANNE KALTENHAUSER
*Concurrent Technologies Corp.*
*Johnstown, PA*

July 20, 2005

# REPORT DOCUMENTATION PAGE

*Form Approved*
*OMB No. 0704-0188*



| 1. REPORT DATE *(DD-MM-YYYY)* | 2. REPORT TYPE | 3. DATES COVERED *(From - To)* |
|---|---|---|
| 20-07-2005 | Memorandum report | March 2000-May 2005 |

**4. TITLE AND SUBTITLE**

Replacement of Chromium Electroplating on Gas Turbine Engine Components Using Thermal Spray Coatings

**5a. CONTRACT NUMBER**

**5b. GRANT NUMBER**

**5c. PROGRAM ELEMENT NUMBER**
63851D8Z

**6. AUTHOR(S)**

Bruce D. Sartwell, Keith O. Legg,* Jerry Schell,† Bob Bondaruk,‡ Charles Alford,‡ Paul Natishan, Steven Lawrence, Gary Shubert,§ Philip Bretz,¶ and Anne Kaltenhauser**

**5d. PROJECT NUMBER**
EPP-0023

**5e. TASK NUMBER**

**5f. WORK UNIT NUMBER**
61-7072

**7. PERFORMING ORGANIZATION NAME(S) AND ADDRESS(ES)**

Naval Research Laboratory, Code 6170
4555 Overlook Avenue, SW
Washington, DC 20375-5320

**8. PERFORMING ORGANIZATION REPORT NUMBER**

NRL/MR/6170--05-8890

**9. SPONSORING / MONITORING AGENCY NAME(S) AND ADDRESS(ES)**

Environmental Security Technology Certification Program
901 North Stuart Street, Suite 303
Arlington, VA 22203

**10. SPONSOR / MONITOR'S ACRONYM(S)**
ESTCP

**11. SPONSOR / MONITOR'S REPORT NUMBER(S)**
EPP-0023-FR

**12. DISTRIBUTION / AVAILABILITY STATEMENT**

Approved for public release; distribution is unlimited.

**13. SUPPLEMENTARY NOTES** *Rowan Technology Group, Libertyville, IL
†GE Aircraft Engines, Cincinnati, OH
‡Propulsion Environmental Working Group (PEWG), Wright-Patterson AFB, OH
§Pratt & Whitney, East Hartford, CT
¶Metcut Research Inc., Cincinnati, OH
**Concurrent Technologies, Corp., Johnstown, PA

**14. ABSTRACT**

Hard chromium electroplating is extensively used by aircraft manufacturers and military maintenance depots to provide wear and/or corrosion resistance or to restore dimensional tolerance to components. However, chrome plating utilizes hexavalent chromium, which is a highly toxic carcinogen, and increasingly, stringent environmental and worker-safety regulations are making chrome plating more expensive for the DoD. This document constitutes the final report on a project to qualify high-velocity oxygen-fuel (HVOF) and plasma thermal spray coatings as a replacement for hard chrome plating on gas turbine engine components. Extensive fatigue, fretting wear, salt-fog corrosion, and carbon-seal wear tests were performed on HVOF WC/17Co, Tribaloy 400, Tribaloy 800, and Cr3C2/20(NiCr), and plasma-sprayed Tribaloy 400 coatings compared to hard chromium. In general, the HVOF WC/17Co coatings demonstrated superior performance. An accelerated test on a TF33 engine containing seven components coated with HVOF WC/17Co showed superior performance to what would have been expected using the standard hard chromium. A cost/benefit analysis indicates that miliary repair depots that overhaul gas turbine engines can realize substantial savings by converting from hard chrome to HVOF.

**15. SUBJECT TERMS**
Thermal spray; HVOF thermal spray; WC/Co coatings; Hard chromium plating; Electrolytic hard chrome; Gas turbine engines; Fatigue; Corrosion; Wear

| 16. SECURITY CLASSIFICATION OF: | | | 17. LIMITATION OF ABSTRACT | 18. NUMBER OF PAGES | 19a. NAME OF RESPONSIBLE PERSON |
|---|---|---|---|---|---|
| | | | | | Bruce D. Sartwell |
| a. REPORT | b. ABSTRACT | c. THIS PAGE | UL | 207 | 19b. TELEPHONE NUMBER *(include area code)* |
| Unclassified | Unclassified | Unclassified | | | (202) 767-0722 |

**Standard Form 298 (Rev. 8-98)**
**Prescribed by ANSI Std. Z39.18**

# TABLE OF CONTENTS

# LIST OF TABLES

# LIST OF FIGURES

## LIST OF ACRONYMS

| | |
|---|---|
| ALC | Air Logistics Center |
| AMS | Aerospace Materials Specification |
| AMT | advanced mission test |
| ANOVA | analysis of variables |
| ANG | Air National Guard |
| ANSI | American National Standards Institute |
| APS | air plasma spray |
| ASTM | American Society for Testing and Materials |
| CBA | cost/benefit analysis |
| CFR | Code of Federal Regulations |
| DARPA | Defense Advanced Research Projects Agency |
| DOD | Department of Defense |
| DOE | design of experiments |
| ECAM | Environmental Cost Accounting Methodology |
| EFH | equivalent flight hours |
| EHC | electrolytic hard chrome |
| EPA | Environmental Protection Agency |
| ESTCP | Environmental Security Technology Certification Program |
| FPI | fluorescent penetrant inspection |
| GEAE | GE Aircraft Engines |
| GTE | gas turbine engine |
| HCAT | Hard Chrome Alternatives Team |
| HCF | high-cycle fatigue |
| hex-Cr | hexavalent chromium |
| HPT | high-pressure turbine |
| HVOF | high-velocity oxygen-fuel |
| IARC | International Agency for Research on Cancer |
| IRR | internal rate-of-return |
| JG-PP | Joint Group on Pollution Prevention |
| JTP | joint test protocol |
| JTR | joint test report |
| LCF | low-cycle fatigue |
| LPT | low-pressure turbine |
| NADEP-CP | Naval Air Depot Cherry Point |
| NADEP-JAX | Naval Air Depot Jacksonville |
| NAVAIR | Naval Air Systems Command |
| NAVSEA | Naval Sea Systems Command |
| NG | natural gas |
| NPV | net present value |
| OC-ALC | Oklahoma City Air Logistics Center |
| OEM | original equipment manufacturer |
| OSHA | Occupational Safety and Health Administration |

| | |
|---|---|
| P&W | Pratt & Whitney |
| PEL | permissible exposure limit |
| PEWG | Propulsion Environmental Working Group |
| PPE | personal protective equipment |
| PS | plasma spray |
| PVD | physical vapor deposition |
| QC | quality control |
| rpm | rotations per minute |
| SAE | Society of Automotive and Aerospace Engineers |
| SOR | source of repair |
| T-400 | Tribaloy 400 |
| T-800 | Tribaloy 800 |
| TWA | time-weighted average |
| UHS | ultra-high sensitivity |

## ACKNOWLEDGMENTS

The financial and programmatic support of the Environmental Security Technology Certification Program, under the direction of Dr. Jeffrey Marqusee, Director, and Mr. Charles Pellerin, Program Manager for Pollution Prevention, is gratefully acknowledged. In addition, the financial and programmatic support of the Propulsion Environmental Working Group is also gratefully acknowledged.

The authors would also like to express thanks to the following individuals who made substantial contributions to the execution of the project:

Mr. Robert Bondaruk and Mr. Charles Alford, U.S. Air Force Aeronautical Systems Center (Propulsion Environmental Working Group)

Mr. Johnny Tsiao and Mr. Jeff Marnix, Oklahoma City Air Logistics Center

Mr. Jerry Schell, GE Aircraft Engines

Mr. Gary Shubert, Pratt & Whitney

Mr. Phil Bretz, Metcut Research, Inc.

Mr. Richard Vanderstraten, Hitemco, Inc.

Mr. Peter Ruggiero, Engelhard Corporation



Principal Investigators: Mr. Bruce D. Sartwell
Naval Research Laboratory
Dr. Keith Legg
Rowan Technology Group

# 1. Executive Summary

**Background:** Electrolytic hard chrome (EHC) plating is a technique that has been in commercial production for over 50 years. It is a critical process that is used both for applying hard coatings to a variety of aircraft components in manufacturing operations and for general re-build of worn or corroded components that have been removed from aircraft during overhaul. Chromium plating baths contain chromic acid, in which the chromium is in the hexavalent state, with hexavalent chromium (hex-Cr) being a known carcinogen. During operation, chrome plating tanks emit a hex-Cr mist into the air, which must be ducted away and removed by scrubbers. Wastes generated from plating operations must be disposed of as hazardous waste and plating operations must abide by U.S. Environmental Protection Agency (EPA) emissions standards and Occupational Safety and Health Administration (OSHA) permissible exposure limits (PEL). Recent studies have clearly shown that there are a significant number of excess deaths at the current PEL of 100 $\mu g/m^3$. OSHA is currently under court order to establish a new hex-Cr PEL by January 2006 and in October 2004 the agency proposed a new PEL of 1 $\mu g/m^3$. A Navy/Industry task group concluded that the cost of compliance for all Navy operations that utilize hex-Cr (i.e., not just plating) would be in excess of $10 million annually if the PEL was reduced to less than 5 $\mu g/m^3$.

Previous research and development efforts had established that high-velocity oxygen-fuel (HVOF) thermal spray coatings are the leading candidates for replacement of hard chrome. HVOF thermal spraying can be used to deposit both metal alloy and ceramic/metal (cermet) such as tungsten carbide/cobalt (WC/Co) coatings that are dense and highly adherent to the base material. They also can be applied to thicknesses in the same range as what is currently being used for EHC. Currently, there are HVOF thermal spray systems commercially available. Although there are a wide number of applications for these coatings, their qualification as an acceptable replacement for hard chrome plating has not been adequately demonstrated, particularly for fatigue-sensitive aircraft and engine components. The Hard Chrome Alternatives Team (HCAT) was formed to perform the demonstration/validation for the HVOF coatings.

**Objectives of the Demonstration:** The objectives were to demonstrate through materials and component testing that the performance of several HVOF and plasma spray coatings on gas turbine engine (GTE) components was equal or superior to that of EHC coatings. Materials testing included axial fatigue, fretting wear, salt-fog corrosion and carbon seal wear.

**Regulatory Drivers:** EHC plating operations must comply with 40 Code of Federal Regulations (CFR) Part 63 (National Emissions Standards for Hazardous Air Pollutants) and 40 CFR Part 50 (National Primary and Secondary Ambient Air Quality Standards). The workplace environment must comply with an OSHA PEL of 100 $\mu g/m^3$ for hex-Cr. As stated above, OSHA has proposed reducing the hex-Cr PEL to 1 $\mu g/m^3$. In the Netherlands, there is pending legislation to reduce allowable hex-Cr exposure to 1.5 $\mu g/m^3$ and the UK's Ministry of Defense is proposing an even stricter standard of 0.5 $\mu g/m^3$. If OSHA adopts the proposed PEL, then the costs associated with EHC plating will significantly increase and it is possible that EHC operations will have to shut down at many Department of Defense (DOD) facilities.

**Demonstration Results:**

- Fatigue: Low-cycle fatigue tests under strain control and high-cycle fatigue tests under load control were conducted at 300º F and 750º F on IN-718, A-286, AMS-355, 9310, IN-901, 4340 and 17-4PH alloy specimens coated with EHC, HVOF WC/17Co, Tribaloy 400, Tribaloy 800 and $Cr_3C_2$/NiCr, and plasma spray Tribaloy 400 to thicknesses of 0.003" or 0.015". Cycles-to-failure at different levels of maximum stress or strain were measured. In general, the average number of cycles-to-failure at any stress or strain level for the thermal-

spray-coated specimens was equal to or greater than for EHC-coated specimens except for IN-718 and 17-4PH substrates where approximately half of the specimens showed fatigue performance inferior to EHC.

- Wear: Fretting wear tests were conducted at 300º F and 750º F for 4340 blocks coated with EHC, HVOF WC/17Co, Tribaloy 800 and $Cr_3C_2$/NiCr, and plasma spray Tribaloy 400 to a thickness of 0.003" sliding against M50, IN-718, IN-901 or 17-4PH. For tests conducted at 750º F, HVOF WC/Co coatings performed significantly better than EHC and the other thermal spray coatings when sliding against all of the mating materials, except IN-718 where the coating performance was equivalent to EHC. For tests conducted at 300º F, the results were less definitive but in the majority of cases, WC/Co performance was equivalent or superior to EHC, with the performance of the other thermal spray coatings generally below that of EHC.
- Corrosion: ASTM B117 salt fog exposure tests were conducted on 4340 rod and plate specimens and IN-718 rod specimens coated with EHC, HVOF Tribaloy 400, Tribaloy 800 and $Cr_3C_2$/NiCr, and plasma spray Tribaloy 400 to thicknesses of 0.003" or 0.015". After 1000 hours exposure, the average appearance ratings for the 0.003"-thick thermal spray coatings were lower than for the EHC coatings on 4340. The average appearance ratings for the 0.015"-thick thermal spray coatings were equivalent to the EHC coatings. Very little corrosion was observed on any coatings on the IN-718 substrates.
- Carbon Seal Wear: Tests consisted of the rotational sliding of shafts coated with EHC, HVOF WC/17Co, Tribaloy 400, Tribaloy 800 and $Cr_3C_2$/NiCr, and plasma spray Tribaloy 400 to a thickness of approximately 0.004" against two different grades of carbon seals. In general, the performance of the HVOF WC/Co coatings was equivalent to EHC in terms of both the wear of the coating and the mating carbon seal material whereas the performance of the other thermal spray coatings was inferior to the EHC coatings. However, the wear rate was so low that almost any of the coatings would perform satisfactorily.
- Component Testing: An Advanced Mission Test (AMT) was conducted on a TF33 engine in which seven components that are normally coated with EHC were instead coated with HVOF WC/17Co. Oil analysis conducted during the test and analysis of oil filters conducted subsequent to the test indicated virtually no degradation of the WC/Co coatings. Inspection of the coatings subsequent to the test indicated performance superior to what would be expected for EHC. The components will be installed in another AMT engine for additional testing to assess ultimate life.
- Cost Assessment: A detailed cost/benefit analysis was conducted using the Environmental Cost Accounting Methodology (ECAM) at a military gas turbine engine overhaul facility that processes more than 1000 components per year. For a constant throughput of components, the analysis showed an annual cost avoidance of approximately $50,000. For a declining throughput based on improved component performance, there was a 15-year net present value of $362,000. If all hard chrome plating could be eliminated from the depot, then the 15-year net present value was more than $1.1 million. If the new proposed hex-Cr PEL of 1$\mu g/m^3$ is implemented, then the 15-year net present value for the constant-throughput, declining-throughput and chrome-elimination cases would increase to $350,000, $700,000 and $2.9 million, respectively.

**Stakeholder/End-User Issues:** The success of the materials testing and the TF33 AMT has resulted in the Air Force proceeding with implementation of HVOF coatings on that and other gas turbine engines through the Component Improvement Program, with the ultimate goal of eliminating hard chrome plating on all components for which thermal spray is amenable (i.e., where line-of-sight is not an issue). This includes repair of the F100, F101, F110, F118 and T56 engines. Naval Air Depot Jacksonville has implemented HVOF coatings on the TF34 engine and is exploring the qualification of the coatings on other engine components.

# 2. Background and Introduction

The replacement of hard chrome plating in aircraft manufacturing activities and maintenance depots is a high priority for the U.S. Department of Defense (DOD). Hard chrome plating is a technique that has been in commercial production for over 50 years and is a critical process that is used both for applying hard coatings to a variety of aircraft components in manufacturing operations and for general re-build of worn or corroded components that have been removed from aircraft during overhaul. In particular, chrome plating is used extensively on gas turbine engine (GTE) components such as shafts and bearing journals. Chromium plating baths contain chromic acid, in which the chromium is in the hexavalent state, with hexavalent chromium (hex-Cr) being a known carcinogen having a level of toxicity greater than arsenic or cadmium. During operation chrome plating tanks emit a hex-Cr mist into the air, which must be ducted away and removed by scrubbers. Wastes generated from plating operations must be disposed of as hazardous waste and plating operations must abide by EPA emissions standards and OSHA permissible exposure limits (PEL).

A significant lowering of the hex-Cr PEL would most likely have the greatest cost impact on military and commercial repair facilities. Such a change has been expected since the mid 1990's. But it was only in 2004 that OSHA began the process to issue a new PEL as a result of a lawsuit filed in 2002 by a citizens group and union that petitioned OSHA to issue a lower PEL, and a subsequent ruling by a Federal District Court upholding the petition [1]. The court ruling required OSHA to publish a new draft hex-Cr PEL in the Federal Register no later than October 2004. Public review and hearings would be conducted in 2005, with a final rule issued in January 2006. In October 2004 OSHA proposed a new PEL of 1 $\mu g/m^3$ with a 0.5 $\mu g/m^3$ action level, which represents a two-order-of-magnitude reduction from the current PEL of 100 $\mu g/m^3$. The expected compliance costs in all industries including electroplating, welding, painting and chromate production is $226 million.

As stated above, a change in the hex-Cr PEL has been expected since the mid 1990's. In anticipation of the change, in 1995 a Navy/Industry task group [2] under the coordination of the Naval Sea Systems Command studied the technical and economic impact of a reduction in the hex-Cr PEL. At the time, a reduction in the 8-hour time-weighted average (TWA) from the existing 100 $\mu g/m^3$ to between 0.5 and 5.0 $\mu g/m^3$ was being considered. The Navy/Industry task group performed the following tasks:

- Identified the manufacturing and repair operations, materials and processes that are used in Navy ships, aircraft, other weapons systems and facilities where worker exposure to hex-Cr would be expected
- Developed data on current worker exposure levels to hex-Cr using OSHA Method 215
- Estimated the technical and economic impact of the anticipated reductions in hex-Cr exposure on Navy ships, aircraft, other weapons systems and facilities
- Identified future actions required to comply with the anticipated PEL reductions

The following operations within the Navy were identified as having the potential for exposing workers to hex-Cr:

- Metal cleaning (including abrasive blasting and grinding) of chromate-coated materials
- Electroplating of chromium
- Painting and application of chromate paints and coatings
- Welding, thermal spraying and thermal cutting

The following conclusions were reached by the task group:

1. Regulated areas for hex-Cr would have to be created in much greater numbers than have been required for cadmium or lead exposure
2. Local exhaust ventilation, which is the presently available engineering control, is not completely effective in reducing exposure to below 0.5 $\mu g/m^3$ for many operations or even below 5 $\mu g/m^3$ in some cases
3. The inability of engineering controls to consistently reduce worker exposure below the anticipated PEL levels will significantly increase the use of respirators
4. The costs of reducing the hex-Cr PEL will include costs for training, exposure monitoring, medical surveillance, engineering controls, personal protective equipment, regulated areas, hygiene facilities, housekeeping and maintenance of equipment. There will also be costs due to reduced efficiency of not only the operations involving hex-Cr but adjacent operations and personnel as well.
5. The estimated costs for compliance with a PEL of 0.5 $\mu g/m^3$ at Navy facilities include an initial, one-time cost of about $22,000,000 and annual costs of about $46,000,000 per year.
6. The estimated costs for compliance with a PEL of 5.0 $\mu g/m^3$ at Navy facilities include an initial, one-time cost of about $3,000,000 and annual costs of about $5,000,000 per year
7. In addition to the greatly increased cost that would be associated with chrome plating, turnaround times for processing of components would be significantly increased as well, impacting mission readiness.

Based on the projections of the metal finishing industry and the study conducted by NAVSEA in 1995, it is clear that a reduction of the hex-Cr PEL to a range near 1 $\mu g/m^3$ will greatly increase the cost and processing times associated with hard chrome plating within DOD.

Previous research and development efforts [3,4] had established that high-velocity oxygen-fuel (HVOF) thermal spray coatings are the leading candidates for replacement of hard chrome. Using commercially available thermal spray systems, HVOF thermal spraying can be used to deposit both metal alloy and ceramic/metal (e.g., WC/Co) coatings that are dense and highly adherent to the base material. They also can be applied to thicknesses in the same range as that currently being used for chrome plating.

In order to conduct the advanced development work required for qualification of the HVOF coatings, a project titled, "Tri-Service Dem/Val of Chromium Electroplating Replacements," principally sponsored by the Environmental Security Technology Certification Program (ESTCP), was established in March 1996. A project team, designated the Hard Chrome Alternatives Team (HCAT) was established to execute the project. From 1996 to early 1998, the HCAT acquired and installed HVOF thermal spray systems at the Naval Aviation Depot in Cherry Point, North Carolina and the Corpus Christi Army Depot. It also performed some generic fatigue and corrosion testing on HVOF WC/17Co and Tribaloy 400 coatings compared to electrolytic hard chrome (EHC) coatings. In general, the performance of the HVOF coatings was superior to that of the EHC coatings.

While these studies were valuable, it was realized in early 1998 that because hard chrome plating was being used on such a wide variety of aircraft components, it would be impossible to develop one test plan or conduct one series of tests that would address all materials and component qualification requirements. It was therefore decided to develop separate projects related to categories of aircraft components onto which hard chrome was being used. At the same time, the

DOD Joint Group on Pollution Prevention (JG-PP) decided to partner with the HCAT on development and execution of the various projects. JG-PP is chartered by the Joint Logistics Commanders to coordinate joint service pollution prevention activities during the acquisition and sustainment of weapons systems. It was jointly determined by the HCAT and JG-PP that the first projects to be executed would be on landing gear and propeller hubs, with projects on hydraulic actuators and helicopter dynamic components to come later. The landing gear and propeller hub projects have now been completed with extensive materials testing generally showing that HVOF coatings such as WC/17Co demonstrate performance superior in fatigue, wear and corrosion to EHC coatings. Rig and flight tests on WC/17Co-coated components showed acceptable performance for the HVOF coatings and, in many cases, superior performance to what would be expected had the components been coated with EHC. As a result of these projects, HVOF is being implemented at a number of Air Force and Navy repair facilities for processing of landing gear and propeller hub components.

The Propulsion Environmental Working Group (PEWG) was founded in the late 1980s to address environmental issues impacting the DOD propulsion community and the military gas turbine engine industry. They have executed a number of demonstration/validation projects related to qualifying new, environmentally friendly technologies associated with aircraft and land-based gas turbine engines. In the Summer of 1999, the PEWG and HCAT partnered to present a proposal to ESTCP for the qualification of thermal spray coatings as a hard chrome replacement on GTE components. The project was approved and initiated in February 2000.

An analysis was first conducted of the extent of hard chrome plating within the propulsion community. Table 2-1 summarizes the current applications for EHC plating on GTE components and the current specifications used for that application. Table 2-2 lists the DOD gas turbine engines onto which hard chrome is currently being applied to at least one component (delineated according to the U.S. DOD aviation depot at which the overhaul of the engine takes place). It indicates the manufacturer, the aircraft utilizing the engine, and the number of parts identified on that engine that have hard chrome applied either by the manufacturer or in overhaul.

**Table 2-1 Summary of Targeted Process, Applications and Specifications**

| Target HazMat | Current Process | Application | Current Specifications | Candidate Parts/ Substrates |
|---|---|---|---|---|
| Hexavalent Chromium | Hard Chromium Electro-plating | Rebuilding Worn Components<br>Wear-resistant Coating<br>Corrosion-resistant Coating | DOD-STD-2182<br>MIL-C-20218F<br>MIL-STD-1501C<br>QQ-C-320B<br>AMS 2408 | Gas Turbine Components |

Subsequent to conducting this analysis, it was decided among the stakeholders that a Joint Test Protocol (JTP) would be developed to cover only the materials testing related to all engines. This document was produced through meetings and electronic communication involving all of the stakeholders and delineated all of the materials testing required to qualify thermal spray coatings as a hard chrome plating replacement. In conjunction with the materials testing, it was decided that each DOD service and GTE manufacturer would evaluate the hardware under consideration for thermal spray coating and decide if additional component or engine testing beyond the materials JTP would be necessary. Such additional testing could be required due to the critical nature of the mechanical system response for some specific GTE components. A demonstration plan was developed for the TF33 engine and an advanced mission test (AMT) was conducted in which seven components that are normally coated with EHC were instead coated with HVOF

**Table 2-2 Summary of Gas Turbine Engines Categorized by Depot Where Engine is Overhauled, the Manufacturer, End-use Aircraft and Number of Parts onto which Hard Chrome is Applied**

| Depot | Engine TMS | OEM | End Use | # Parts |
|---|---|---|---|---|
| NADEP - Cherry Point | T58 | GEAE | CH-46 Helicopter (Navy and Marines | 29 |
| | T64 | GEAE | CH-53 Helicopter (Navy and USAF) | 27 |
| | T-400 | P&W Canada | UH-1N (Marines) | 6 |
| | F402 | RR UK | AV-8B (Marines) | 3 |
| NADEP – North Island | LM2500 (TF39 Core) | GEAE | Military Marine (U.S. Navy and 23 International Navies) | 22 |
| NADEP – Jacksonville | TF34 | GEAE | S-3 (Navy); A-10 (Air Force) | 29 |
| | F404 | GEAE | F/A-18 (Navy); F-117 (Air Force) | 5 |
| | J52 | P & W | A-4; A-6; EA-6B | 6 |
| Oklahoma City – ALC | TF33- P3/P103 | P & W | B-52H (Air Force) | 12 |
| | TF33-P7A | P & W | C-141 (Air Force) | |
| | TF33-P100 | P & W | E-3 (Air Force) | |
| | TF33-P102A/B | P & W | KC-135; C-18; E-8 (AF) | |
| | F100 | P & W | F-15, F-16 (Air Force) | 41 |
| | F118 | GEAE | B-2 (Air Force) | 3 |
| | F110-100/129 | GEAE | F-16 (Air Force) | |
| | F110-400 | GEAE | F-14 (Navy) | |
| San Antonio ALC | T56 | RR Allison | C-130 | 42 |
| Corpus Christi Army Depot | T700 | GEAE | H-60, AH-64, SH-2 Helicopters | 10 |
| TOTAL | | | | 235 |

WC/17Co.

This Final Report provides detailed information on all work performed under the project.

Section 3 provides a description of HVOF and plasma spray technology including a discussion of the advantages and disadvantages of the technologies for hard chrome replacement.

Section 4 provides results for all of the work performed under the JTP including a description of the procedures for optimization of the coatings deposition parameters plus results of the fatigue, wear, corrosion and carbon seal testing.

Section 5 presents the results of the TF33 AMT that included an analysis of the seven WC/Co-coated components.

Section 6 presents the results of a cost/benefit analysis for replacement of EHC with HVOF thermal spray for processing of components at a GTE repair facility.

Finally, Section 7 discusses issues associated with implementation of thermal spray technology at GTE repair facilities.

In this report there are a number of references to specific standards related to materials processing and testing. These are listed in Table 2-3.

**Table 2-3 Applicable Materials Processing, Coating Deposition, and Test Standards.**

| | |
|---|---|
| ASTM E466: | Standard Practice for Fatigue testing |
| ASTM E606: | Standard Practice for Strain Controlled Fatigue Testing |
| ASTM B117: | Standard Practice for Salt Spray (fog) Apparatus, Operating |
| ASTM B537: | Standard Practice for Ranking Electroplated Panels Subject to Atmospheric Exposure |
| Boeing Aircraft Corporation (BAC) Standards: | |
| BAC 5851: | Deposition of HVOF thermal spray coatings |
| Military Specifications: | |
| MIL-H-6875: | Heat Treatment of 4340 Steel |
| MIL-STD-1501: | Chromium Plating Low Embrittlement, Electrodeposition |
| MIL-STD-866: | Grinding of Chrome Plated Steel and Steel Parts Heat Treated to 180,000 psi or over |
| MIL-STD-1504: | Abrasive Blasting |
| QQ-C-320: | Chromium Plating (Electrodeposited) |
| QQ-N-290: | Sulfamate Nickel Plating |
| SAE Standards: | |
| AMS-2432: | Shot Peening, Computer Controlled |
| AMS-5604: | Heat Treatment of 17-4PH Steel |
| AMS-5660: | Heat Treatment of IN-901 Alloy |
| AMS-6875: | Heat treating of high strength Steels |
| GE Aircraft Engine (GEAE) Specifications: | |
| C50TF103, Class B: | Forging of IN-718 |
| C50TF58, Class A: | Forging of A-286 |
| C50TF53, Class A or B: | Forging and heat treatment of AM-355 |
| C50TF37, Class B: | Heat treatment for IN-718 |
| C50TF20, Class A: | Heat treatment for A-286 |
| C50TF50-S8: | Heat treatment and carburization of 9310 |
| Word Drawing 4013195-990: | Low-stress grinding of materials |

# 3. Technology Description

## 3.1. Technology Development and Application

The primary technology used in this program was HVOF thermal spray, although Air Plasma Spray (APS) Tribaloy 400 and WC-Co were evaluated in some materials tests.

**Technology background and theory of operation**: HVOF and APS are thermal spray processes. HVOF is a standard commercial thermal spray process in which a powder of the material to be sprayed is injected into a supersonic flame of a fuel (usually hydrogen, propylene or kerosene), as shown in Figure 3-1. The powder particles are accelerated to high speed and soften in the flame, forming a dense, well-adhered coating on the substrate. The coating material is usually a metal or alloy (such as Tribaloy or stainless steel), or a cermet (such as cobalt-

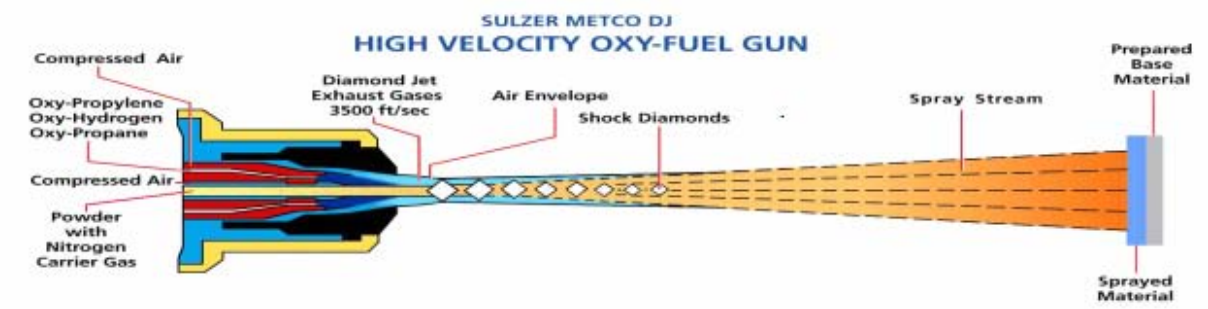


**Figure 3-1. Schematic of HVOF gun and process (Sulzer Metco DiamondJet).**

cemented tungsten carbide, WC/Co). The technology is used to deposit coatings about 0.003" thick on OEM parts, and to rebuild worn components by depositing layers up to 0.015" thick.

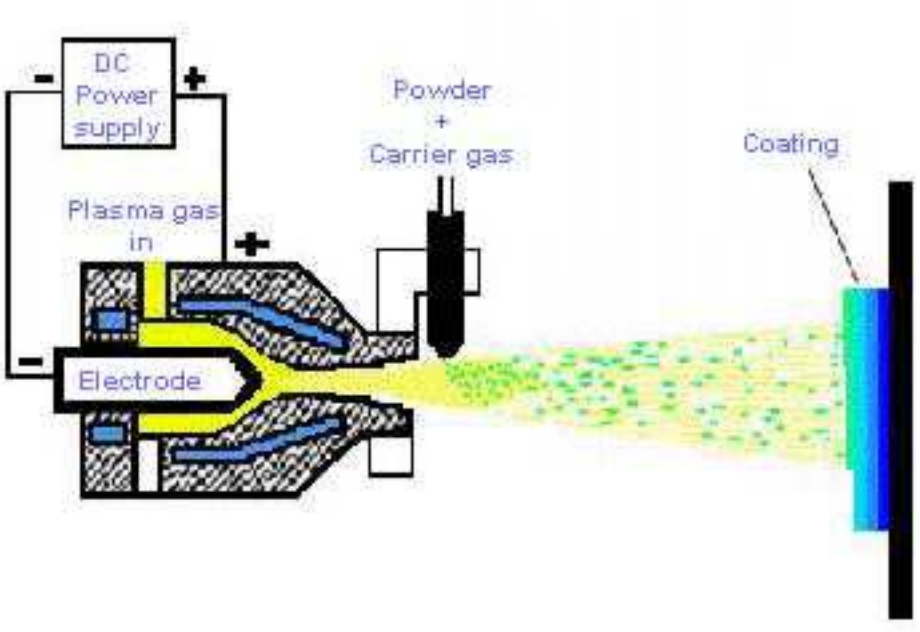


**Figure 3-2. Schematic of plasma spray gun and process.**

APS is a similar process (Figure 3-2), the primary difference being that the heat source is a plasma created by an intense arc and the gas stream is subsonic. Thus there are no fuel gases, and

the gun runs primarily on argon with some nitrogen or hydrogen, depending on the powder used. This combination of design features makes plasma spray particles slower but potentially hotter. Plasma spray coatings are high quality, but they are generally more porous and have lower adhesion and less compressive stress than HVOF coatings.

**Applicability**: High Velocity Oxygen Fuel (HVOF) was originally developed primarily for gas turbine engine (GTE) applications. The primary thermal spray processes are Flame Spray, Plasma Spray, Arc Spray, HVOF, and the recently-developed cold spray. The original high velocity spray technology was the pulsed deposition detonation gun (D-gun) developed by Union Carbide (later Praxair). The quality of the wear and erosion resistant spray coatings produced by this method was much better than the lower speed methods, and continuous flame HVOF was developed as a competitive response.

The original applications for HVOF were wear components in GTEs, such as shafts and bearing journals. As the availability and use of the technology grew, it began to be applied to a wide range of other types of coatings and applications, including a variety of aircraft components such as flap and slat tracks, landing gear and hydraulics for commercial aircraft. It is now being used in many applications outside the aircraft industry, such as industrial rolls and vehicle hydraulics. The original aircraft wear applications, primarily used by Boeing, were for otherwise-intractable spot problems that neither the original alloy nor chrome plate could solve.

The technology can be used to spray a wide variety of alloys and cermets. It is limited for high temperature materials such as oxides, most of which cannot be melted in the flame. The areas to be coated must be accessible to the gun – i.e. they must be line-of-sight.

APS is widely used in the aircraft industry, including the depots. Because the heat source is a plasma APS is widely used to spray refractory zirconium oxide ceramics as thermal barrier coatings in GTE hot section liners, as well as cermets such as WC-Co and alloys for other engine applications.

**Material to be replaced**: HVOF and APS coatings are used to replace hard chrome plate (especially using carbide cermets and high temperature oxidation-resistant Tribaloys). The combination of HVOF NiAl with an overlayer carbide is also used to replace the combination sulfamate Ni/hard chrome. HVOF coatings can also be used to replace some hard Ni and electroless Ni coatings on such components as flap tracks and propeller hubs. In the HCAT program the primary application is hard chrome replacement.

## 3.2. Process Description

**Installation and operation**: Both HVOF and APS systems operate in a similar manner, using a similar spray booth. The spray gun can be hand-held and used in an open-fronted booth. However, the gas stream is extremely loud (especially in the supersonic HVOF process) and requires that the operator use very good ear protection. For this reason the unit is usually installed on a six-axis robot arm in a sound-proof booth, programmed and operated remotely. Most depots, even those new to HVOF, already use this type of booth for their existing plasma spray operations. Since thermal spray is frequently used for cylindrical items the most common arrangement is to rotate the component on a horizontal rotating table and move the gun up and down the axis. Figure 3-3 shows an example of application of an HVOF coating to a landing gear inner cylinder. A similar set-up would be used for application of HVOF coatings to components such as shafts from gas turbine engines.

**Figure 3-3. HVOF Spray of Landing Gear Inner Cylinder.**

**Facility design**: The installation requires

- A soundproof booth. Booths are typically 15 feet square, with a separate operator control room, an observation window, and a high volume air handling system drawing air and dust out of the booth through a louvered opening (shown in Figure 3-3).
- Gun and control panel. The HVOF gun burns the fuel and oxygen inside its combustion chamber and injects the powder axially into the flame. The gas exits the gun at supersonic speed, while the particles are accelerated to high velocity but usually remain subsonic. The APS gun uses Ar as the primary gas. The control panel controls the gas flows, cooling water, etc.
- Powder feeder. Powder is typically about 60μm in diameter and is held in a powder feeder, which meters the powder to the gun at a steady rate, carried on a gas stream. Two powder feeders are commonly used to permit changeover from one coating to another without interrupting the spraying.
- 6-axis industrial robot and controller. Most installations use an industrial robot to manipulate the gun and ensure even spraying. The robot is often suspended from above to leave the maximum possible floor space for large items.
- Supply of oxygen (HVOF). This is frequently a bulk storage container outside the building. Alternatively bottled gas can be used, but because of the high usage rate of up to 2,000 scfh (see Table 3-1), even a standard 12-bottle setup lasts only a few hours in production.
- Supply of fuel gas or kerosene (bottled or bulk, HVOF). Hydrogen is the most common fuel, supplied in bulk or in bottles. Praxair (TAFA) guns use kerosene, which is

significantly cheaper and less dangerous.

- Supply of argon (APS). Argon is supplied from a standard gas cylinder since the flow rate is far lower than that used in HVOF.
- Dust extractor and bag-house filter system. The air extracted from the booth is laden with overspray – particles that have failed to stick to the surface (often 20-50% of the total sprayed). The air is blown into a standard bag house, often located outside the building, where the dust is removed.
- Dry, oil-free compressed air for cooling the component and gun. Air cooling prevents the components being overheated (temperatures must be kept below about 400°F for most high strength steels).
- Water cooling for gun. Not all guns are water cooled, but most are.

The facility must be capable of supplying the material pressures and flows of Table 3-1. Standard commercial equipment currently in service already meet these requirements. Equipment vendors are able to supply turnkey systems.

**Table 3-1 Optimized Deposition Conditions for WC-17Co - DJ 2600 and JP 5000 HVOF Guns [5].**

| | | | |
|---|---|---|---|
| **Equipment** | **Gun** | Model 2600 hybrid gun | Model 5220 gun with 8" nozzle |
| | **Console** | Model DJC | Model 5120 |
| | **Powder feeder** | Model DJP powder feeder | Model 5500 powder feeder |
| **Powder feed** | **Powder** | Diamalloy 2005 | Stark Amperit 526.062 |
| | **Powder Feed Rate:** | 8.5 lb/hr | 80 gm/min (325 rpm, 6 pitch feeder screw) |
| | **Powder Carrier Gas** | Nitrogen | Argon |
| | Carrier gas pressure | 148 psi | 50 psi |
| | Flow rate | 28 scfh | 15 scfh |
| **Combustion Gases** | **Fuel** | Hydrogen | Kerosene, Type 1-K |
| | Console supply pressure | | 162-168 psi |
| | Gun supply pressure | 135 psi | 121-123 psi |
| | Flow rate | 1229 scfh | 5.0 gph |
| | **Oxidizer** | Oxygen | Oxygen |
| | Pressure | 148 psi | 138-140 psi |
| | Mass flow | 412 scfh | 2000 scfh |
| **Gun Compressed Air** | **Pressure** | 105 psi | |
| | **Mass flow** | 920 scfh | |
| **Gun Cooling Water Flow** | **Flow rate**<br>**Water Temperature to Gun:** | 5.3-5.7 gph (factory set)<br>65-80°F typical (ground water, temp varies) | 8.3-8.7 gph<br>64-72°F |
| **Specimen Rotation** | | 2,336 rpm for round bars (0.25 inch dia.) – 1835 in/min surface speed | 600 rpm for round bars (0.25 inch diam.); 144 rpm for rectangular bars (at 6.63 inch diam.) |
| **Gun Traverse Speed** | | 400 linear in/min for round bars | 70 in/min for round bars |
| **Spray Distance** | | 11.5 inches | 18 inches |
| **Cooling Air** | **Pressure** | 90-110 psi | 90-110 psi |
| | **Location** | 2 stationary nozzle tips at 6 inches pointed at coating area | 2 gun-mounted air jets at 14 inches; 1 stationary air jet at 4-6 inches pointed at coating area |

**Performance**: From Table 3-1 HVOF guns deliver about 4-5 kg per hour, of which 65% typically enters the coating, for a coating rate of about 3 kg/hour. For a common 0.010" WC/Co rebuild coating (which will be sprayed to a thickness of 0.013-0.015"), an HVOF gun can deposit about 900in$^2$/hr. This permits application of a 0.010"-thick coating onto the outer surface of a cylinder that is 2 feet long by 4 inches in diameter in about 30 minutes, compared with about 10-

15 hours for chrome plating. The deposition rate for APS is similar.

**Specifications**: The following specifications and standards apply to HVOF coatings:

- Prior to the HCAT program the only aerospace specifications were those issued by primes such as Boeing, whose BAC 5851 thermal spray specification, supported by BMS 10-67G powder specification, is still one of the most quoted standards. This specification includes both HVOF and plasma spray processes.
- Aerospace Materials Specification (AMS) 2447 was developed with the assistance of the HCAT team and issued by SAE in 1998. It is now a widely used standard in the aerospace industry.
- AMS 2437 is the standard AMS specification for plasma spray.
- In order to provide specifications for spraying high strength aircraft steels at depots and vendors, HCAT has worked through SAE to promulgate several standards:
    - AMS 7881 is a powder specification for WC/Co and AMS 7882 is a powder specification for WC/CoCr that were both issued in April 2003.
    - AMS 2448 is a specification describing procedures for spraying WC/Co and WC/CoCr coatings using HVOF that was issued in August 2004
    - AMS 2449 is a specification describing procedures for low-stress grinding of HVOF WC/Co and WC/CoCr coatings that was issued in August 2004.

**Training**: Just as plating shops typically have several personnel who handle masking, racking, demasking, etc. it is common for thermal spray shops to have 3 or 4 technicians dedicated to masking and spraying. Thermal spray training is essential, and is usually provided by equipment vendors such as Praxair and Sulzer Metco. Training is also available through the Thermal Spray Society. Depot personnel taking part in the HCAT program have been trained by Jerry Schell, thermal spray coatings expert at GE Aircraft Engines. Since thermal spray is a more complex technology than electroplating, plating line personnel cannot be transferred successfully to a thermal spray shop without extensive retraining.

**Health and safety**: The thermal spray process does not produce air emissions or toxic wastes. Co powder is an IARC (International Agency for Research on Cancer) Group 2B material, which means that "The agent (mixture) is possibly carcinogenic to humans", whereas $Cr^{6+}$ is an IARC Group 1 material, "Known to be carcinogenic to humans". However, the OSHA PEL for Co (8hr TWA) of 0.1 mg(Co)/$m^3$, is lower than the 1 mg(Cr)/$m^3$ for metallic chrome, and is the same as the 0.1 mg(Cr)/$m^3$ for $Cr^{6+}$. Unlike chrome plating the Co is not emitted into the air. Excess Co-containing powder is drawn from the spray booth and captured in the bag house. Nevertheless personnel should wear a dust respirator when handling the powder, working in the booth, or grinding the coating. While the powders are usually about 60 μm in diameter, they can break apart on impact, producing 10 μm or smaller particles. The American Welding Society recommends the use of a respirator complying with ANSI Z88.2

**Ease of operation**: Since in commercial systems the entire system is programmable, including the gun control and robot, it is generally easy to operate. The operator must create masking (usually shim stock shadow masks) and must develop the correct spray parameters and gun motions. While vendors supply standard operating conditions for different materials, these may have to be optimized experimentally for new materials and powders, and must be adjusted for different components to ensure proper coating speed and gun traverse rate. Small diameter components, for example, must be rotated faster than large ones to maintain the same deposition rate and coating structure. In this respect operating a thermal spray system is considerably more

complex than electroplating.

## 3.3. Previous Testing of the Technology

Prior to the HCAT program HVOF technology had been successfully used by Boeing for a number of years for their commercial aircraft and by GEAE for GTEs. In the period 1993-1996 Keith Legg, Bruce Sartwell, GEAE, Cummins Diesel, and Corpus Christi Army Depot carried out a DARPA-funded evaluation of chrome alternatives [4]. The program evaluated HVOF, PVD, and laser cladding, and concluded that HVOF was the best overall alternative for use in depots and most OEM aircraft applications. At the beginning of the HCAT program Lufthansa successfully completed flight tests of HVOF coatings on commercial landing gear and Delta began to carry out similar flight tests.

## 3.4. Advantages and Limitations of the Technology

Replacing hard chrome plating is a great deal more complex than simply putting down a hard coating. The alternative must not only work technically, but it must fit with the entire life cycle of use and maintenance, and it must be a reasonable, mature technology for depot use. The advantages and limitations of HVOF are summarized in Table 3-2.

APS has similar advantages and limitations, except that it can be used to coat IDs above about 2.5" diameter.

**Table 3-2. Advantages and Limitations of HVOF as a Chrome Replacement.**

| Advantages/strengths | Disadvantages/limitations |
|---|---|
| **Technical:** | |
| Higher hardness, better wear resistance, longer overhaul cycle, less frequent replacement | Brittle, low strain-to-failure – can spall at high load. Issue primarily for carrier-based aircraft |
| Better fatigue, corrosion, embrittlement | Line-of-sight. Cannot coat IDs |
| Material can be adjusted to match service requirements | More complex than electroplating. Requires careful QC |
| **Depot and OEM fit:** | |
| Most depots already have thermal spray expertise and equipment | WC-Co requires diamond grinding wheel. Only HVOF alloys can be plunge ground |
| Can coat large areas quickly | |
| Can be chemically stripped | |
| Many commercial vendors | |
| **Environmental:** | |
| No air emissions from plating tanks, no high volume rinse water | Co toxicity |
| No requirement for use of perchloroethylene as a post-plating cleaner as with hard chrome | |

# 4. Materials Testing

## 4.1. Development of Materials JTP

Performance objectives established under the JTP consisted of materials testing performed on coupons manufactured from the same base materials from which hard-chrome-plated GTE components are fabricated. The objectives were established by the following stakeholders in the project:

Air Force Aeronautical Systems Center

Air Force Propulsion Single Item Manager

Oklahoma City Air Logistics Center (OC-ALC)

Naval Air Systems Command (NAVAIR)

Naval Air Depot Jacksonville (NADEP-JAX)

Naval Air Depot Cherry Point (NADEP-CP)

GE Aircraft Engines (GEAE) (OEM)

Pratt & Whitney (P&W) (OEM)

Rolls-Royce/Allison (OEM)

Coordination of the development and execution of the JTP was provided by the Naval Research Laboratory and Rowan Technology Group.

As indicated in Section 2, an analysis was first conducted of the components from the various DOD GTEs onto which hard chrome is currently applied, with the results of that analysis shown in Table 2-2. Most of the components could be grouped by function in a few families which included shafts, housings, gears and seals. Then the stakeholders analyzed the types of conditions to which the EHC-coated components were subjected (e.g., cyclic stresses, sliding wear, corrosion). From these analyses, the materials testing requirements were established. A stakeholders meeting was held in October 2000 to discuss the testing requirements and create an outline of a Joint Test Protocol (JTP). A first draft of the JTP was produced by Jerry Schell from GEAE and was distributed to the stakeholders. There were numerous revisions generated through additional meetings and electronic correspondence, with a final version [6] approved by the stakeholders in September 2001. The specific types of materials testing delineated in the JTP were fatigue, wear (both sliding wear and carbon seal wear) and corrosion. A detailed description of these tests can be found later in this section. The performance objectives, also called acceptance criteria, were as follows:

Fatigue: Cycles-to-failure at different stress or strain levels were measured for fatigue specimens coated with either EHC or a thermal spray coating. These data were plotted with stress/strain on the vertical axis and cycles-to-failure on the horizontal axis and smooth curves were fit to the data points. If the curves for the thermal spray coatings fell on or above those for the EHC, then the thermal spray coatings were considered to have passed the acceptance criteria.

Wear: Fretting wear tests were conducted for specimens coated with EHC and various thermal spray coatings with different materials as the mating surfaces. If the average wear volume for the thermal spray coatings was equal to or less than for EHC coatings, then the thermal spray coatings were considered to have passed the acceptance criteria.

Corrosion: American Society for Testing and Materials (ASTM) B117 salt-fog exposure tests were conducted on specimens coated with EHC and various thermal spray coatings. Protection ratings were determined in accordance with ASTM specifications. If the average ratings for the thermal spray coatings were greater than or equal to those for EHC, then the thermal spray coatings were considered to have passed the acceptance criteria.

Carbon Seal Testing: Tests consisting of the rotational sliding of EHC- or thermal-spray-coated shafts against two different grades of carbon seals were conducted. If the average wear volume for the carbon seals and thermal spray mating coatings was equal to or less than the wear volume for the carbon seals and EHC mating coatings, then the thermal spray coatings were considered to have passed the acceptance criteria.

## 4.2. Substrate Material Selection

This project differed from the previous HCAT projects in that a GTE is a complete mechanical system that consists of a wide variety of components with different design considerations, operating conditions and parent materials. The other HCAT projects focused on a specific family of components such as landing gear and propeller hubs that have similar design considerations, operating conditions and are fabricated from relatively few parent materials. The survey of the 235 different GTE components listed in Table 2-2 that are currently coated with EHC included a determination of the alloy from which each component was fabricated and these are listed in Table 4-1. It obviously was not possible to conduct materials tests for thermal spray and EHC coatings on all of these 18 alloys. A total of seven alloys as indicated in Table 4-2 were selected for testing based on volume of use, as generic alloy family representatives and for special considerations such as low-tempering temperatures (e.g., 9310 steel) or very complex multi-step heat-plus-cryogenic treatments (e.g., AM355). All materials were tested in an appropriate heat treat condition as defined in Table 4-3. The GTE components represented by these alloys may have varied heat treat conditions depending on the engine and component so heat treatments representative of the most demanding applications were selected.

**Table 4-1 List of Alloys Used to Fabricate GTE Components onto which EHC Plating is Applied**

| | | |
|---|---|---|
| IN-718 | 4140 | 17-4PH |
| IN-901 | 4340 | 410 SS |
| Inco W | 8630 | L605 |
| AM-355 | 8740 | C-355 |
| A-286 | 9310 | |
| Greek Ascolloy | 17-22H | |
| | Nitralloy 135 | |
| | Lapelloy C | |

The components being represented may have varied heat treat conditions depending on the engine and component so heat treatments representative of the most demanding applications were selected. The sample geometries used for the materials testing are defined in each of the respective sections of this report. In general, samples for all testing were shot peened prior to coating application with cut wire (CW-14) to an intensity of 6-8A in accordance with AMS 2432.

**Table 4-2 Alloys Selected for Testing and Their Compositions**

| Selection | | Composition in Weight % | | | | | | | | | | | |
|---|---|---|---|---|---|---|---|---|---|---|---|---|---|
| Alloy | AMS Spec | Ni (+Co) | Cr | Fe | Mo | Nb+Ta | Ti | Al | C | Mn | Cu | Si | B, other |
| IN-718 | 5663 | 50-55 | 19.0 | 19.0 | 3.0 | 5.1 | 0.9 | 0.50 | 0.08 | 0.35 max | 0.75 max | 0.45 max | 0.006 max |
| IN-901 | 5660 5661 | 41-44 | 13.5 | 35.0 | 6.0 | ---- | 2.7 | 0.25 | 0.05 | ---- | ---- | ---- | 0.01 |
| AM-355 | 5743 | 4.5 | 15.5 | 75.5 | 2.9 | ---- | ---- | ----- | 0.13 | 0.85 | ---- | 0.5 | 0.1 Nit |
| A-286 | 5731 | 26.0 | 15.0 | 52.7 | 1.3 | ---- | 2.1 | 0.3 | 0.04 | 1.5 | ---- | 0.7 | 0.005, 0.3 V |
| 17-4PH | 5355 | 4.1 | 16.0 | 76.4 | ---- | 0.28 | ---- | ---- | ---- | ----- | 3.2 | ---- | ---- |
| 4340 | 6415 | 1.75 | 0.8 | 95.8 | 0.25 | ---- | ---- | ---- | 0.40 | 0.70 | ---- | 0.3 | ---- |
| 9310 | 6260 6265 | 3.25 | 1.2 | 94.1 | 0.12 | ---- | ---- | ---- | 0.10 | 0.55 | 0.35max | 0.3 | ---- |

**Table 4-3 Heat Treatment Parameters for Alloys Selected for Testing**

| Material | Heat Treat |
|---|---|
| IN-718 | C50TF37, CL-B |
| IN-901 | AMS 5660 |
| A-286 | C50TF20, CL-A |
| AM-355 | C50TF53, CL-A or B |
| 4340 | MIL-H-6875 (HRc 48-50) |
| 9310 | C50TF50-S8 (HRc 37-38) |
| 17-4PH | AMS 5604 (H1000 temper) |

## 4.3. Coatings Selected for Evaluation

Because of the large number of GTE components onto which EHC is currently applied and because of the wide range of stresses, mating materials and environmental conditions to which the components are subjected, it was decided to perform testing on four different HVOF coatings: (1) WC/17Co, (2) $Cr_3C_2$-20NiCr, (3) Co-28Mo-17Cr-3Si (Tribaloy 800 (T-800)), (4) Co-28Mo-8Cr-2Si (Tribaloy 400 (T-400)). Because of the difficulty of stripping HVOF coatings (which generally involve electrolytic processes) and because at least one GTE OEM has indicated that they prefer not to expose any rotating GTE components to an electrolytic process, it was decided to perform tests on two air plasma-sprayed (APS) coatings which can be stripped using non-electrolytic processes such as high-velocity water-jet. Those coatings were WC/17Co and Co-28Mo-8Cr-2Si (Tribaloy 400). Materials testing was also conducted on EHC-coated samples to form the baseline data to which the results for the HVOF and plasma-sprayed coatings would be compared. The coatings selected for testing are summarized in Table 4-4 which also indicates the powder used for coatings application.

**Table 4-4 Coatings Selected for Testing**

| **HVOF Process** | | **APS Process** | |
|---|---|---|---|
| Composition, Wgt % | Powder | Composition, Wgt % | Powder |
| WC/17Co | Diamalloy 2005 | WC/17Co | Metco 73F-NS-1 |
| $Cr_3C_2$-20 (Ni,Cr) | Amdry 5260/Diam 3007 | Co-28 Mo-8 Cr-2 Si** | Metco 66F-NS |
| Co-28 Mo-17 Cr-3 Si* | Diamalloy 3001 | | |
| Co-28 Mo-8 Cr-2 Si** | Diamalloy 3002 | | |

* Tribaloy 800
** Tribaloy 400

## 4.4. Coating Optimization, Deposition and Characterization

### 4.4.1. Data Summary

**Table 4-5 Quick Reference to Primary Data. Click Blue Links t o Jump to Data**

| Item | Item Number |
|---|---|
| GTE JTP Coatings | Table 4-7 |
| Thermal Spray Process/QC Inputs/Outputs | Table 4-6 |
| HVOF WC/17Co spray parameters | Table 4-10 |
| HVOF T-400 spray parameters | Table 4-13 |
| HVOF T-800 spray parameters | Table 4-14 |
| HVOF Chrome Carbide-20NiCr parameters | Table 4-15 |
| Plasma WC/Co DOE | Figure 4-7, Table 4-18, and Table 4-19 |
| Plasma T-400 spray parameters | Table 4-21 |
| Hydrogen vs. Natural Gas Comparison | Table 4-17 |
| Quality Control Data For GTE Spray Runs | Table 4-22, Table 4-23, and Table 4-24 |

### 4.4.2. General

The main thrust of the Joint Test Protocol (JTP) was to compare the performance of EHC to that of alternative coatings in materials tests relevant to GTE applications. In order to have a valid comparison, it was necessary to consider the optimization, control, and characterization of the alternative coatings being deposited.

EHC is a known and optimized process for both OEMs and repair depots on all the current GTE applications. In contrast, the thermal spray coatings considered as EHC replacements have not been fully optimized and it has been necessary within the HCAT program to optimize process parameters for the varied materials. The coatings for the GTE work were listed in Table 4-4. With the exception of HVOF WC/17Co and T-400 (optimized in earlier HCAT work), coating optimization studies were conducted on the remaining materials.

Also, for the GTE work, there are three major differences concerning coating deposition compared to previous HCAT work:

- More coatings (six) were considered than in previous HCAT protocols
- Plasma spray work was included along with HVOF coatings (HVOF coatings in all other work)
- Inclusion of natural gas as a fuel for HVOF coating deposition in lieu of the hydrogen fuel evaluated in all other HCAT protocols

Therefore, in the subsequent subsections, the following information is provided:

- The logic and purpose of coating optimization
  - Rationale
  - Methodology (Design of Experiment (DOE))
- A summary of the optimization work that was conducted for the GTE coatings listed in Table 4-4.
- The quality control (QC ) results and characterization of the coating process used in the spraying of the GTE test specimens.

## 4.4.3. Rationale of the HCAT Coating Optimization

#### 4.4.3.1.Rationale of Coating Optimization

As with any manufacturing output, the properties and performance of the final product depend upon both an optimized and well controlled process. With thermal spray coatings or chrome plating, optimal coating properties can therefore only be obtained when the critical deposition parameters are in the proper range. In chrome plating the coating properties are primarily governed by solution chemistry, temperature, current density, and anode/geometry placement. As stated earlier, procedures governing EHC plating are well documented and quality control procedures in place for adequate monitoring of the final product. Thermal spray, with obvious emphasis on HVOF, is more complex to optimize since there are many more variables in the deposition process.

Table 4-6 is a list of the parameters/quality control (QC) outputs which are critical for thermal spray processing. These factors must therefore be considered in a successful optimization investigation.

##### 4.4.3.1.1. Background History of HCAT Coating Optimization and Deposition Philosophy

In order to optimize a coating, it is important to decide at the outset what property, or set of properties, is to be optimized. This is especially true for thermal spray coatings, where it has been found, for example, that a coating optimized for minimum wear can behave poorly in fatigue. Within the HCAT, the fatigue critical nature of applications such as landing gear, actuators, propeller hub components, and, for this protocol, gas turbine engine parts, was quickly identified as the major life limiting characteristic that governs acceptance of those chrome alternatives by the user community. This does not eliminate the need to evaluate other characteristics such as corrosion, wear, hydrogen embrittlement, etc. but coating optimization initially concentrated on fatigue performance, with modifications for other properties as necessary. This approach was adopted as the philosophy of the HCAT stakeholders from the onset of the program, as evidenced by the heavy concentration on fatigue in the test protocols.

**Table 4-6 Thermal Spray Process and Quality Control Inputs/Outputs.**

| Input | Output |
|---|---|
| Powder size and feed rate | Hardness |
| Gas flow | Microstructure |
| Gas ratio-fuel to oxygen | Almen strip |
| Spray distance | Tensile |
| Carrier gas flow | Coating deposition rate |
| Air flow | |
| Traverse speed | |

For the HCAT program in general, the coating optimization process began with the initial "generic" protocol (i.e. not associated with any type of aircraft component) in 1996 and has been evolving to the present time. A design of experiment (DOE) test methodology (which will be discussed in a later section) was chosen as the mechanism to provide an optimized coating deposit. The variables in the process are identified and experiments conducted to determine the best parameter set for optimum results. In past JTPs, general work has been performed using several commercial systems such as the JP-5000 (Praxair/TAFA-using kerosene fuel) and the DJ 2600 (Sulzer Metco-using hydrogen fuel) units. Optimization of the process is carried out for three important reasons:

1. To define a thermal spray process that will achieve the desired performance and property goals.
2. To establish manufacturing robustness and the process window for a reliable process.
3. To understand the process and trends that give an indication of (and can later be used as) a trouble shooting guide. When parameters are identified as significant, these variables will be the first areas of investigation in problem solving.

In optimizing the thermal spray process, it is important to understand the difference between the general output of the process and the characteristics/properties of the final coating deposit. As stated earlier, the final goal of the coating optimization is maximized fatigue performance with close emphasis on other properties such as corrosion, wear, etc. However, when the coating is initially sprayed, only a set of simple measurements (also listed in Table 4-6) are used for quality control of the process, as follows:

- Microstructure (primarily measurement of porosity, unmelted particles, and oxides)
- Hardness (both macro and micro)
- Almen strip (residual stress)
- Substrate temperature (during coating)
- Deposition rate

The total outcome of these measurements has proven to be adequate to define the coating for the purpose of quality control. It makes technical sense that characteristics such as microstructure and hardness will ultimately determine coating performance in areas such as wear or corrosion resistance, while residual stress and substrate temperature are known to strongly influence fatigue. Thus, even though the ultimate goal is enhanced fatigue performance, that performance can be ensured indirectly by measuring other coating properties for quality control.

Once the deposition process is known to be uniform and stable, these measurements can be

routinely made on test samples set up and sprayed in a manner similar to components being coated. These test samples may be sprayed prior to part coating (for daily spray booth qualification), or sprayed during actual coating deposition on components (for quality control).

## 4.4.4. DOE Methodology for the Coating Optimization

### 4.4.4.1. General Methodology

For HCAT optimization studies, the design of experiment (DOE) methodology has been chosen as the vehicle to deliver the best spray parameter set. This method is used in many manufacturing environments when numerous variables exist and there are insufficient time and financial resources to analyze each individual process input (i.e. to carry out a full matrix test). Pre-DOE experiments are usually run on an iterative basis to determine the limits of the various parameters and determine which have the most significant effect on the output of the process. A DOE matrix is then designed using standard experimental design protocols in which the variables selected are usually assigned high and low values for the numerous DOE test runs. Statistical analysis through Analysis of Variables (ANOVA), is applied and each variable assigned a rank as to the effect on the final process output. In subsequent experimentation, insignificant variables are eliminated from the analysis and the final outcome is a full parameter set for the process in question. For the HCAT program the experimental design was done using commercial software made by Minitab, Inc.

### 4.4.4.2. Thermal Spray Optimization

As stated earlier, even with the DOE methodology, there must be a general starting or reference point. This was provided by the earlier thermal spray work conducted by Boeing and some general experience from Jerry Schell of GE Aircraft Engines. With this knowledge and the ultimate goal of fatigue performance, three QC outputs (from Table 4-6 ) were identified as the major drivers to achieve the end goal:

***Hardness –*** tends to be a general gage of wear resistance, but more importantly an indicator of carbide solutioning and phase change

***Almen Strip –*** indication of coating residual stress and hence probable fatigue performance

***Substrate Temperature –*** should generally be below 350 °F to avoid degrading substrate fatigue material properties

This information shaped the methodology involved for this optimization, which included:

***Pre-DOE –*** A series of general experimental runs to achieve a common-sense understanding of the process. For example, it would not make sense to pick a parameter range for the thermal spray system setting that would not allow the gun to spray in an efficient manner or provides no Almen Strip response. This initial set identifies some reasonable responses for the actual DOE experimentation.

***Actual DOE*** – When a reasonable set of process inputs and ranges have been identified, a number of runs/experiments are conducted according to a test matrix defined by the DOE software. Outputs are analyzed and trends determined. Dependent upon time and funding, further more refined studies can be run or the process fine-tuned at this point.

***Validation Runs –*** Using the optimum settings determined from the DOE, a small set of runs is made to verify the parameter set and repeat spray cycles are conducted to

establish consistency.

#### 4.4.4.3. Optimization Results for the GTE Coatings

##### 4.4.4.3.1. General

The ultimate goal of the optimization work under the GTE protocol was fully characterized and optimized spray parameter sets for all the coatings shown in Table 4-7. As stated earlier, work for the HVOF WC/17Co and HVOF T-400 had already been completed and reported in the under the Landing Final Report [7].

However, during the time frame of the protocol, manpower and resource constraints did not allow

**Table 4-7 GTE Coatings. Coatings Selected for Testing**

| ***HVOF Process*** | | ***Optimization*** | |
|---|---|---|---|
| *Composition, Wgt %* | *Powder* | *Full DOE Other HCAT Work* | *Limited DOE GTE Work* |
| WC/17Co | Diamalloy 2005 | Yes | -- |
| $Cr_3C_2$-20 (Ni,Cr) | Amdry 5260/Diam 3007 | -- | Yes |
| Co-28 Mo-17 Cr-3 Si* | Diamalloy 3001 | -- | Yes |
| Co-28 Mo-8 Cr-2 Si** | Diamalloy 3002 | Yes | -- |
| | | | |
| ***PS Process*** | | | |
| WC/17Co | Metco 73F-NS-1 | -- | Yes-unsuccessful |
| Co-28 Mo-8 Cr-2 Si** | Metco 66F-NS | -- | Very limited |

* Tribaloy 800 ** Tribaloy 400

performance of a complete DOE study for the remaining coatings. The final coating parameter sets were therefore determined by a limited DOE process. *Limited DOE work* is defined as selection of coating parameters based upon data generated by the DOE methodology but not based upon a full DOE process with finalized validation runs. For plasma WC/17Co, optimization work was unsuccessful as will be explained later in this section, and the coating was subsequently dropped from the test protocol, except for carbon seal testing.

For completeness, this section details both the prior optimizations of HVOF coatings (which fully illustrates a total DOE analysis) and the limited DOE work used to optimize the remaining coatings.

##### 4.4.4.3.2. HVOF WC/Co Sulzer Metco DJ 2600 System (Landing Gear program)

The first example of coating optimization is the DOE work at Hitemco for the HVOF WC/Co in the Landing Gear project. Although this work was performed earlier in the HCAT program, a quick synopsis is in order to illustrate the full DOE process and the amount of work required.

## Table 4-8 Random Runs for HVOF WC/Co DOE

| | | A factor | | (B,C) Combined Factors | | | D factor |
|---|---|---|---|---|---|---|---|
| Run No. | Std.Ord | Turn Table RPM | Robot Trav Sp mm/s | Hydrogen psi/FMR | Oxygen psi/FMR | Air psi, FMR | Sp Dist inches |
| 1 | 9 | 252 | 14.8 | 135 psi, 50.4 | 148 psi, 23.1 | 105 psi, 50.5 | 11.5 |
| 2 | 1 | 212 | 10.6 | 135 psi, 47.2 | 148 psi, 17.8 | 105 psi, 50.5 | 10 |
| 3 | 2 | 292 | 21.2 | 135 psi, 47.2 | 148 psi, 17.8 | 105 psi, 50.5 | 13 |
| 4 | 3 | 212 | 10.6 | 135 psi, 56.5 | 148 psi, 23.8 | 105 psi, 50.5 | 13 |
| 5 | 4 | 292 | 21.2 | 135 psi, 56.5 | 148 psi, 23.8 | 105 psi, 50.5 | 10 |
| 6 | 10 | 252 | 14.8 | 135 psi, 50.4 | 148 psi, 23.1 | 105 psi, 50.5 | 11.5 |
| 7 | 5 | 212 | 10.6 | 135 psi, 44.6 | 148 psi, 21.8 | 105 psi, 50.5 | 13 |
| 8 | 6 | 292 | 21.2 | 135 psi, 44.6 | 148 psi, 21.8 | 105 psi, 50.5 | 10 |
| 9 | 7 | 212 | 10.6 | 135 psi, 53.4 | 148 psi, 28.7 | 105 psi, 50.5 | 10 |
| 10 | 8 | 292 | 21.2 | 135 psi, 53.4 | 148 psi, 28.7 | 105 psi, 50.5 | 13 |
| 11 | 11 | 252 | 14.8 | 135 psi, 50.4 | 148 psi, 23.1 | 105 psi, 50.5 | 11.5 |

Table 4-8 represents the random run sequence for the DOE and Table 4-9 shows the general matrix.

Figure 4-1, Figure 4-2, and Figure 4-3 show the general trends for microhardness, substrate temperature, and Almen strip responses, respectively.

## Table 4-9 DOE Matrix for Hitemco Analysis

*Design 1: Use L8 design plus Center Points, 11 runs total*

| FACTORS: | | Levels -1 | +1 | C Pt |
|---|---|---|---|---|
| A | Surf Speed,Feed Rate | 1335, 5.1 | 1835, 3.5 | 1585 ipm, 4.3 |
| B | Combustion Gas | 1525 scfh | 1825 scfh | 1675 scfh |
| C | Stoic Ratio | 0.405 | 0.485 | 0.445 |
| D | Spray Distance | 10 inch | 13 inch | 11.5 inch |

| A Factor: | Turntable RPM | Robot Spd ipm | mm/sec | Robot % @ 750 mm/sec | Spots/Rev |
|---|---|---|---|---|---|
| (-1) | 212 | 25 | 10.6 | 1.41% | 5.1 |
| C Pt | 252 | 35 | 14.8 | 1.98% | 4.3 |
| (+1) | 292 | 50 | 21.2 | 2.82% | 3.5 |

**(B,C) Factor Combinations:**

| Comb Gas | Stoic Ratio | Hyd SCFH | Oxy SCFH | Air SCFH | Point (CG,SR) |
|---|---|---|---|---|---|
| 1675 | 0.445 | 1159 | 332 | 920 | ( 0, 0) |
| 1525 | 0.405 | 1085 | 258 | 920 | (-1,-1) |
| 1525 | 0.485 | 1027 | 314 | 920 | (-1,+1) |
| 1825 | 0.405 | 1299 | 342 | 920 | (+1,-1) |
| 1825 | 0.485 | 1229 | 412 | 920 | (+1,+1) |

**FIXED:**

54 grit alumina grit blast at 40 psi, 6 inches
Substrate is 4340 steel, 260-280 ksi
Powder size/type is WC-17Co, Diamalloy 2005, Lot 54480
Powder Feed Rate** 8.5 lbs/hr
Spray angle is 90 degrees
100 psi cooling air, 4 AJs @ 6 inch spaced over coupon area
Carrier gas $N_2$ at 148 psi, 55 flow, air vib @ 20 psi
Spray pattern length Approximately 13 inch
Fixture diameter 2 inch

| RESPONSES: | RELATED CTG FUNCTION: |
|---|---|
| 1) Part temperature | Fatigue |
| 2) Almen strip | Fatigue, ctg residual stress |
| 3) Hardness, $HV_{300}$ | Wear |
| 4) Coating dep/pass | Cost |
| 5) Porosity | Ctg quality, corrosion |
| 6) Oxides | Ctg quality |
| 7) Carbides | Ctg quality, wear |
| 8) Tensile bond | Adhesion/cohesion |

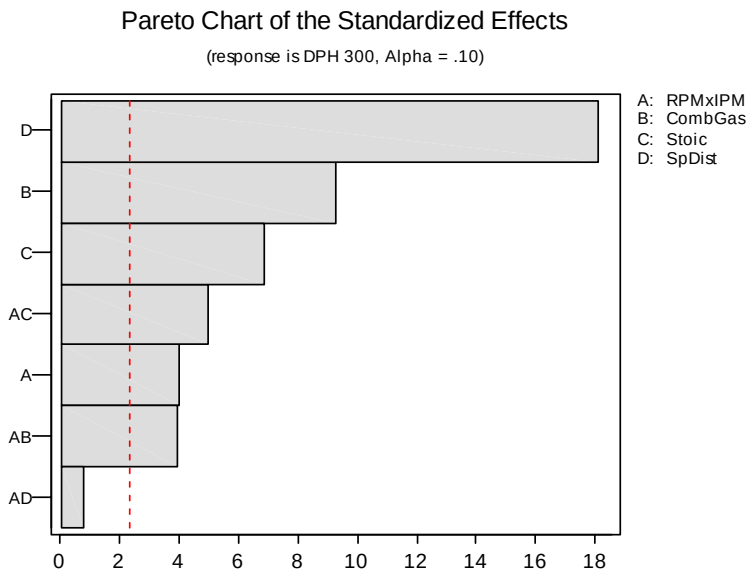


**Figure 4-1 Microhardness Response for the HVOF WC/Co DOE**

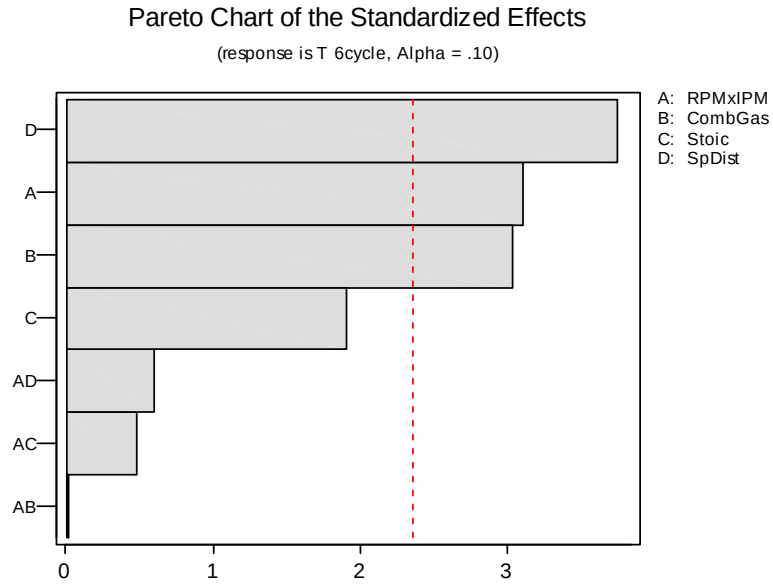


**Figure 4-2 Substrate Temperature Response for HVOF WC/Co DOE**

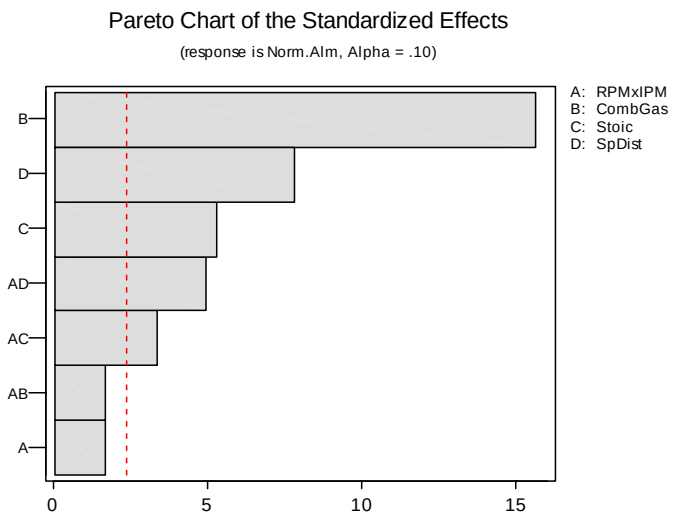


**Figure 4-3 Almen Strip Response for HCAT HVOF WC/Co DOE**

This initial work helped to shape the expectations for all subsequent DOE work within HCAT. Some of the major trends identified for HVOF were:

- Combustion gas content and stand-off distance are the major factors in the spray process. The data for microhardness, Almen strip values, and substrate temperature identifies these variables as the critical parameters for control and the obvious areas to investigate in subsequent problem troubleshooting.
- The deposition rate of the coating is obviously controlled not only by powder feed rate but traverse speed of the part being sprayed. This will have a substantial effect on Almen and substrate temperature because of the heat being transferred to the part. It is therefore critical to keep the deposition rate constant in spraying test bars, Almen strips, or parts to best approximate a consistent and repeatable process

Stoichiometry was also identified as a major factor in microhardness results. Stoichiometry is the ratio of fuel gas to oxygen in the gun, and because it controls flame temperature, it affects melting of the matrix Co and dissolution of the carbides. High flame temperatures tend to put the carbides in solution, resulting in hardness changes and alloying of the binder, both of which affect mechanical properties of the coating. Stoichiometry must therefore be included in the process control.

Table 4-10 is the final spray parameter set for spraying of test coupons with HVOF WC/Co.

**Table 4-10 Final Deposition Parameters HCAT HVOF WC/Co**

| Description | Required Value |
|---|---|
| **Gun** | Model 2600 hybrid gun |
| **Injector** | #8 |
| **Shell** | #8 |
| **Insert** | #8 |
| **Siphon plug** | #8 |
| **Aircap** | DJ2603 |
| **Powder** | Diamalloy 2005 |
| **Powder Feed Rate:** | 8.5 lb/hr |
| **Powder Carrier Gas** | Nitrogen |
| Carrier gas pressure | 148 psi |
| FMR | 55 |
| Flow rate | 28 scfh |
| **Fuel** | Hydrogen |
| Gun supply pressure | 135 psi |
| FMR | 53.4 |
| Flow rate | 1229 scfh |
| **Oxidizer** | Oxygen |
| Pressure | 148 psi |
| FMR | 28.7 |
| Mass flow | 412 scfh |
| **Air** | Air |
| Pressure | 105 psi |
| FMR | FMR – 50.5 |
| Mass flow | 920 scfh |
| **Rotational Speed** | 2,336 rpm for round bars (0.25 inch dia.) – 1835 in/min surface speed |
| **Traverse Rate** | 169 mm/sec for round bars |
| **Stand-off distance** | 11.5 inches |
| **Cooling air** | |
| Pressure | 90-110 psi |
| Location | 2 stationary nozzle tips at 6 inches pointed at coating area |

### 4.4.4.3.3. HVOF T-400 Sulzer Metco DJ 2600 System (Landing Gear program) at NADEP Cherry Point

The work performed at Cherry Point centered around optimization of the HVOF T-400 coating. Table 4-11 and Table 4-12 show the DOE matrix for this optimization.

**Table 4-11 DOE Matrix for Optimization of T-400 at NADEP Cherry Point**

| DOE Design | | | | | | Assigned Levels | | | | RESPONSES | | | | | | |
|---|---|---|---|---|---|---|---|---|---|---|---|---|---|---|---|---|
| | | C | B | A | D | C | B | A | D | | | | | | | |
| Notes ID | Std. Order | Stoic | CombGas | RPMxTrSp | PFR | Stoic | CombGas | RPMx TrSp | PFR | Tmax | Norm Almen | Dep/ Pass | Hardness | % Porosity | % Oxides | Tensile |
| **i** | 1 | - | - | - | - | 0.409 | 2240 | 170x30 | 4.2 | 497 | 4.1 | 0.200 | 51.5 | 0.175 | 0.750 | 7391 |
| **A** | 2 | - | - | + | + | 0.409 | 2240 | 340x68 | 6.3 | 315 | 4.4 | 0.142 | 50.0 | 0.175 | 0.750 | 8792 |
| **D** | 3 | - | + | - | + | 0.409 | 2000 | 170x30 | 6.3 | 262 | 1.9 | 0.142 | 53.3 | 0.375 | 0.400 | 9097 |
| **F2** | 4 | - | + | + | - | 0.409 | 2000 | 340x68 | 4.2 | 270 | 1.6 | 0.129 | 55.0 | 1.000 | 0.500 | 10700 |
| **G** | 5 | + | - | - | + | 0.445 | 2240 | 170x30 | 6.3 | 385 | 4.1 | 0.229 | 49.9 | 0.675 | 1.000 | 8767 |
| **C** | 6 | + | - | + | - | 0.445 | 2240 | 340x68 | 4.2 | 300 | 4.5 | 0.117 | 46.6 | 0.500 | 0.500 | 9717 |
| **B** | 7 | + | + | - | - | 0.445 | 2000 | 170x30 | 4.2 | 320 | 5.3 | 0.167 | 51.4 | 0.175 | 0.750 | 8458 |
| **ii** | 8 | + | + | + | + | 0.445 | 2000 | 340x68 | 6.3 | 295 | 1.9 | 0.167 | 54.5 | 0.175 | 1.000 | 4780 |

Figure 4-4, Figure 4-5, and Figure 4-6 show examples of the response functions from the DOE and how the variables affect the final outputs. The same general trends as summarized for the WC/17Co DOE trials (Section 4.4.4.3.2) with regard to combustion gas, stand-off distance, and deposition rate were also observed for T-400 and therefore not summarized again in this section. Table 4-13 provides the final spray parameters for T-400.

**Table 4-12 DOE Random Order Process Information for T-400**

| Powder | DATE | Std Order | RUN # | Diam | Part | Trav | Y Speed ipm | Part RPM | Inch/min | Overlaps | Cycles | Tot Cy | Spray Dist | PFR lbs/hr | Feed RPM | Stoic Ratio | Comb Gas |
|---|---|---|---|---|---|---|---|---|---|---|---|---|---|---|---|---|---|
| T-400 (Diam 3002) | 2/11/99 | **1** | **99.09** | | 6.63' fixture | 19% | 30 | 170 | 3539 | 3.4 | 8+16 | 24 | 10 | 4.2 | 8% | 0.409 | 2240 |
| T-400 (Diam 3002) | 2/11/99 | **8** | **99.10** | | 6.63' fixture | 38% | 68 | 340 | 7078 | 3.0 | 12+18 | 30 | 10 | 6.3 | 12% | 0.445 | 2000 |
| T-400 | 3/5/99 | **7** | **99.13** | | 6.63' fixture | 19% | 30 | 170 | 3539 | 3.4 | 12+12 | 24 | 10 | 4.2 | 8% | 0.445 | 2000 |
| T-400 | 3/5/99 | **2** | **99.14** | | 6.63' fixture | 38% | 68 | 340 | 7078 | 3.0 | 12+12 | 24 | 10 | 6.3 | 12% | 0.409 | 2240 |
| T-400 | 3/5/99 | **6** | **99.15** | | 6.63' fixture | 38% | 68 | 340 | 7078 | 3.0 | 12+12 | 24 | 10 | 4.2 | 8% | 0.445 | 2240 |
| T-400 | 3/5/99 | **3** | **99.17** | | 6.63' fixture | 19% | 30 | 170 | 3539 | 3.4 | 12+12 | 24 | 10 | 6.3 | 12% | 0.409 | 2000 |
| T-400 | 3/8/99 | **5** | **99.18** | | 6.63' fixture | 19% | 30 | 170 | 3539 | 3.4 | 12+12 | 24 | 10 | 6.3 | 12% | 0.445 | 2240 |
| T-400 | 3/8/99 | **4** | **99.19** | | 6.63' fixture | 38% | 68 | 340 | 7078 | 3.0 | 12+12 | 24 | 10 | 4.2 | 8% | 0.409 | 2000 |

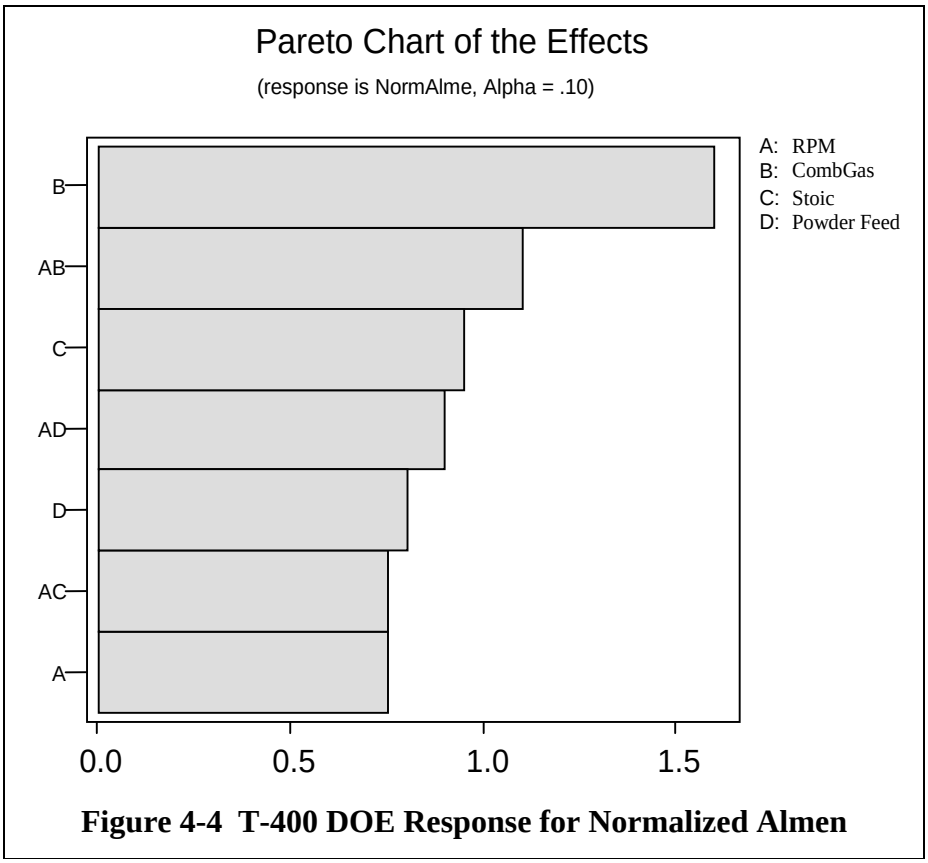


**Figure 4-4 T-400 DOE Response for Normalized Almen**

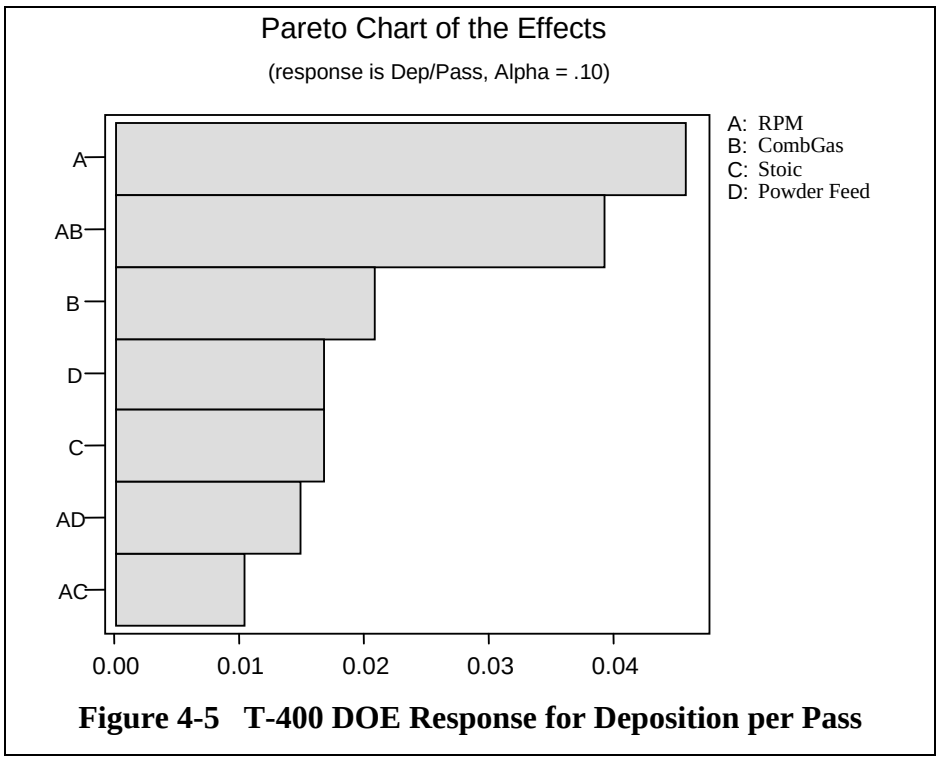


**Figure 4-5 T-400 DOE Response for Deposition per Pass**

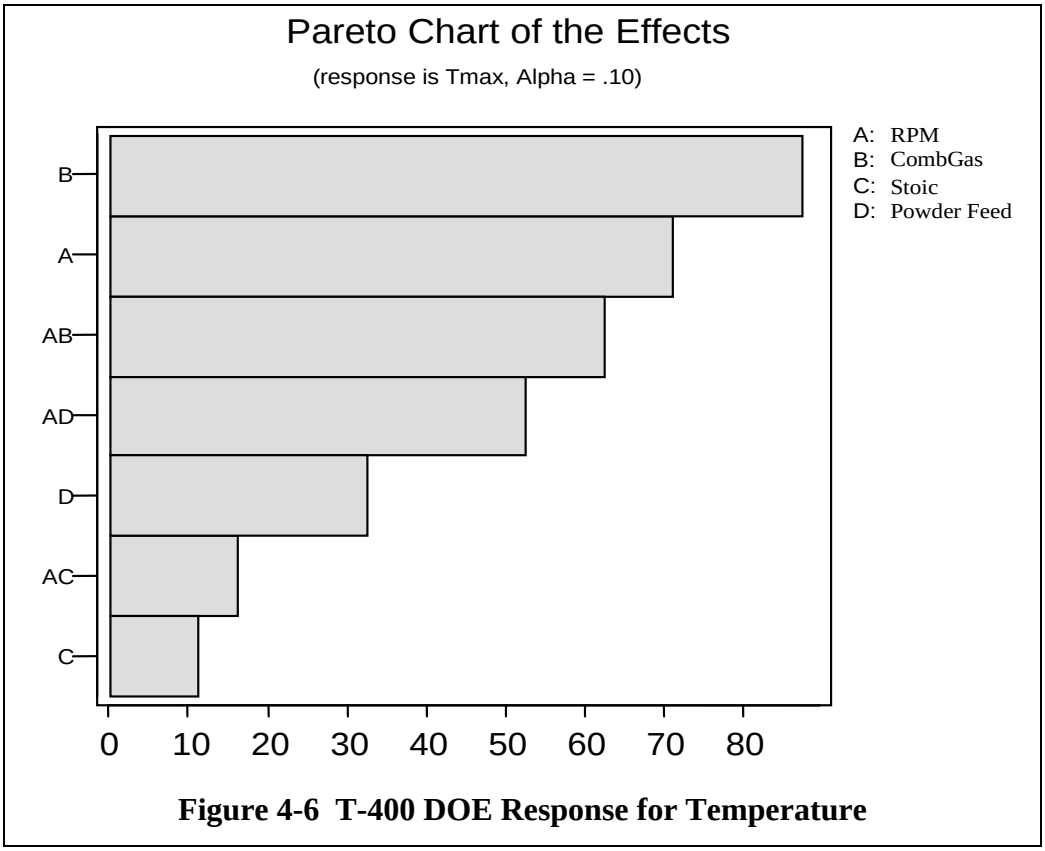


**Figure 4-6 T-400 DOE Response for Temperature**

#### 4.4.4.3.4. HVOF T-800 Coating Optimization

As stated earlier, limited DOE work was performed on HVOF T-800 due to manpower and resources constraints. This work involved approximately 17 runs with review of outputs from Almen, tensile, porosity, and hardness. Based upon analysis of the results, Run 18 (as highlighted in green) was selected as the spray parameter set for the GTE specimens as highlighted in Table 4-14.

**Table 4-13 Final Spray Parameters for HVOF T-400**

| DESCRIPTION | REQUIRED VALUE (RANGE) |
|---|---|
| **GUN TYPE** | DIAMOND JET |
| **NOZZLE SHELL** | 8 |
| **NOZZLE INSERT** | 8 |
| **INJECTOR** | 8 |
| **AIRCAP** | 2603 |
| **SIPHON PLUG** | 8 |
| **OXIDIZER** | OXYGEN |
| **PSI** | 150 |
| **FLOW** | 26.8 (388 scfh) |
| **AIR** | AIR |
| **PSI** | 105 |
| **FLOW** | 52.9 (965 scfh) |
| **FUEL** | HYDROGEN |
| **PSI** | 150 |
| **FLOW** | 58.8 (1418.89 scfh) |
| **CARRIER GAS** | NITROGEN |
| **PSI** | 145 |
| **FLOW** | 55 |
| **POWDER FEED RATE** | 6.3 |
| **SPRAY DISTANCE** | 10" |
| **SPRAY ANGLE** | 90° +/- 10° |
| **ROTATIONAL SPEED** | 3000 rpm |
| **GUN TRAVERSE RATE** | 225 MM/sec |
| **GUN AIRJETS(LOCA.)** | N/A |
| **GUN AIRJETS(PSI.)** | N/A |
| **AUX.COOLING(LOCA.)** | 170 degrees form spray |
| **AUX.COOLING(PSI.)** | 80 psi |
| **COATING THICKNESS** | .0067" |
| **# OF PASSES (ref. Only!)** | 22 (.0003"/pass) |
| **Almen deflection (normalized)- .004"-.006"** | |

#### 4.4.4.3.5. HVOF Chrome Carbide Coating Optimization

As stated earlier, limited DOE work was performed on the HVOF $Cr_3C_2$/20NiCr due to manpower and resources constraints. This work involved approximately 8 runs with review of outputs for Almen, tensile, porosity and hardness. Based upon an analysis of the results, Run 45 (as highlighted in green) was selected as the spray parameter set for the GTE specimens as highlighted in Table 4-15.

#### 4.4.4.3.6. Hydrogen vs. Natural Gas Comparison for HVOF Coatings

HVOF spraying using natural gas as the fuel was performed at Sulzer Metco in Westbury, NY using the hydrogen parameters as a starting point. Table 4-16 highlights the limited DOE trials for the natural gas optimization. Table 4-17 compares the final spray parameters from hydrogen and natural gas spraying.

As can be seen, the differences between the parameters are minor. There are obviously stoichiometric issues because of the BTU differences between the fuels but nothing major has changed in the other settings. Note that Table 4-17 is a comparison of work on fatigue only. No other specimens were sprayed in this comparison. There are some differences in speeds/traverse rates between the hydrogen/natural gas settings. This is acceptable since the Almen strip values are equivalent even though the deposition rates are different.

#### 4.4.4.3.7. Plasma WC/Co Coating Optimization

A full DOE analysis was run to obtain optimum parameters for plasma WC/Co in this protocol. Unfortunately, with limited time and resources, a coating could not be sprayed with the desired compressive Almen values. As stated earlier, the desire for compressive Almen is driven by fatigue concerns in GTE applications. Normal plasma parameters usually result in tensile residual stresses in the deposit. This situation was clearly evident in spraying of .015" thick specimens during early trials where the coating completely delaminated due to high tensile residual stress. Figure 4-7, Table 4-18, and Table 4-19 summarize the work performed in this analysis. Because of the inability to obtain acceptable values of residual stress, PS WC/Co coatings were not evaluated in the test protocol, except for the carbon seal tests.

#### 4.4.4.3.8. Plasma T-400 Coating Optimization

For the plasma T-400 , limited DOE work was performed due to manpower and resources constraints. This work involved approximately 14 runs with review of outputs from Almen, tensile, porosity, and hardness (Table 4-20) . After this work was performed, the data analysis did not result in a satisfactory set of parameters. Given time constraints, a decision was made to use prior GEAE approved production parameters, as indicated in Table 4-21. However, it must be noted that these parameters were not optimized for fatigue performance and residual stress was neutral to slightly tensile as opposed to compressive which was the original goal.

## Table 4-14 HVOF T-800 Limited DOE Work

| ***T-800 Data on 3.3" OD*** | **Diamalloy 3001** | | **OPTIMIZATION** | **RUNS** | | **SELECTED PARAMETER SET** | | | |
|---|---|---|---|---|---|---|---|---|---|
| *Date* | 8/15/01 | 8/15/01 | 8/15/01 | 8/15/01 | 8/15/01 | 8/15/01 | 3/27/02 | 3/27/02 | 3/27/02 |
| *Run Number* | 13 | 14 | 15 | 16 | 17 | 18 | 51 | 52 | 53 |
| *Gun Type* | DJ 2600 | DJ 2600 | DJ 2600 | DJ 2600 | DJ 2600 | DJ 2600 | DJ 2600 | DJ 2600 | DJ 2600 |
| *Oxygen Pressure* | 175 | 175 | 150 | 150 | 150 | 150 | 150 | 145 | 170 |
| *Oxygen Flow* | 33.5 | 33.5 | 29 | 30 | 27 | 32 | 32 | 28.5 | 32 |
| *Air Pressure* | 105 | 105 | 103 | 109 | 105 | 105 | 105 | 105 | 105 |
| *Air Flow* | 41 | 41 | 53 | 44 | 53 | 53 | 53 | 49 | 49 |
| *Fuel Pressure* | 148 | 148 | 148 | 145 | 145 | 145 | 145 | 145 | 145 |
| *Fuel Flow* | 63 | 63 | 58 | 51 | 60 | 56.5 | 56.5 | 55.5 | 58 |
| *Carrier Gas Pressure* | 150 | 150 | 150 | 150 | 150 | 150 | 150 | 150 | 150 |
| *Carrier Gas Flow* | 55 | 55 | 55 | 55 | 55 | 55 | 55 | 55 | 55 |
| *Powder Feed Rate* | 4 | 4 | 4.5 | 3.8 | 4 | 4.3 | 4.3 | 5 | 5 |
| *Spray Distance* | 9" | 9" | 11" | 11" | 11" | 11" | 11" | 10" | 11" |
| *Spray Angle* | 90° | 90° | 90° | 90° | 90° | 90° | 90° | 90° | 90° |
| *Rotational Speed* | 267 rpm | 267 rpm | 267 rpm | 267 rpm | 267 rpm | 267 rpm | 267 rpm | 300 rpm | 300 rpm |
| *Gun Traverse Rate* | 24.75 mm/sec | 24.75 mm/sec | 24.75 mm/sec | 24.75 mm/sec | 24.75 mm/sec | 24.75 mm/sec | 24.75 mm/sec | 31.8 mm/sec | 31.8 mm/sec |
| *Deposition Rate* | 0.00019 per pass | 0.0002 per pass | 0.00019 per pass | 0.00024 per pass | 0.00019 per pass | 0.0002 per pass | 0.0015 per pass | 0.0014 per pass | 0.0002 per pass |
| *Max Temperature* | 575 ° | 490 ° | 382 ° | 300 ° | 395 ° | 355 ° | 355 ° | 400 ° | 382 ° |
| *Normalized Almen Deflection* | + .0076 | + .0062 | + .0076 | 0.0 | + .0066 | + .0054 | + .0043 | + .0055 | + .0049 |
| *Bond Strength Avg.* | 7,948 | 7,457 | 6,602 | 5,470 | 6,262 | 7,670 | 9,444 | 7,671 | 8,162 |
| *Hardness Avg.* | 736 | 785 | 628 | 885 | 785 | | 699.6 | 741.6 | 751.4 |
| *Porosity %* | < 3 % | < 3 % | < 5 % | < 5 % | < 5 % | | < 3 % | < 1 % | < 1 % |
| *Oxide Content* | Uniformly Dist. | Uniformly Dist. | Uniformly Dist. | Uniformly Dist. | Uniformly Dist. | | Uniformly Dist. | Uniformly Dist. | Uniformly Dist. |
| ***T-800 Data on 3.3" OD*** | | | | | | | | | |
| *Date* | 3/27/02 | 3/28/02 | 3/28/02 | 3/28/02 | 3/28/02 | 3/28/02 | 3/28/02 | 3/28/02 | |
| *Run Number* | 54 | 55 | 56 | 57 | 58 | 59 | 60 | 61 | |
| *Gun Type* | DJ 2600 | DJ 2600 | DJ 2600 | DJ 2600 | DJ 2600 | DJ 2600 | DJ 2600 | DJ 2600 | |
| *Oxygen Pressure* | 145 | 145 | 145 | 145 | 145 | 170 | 145 | 145 | |
| *Oxygen Flow* | 28.5 | 22.5 | 27.5 | 28.5 | 27.5 | 32 | 22.5 | 28.5 | |
| *Air Pressure* | 105 | 105 | 105 | 105 | 105 | 105 | 105 | 105 | |
| *Air Flow* | 49 | 49 | 49 | 49 | 49 | 49 | 49 | 49 | |
| *Fuel Pressure* | 145 | 145 | 145 | 145 | 145 | 145 | 145 | 145 | |
| *Fuel Flow* | 61.5 | 52.5 | 49.5 | 61.5 | 49.5 | 58 | 52.5 | 55.5 | |
| *Carrier Gas Pressure* | 150 | 150 | 150 | 150 | 150 | 150 | 150 | 150 | |
| *Carrier Gas Flow* | 55 | 55 | 55 | 55 | 55 | 55 | 55 | 55 | |
| *Powder Feed Rate* | 5 | 5 | 5 | 5 | 5 | 5 | 5 | 5 | |
| *Spray Distance* | 9" | 9" | 11" | 11" | 9" | 9" | 11" | 10" | |
| *Spray Angle* | 90° | 90° | 90° | 90° | 90° | 90° | 90° | 90° | |
| *Rotational Speed* | 300 rpm | 300 rpm | 300 rpm | 300 rpm | 300 rpm | 300 rpm | 300 rpm | 300 rpm | |
| *Gun Traverse Rate* | 31.8 mm/sec | 31.8 mm/sec | 31.8 mm/sec | 31.8 mm/sec | 42.45 mm/sec | 21.15 mm/sec | 42.45 mm/sec | 31.8 mm/sec | |
| *Deposition Rate* | 0.00017 per pass | 0.0002 per pass | 0.0002 per pass | 0.0002 per pass | 0.00017 per pass | 0.00021 per pass | 0.00024 per pass | 0.00021 per pass | |
| *Max Temperature* | 518 ° | 442 ° | 362 ° | 440 ° | 380 ° | 485 ° | 337 ° | 408 ° | |
| *Normalized Almen Deflection* | + .0049 | + .0026 | + .0021 | + .0044 | + .0027 | + .005 | + .0012 | + .004 | |
| *Bond Strength Avg.* | 9,957 | 6,987 | 7,628 | 6,624 | 7,543 | 7,372 | 7,949 | 7,265 | |
| *Hardness Avg.* | 748 | 741.8 | 725 | 642.4 | 788.2 | 693.8 | 617.6 | 661.6 | |
| *Porosity %* | < 1 % | < 3 % | < 3 % | < 3 % | < 3 % | < 1 % | < 3 % | < 5 % | |
| *Oxide Content* | Uniformly Dist. | Uniformly Dist. | Uniformly Dist. | Uniformly Dist. | Uniformly Dist. | Uniformly Dist. | Uniformly Dist. | Uniformly Dist. | |

## Table 4-15 HVOF $Cr_3C_2$-NiCr Limited DOE Work

| CrC/NiCr Data on 3.3" OD | OPTIMIZATION | | | SELECTED | | | | | |
|---|---|---|---|---|---|---|---|---|---|
| **Diamalloy 3007** | RUNS | | | PARAMETER SET | | | | | |
| *Date* | 3/26/02 | 3/26/02 | 3/26/02 | 3/26/02 | 3/26/02 | 3/26/02 | 3/26/02 | 3/26/02 | 3/26/02 |
| *Run Number* | 42 | 43 | 44 | 45 | 46 | 47 | 48 | 49 | 50 |
| *Gun Type* | DJ 2600 | DJ 2600 | DJ 2600 | DJ 2600 | DJ 2600 | DJ 2600 | DJ 2600 | DJ 2600 | DJ 2600 |
| *Oxygen Pressure* | 170 | 170 | 170 | 170 | 150 | 150 | 150 | 170 | 170 |
| *Oxygen Flow* | 32 | 32 | 32 | 32 | 27.5 | 27.5 | 30 | 31 | 28.5 |
| *Air Pressure* | 105 | 105 | 105 | 105 | 105 | 105 | 105 | 105 | 105 |
| *Air Flow* | 44 | 44 | 44 | 44 | 48 | 48 | 48 | 48 | 48 |
| *Fuel Pressure* | 140 | 140 | 140 | 140 | 140 | 140 | 140 | 140 | 140 |
| *Fuel Flow* | 62 | 62 | 62 | 62 | 60 | 60 | 58.5 | 57 | 63.5 |
| *Carrier Gas Pressure* | 150 | 150 | 150 | 150 | 150 | 150 | 150 | 150 | 150 |
| *Carrier Gas Flow* | 55 | 55 | 55 | 55 | 55 | 55 | 55 | 55 | 55 |
| *Powder Feed Rate* | 10 | 5 | 5 | 5 | 5 | 5 | 5 | 5 | 5 |
| *Spray Distance* | 9.5" | 9.5" | 11" | 11" | 11" | 11" | 11" | 11" | 11" |
| *Spray Angle* | 90° | 90° | 90° | 90° | 90° | 90° | 90° | 90° | 90° |
| *Rotational Speed* | 173 rpm | 173 rpm | 173 rpm | 173 rpm | 173 rpm | 173 rpm | 173 rpm | 173 rpm | 173 rpm |
| *Gun Traverse Rate* | 18 mm/sec | 18 mm/sec | 18 mm/sec | 27 mm/sec | 27 mm/sec | 27 mm/sec | 27 mm/sec | 27 mm/sec | 27 mm/sec |
| *Deposition Rate* | 0.00045 per pass | 0.00027 per pass | 0.0003 per pass | 0.00021 per pass | 0.0002 per pass | 0.00018 per pass | 0.00022 per pass | 0.00019 per pass | 0.00022 per pass |
| *Max. Temperature* | 562 ° | 510 ° | 462 ° | 438 ° | 425 ° | 440 ° | 443 ° | 418 ° | 470 ° |
| *Normalized Almen Deflection* | + .0027 | + .0059 | + .0028 | + .0035 | + .002 | + .0016 | + .0032 | + .003 | + .004 |
| *Bond Strength Avg.* | 11,795 | 10,919 | 10,833 | 11,624 | 11,453 | No data | 11,517 | 10,171 | 10,149 |
| *Hardness Avg.* | 1,038 | 996 | 977 | 991 | 931 | available | 997 | 930 | 929 |
| *Porosity %* | < 3 % | < 1 % | < 3 % | < 1 % | < 3 % | This was a | < 3 % | < 3 % | < 5 % |
| *Oxide Content* | Uniformly Dist. | Uniformly Dist. | Uniformly Dist. | Uniformly Dist. | Uniformly Dist. | re-run of # 46 | Uniformly Dist. | Uniformly Dist. | Uniformly Dist. |

## Table 4-16 Comparison of Hydrogen vs. Natural Gas Parameters for WC/Co and $Cr_3C_2$-NiCr

| **COATING** | 2005 | 2005 | 3007 | 3007 |
|---|---|---|---|---|
| Fuel | Hydrogen | Nat Gas | Hydrogen | Nat Gas |
| GUN TYPE | DIAMOND JET | DIAMOND JET | DIAMOND JET | DIAMOND JET |
| NOZZLE SHELL | 8 | 9 | 8 | 9 |
| NOZZLE INSERT | 8 | 9 | 8 | 9 |
| INJECTOR | 8 | 9 | 8 | 9 |
| AIRCAP | 2603 | 2701 | DJ 2603 | 2701 |
| SIPHON PLUG | 8 | 9 | 8 | 9 |
| OXIDIZER | OXYGEN | Oxygen | OXYGEN | Oxygen |
| PSI | 148 | 150 | 170 | 150 |
| FLOW | 28.7 | 44 | 32 | 46 |
| AIR | AIR | AIR | AIR | AIR |
| PSI | 105 | 95 | 105 | 100 |
| FLOW | 50.5 | 36 | 44 | 46 |
| FUEL | HYDROGEN | Methane | HYDROGEN | Methane |
| PSI | 135 | 110 | 140 | 110 |
| FLOW | 53.4 | 58 | 62 | 50 |
| CARRIER GAS | NITROGEN | Nitrogen | NITROGEN | Nitrogen |
| PSI | 148 | 150 | 150 | 150 |
| FLOW | 55 | 28.5 | 55 | 28.5 |
| POWDER FEED RATE | 8.5 Lbs/Hr. | 5 lbs/Hr. | 5 lbs./Hr. | 5 lbs./Hr. |
| SPRAY DISTANCE | 11.5" | 9 | 11" | 11" |
| SPRAY ANGLE | 90° +/- 10° | 90° +/- 10° | 90° +/- 10° | 90° +/- 10° |
| ROTATIONAL SPEED | 2236 RPM / 169.5 MM-SEC | 2292 | 2280 RPM | 2300 rpm on .250" diameter fatigue specimen |
| GUN TRAVERSE RATE | 169.5 MM-SEC | 121 mm/sec | 225 MM-SEC | 100 mm/sec |
| GUN AIRJETS (LOCA.) | N/A | Cab coolers 170 degrees from spray | N/A | Cab coolers 170 degrees from spray |
| GUN AIRJETS (PSI.) | N/A | 95 psi | N/A | 95 psi |
| AUX. COOLING (LOCA.) | 170° FROM SPRAY | N/A | 170° FROM SPRAY | N/A |
| AUX. COOLING (PSI.) | 80 PSI | N/A | 80 PSI | N/A |
| COATING THICKNESS | .018/.006 | 0.0181 | .018/.006 | 0.0195 |
| # OF PASSES (ref. Only!) | | 105 (0.00017"/pass) | | 63 (0003"/pass) |
| Almen | .005-.0086 | | .000-004" | |

**Table 4-17 Comparison of Hydrogen vs. Natural Gas Spray Parameters Tribaloy Coatings**

| **COATING** | 3002 | 3002 | 3001 | 3001 |
|---|---|---|---|---|
| Fuel | Hydrogen | Nat Gas | Hydrogen | Nat Gas |
| GUN TYPE | DIAMOND JET | DIAMOND JET | DIAMOND JET | DIAMOND JET |
| NOZZLE SHELL | 8 | 9 | 8 | 9 |
| NOZZLE INSERT | 8 | 9 | 8 | 9 |
| INJECTOR | 8 | 9 | 8 | 9 |
| AIRCAP | 2603 | 2603 | 2603 | 2603 |
| SIPHON PLUG | 8 | | 8 | |
| OXIDIZER | OXYGEN | Oxygen | OXYGEN | Oxygen |
| PSI | 150 | 150 | 150 | 155 |
| FLOW | 26.8 | 38 | 32 | 40 |
| AIR | AIR | | AIR | |
| PSI | 105 | | 105 | |
| FLOW | 52.9 | | 53 | |
| FUEL | HYDROGEN | Methane | HYDROGEN | Methane |
| PSI | 150 | 112 | 145 | 112 |
| FLOW | 58.8 | 65 | 56.5 | 52 |
| CARRIER GAS | NITROGEN | Nitrogen | NITROGEN | Nitrogen |
| PSI | 145 | 153 | 130 | 130 |
| FLOW | 55 | 28.5 | 55 | 55 |
| POWDER FEED RATE | 6.3 | 6.3 | 4.3 lb/hr | 4.3 lb/hr |
| SPRAY DISTANCE | 10" | 10" | 11" | 11" |
| SPRAY ANGLE | 90° +/- 10° | 90° +/- 10° | 90° +/- 10° | 90° +/- 10° |
| ROTATIONAL SPEED | 3000 rpm | 1150 rpm on .250" diameter fatigue specimen | 3525 rpm | 1390 rpm on .250" diameter fatigue specimen |
| GUN TRAVERSE RATE | 225 mm/sec | 60 mm/sec | 135 mm/sec | 75 mm/sec |
| GUN AIRJETS (LOCA.) | N/A | Cab coolers 170 degrees from spray | N/A | Cab coolers 170 degrees from spray |
| GUN AIRJETS (PSI.) | N/A | 95 psi | N/A | 95 psi |
| AUX. COOLING (LOCA.) | 170° FROM SPRAY | N/A | 170° FROM SPRAY | N/A |
| AUX. COOLING (PSI.) | 80 PSI | N/A | 80 PSI | N/A |
| COATING THICKNESS | .018/.006" | 0.019 | .018/.006" | 0.0195 |
| # OF PASSES (ref. Only!) | | 23 (00083"/pass) | | 38 (00051"/pass) |
| Almen | .0032-.0062" | .006” | .005-.0098" | >006” |

## Table 4-18 Plasma WC/Co DOE

| | | | | Plasma | WC/Co | DOE | Results | | | |
|---|---|---|---|---|---|---|---|---|---|---|
| | Base Settings | | Run No. | Almen Thick | Spray Rate | Mils per pass | Almen Norm to .005" | Almen Non-Norm | Sub Temp. | |
| Gun | 3MB | | | | | | | | | |
| Nozzle | | | 1 | 0.011 | 11 | 0.0012 | 0.003 | | | |
| Primary Gas | Argon | | 2 | 0.005 | 8 | 0.0008 | 0.003 | | | |
| Pressure | 100 | | 3 | 0.005 | 8 | 0.0005 | 0.006 | | | |
| Flow | 160 | | 4 | 0.003 | 7.3 | 0.0005 | 0.0035 | | 180 °F | |
| | | | 5 | 0.004 | 6 | 0.0003 | 0.0031 | | 280 °F | |
| 0.004 | Hydrogen | | 6 | | 6 | 0.0004 | 0.0038 | -0.003 (tensile) | 200-300 °F | |
| Pressure | 50 | | 7 | xx | 7.5 | 0.00093 | xx | -0.004 (tensile) | 250-450 °F | |
| Flow | 80% | | 8 | 0.0057 | 6.2 | 0.00057 | 0.004 | -0.0047 (tensile) | 250-350 | |
| Powder Feed | (argon) | DOE Design | | Primary Flow | Spray rate | Surface Speed | Total Power (vary voltage and secondary gas) | | DOE SETTINGS | Plus (+) | Minus (-) |
| Pressure | 100 | | 1 | (-) | (-) | (-) | (-) | | Primary Flow | 140 | 160 |
| Flow | 50 | | 2 | (+) | (-) | (-) | (+) | | Spray rate | 6 | 11 |
| Volts | 55 | | 3 | (-) | (+) | (-) | (+) | | Surface Speed | 7.5 | 15 |
| Amps | 400 | | 4 | (+) | (+) | (-) | (-) | | Total Power (vary voltage and secondary gas) | 55 | 65 |
| Spray Dist. | 3" | | 5 | (-) | (-) | (+) | (+) | | | | |
| | | | 6 | (+) | (-) | (+) | (-) | | | | |
| Rot Speed | 290 | | 7 | (-) | (+) | (+) | (-) | | | | |
| | | | 8 | (+) | (+) | (+) | (+) | | | | |

## Table 4-19 Plasma WC/Co Trials – 3MB Plasma Spray Gun

| | | | | | | | ***Plasma*** | ***WCCo*** | ***Trial*** | ***Runs*** | | |
|---|---|---|---|---|---|---|---|---|---|---|---|---|
| | ***Settings used*** | Volts | Secondary | Run # | | | | Almen Norm-alized | Almen | Traverse | Substrate | Hard-ness |
| | ***for deposition*** | | Gas flow % | | Thick-ness | Spray Rate | Depo Rate | to .005" | Non-Norm-alized | Rate | Temp. | |
| ***Gun/nozzle*** | **3MB/GE** | Nov 2002 runs | | | (inch) | | ("/pass) | | | (mm/sec) | (deg F) | |
| ***Primary Gas*** | **Ar** | Base | Set | A | 0.008 | 8 | 0.0008 | 0.002 tensile | .0035 tensile | 11.25 | 225-325 | |
| ***Pressure*** | **100** | 55 | 80 | 1P | 0.0045 | 8 | 0.00045 | 0.0038 tensile | 0.0035 tensile | 15 | 240 | 875 |
| ***Flow*** | **180** | 60 | 83 | 2P | 0.005 | 8 | 0.0005 | 0.0045 tensile | 0.0045 tensile | 15 | 273 | 903 |
| ***Secondary*** | **$H_2$** | 50 | 77 | 3P | 0.0045 | 8 | 0.00045 | 0.0022 tensile | 0.002 tensile | 15 | 215 | xx |
| ***Pressure*** | **50** | 65 | 87 | 4P | 0.0044 | 8 | 0.00044 | 0.0064 tensile | 0.0057 tensile | 15 | 300 | 941 |
| ***Flow*** | **3** | 65 | 87 | 5P-1 | 0.0054 | 12.6 | 0.0009 | 0.0057 tensile | 0.0062 tensile | 11.25 | 220 | |
| ***Powder Feed gas*** | **Ar** | 65 | 87 | 5P-2 | 0.005 | 10.3 | 0.0005 | 0.006 tensile | 0.006 tensile | 15 | 153 | |
| ***Pressure*** | **100** | 65 | 87 | 5P-3 | 0.006 | 12.2 | 0.0003 | 0.0042 tensile | 0.005 tensile | 30 | 250 | |
| ***Flow*** | **50** | 65 | 87 | 5P-4 | 0.005 | 12.2 | 0.0012 | 0.0052 tensile | 0.0052 tensile | 7.5 | 240 | |
| ***Volts*** | **55** | | | | | | | | | | | |
| ***Amps*** | **400** | Base | Set | 6P | 0.004 | 7.8 | 0.0005 | 0.0046 tensile | 0.0037 tensile | 11.25 mm/sec | 260 | |
| ***Spray Dist.*** | **3"** | | | | | | | | | | | |
| ***Rot Speed*** | **290** | | | | | | | | | | | |
| ***Powder*** | **73 F** | | | | | | | | | | | |
| ***Powder Feed rate*** | **6 lb/hr** | | | | | | | | | | | |
| ***Surface speed*** | **1270 mm/sec** | | | | | | | | | | | |

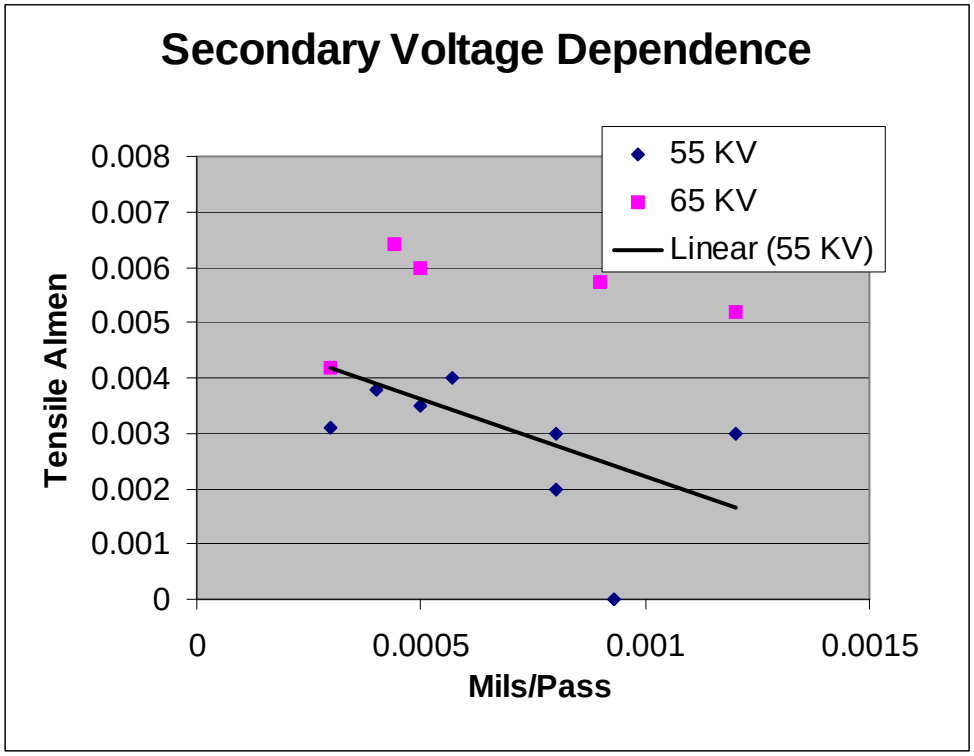


**Figure 4-7 Plasma WC/Co Illustrating Almen Trend with Voltage**

## 4.4.5. GTE Coating Deposition and Characterization

As highlighted earlier, material was sprayed using both hydrogen and natural gas. The work on natural gas spraying was done at the request of NADEP JAX because they intended to use it as a fuel for HVOF.

### 4.4.5.1.Hydrogen Spraying

Table 4-22 and Table 4-23 summarize the quality control testing data for the varied spray runs concerning fatigue, wear, and corrosion testing. As a matter of convention, negative values in the Almen data mean a tensile residual stress. The goal for HVOF is compressive residual stress so this convention has been adopted as the positive listings in the data tables.

The plasma T-400 data is also included in Table 4-24 for completeness.

### 4.4.5.2.Natural Gas Spraying

As stated earlier, comparative runs were made between the hydrogen and natural gas fuel. Table 4-16 and Table 4-17 compare the spray parameters from hydrogen and natural gas spraying. As can be seen, there are no real substantial differences between the parameters. There are obviously stoichiometric issues because of the BTU differences between the fuels but nothing major has changed in the other parameters. Table 4-24 shows the quality control spray data for the natural gas.

## Table 4-20 Plasma T-400 Limited DOE

| ***Plasma T-400*** | ***Limited DOE*** | ***66F*** | ***2.25 ID*** | ***Fixture*** | | | |
|---|---|---|---|---|---|---|---|
| Date | 10/4/2001 | 10/5/2001 | 10/5/2001 | 10/5/2001 | 10/5/2001 | 10/5/2001 | 10/5/2001 |
| Run Number | 28 | 29 | 30 | 31 | 32 | 33 | 34 |
| Gun Type | 3 MB | 3 MB | 3 MB | 3 MB | 3 MB | 3 MB | 3 MB |
| Nozzle | GH | GP | GP | GP | GP | GP | GP |
| Powder Port | # 2 | # 2 | # 2 | # 2 | # 2 | # 2 | # 2 |
| Primary PSI (Argon) | 100 | 100 | 100 | 100 | 100 | 100 | 100 |
| Primary Flow | 150 | 150 | 150 | 150 | 150 | 180 | 180 |
| Secondary PSI (Hydro) | 50 | 50 | 50 | 50 | 50 | 50 | 50 |
| Secondary Flow | 5 | 5 | 10 | 3.2 | 3.2 | 3.2 | 2 |
| Carrier Gas PSI (Argon) | 100 | 100 | 100 | 100 | 100 | 100 | 100 |
| Carrier Gas Flow | 37 | 37 | 37 | 37 | 37 | 37 | 37 |
| Powder Feed Rate | 5.8 | 5.5 | 5.5 | 4.2 | 5.5 | 5.5 | 5.5 |
| Voltage | 70 | 70 | 78 | 62 | 62 | 62 | 52.5 |
| Amperage | 525 | 525 | 525 | 525 | 525 | 525 | 525 |
| Spray Distance | 4.5" | 4.5" | 4.5" | 4.5" | 4.5" | 4.5" | 4.5" |
| Spray Angle | 60° | 60° | 60° | 60° | 60° | 60° | 60° |
| Gun Air Jets | Cross @ 5.5" | Cross @ 5.5" | Cross @ 5.5" | Cross @ 5.5" | Cross @ 5.5" | Cross @ 5.5" | Cross @ 5.5" |
| Gun Air Jets PSI | 40 | 100 | 100 | 100 | 100 | 100 | 100 |
| Rotational Speed | 364 rpm | 364 rpm | 364 rpm | 364 rpm | 364 rpm | 364 rpm | 364 rpm |
| Gun Traverse Rate | 33.75 mm/sec | 33.75 mm/sec | 33.75 mm/sec | 33.75 mm/sec | 33.75 mm/sec | 33.75 mm/sec | 33.75 mm/sec |
| Deposition Rate | 0.00036 per pass | 0.00029 per pass | 0.00031 per pass | 0.00024 per pass | 0.00029 per pass | 0.00023 per pass | 0.00024 per pass |
| Max. Temperature | 470 ° | 340 ° | 380 ° | 275 ° | 275 ° | 285 | 195 ° |
| Normalized Almen Deflection | - .0014 | - .0017 | - .0019 | - .0016 | - .0016 | - .0013 | - .0014 |
| Bond Strength Avg. | 3,782 | 3,205 | 3,846 | 3,333 | 3,077 | 3,141 | 2,821 |
| Hardness Avg. | 647 | 535 | 571 | 599 | 554 | 588 | 545 |
| Porosity % | < 10 % | < 10 % | < 5 % | < 12 % | < 5 % | < 20 % | < 25 % |
| Oxide Content | Uniformly Dist. | Not Uniform | Not Uniform | Heavy Stringers | Uniformly Dist. | Not Uniform | Not Uniform |
| Date | 10/5/2001 | 10/8/2001 | 10/8/2001 | 10/4/2001 | 10/4/2001 | 10/4/2001 | 10/4/2001 |
| Run Number | 35 | 36 | 37 | 38 | 39 | 40 | 41 |
| Gun Type | 3 MB | 3 MB | 3 MB | 3 MB | 3 MB | 3 MB | 3 MB |
| Nozzle | 704 | 704 | 704 | GH | GH | GH | GE |
| Powder Port | # 2 | # 2 | # 2 | # 2 | # 2 | # 2 | # 2 |
| Primary PSI (Argon) | 100 | 100 | 100 | 100 | 100 | 100 | 100 |
| Primary Flow | 150 | 150 | 175 | 150 | 175 | 175 | 180 |
| Secondary PSI (Hydro) | 50 | 50 | 50 | 50 | 50 | 50 | 50 |
| Secondary Flow | 5.5 | 3 | 1 | 3.5 | 3 | 8 | 1.5 |
| Carrier Gas PSI (Argon) | 100 | 100 | 100 | 100 | 100 | 100 | 100 |
| Carrier Gas Flow | 37 | 37 | 37 | 37 | 37 | 37 | 37 |
| Powder Feed Rate | 5.5 | 5.5 | 5.4 | 5.4 | 5.4 | 5.5 | 5.4 |
| Voltage | 70 | 62 | 55 | 55 | 55 | 70 | 52.5 |
| Amperage | 525 | 525 | 525 | 525 | 525 | 525 | 525 |
| Spray Distance | 4.5" | 4.5" | 4.5" | 4.5" | 4.5" | 6" | 4.5" |
| Spray Angle | 60° | 60° | 60° | 60° | 60° | 60° | 60° |
| Gun Air Jets | Cross @ 5.5" | Cross @ 5.5" | Cross @ 5.5" | Cross @ 5.5" | Cross @ 5.5" | Cross @ 7" | Cross @ 5.5" |
| Gun Air Jets PSI | 100 | 100 | 100 | 100 | 100 | 100 | 100 |
| Rotational Speed | 364 rpm | 364 rpm | 364 rpm | 364 rpm | 364 rpm | 364 rpm | 364 rpm |
| Gun Traverse Rate | 33.75 mm/sec | 33.75 mm/sec | 33.75 mm/sec | 33.75 mm/sec | 33.75 mm/sec | 33.75 mm/sec | 33.75 mm/sec |
| Deposition Rate | 0.00022 per pass | 0.00017 per pass | 0.0001 per pass | 0.0001 per pass | 0.00036 per pass | 0.00036 per pass | 0.00021 per pass |
| Max. Temperature | 268 ° | 208 ° | 188 ° | 292 ° | 325 ° | 280 ° | 260 ° |
| Normalized Almen Deflection | - .0018 | - .0025 | - .0012 | - .0012 | - .0017 | - .0018 | - .0014 |
| Bond Strength Avg. | 4,231 | 3,974 | 3,846 | 3,590 | 4,487 | 4,103 | 2,564 |
| Hardness Avg. | 515 | 563 | 497 | 575 | 540 | 594 | 585 |
| Porosity % | < 20 % | < 20 % | < 20 % | < 10 % | < 15 % | > 20 % | < 20 % |
| Oxide Content | Not Uniform | Not Uniform | Not Uniform | Uniformly Dist. | Not Uniform | Not Uniform | Not Uniform |

## Table 4-21 Final Plasma T-400 Parameters

| ***COATING*** | **66F** | **Plasma T-400** | | |
|---|---|---|---|---|
| ***Fuel*** | Hydrogen | | ***ROTATIONAL SPEED*** | 3828 RPM |
| ***GUN TYPE*** | 9 MB PLASMA | | ***GUN TRAVERSE RATE*** | 148.5 MM-SEC |
| ***NOZZLE SHELL*** | GH | | ***GUN AIRJETS (LOCA.)*** | N/A |
| ***NOZZLE INSERT*** | 9MB 63 ELECTRODE | | ***GUN AIRJETS (PSI.)*** | N/A |
| ***INJECTOR*** | # 5 POWDER PORT | | ***AUX. COOLING (LOCA.)*** | 170° FROM SPRAY |
| ***OXIDIZER*** | ARGON | | ***AUX. COOLING (PSI.)*** | 80 PSI |
| ***PSI*** | 100 PSI | | ***COATING THICKNESS*** | .018" |
| ***FLOW*** | 150 FLOW | | ***# OF PASSES (ref. Only!)*** | |
| ***FUEL*** | HYDROGEN | | ***Almen*** | Neutral |
| ***PSI*** | 50 PSI | | | |
| ***FLOW*** | 20 FLOW | | | |
| ***CARRIER GAS*** | ARGON | | | |
| ***PSI*** | 100 PSI | | | |
| ***FLOW*** | 37 FLOW | | | |
| ***Volts*** | 80 | | | |
| ***Amps*** | 600 | | | |
| ***POWDER FEED RATE*** | 7 lbs./Hr. | | | |
| ***SPRAY DISTANCE*** | 5.5" | | | |
| ***SPRAY ANGLE*** | 90° +/- 10° | | | |

## Table 4-22 WC/Co and $Cr_3C_2$-NiCr HVOF Hydrogen Data

| Coating | Specimen Type | Voids [%] | Interface [visual] | Oxides [%] | HV300 Micro Hard | Tensile [PSI] | Thick [inch] | Norm Almen Deflection | Max Temp [deg. F] | Depo Rate [inch per pass] |
|---|---|---|---|---|---|---|---|---|---|---|
| D2005 HVOF | FATIGUE | < 1% | OK | < 1% | 1103.8 | 11111 | .018/.006 | 0.0049 | 180° | 0.0025 |
| D2005 HVOF | FATIGUE | < 1% | OK | < 1% | 1062.8 | 11282 | .018/.006 | 0.005 | 190° | 0.0025 |
| D2005 HVOF | FATIGUE | < 1% | OK | < 1% | 1012.1 | 11004 | .018/.006 | 0.0056 | 170° | 0.0025 |
| D2005 HVOF | FATIGUE | < 1% | OK | < 1% | 1027.5 | 10128 | .018/.006 | 0.0078 | 155° | 0.0025 |
| D2005 HVOF | FATIGUE | < 1% | OK | < 1% | 1050.2 | 10855 | .018/.006 | 0.0083 | 145° | 0.0025 |
| D2005 HVOF | FATIGUE | < 1% | OK | < 1% | 1072.2 | 10748 | .018/.006 | 0.006 | 136° | 0.0025 |
| D2005 HVOF | FATIGUE | < 1% | OK | < 1% | 1101.1 | 10192.3 | 0.019 | 0.0086 | 175° | 0.0025 |
| D2005 HVOF | WEAR PLATES | < 1% | OK | < 1% | 1003.4 | 10534 | .018/.006 | 0.0063 | 175° | 0.0003 |
| D2005 HVOF | WEAR PLATES | < 1% | OK | < 1% | 1044.3 | 10961.3 | .018/.006 | 0.0057 | 165° | 0.0025 |
| D3007 HVOF | FATIGUE | < 1% | OK | < 1% | 1046.2 | 10897 | 0.006 | 0.0041 | 240° | 0.0013 |
| D3007 HVOF | FATIGUE | < 1% | OK | < 1% | 905.3 | 10214 | 0.018 | Neutral | 340° | 0.0011 |
| D3007 HVOF | WEAR PLATES | < 1% | OK | < 1% | 853.4 | 9914.67 | .006/.018 | 0.0022 | 320° | 0.0015 |
| D3007 HVOF | WEAR PLATES | < 1% | OK | < 1% | 832.6 | 11165.5 | .006/.018 | 0.0061 | 275° | 0.0013 |
| D3007 HVOF | COROSION BAR | < 1% | OK | < 1% | 948.4 | 10940 | 0.018 | 0.0019 | 250° | 0.0013 |

**Table 4-23 GTE Coating Data for HVOF T-400 and T-800 Sprayed with Hydrogen**

| Coating | Specimen Type | Voids [%] | Interface [visual] | Oxides [%] | HV300 Micro Hard | Tensile [PSI] | Thick [inch] | Norm Almen Deflection | Max Temp [deg. F] | Depo Rate [inch per pass] |
|---|---|---|---|---|---|---|---|---|---|---|
| D3001 HVOF | FATIGUE | < 1% | OK | < 1% | 1079.1 | 10384 | .018/.006 | 0.007 | 318° | 0.00023 |
| D3001 HVOF | WEAR PLATES | < 1% | OK | < 1% | 559.4 | 5363.33 | .018/.006 | 0.0033 | 320° | 0.00023 |
| D3001 HVOF | FATIGUE | < 1% | OK | < 1% | 646.2 | 6154 | .018/.006 | 0.005 | 350° | 0.00023 |
| D3001 HVOF | FATIGUE | < 1% | OK | < 1% | 635.7 | 7799 | .018/.006 | 0.0098 | 315° | 0.00023 |
| D3001 HVOF | FATIGUE | < 1% | OK | < 1% | 644.7 | 6389 | .018/.006 | 0.0076 | 315° | 0.00023 |
| D3001 HVOF | WEAR PLATES | < 1% | OK | < 1% | 477.8 | 4699.33 | .018/.006 | 0.005 | 185° | 0.00023 |
| D3001 HVOF | COROSION BAR | < 1% | OK | < 1% | 555 | 6111 | .018/.006 | 0.0056 | 230° | 0.00023 |
| D3001 HVOF | WEAR PLATES | < 1% | OK | < 1% | 559.4 | 5363.33 | .018/.006 | 0.0033 | 215° | 0.00023 |
| D3002 HVOF | FATIGUE | < 1% | OK | < 1% | 928.2 | 10278 | 0.014 | 0.0054 | 170° | 0.00039 |
| D3002 HVOF | FATIGUE | < 1% | OK | < 1% | 1058.58 | 10834 | .006/.018 | 0.0062 | 170° | 0.00039 |
| D3002 HVOF | FATIGUE | < 1% | OK | < 1% | 1029.4 | 10321 | .006/.018 | 0.0062 | 190° | 0.00039 |
| D3002 HVOF | FATIGUE | < 1% | OK | < 1% | 690.1 | 8723 | .006/.018 | 0.0053 | 164° | 0.00039 |
| D3002 HVOF | FATIGUE | < 1% | OK | < 1% | 680.7 | 9135 | 0.018 | 0.0032 | 160° | 0.00039 |
| D3002 HVOF | FATIGUE | < 1% | OK | < 1% | 673.7 | 10406 | .006/.018 | 0.0039 | 180° | 0.00039 |
| D3002 HVOF | FATIGUE | < 1% | OK | < 1% | 954.5 | 10107 | .006/.018 | 0.0082 | 200° | 0.00039 |
| D3002 HVOF | WEAR PLATES | < 1% | OK | < 1% | 655.1 | 10000 | .006/.018 | 0.0044 | 250° | 0.00039 |
| D3002 HVOF | WEAR PLATES | < 1% | OK | < 1% | 575.2 | 10299.3 | .006/.018 | 0.0044 | 260° | 0.00039 |
| D3002 HVOF | COROSION BAR | < 1% | OK | < 1% | 625.8 | 9337.67 | .006/.018 | 0.0043 | 235° | 0.00039 |
| 66F PLASMA | FATIGUE | V2 | OK | X3 | 584 | 7009 | .006/.018 | 0.0013 | 280° | 0.00025 |
| 66F PLASMA | FATIGUE | V2 | OK | X3 | 817.4 | 5940 | 0.018 | -0.002 | 320° | 0.00022 |
| 66F PLASMA | COROSION BAR | V-1 | OK | X-2 / X-3 | 522 | 5684 | .006/.018 | -0.003 | 300° | 0.00018 |
| 66F PLASMA | WEAR PLATES | V-1 | OK | X-2 | 459 | 4850.33 | .006/.018 | -0.003 | 185° | 0.00054 |

**Table 4-24 Testing Data From the Natural Gas Spraying**

| Coating | Porosity [%] | Interface [visual] | Oxides [%] | HV300 Micro Hardness | 15N Macro Hardness | Tensile [PSI] | Thickness [inch] | Net Almen Deflection | Max Temp [deg. F] | Depo Rate [inch per pass] |
|---|---|---|---|---|---|---|---|---|---|---|
| D2005 HVOF | | | | | | | 0.006 | 0.0127 | 320 | 0.00028 |
| | | | | | | | 0.016 | 0.0188 | 320 | 0.00028 |
| | <1 | Clean, good bonding | <1 | 1000 | 92.52 | 12,585 | 0.015 | | 320 | 0.00028 |
| D3002 HVOF | | | | | | | 0.006 | 0.0063 | 255 | 0.00083 |
| | | | | | | | 0.016 | 0.0155 | 255 | 0.00083 |
| | 1.61 | Clean, good bonding | 2.97 | 685 | 85.7 | 8,963 | 0.011 | | 255 | 0.00083 |
| D 3001 HVOF | | | | | | | 0.006 | 0.006 | 230 | 0.0005 |
| | | | | | | | 0.016 | 0.015 | 230 | 0.0005 |
| | <1 | Clean, good bonding | 18.8 | 755 | 86.5 | 8,460 | 0.011 | | 230 | 0.0005 |
| D3007 HVOF | | | | | | | 0.006 | 0.0062 | 270 | 0.0003 |
| | | | | | | | 0.016 | 0.0144 | 270 | 0.0003 |
| | | | | | | 10,364 | 0.011 | | 270 | 0.0003 |
| | <1 | Clean, good bonding | 22.2 | 938 | 92.4 | | 0.011 | | 270 | 0.0003 |

## 4.4.6. Lessons Learned-Almen Strip and Temperature Measurement Procedures

During coating optimization work in HCAT, Almen strip and substrate temperature measurement were identified as two of the more critical areas for process control. In the initial HVOF trials, it was assumed that these measurements were well defined and would not create any inconsistencies. Subsequent experience has shown that this is not the case.

Almen strip results were found to be strongly influenced by preparation and spraying methods, leading to large systematic differences between spray sites. Factors to consider are:

- *Grit blasting of one side vs. both sides of the strip* This can result in a 0.003”-0.004” difference in Almen results when spraying.
- *Orientation of the strip (i.e. torch traverse along or across the strip* This can result in a 0.001”-0.002” difference in Almen results when spraying.
- *Cleaning of Almen block* If not performed properly and frequently, coating will build

up on the block, preventing proper thermal contact and leading to improper readings

- *Reduction in Almen Response with Increasing Thickness* As thickness increases, the Almen response appears to level off. Another Almen strip type may be required for more substantial deflections
- *Normalized Almen Values* Based upon the issue of thickness, many initial values have been reported for the .003-.005" thickness range due to interest in those areas. However, values for Almen response can vary even over a .002" range. HCAT has therefore defined Almen stress as the value measured on a 0.005" thick coating.

To summarize, the correct procedure is to grit blast both sides, spray across the longitudinal direction, and normalize all Almen spraying to 0.005" nominal coating thickness.

It is common practice in many spray shops to measure substrate temperature with a contact probe at the end of the spray run. This approach provides no information on the true temperature excursions that occur during spraying. The HCAT team therefore adopted the approach of continuous infrared temperature measurement during spraying.

For substrate temperature measurement, the following issues have been identified:

- *Use of real time measurement vs. touch probe* Temperatures can be as much as 100 ºF higher with instantaneous measurement (IR pyrometer) vs. touch probe after all spraying is complete.
- *Spot size of IR system* When spraying small test bars (as was required for this project), the spot size is normally bigger than the specimen diameter. This requires a compensation factor when spraying test bars. If the actual reading is used, it will give a false indication which is lower than the actual bar value and substrate overheating may result.
- *Co-ordination of touch probes and IR system via emissivity corrections* As stated earlier, temperatures can be as much as 100 degrees hotter with instantaneous measurement (IR pyrometer) vs. touch probe after all spraying is complete. The IR unit must therefore be calibrated to define an emissivity setting that can be used as a default value. Although the IR system may not be an exact value, it can be used as a conservative guideline to control the process.

The correct procedure is therefore to require instantaneous temperature measurement via an IR pyrometer. Varied techniques are allowed but this must be verified and calibrated against touch probe data.

A complete guideline for Almen Strip/Substrate Temperature measurement can be found on the relevant specification document on the HCAT web site [8].

## 4.4.7. Discussion

### 4.4.7.1. Information from Full DOE Analyses

Although the full DOE work was not performed on all the GTE coatings, the lessons learned in full DOE analyses were again illustrated in the limited DOE work and the combined trends are summarized in Table 4-25.

- The primary effects are not unexpected for the substrate temperature and Almen values as the amount of combustion gas will drive the achievable flame temperature, while spray distance (end of nozzle to part) will have a substantial effect on how much of that heat input is transferred to the part.

- The secondary effects of nozzle and powder size are controlled by a standard choice for each of these parameters. When selected, these variables will be fixed but powder size must still be a part of the troubleshooting guide if size/particle distribution issues are identified at the powder vendor.

**Table 4-25 Primary and Secondary Determinants of Coating Properties.**

| Property | Primary | Secondary |
|---|---|---|
| Almen | Combustion Gas<br>Spray Distance | Nozzle<br>Powder size |
| Microhardness | Combustion Gas<br>Spray Distance | Powder size |
| Substrate temperature | Combustion Gas<br>Spray Distance | Nozzle |

As stated earlier, the spray parameter sets must be well characterized and documented to achieve repeatable results. The pedigree of the optimized spray parameters is also a very critical consideration. It has been stressed in this section that fatigue was chosen as the most important factor for HCAT coating optimization.

### 4.4.8. Conclusions

The HVOF and plasma processes were successfully implemented for the majority of the GTE coatings, meeting the necessary quality control requirements. Natural gas parameters were also developed for the HVOF materials. However, further optimization may also be necessary for the HVOF T-800, HVOF $Cr_3C_2$/20NiCr, and plasma T-400.

For plasma WC/17Co, with the time and manpower available, a compressive residual stress could not be obtained for this material type. Further work may be performed to understand if a compressive stress can actually be obtained with plasma WC/17Co.

.

## 4.5. Fatigue Data

### 4.5.1. Data Summary

**Table 4-26. Quick Reference to Primary Data. Click Blue Links to Jump to Data.**

| Item | Item Number |
|---|---|
| Fatigue testing variables | Table 4-27 |
| Materials evaluated for fatigue testing | Table 4-28 |
| Fatigue test matrix | $H_2$ fuel Table 4-31, Natural gas Table 4-32 |
| IN-718 | Figure 4-11 to Figure 4-15; NG Figure 4-40, Figure 4-43 |
| A-286 | Figure 4-16 to Figure 4-19 |
| AMS-355 | Figure 4-20 to Figure 4-23; NG Figure 4-44, Figure 4-45 |
| 9310 | Figure 4-24 to Figure 4-26 |
| IN-901 | Figure 4-27 to Figure 4-31 |
| 4340 | Figure 4-32 to Figure 4-35; NG Figure 4-47, Figure 4-46 |
| 17-4PH | Figure 4-34 to Figure 4-39 |

### 4.5.2. Test Rationale

Fatigue is a very critical property in the aerospace industry, because of the repeated cyclic loading for landing gear, actuators, airframe parts, and gas turbine engine components. There is an extensive amount of fatigue data on alloys that are used in gas turbine engines. When coatings are applied to the alloys, the evaluation of fatigue essentially is the analysis of how the application of the coating affects the fatigue strength of the alloy, i.e., a comparison is made between the cycles-to-failure at selected stress/strain values for coated and uncoated specimens. It is generally recognized that when EHC is applied to most alloys used in gas turbine engines the fatigue strength will be reduced because there are microcracks and residual tensile stresses in the coatings.

Although plasma spray processes have seen widespread use in the aerospace industry for many years, they have tended to be limited to non-fatigue-critical applications, largely due to the heat input of the process and tensile coating stresses. The commercial development of the HVOF process, which relies more on kinetic than thermal energy for final coating properties and permits compressive coating stress, has started to move the design community towards thermal spray in fatigue-driven components. Since fatigue performance is driven by material strength and is especially related to near-surface effects, fatigue-critical applications require careful definition and control of the thermal spray process such that: (1) the coatings are deposited in a state of residual compressive stress which will tend to reduce crack propagation and thus minimize any fatigue debit associated with the coating application, and (2) deposition of the coatings is performed with a minimum of surface heating so as to prevent a loss of mechanical properties.

Since there are several different types of fatigue tests, it is essential to define the one that best represents the conditions that a gas turbine engine component would encounter in service. For most chrome-replacement testing to date in other projects (e.g., landing gear), axial fatigue testing (ASTM E466-96), as opposed to bend testing, has provided the most useful data for evaluation. This was also considered the case for testing in this project since axial fatigue testing has been conducted in the majority of previous measurements on uncoated alloys.

In designing the fatigue tests, there were other considerations in addition to type of test:

Specimen Geometry. In axial fatigue testing there are two principal geometries:

- Hourglass: The gage section has a smoothly varying cross section, with the minimum diameter (and thus maximum stress) confined to one location at the center of the specimen. For testing coated hourglass specimens, the coating will obviously be applied at and adjacent to the point of minimum diameter and this will virtually ensure that the failure will occur under the coating.
- Smooth Gage Section: The gage section has a constant cross-sectional area over a specified length at the center of the specimen. Thus, the maximum stress is distributed over this length. Because this is the most prevalent geometry selected for gas turbine engine evaluations (as specified in MIL-HDBK-5 [9]), it was selected for the testing in this project. It was also decided that the coating would not be applied over the entire constant-diameter section of the specimen which would allow for failure to occur in either the coated or uncoated portion.

Number of cycles and type of control (load or strain). The need for low-cycle-fatigue (LCF) testing in GTE applications is driven by design consideration for the number of engine take-off/landing cycles. During this time period, engine parts experience the most severe loading environment of very high constant strain and can exhibit failure in a low number of cycles. In this type of control mode, the load will actually drop as the specimen begins to fail to maintain the constant strain condition. An extensometer is used during testing to ensure that constant strain is maintained. The need for high-cycle-fatigue (HCF) testing in GTE applications, in conjunction with the LCF studies, is driven by components which experience a high number of cycles during extended flight times. With HCF, the critical element is not strain but a constant load – thus the term "load control". In contrast to strain control, an extensometer is not used and the load is the same through the test and into the failure regime. For this project, it was decided to conduct both LCF testing under strain control and HCF testing under load control.

Stress/Strain Ratios. The maximum and minimum values of stress (in load control) or strain (in strain control) testing must be determined. In axial fatigue testing, it is possible to conduct tests in which the specimen is placed only in tension or in which the specimen is placed in both tension and compression. The stress or strain ratios can be expressed in terms of R values or A values where:

R ratio is defined as *min load or strain / max load or strain*

A ratio is defined as *alternating load or strain / mean load or strain*

where alternating is *( max – min ) / 2*

mean is *( max + min ) / 2*

Hence

$$A = \frac{1-R}{1+R} \quad \text{and} \quad R = \frac{1-A}{1+A}$$

Because of the types of stresses encountered by most gas turbine engine components, the fatigue test specimens in this project were only subjected to tensile stresses. Exact parameters are given in Section 3.5.

## 4.5.3. Specimen Fabrication

### 4.5.3.1. Specimen Geometry and Materials

The alloys selected for fatigue testing were indicated in Table 4-4 (note that only HVOF coatings were fatigue tested as APS coatings could not be deposited with compressive residual stress). These substrate materials are not readily available or generally used in the same form for the fabrication of gas turbine engine components. Based on discussions with representatives of the GTE OEM community and a review of potential applications for thermal spray coatings on GTE components, it was determined that some alloys would be acquired as round bar and some would be acquired as forgings as indicated in Table 4-27. The heat treat condition for all alloys was indicated in Table 4-3.

**Table 4-27 Material Forms**

| Material Form | Alloy | Comments |
|---|---|---|
| Round bar | IN-901, 17-4PH, 4340, 9310 | Same lot<br>Single furnace load |
| Forgings | IN-718, A-286, AM-355** | Single forging<br>Same billet heat |

** Material came from multiple forgings

For the fatigue specimen configuration, a 250”-diameter smooth gage specimen was selected as indicated in Figure 4-8. The length of the constant-diameter gage section was 0.75”.

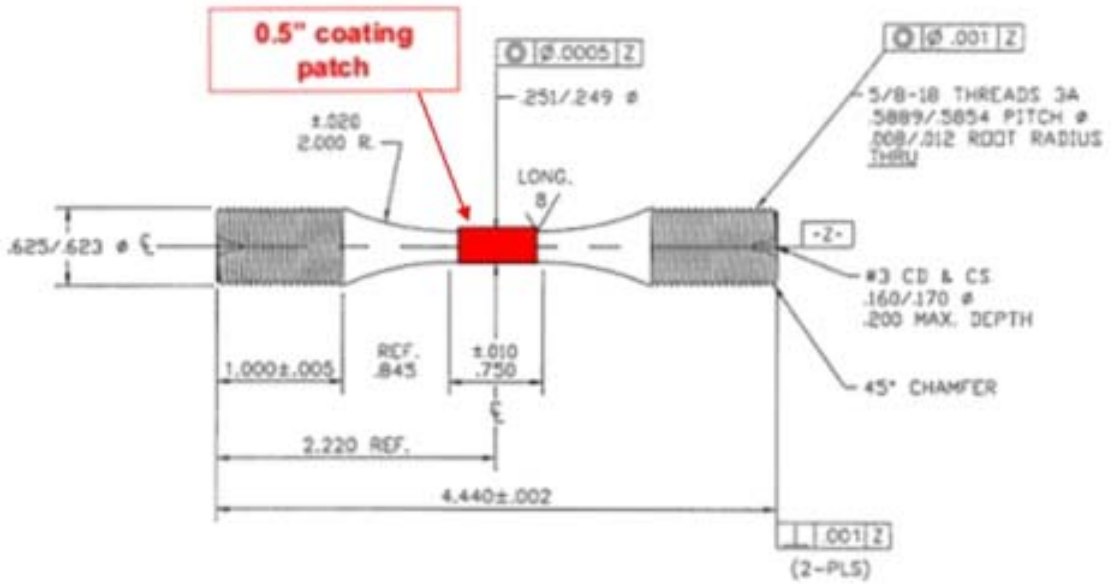


**Figure 4-8 Smooth Bar Fatigue Specimen.**

#### 4.5.3.2. Specimen Preparation

Fatigue performance is to a large degree driven by the surface condition of the specimen. This is especially critical for this project since it is an investigation of the effect of coatings on baseline properties. It is therefore essential to produce a consistent machined surface to reduce fatigue test data scatter.

To achieve a repeatable fatigue specimen, there are three major steps in the fabrication process:

- Rough grinding
- Finish grinding
- Final polishing

For the GTE specimens, both the rough and finish grinding were performed to MIL-STD-866 and GEAE word drawing 4013195-990 (which defines low stress or finish grinding). Low stress grinding involves the use of documented lubricant/grinding wheel/in-feed combinations that result in a thin layer of compressive residual stress at the surface. With this grinding methodology, a consistent surface is produced and the results represent a true analysis of material fatigue performance.

After grinding, the samples were polished in the longitudinal direction using a 320/400/600 grit paper combination to remove a minimum of 0.001" on all gages. This step was necessary to remove the circumferential grinding marks and produce the low-stress surface conditions.

Given the extensive use of shot peening in OEM applications, the majority of the specimens in this protocol were shot peened as part of the sample fabrication process (baseline data without shot peening the specimens was also obtained). Two separate shot peening steps were performed. For the actual gage area where the coating was applied, shot peening via computer control was conducted to AMS-2432 with cut wire and 100% surface coverage. To prevent thread failures during testing, the threaded areas were peened with S7 steel shot (average diameter of .007") to ensure at least 50% coverage in the thread roots.

The fabrication of the fatigue specimens was such that it would be possible to repeatedly grind coatings that had been deposited to produce a consistent thickness for testing.

### 4.5.4. Coating Deposition Methodology

For this protocol, EHC, plasma and HVOF thermal spray coatings were applied to the fatigue specimens. Prior to application of the coatings, each specimen was grit blasted using the media and conditions as indicated in Table 4-28. The grit blasting was carried out not more than 2 hours prior to plating or coating.

**Table 4-28 Grit Blasting**

| | Media | Stand-off |
|---|---|---|
| Prior to chrome plating | #13 glass beads<br>or<br>220 grit aluminum oxide ( QQ-C-320) | 4-6 “ |
| Prior to thermal spray coating | 54 grit aluminum oxide<br>MIL-STD-1504 | 4-6”<br>60 psi<br>45 angle |

**EHC Plating**

To best represent a hard chrome baseline, especially at a depot site, the EHC plating was done at NADEP JAX to the guidelines of MIL-STD-1501C, Class 1, Type 1. All of the fatigue specimens were solvent wiped with reagent grade acetone and/or isopropyl alcohol prior to plating. The electroplating was applied in a patch 0.5” long centered on the middle of the bar (see Figure 4-8) and feathered at the patch ends to limit stress concentrations. The final thickness values for plating were 0.003” and 0.015” ± 0.0005” with the as-deposited values approximately 0.002” to 0.004” thicker than specified for grinding to final dimension. No interfacial layer or sealer was applied in deposition of the EHC. Specimens were given a typical hydrogen bake for 24 hrs at 350 ± 25 $^{o}$F within 4 hrs of plating.

**Thermal Spray**

As summarized in Section 2 on Coating Optimization, final coating deposition conditions were established via Design of Experiment (DOE) studies either in the current GTE effort or in previous HCAT programs. This analysis was performed for both the plasma and HVOF coatings. For the plasma WC/Co, an optimized parameter set to obtain a neutral or compressive residual stress could not be developed; this coating was therefore dropped from the testing protocol. Table 4-30 summarizes the thermal spray system used, and the coating method for each type of coating.

With the thermal spray deposition, a number of special considerations were necessary:

- Maximum surface temperature did not exceed 350 $^{o}$F for all alloys (except 9310, which was kept below 300 $^{o}$F), as measured by an optical pyrometer.
- The fatigue bar specimens were coated individually while rotating on-axis and being traversed parallel to the length.

**Table 4-29 Coating Methods**

| System | Vendor | Method | Coatings |
|---|---|---|---|
| Sulzer HVOF DJ 2600 | Hitemco Westbury, NY | HVOF Hydrogen | WC/17Co, T-800, T-400, $Cr_2C_3$/20NiCr |
| Sulzer HVOF DJ 2600 | Sulzer Westbury, NY | HVOF Natural gas | WC/17Co, T-800, T-400, $Cr_2C_3$/20NiCr |
| Sulzer Plasma 3M | Hitemco Westbury, NY | Plasma | T-400 |

- A pair of shadow masks restricted coating deposition to the desired 0.5"-long region centered in the gage section and ensured proper feathering of the patch ends.
- Tape masking restricted grit blasting and the coating overspray area to a slightly wider area (0.6" maximum)
- For process control in this protocol, Almen strips were sprayed to monitor the presence of the desired compressive residual stress in the deposit. All HVOF coatings were sprayed to an Almen of 4 to 12 compressive and the plasma T-400 coatings were sprayed to an Almen of 0 to -2 tensile.

As with chrome, the final thickness values for the coatings were 0.003" and 0.015" ± 0.0005" with the as-deposited values approximately 0.002" to 0.004" thicker than specified for grinding to final dimension. The grinding of the coatings followed the procedures specified in AMS 2449. Even with low-stress grinding techniques applied, it is still possible that the grinding could introduce additional stresses into the coating which could affect fatigue performance. In service, almost all HVOF coatings will be ground and therefore it was important to use the same grinding techniques as would be used on actual components so that the fatigue data would be representative of those situations.

### 4.5.5. Test Methodology

The axial low cycle fatigue (LCF) test used in this protocol was a strain-controlled constant total strain (elastic strain + plastic strain) methodology in accordance with ASTM E606. A 5/8" extensometer clipped directly to the uncoated gage at points just beyond each end of the 0.5" coating patch was used for the strain control measurement. The strain controlled tests were conducted at a frequency of 0.5 Hz for the first 24 hours or until the work hardening hysteresis loop stabilized, whichever was longer, and then switched to load control at 5 Hz until failure or runout at $10^5$ cycles. The input strain waveform was triangular and the strain rate for each given test was the result of the total strain value and the frequency. Figure 4-9 shows the specimen configuration for LCF testing.

The axial high cycle fatigue (HCF) test used in this protocol was a load-controlled constant amplitude methodology in accordance with ASTM E466. HCF runout was defined at $10^7$ cycles. Figure 4-10 shows the specimen `configuration for HCF testing.

The test parameters are given in Table 4-30.

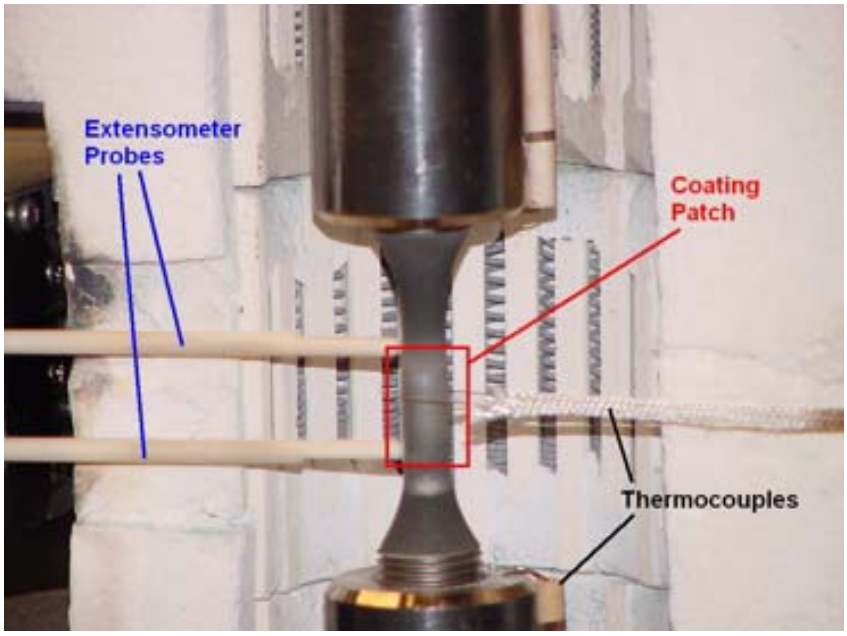


**Figure 4-9 Low Cycle (LCF) Fatigue Set-up**

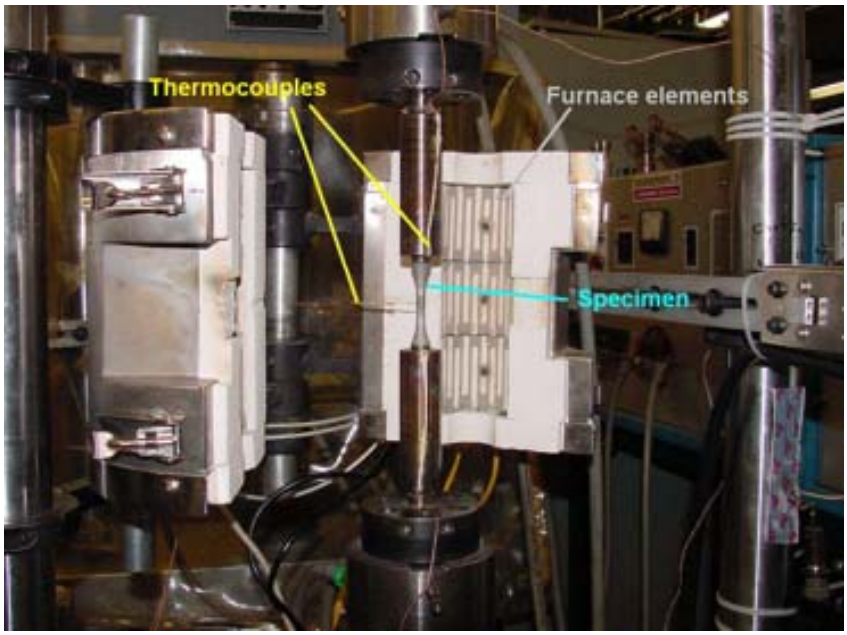


**Figure 4-10 High Cycle Fatigue (HCF) Set-up**

The two temperatures selected for testing reflected the range of temperatures encountered by EHC-coated components in gas turbine engines. The rationale for the two control modes utilized was given in Section 4.5.2. The cyclic frequency for applying the stresses or strains to the specimens was selected to ensure that overheating did occur that could impact the results. The entire fatigue test matrix is given in Table 4-31 except for HVOF coatings deposited using natural gas where the test matrix is given in Table 4-32.

After testing, the data were plotted in the standard manner with stress on the vertical axis and cycles-to-failure on the horizontal axis (designated an S/N plot). For all of the coated specimens, stress was calculated based on the uncoated gage diameter of 0.25". A least-squares curve was fit to the EHC data points to establish a baseline and then least-squares curves were fit to the thermal spray data points. If the data points from the thermal spray coatings fell on or above the curves for the EHC, then the thermal spray coatings were considered to have met the acceptance criteria.

**Table 4-30 Fatigue Test Parameters**

| **Parameter** | **Value** |
|---|---|
| *Environment* | 300 and 750 $^{o}$F in air |
| *Control modes* | *Strain control*<br>*Low cycle fatigue (LCF)*<br>A ratio of 0.95<br>or<br>R ratio of 0.026<br>Frequency of 0.5-5.0 Hz<br>Triangular input strain waveform |
| | *Load control*<br>*High cycle fatigue (HCF)*<br>A ratio of 0.5<br>or<br>R ratio of 0.33<br>Frequency of 5-59 Hz<br>Sine wave load input signal |
| *Number of specimens* | 10 uncoated baseline per alloy<br>6 coated per alloy/coating combination<br>Minimum of 3 stress levels per group<br>Select stress levels to fit curves |

## Table 4-31 Fatigue Test Matrix, HVOF by Hydrogen Process

| ALLOY | PEEN | COATING | THICKNESS (inches) | A-RATIO (LCF or HCF) | TEST TEMP. (Deg. F) | NO. SPECIMENS |
|---|---|---|---|---|---|---|
| IN-718 | No | None | NA | 0.95 | 300 | 10 |
| IN-718 | Yes | None | NA | 0.95 | 300 | 10 |
| IN-718 | Yes | EHC | 0.015 | 0.95 | 300 | 6 |
| IN-718 | Yes | HVOF WC/17Co | 0.015 | 0.95 | 300 | 6 |
| IN-718 | Yes | HVOF $Cr_3C_2$-20NiCr | 0.015 | 0.95 | 300 | 6 |
| IN-718 | Yes | HVOF Tribaloy 800 | 0.015 | 0.95 | 300 | 6 |
| IN-718 | Yes | HVOF Tribaloy 400 | 0.015 | 0.95 | 300 | 6 |
| IN-718 | Yes | PS Tribaloy 400 | 0.015 | 0.95 | 300 | 6 |
| IN-718 | Yes | EHC | 0.015 | *0.5* | 300 | 6 |
| IN-718 | Yes | HVOF WC/17Co | 0.015 | *0.5* | 300 | 6 |
| IN-718 | Yes | HVOF $Cr_3C_2$-20NiCr | 0.015 | 0.5 | 300 | 6 |
| IN-718 | Yes | HVOF Tribaloy 800 | 0.015 | *0.5* | 300 | 6 |
| IN-718 | Yes | HVOF Tribaloy 400 | 0.015 | *0.5* | 300 | 6 |
| IN-718 | Yes | PS Tribaloy 400 | 0.015 | *0.5* | 300 | 6 |
| IN-718 | No | None | NA | 0.95 | 750 | 10 |
| IN-718 | Yes | None | NA | 0.95 | 750 | 10 |
| IN-718 | Yes | EHC | 0.015 | 0.95 | 750 | 6 |
| IN-718 | Yes | HVOF WC/17Co | 0.015 | 0.95 | 750 | 6 |
| IN-718 | Yes | HVOF $Cr_3C_2$-20NiCr | 0.015 | 0.95 | 750 | 6 |
| IN-718 | Yes | HVOF Tribaloy 800 | 0.015 | 0.95 | 750 | 6 |
| IN-718 | Yes | HVOF Tribaloy 400 | 0.015 | 0.95 | 750 | 6 |
| IN-718 | Yes | PS Tribaloy 400 | 0.015 | 0.95 | 750 | 6 |
| IN-718 | Yes | EHC | *0.003* | 0.95 | 750 | 6 |
| IN-718 | Yes | HVOF WC/17Co | *0.003* | 0.95 | 750 | 6 |
| IN-718 | Yes | HVOF $Cr_3C_2$-20NiCr | *0.003* | 0.95 | 750 | 6 |
| IN-718 | Yes | HVOF Tribaloy 800 | *0.003* | 0.95 | 750 | 6 |
| IN-718 | Yes | HVOF Tribaloy 400 | *0.003* | 0.95 | 750 | 6 |
| IN-718 | Yes | PS Tribaloy 400 | *0.003* | 0.95 | 750 | 6 |
| **IN-718 Total** | | | | | | **184** |
| | | | | | | |
| A-286 | No | None | NA | 0.95 | 300 | 10 |
| A-286 | Yes | None | NA | 0.95 | 300 | 10 |
| A-286 | Yes | EHC | 0.015 | 0.95 | 300 | 6 |
| A-286 | Yes | HVOF WC/17Co | 0.015 | 0.95 | 300 | 6 |
| A-286 | Yes | HVOF Tribaloy 400 | 0.015 | 0.95 | 300 | 6 |
| A-286 | Yes | PS Tribaloy 400 | 0.015 | 0.95 | 300 | 6 |
| A-286 | Yes | EHC | 0.015 | *0.5* | 300 | 6 |
| A-286 | Yes | HVOF Tribaloy 400 | 0.015 | *0.5* | 300 | 6 |
| A-286 | Yes | PS Tribaloy 400 | 0.015 | *0.5* | 300 | 6 |
| A-286 | No | None | NA | 0.95 | 750 | 10 |
| A-286 | Yes | None | NA | 0.95 | 750 | 10 |

**Table 4-31 continued -1**

| ALLOY | PEEN | COATING | THICKNESS (inches) | A-RATIO (LCF or *HCF*) | TEST TEMP. (Deg. F) | NO. SPECIMENS |
|---|---|---|---|---|---|---|
| A-286 | Yes | EHC | 0.015 | 0.95 | 750 | 6 |
| A-286 | Yes | HVOF WC/17Co | 0.015 | 0.95 | 750 | 6 |
| A-286 | Yes | HVOF Tribaloy 400 | 0.015 | 0.95 | 750 | 6 |
| A-286 | Yes | PS Tribaloy 400 | 0.015 | 0.95 | 750 | 6 |
| A-286 | Yes | EHC | *0.003* | 0.95 | 750 | 6 |
| A-286 | Yes | HVOF Tribaloy 400 | *0.003* | 0.95 | 750 | 6 |
| A-286 | Yes | PS Tribaloy 400 | *0.003* | 0.95 | 750 | 6 |
| **A-286 Total** | | | | | | **124** |
| | | | | | | |
| AM-355 | No | None | NA | 0.95 | 300 | 10 |
| AM-355 | Yes | None | NA | 0.95 | 300 | 10 |
| AM-355 | Yes | EHC | 0.015 | 0.95 | 300 | 6 |
| AM-355 | Yes | HVOF WC/17Co | 0.015 | 0.95 | 300 | 6 |
| AM-355 | Yes | HVOF Tribaloy 400 | 0.015 | 0.95 | 300 | 6 |
| AM-355 | Yes | PS Tribaloy 400 | 0.015 | 0.95 | 300 | 6 |
| AM-355 | Yes | EHC | 0.015 | *0.5* | 300 | 6 |
| AM-355 | Yes | HVOF WC/17Co | 0.015 | *0.5* | 300 | 6 |
| AM-355 | Yes | PS Tribaloy 400 | 0.015 | *0.5* | 300 | 6 |
| AM-355 | No | None | NA | 0.95 | 750 | 10 |
| AM-355 | Yes | None | NA | 0.95 | 750 | 10 |
| AM-355 | Yes | EHC | 0.015 | 0.95 | 750 | 6 |
| AM-355 | Yes | HVOF WC/17Co | 0.015 | 0.95 | 750 | 6 |
| AM-355 | Yes | HVOF Tribaloy 400 | 0.015 | 0.95 | 750 | 6 |
| AM-355 | Yes | PS Tribaloy 400 | 0.015 | 0.95 | 750 | 6 |
| AM-355 | Yes | EHC | *0.003* | 0.95 | 750 | 6 |
| AM-355 | Yes | HVOF WC/17Co | *0.003* | 0.95 | 750 | 6 |
| AM-355 | Yes | PS Tribaloy 400 | *0.003* | 0.95 | 750 | 6 |
| **AM-355 TOTAL** | | | | | | **124** |
| | | | | | | |
| 9310 | No | None | NA | 0.95 | 300 | 10 |
| 9310 | Yes | None | NA | 0.95 | 300 | 10 |
| 9310 | Yes | EHC | 0.015 | 0.95 | 300 | 6 |
| 9310 | Yes | HVOF WC/17Co | 0.015 | 0.95 | 300 | 6 |
| 9310 | Yes | HVOF Tribaloy 400 | 0.015 | 0.95 | 300 | 6 |
| 9310 | Yes | PS Tribaloy 400 | 0.015 | 0.95 | 300 | 6 |
| 9310 | Yes | EHC | 0.015 | *0.5* | 300 | 6 |
| 9310 | Yes | HVOF WC/17Co | 0.015 | *0.5* | 300 | 6 |
| 9310 | Yes | EHC | *0.003* | *0.5* | 300 | 6 |
| 9310 | Yes | Plasma WC/17Co | *0.003* | *0.5* | 300 | 6 |
| 9310 | Yes | HVOF WC/17Co | *0.003* | *0.5* | 300 | 6 |
| **9310 Total** | | | | | | **78** |
| | | | | | | |
| IN-901 | No | None | NA | 0.95 | 300 | 10 |
| IN-901 | Yes | None | NA | 0.95 | 300 | 10 |
| IN-901 | Yes | EHC | 0.015 | 0.95 | 300 | 6 |
| IN-901 | Yes | HVOF WC/17Co | 0.015 | 0.95 | 300 | 6 |
| IN-901 | Yes | HVOF Tribaloy 800 | 0.015 | 0.95 | 300 | 6 |

**Table 4-31 continued - 2**

| ALLOY | PEEN | COATING | THICKNESS (inches) | A-RATIO (LCF or *HCF*) | TEST TEMP. (Deg. F) | NO. SPECIMENS |
|---|---|---|---|---|---|---|
| IN-901 | Yes | HVOF Tribaloy 400 | 0.015 | 0.95 | 300 | 6 |
| IN-901 | Yes | HVOF Cr3C2-NiCr | 0.015 | 0.95 | 300 | 6 |
| IN-901 | Yes | PS Tribaloy 400 | 0.015 | 0.95 | 300 | 6 |
| IN-901 | Yes | EHC | 0.015 | *0.5* | 300 | 6 |
| IN-901 | Yes | HVOF WC/17Co | 0.015 | *0.5* | 300 | 6 |
| IN-901 | Yes | HVOF Tribaloy 800 | 0.015 | *0.5* | 300 | 6 |
| IN-901 | Yes | HVOF Tribaloy 400 | 0.015 | *0.5* | 300 | 6 |
| IN-901 | Yes | HVOF Cr3C2-NiCr | 0.015 | *0.5* | 300 | 6 |
| IN-901 | Yes | PS Tribaloy 400 | 0.015 | *0.5* | 300 | 6 |
| IN-901 | No | None | NA | 0.95 | 750 | 10 |
| IN-901 | Yes | None | NA | 0.95 | 750 | 10 |
| IN-901 | Yes | EHC | 0.015 | 0.95 | 750 | 6 |
| IN-901 | Yes | HVOF WC/17Co | 0.015 | 0.95 | 750 | 6 |
| IN-901 | Yes | HVOF Tribaloy 800 | 0.015 | 0.95 | 750 | 6 |
| IN-901 | Yes | HVOF Tribaloy 400 | 0.015 | 0.95 | 750 | 6 |
| IN-901 | Yes | HVOF Cr3C2-NiCr | 0.015 | 0.95 | 750 | 6 |
| IN-901 | Yes | PS Tribaloy 400 | 0.015 | 0.95 | 750 | 6 |
| IN-901 | Yes | EHC | *0.003* | 0.95 | 750 | 6 |
| IN-901 | Yes | HVOF WC/17Co | *0.003* | 0.95 | 750 | 6 |
| IN-901 | Yes | HVOF Tribaloy 800 | *0.003* | 0.95 | 750 | 6 |
| IN-901 | Yes | HVOF Tribaloy 400 | *0.003* | 0.95 | 750 | 6 |
| IN-901 | Yes | HVOF Cr3C2-NiCr | *0.003* | 0.95 | 750 | 6 |
| IN-901 | Yes | PS Tribaloy 400 | *0.003* | 0.95 | 750 | 6 |
| **IN-901 Total** | | | | | | **184** |
| | | | | | | |
| 4340 | No | None | NA | 0.95 | 300 | 10 |
| 4340 | Yes | None | NA | 0.95 | 300 | 10 |
| 4340 | Yes | EHC | 0.015 | 0.95 | 300 | 6 |
| 4340 | Yes | HVOF WC/17Co | 0.015 | 0.95 | 300 | 6 |
| 4340 | Yes | HVOF $Cr_3C_2$-20NiCr | 0.015 | 0.95 | 300 | 6 |
| 4340 | Yes | HVOF Tribaloy 400 | 0.015 | 0.95 | 300 | 6 |
| 4340 | Yes | PS Tribaloy 400 | 0.015 | 0.95 | 300 | 6 |
| 4340 | Yes | EHC | *0.003* | 0.95 | 300 | 6 |
| 4340 | Yes | HVOF WC/17Co | *0.003* | 0.95 | 300 | 6 |
| 4340 | Yes | PS Tribaloy 400 | *0.003* | 0.95 | 300 | 6 |
| 4340 | No | None | NA | *0.5* | 300 | 10 |
| 4340 | Yes | None | NA | *0.5* | 300 | 10 |
| 4340 | Yes | EHC | 0.015 | *0.5* | 300 | 6 |
| 4340 | Yes | HVOF WC/17Co | 0.015 | *0.5* | 300 | 6 |
| 4340 | Yes | HVOF $Cr_3C_2$-20NiCr | 0.015 | 0.5 | 300 | 6 |
| 4340 | Yes | PS Tribaloy 400 | 0.015 | *0.5* | 300 | 6 |
| 4340 | Yes | EHC | *0.003* | *0.5* | 300 | 6 |
| 4340 | Yes | HVOF WC/17Co | *0.003* | *0.5* | 300 | 6 |
| 4340 | Yes | PS Tribaloy 400 | *0.003* | *0.5* | 300 | 6 |

**Table 4-31 continued - 3**

| ALLOY | PEEN | COATING | THICKNESS (inches) | A-RATIO (LCF or *HCF*) | TEST TEMP. (Deg. F) | NO. SPECIMENS |
|---|---|---|---|---|---|---|
| | | | | | | |
| 17-4PH | No | None | NA | 0.95 | 300 | 10 |
| 17-4PH | Yes | None | NA | 0.95 | 300 | 10 |
| 17-4PH | Yes | EHC | 0.015 | 0.95 | 300 | 6 |
| 17-4PH | Yes | HVOF WC/17Co | 0.015 | 0.95 | 300 | 6 |
| 17-4PH | Yes | HVOF Tribaloy 800 | 0.015 | 0.95 | 300 | 6 |
| 17-4PH | Yes | HVOF Tribaloy 400 | 0.015 | 0.95 | 300 | 6 |
| 17-4PH | Yes | PS Tribaloy 400 | 0.015 | 0.95 | 300 | 6 |
| 17-4PH | Yes | EHC | 0.015 | *0.5* | 300 | 6 |
| 17-4PH | Yes | HVOF WC-17C | 0.015 | *0.5* | 300 | 6 |
| 17-4PH | Yes | HVOF Tribaloy 800 | 0.015 | *0.5* | 300 | 6 |
| 17-4PH | Yes | HVOF Tribaloy 400 | 0.015 | *0.5* | 300 | 6 |
| 17-4PH | Yes | PS Tribaloy 400 | 0.015 | *0.5* | 300 | 6 |
| 17-4PH | No | None | NA | 0.95 | 750 | 10 |
| 17-4PH | Yes | None | NA | 0.95 | 750 | 10 |
| 17-4PH | Yes | EHC | 0.015 | 0.95 | 750 | 6 |
| 17-4PH | Yes | HVOF WC/17Co | 0.015 | 0.95 | 750 | 6 |
| 17-4PH | Yes | HVOF Tribaloy 800 | 0.015 | 0.95 | 750 | 6 |
| 17-4PH | Yes | HVOF Tribaloy 400 | 0.015 | 0.95 | 750 | 6 |
| 17-4PH | Yes | PS Tribaloy 400 | 0.015 | 0.95 | 750 | 6 |
| 17-4PH | Yes | EHC | *0.003* | 0.95 | 750 | 6 |
| 17-4PH | Yes | HVOF WC/17Co | *0.003* | 0.95 | 750 | 6 |
| 17-4PH | Yes | HVOF Tribaloy 800 | *0.003* | 0.95 | 750 | 6 |
| 17-4PH | Yes | HVOF Tribaloy 400 | *0.003* | 0.95 | 750 | 6 |
| 17-4PH | Yes | PS Tribaloy 400 | *0.003* | 0.95 | 750 | 6 |
| **17-4PH Total** | | | | | | **160** |
| **GRAND TOTAL** | | | | | | **988** |

**Table 4-32 Fatigue Test Matrix, all HVOF by Natural Gas Process**

| ALLOY | PEEN | COATING | THICKNESS (inches) | A-RATIO (LCF or HCF) | TEST TEMP. (Deg. F) | NO. SPECIMENS |
|---|---|---|---|---|---|---|
| IN-718 | Yes | WC/17Co | .015 | .95 | 300 | 5 |
| IN-718 | Yes | $Cr_3C_2$-20NiCr | .015 | .95 | 300 | 5 |
| IN-718 | Yes | Tribaloy 400 | .015 | .95 | 300 | 5 |
| IN-718 | Yes | Tribaloy 800 | .015 | .95 | 300 | 5 |
| IN-718 | Yes | WC/17Co | .015 | .5 | 300 | 5 |
| IN-718 | Yes | $Cr_3C_2$-20NiCr | .015 | .5 | 300 | 5 |
| IN-718 | Yes | Tribaloy 400 | .015 | .5 | 300 | 5 |
| IN-718 | Yes | Tribaloy 800 | .015 | .5 | 300 | 5 |
| IN-718 | Yes | WC/17Co | .015 | .95 | 750 | 5 |
| IN-718 | Yes | $Cr_3C_2$-20NiCr | .015 | .95 | 750 | 5 |
| IN-718 | Yes | Tribaloy 400 | .015 | .95 | 750 | 5 |
| IN-718 | Yes | Tribaloy 800 | .015 | .95 | 750 | 5 |
| IN-718 | Yes | WC/17Co | .015 | .5 | 750 | 5 |
| IN-718 | Yes | $Cr_3C_2$-20NiCr | .015 | .5 | 750 | 5 |
| **ALLOY** | **PEEN** | **COATING** | **THICKNESS (inches)** | **A-RATIO (LCF or HCF)** | **TEST TEMP. (Deg. F)** | **NO. SPECIMENS** |
| IN-718 | Yes | Tribaloy 400 | .015 | .5 | 750 | 5 |
| IN-718 | Yes | Tribaloy 800 | .015 | .5 | 750 | 5 |
| **IN-718 Total** | | | | | | **80** |
| 4340 | Yes | WC/17Co | .015 | .95 | 300 | 6 |
| 4340 | Yes | $Cr_3C_2$-20NiCr | .015 | .95 | 300 | 6 |
| 4340 | Yes | Tribaloy 400 | .015 | .95 | 300 | 6 |
| 4340 | Yes | Tribaloy 800 | .015 | .95 | 300 | 6 |
| 4340 | Yes | WC/17Co | .015 | .5 | 300 | 6 |
| 4340 | Yes | $Cr_3C_2$-20NiCr | .015 | .5 | 300 | 6 |
| 4340 | Yes | Tribaloy 400 | .015 | .5 | 300 | 6 |
| 4340 | Yes | Tribaloy 800 | .015 | .5 | 300 | 6 |
| **4340 Total** | | | | | | **48** |
| AM-355 | Yes | WC/17Co | .015 | .95 | 300 | 6 |
| AM-355 | Yes | $Cr_3C_2$-20NiCr | .015 | .95 | 300 | 6 |
| AM-355 | Yes | Tribaloy 400 | .015 | .95 | 300 | 6 |
| AM-355 | Yes | Tribaloy 800 | .015 | .95 | 300 | 6 |
| AM-355 | Yes | WC/17Co | .015 | .5 | 300 | 6 |
| AM-355 | Yes | $Cr_3C_2$-20NiCr | .015 | .5 | 300 | 6 |
| AM-355 | Yes | Tribaloy 400 | .015 | .5 | 300 | 6 |
| AM-355 | Yes | Tribaloy 800 | .015 | .5 | 300 | 6 |
| **AM-355 Total** | | | | | | **48** |
| **GRAND TOTAL** | | | | | | **176** |

### 4.5.6. Test Results

A comparison of the similarities/differences as compared to previous HCAT testing protocols is shown in Table 4-33. The main difference with the current GTE JTP is testing at the elevated temperatures of 300 and 750 °F

**Table 4-33 Comparison of Testing Protocols**

| Condition | Previous Protocols | GTE Protocol |
|---|---|---|
| Test bar | Smooth and hourglass | Smooth |
| R ratios | .1 to -1 | 0.026 and 0.33 |
| Test Temperatures | RT | 300 and 750 °F |
| Type of control | Strain and/or load | Strain and load |

Within the GTE JTP, the primary comparisons made between the variables were:

**Coating:** EHC vs. varied coatings

**Peening***:* Peened vs. unpeened

**Thickness:** .003" vs. .015"

**Temperature:** 300 and 750 °F.

The primary goal of this program was to generate comparative S-N curves to assess fatigue performance. With elevated temperature testing, the issues of coating integrity (cracking/spalling) could not be carefully monitored during each test. For this reason, observations regarding coating integrity reported herein were limited to post-test assessments only.

#### 4.5.6.1. Coatings Made with Hydrogen Fuel

##### 4.5.6.1.1. IN-718 Substrate

The comparisons as outlined above were made for the IN-718 substrate material.

General comments on the comparisons are:

- Figure 4-11 shows the comparison of the bare material at the varied elevated temperatures and unpeened vs. peened data.
- Figure 4-12 shows the data for HCF testing at 300 °F at a thickness of .015". The HVOF carbide coatings (WC/Co and chrome carbide) in addition to the plasma spray T-400 fall below the chrome (EHC ) curve in this situation.
- Figure 4-13 shows the data for LCF testing at 300 °F at a thickness of .015". In this case, all coatings are equal to or better than EHC.
- Figure 4-14 and Figure 4-15 show the data for LCF testing at 750 °F and compares the thickness values of .003 and .015". The carbide coatings (WC/Co and $Cr_3C_2$-NiCr) in Set 1 fall below the chrome (EHC ) curve in this situation. The HVOF Tribaloy coatings T-400/800 in addition to the plasma T-400 are equal or better than chrome.

Comparisons of natural gas work on IN-718 are made in later section of the report.

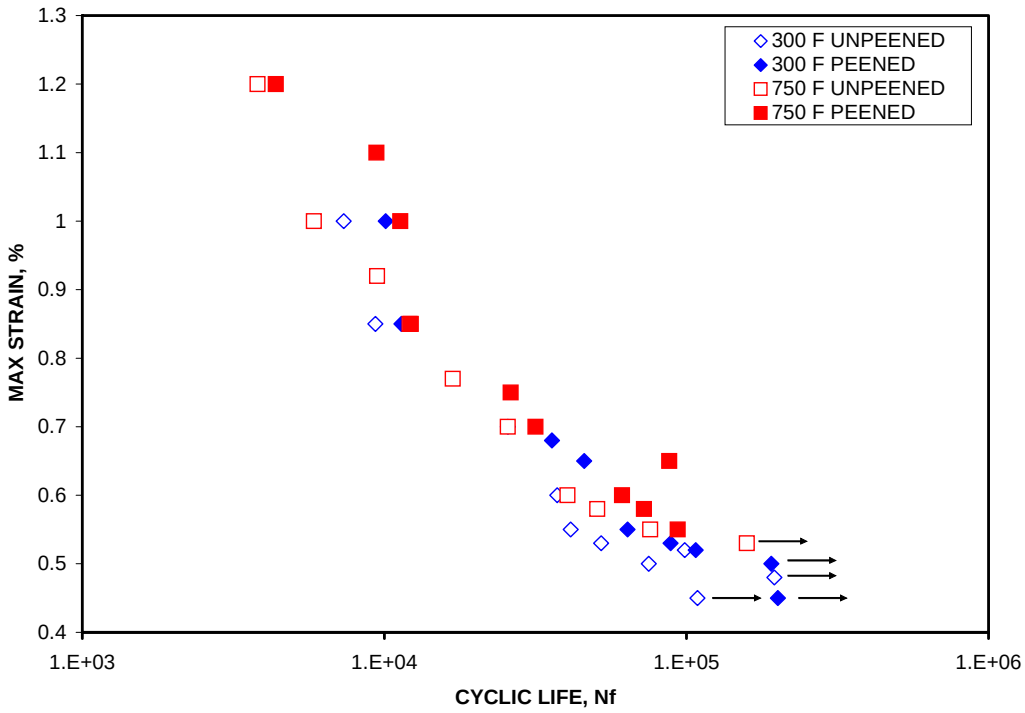


**Figure 4-11. Strain Control, A=0.95, IN-718 BARE**

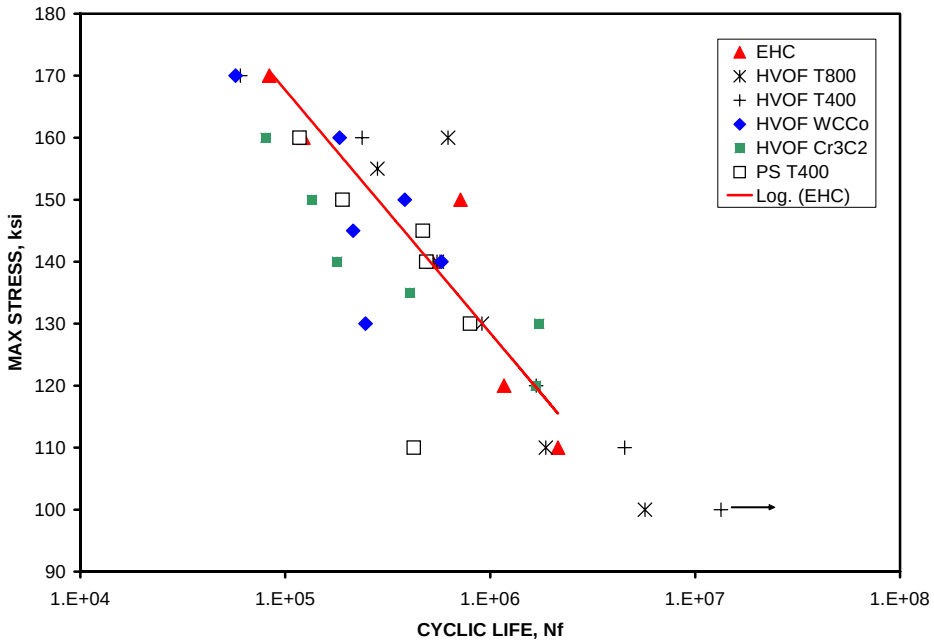


**Figure 4-12 Load Control A=0.5, IN-718/0.015", 300 °F**

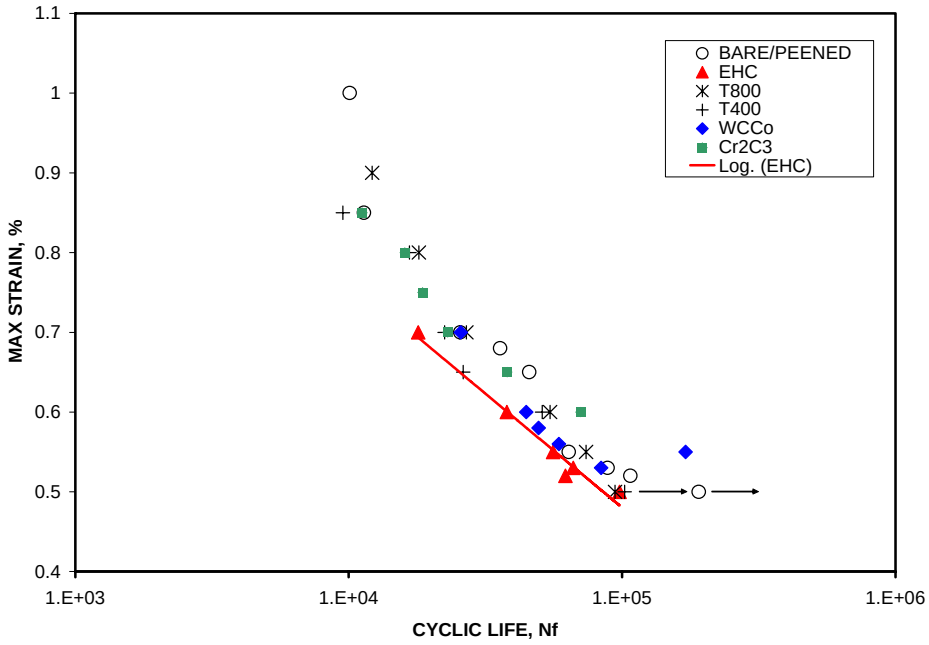


**Figure 4-13 Strain Control, A=0.95, IN-718/0.015", 300 °F**

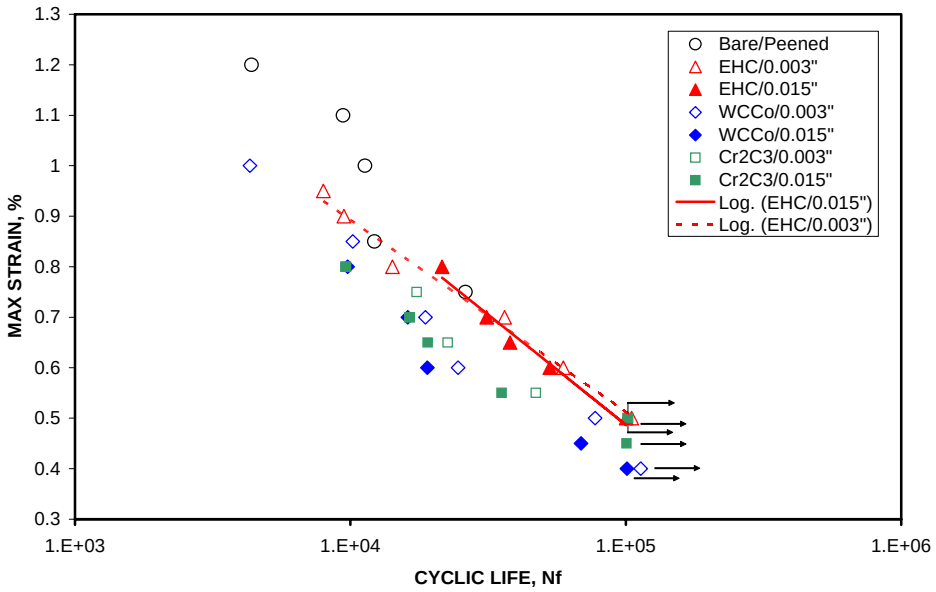


**Figure 4-14 Strain Control, A=0.95, IN-718, 750 °F Set 1**

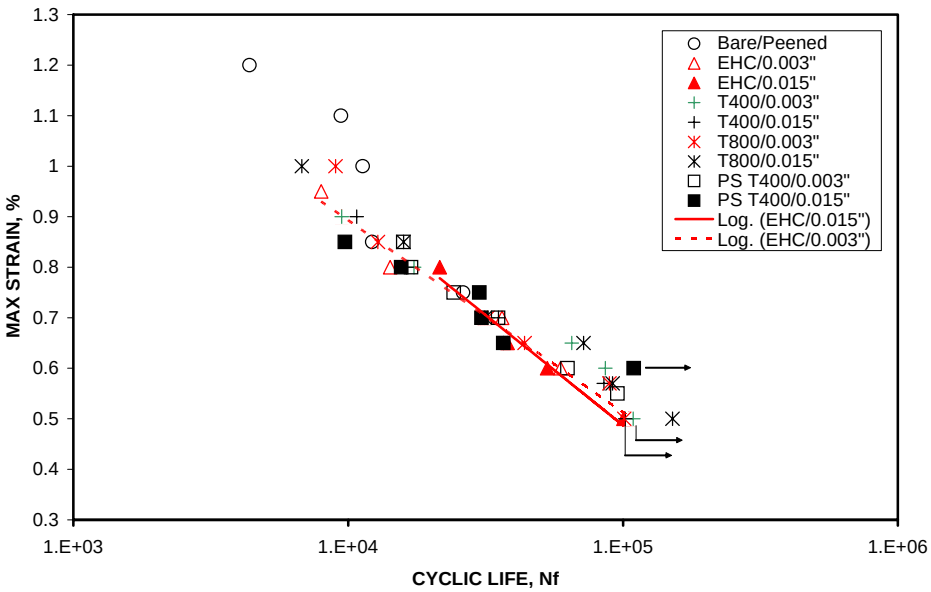


**Figure 4-15 Strain Control, A=0.95, IN-718, 750 °F Set 2**

#### 4.5.6.1.2. A-286 Results

The comparisons for A-286 are very similar. General comments on the comparisons are:

- Figure 4-16 shows the comparison of the bare material at the varied elevated temperatures and unpeened vs. peened data.
- Figure 4-17 shows the data for HCF testing at 300 °F at a thickness of .015". In this case, all coatings are equal to or better than EHC.
- Figure 4-18 shows the data for LCF testing at 300 °F at a thickness of .015". In this case, all coatings are equal to or better than EHC.
- Figure 4-19 shows the data for LCF testing at 750 °F and compares the thickness values of .003 and .015". In this case, all coatings are equal to or better than EHC.

#### 4.5.6.1.3. AM-355 Results

The comparisons for AM-355 are very similar. General comments on the comparisons are:

- Figure 4-20 shows the comparison of the bare material at the varied elevated temperatures and unpeened vs. peened data.
- Figure 4-21 shows the data for HCF testing at 300 °F at a thickness of .015". In this case, all coatings are equal to or better than EHC.
- Figure 4-22 shows the data for LCF testing at 300 °F at a thickness of .015". In this case, all coatings are equal to or better than EHC.
- Figure 4-23 shows the data for LCF testing at 750 °F and compares the thickness values of .003 and .015". In this case, all coatings are equal to or better than EHC except the HVOF WC/Co at the .003" thickness

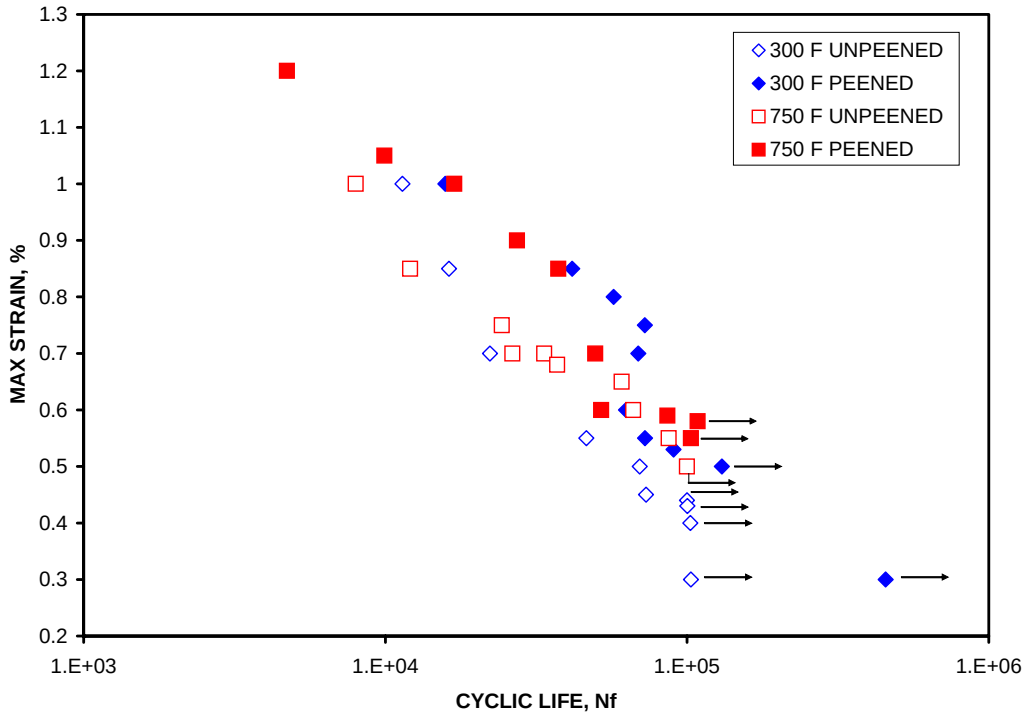


**Figure 4-16 Strain Control, A=0.95, A-286 BARE**

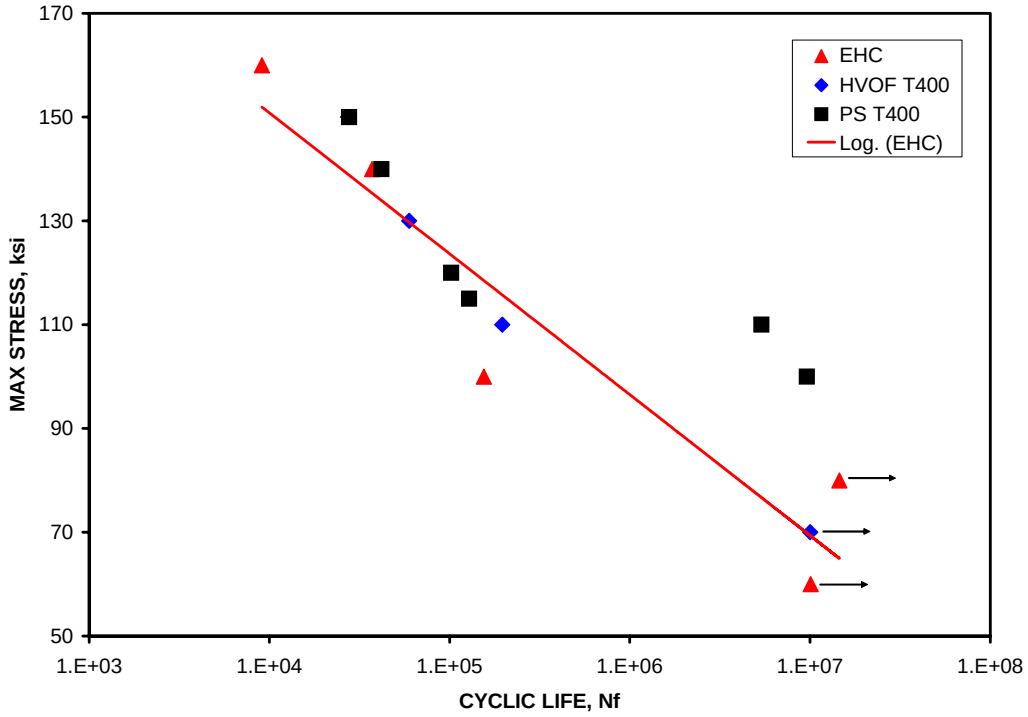


**Figure 4-17 Load Control A=0.5, A-286/0.015", 300 °F**

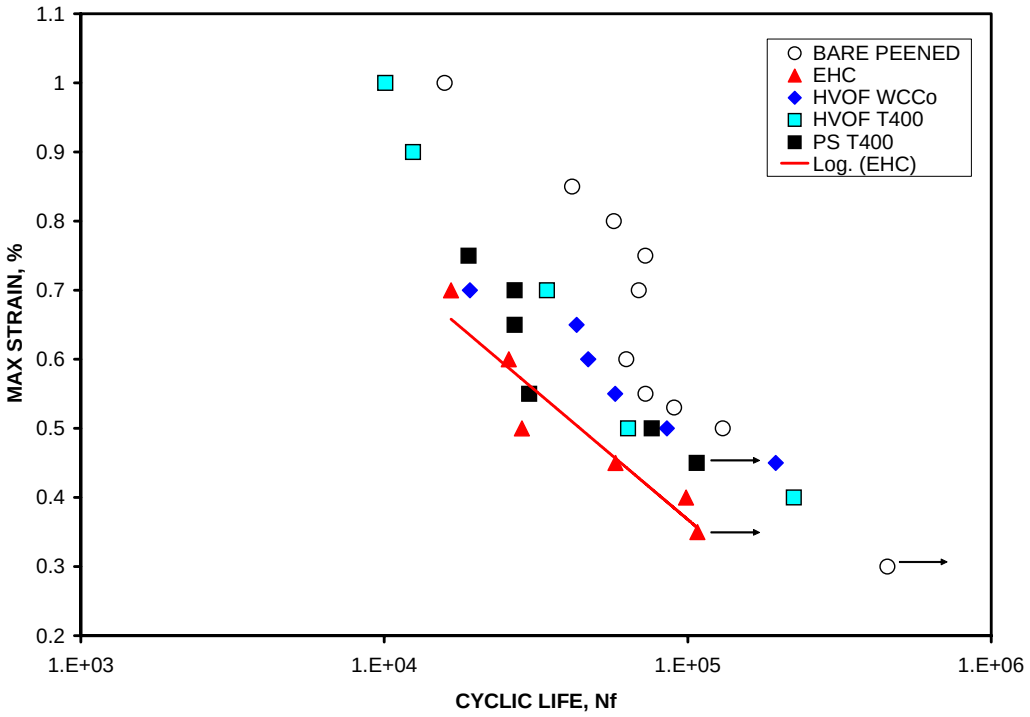


**Figure 4-18 Strain Control A=0.95, A-286/0.015", 300 °F**

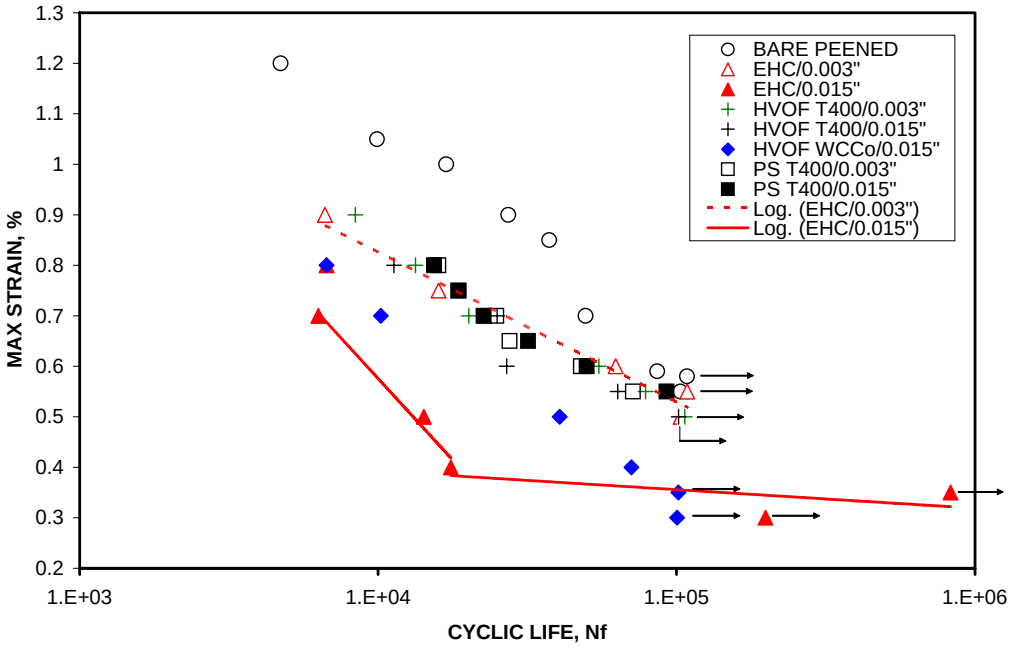


**Figure 4-19 Strain Control A=0.95, A-286, 750 °F**

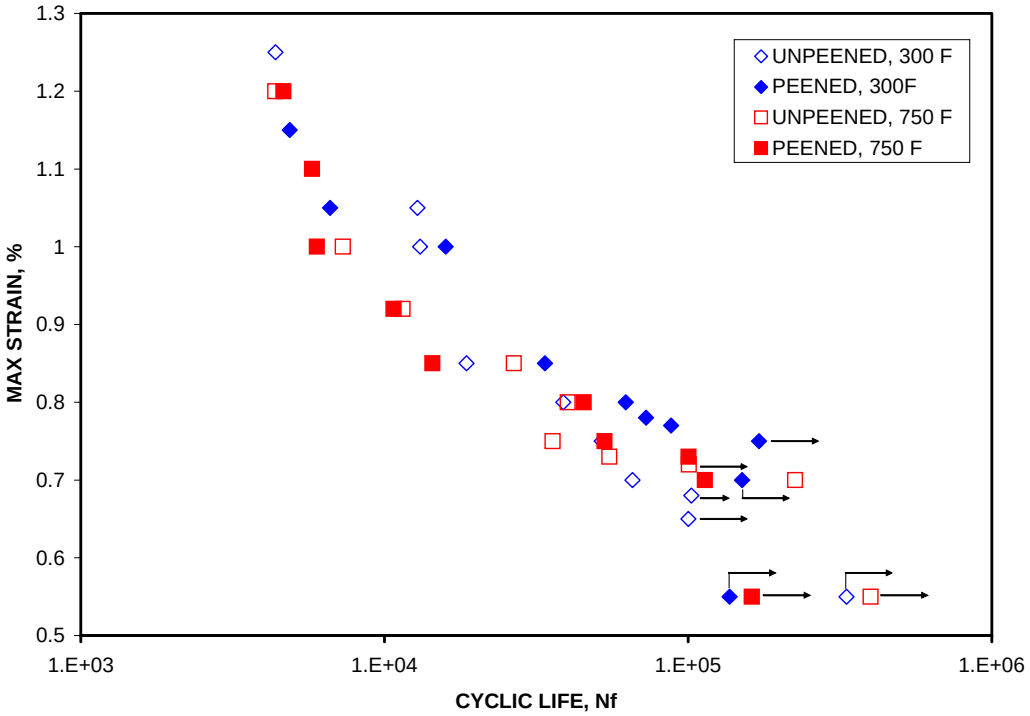


**Figure 4-20 Strain Control A=0.95 AM-355 BARE**

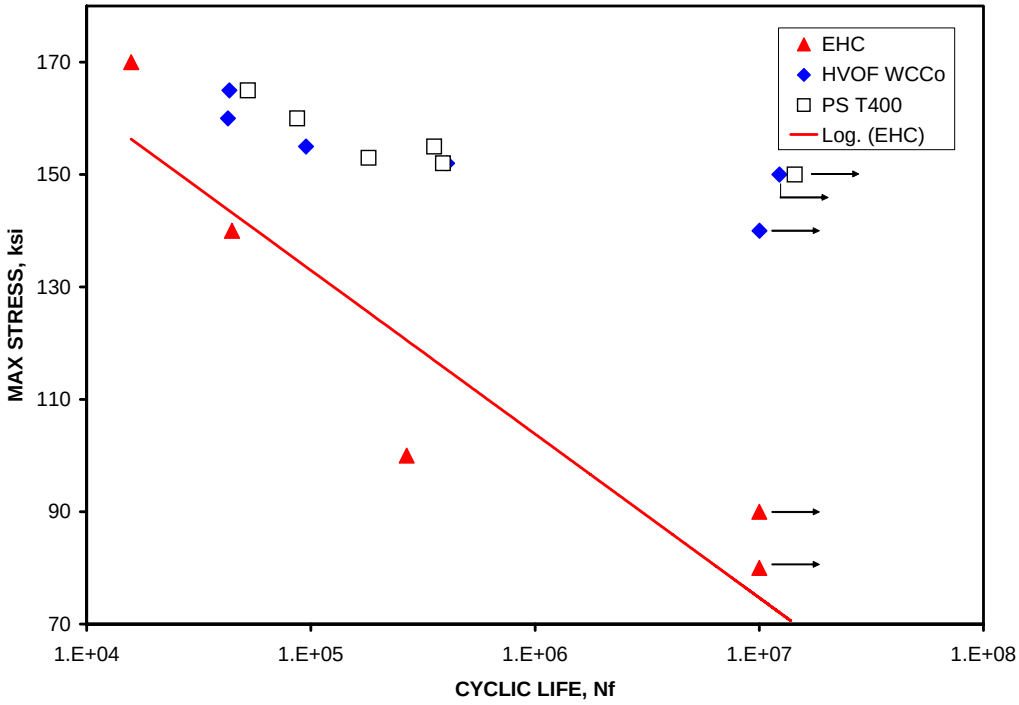


**Figure 4-21 Load Control A=0.5, AM-355/0.015", 300 °F**

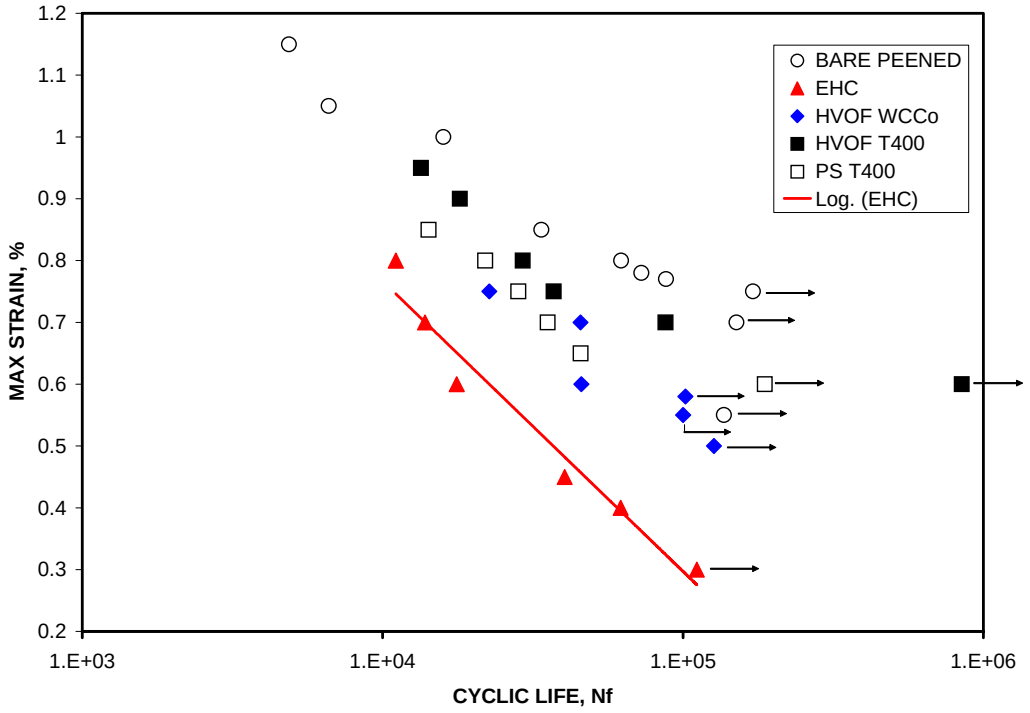


**Figure 4-22 Strain Control A=0.95, AM-355/0.015", 300 °F**

#### 4.5.6.1.4. 9310 Results

The comparisons for 9310 are very similar. General comments on the comparisons are:

- Figure 4-24 shows the comparison of the bare material at the varied elevated temperatures and unpeened vs. peened data.
- Figure 4-25 shows the data for HCF testing at 300 °F at both the thickness values of .003 and .015". In this case, all coatings are equal to or better than EHC.
- Figure 4-26 shows the data for LCF testing at 300 °F at a thickness of .015". In this case, all coatings are equal to or better than EHC.

#### 4.5.6.1.5. IN-901 Results

The comparisons for IN-901 are very similar. General comments on the comparisons are:

- Figure 4-27 shows the comparison of the bare material at the varied elevated temperatures and unpeened vs. peened data.
- Figure 4-28 shows the data for LCF testing at 300 °F at a thickness of .015". In this case, all coatings are *marginally* equal to or better than EHC.
- Figure 4-29 shows the data for HCF testing at 300 °F at a thickness of .015". In this case, all coatings are equal to or better than EHC.
- Figure 4-30 and Figure 4-31 show the data for LCF testing at 750 °F and compares the thickness values of .003 and .015". In this case, the Set 1 graph shows that .015" thick HVOF WC/Co falls below the EHC curve. For Set 2, all coatings are equal to or better than EHC.

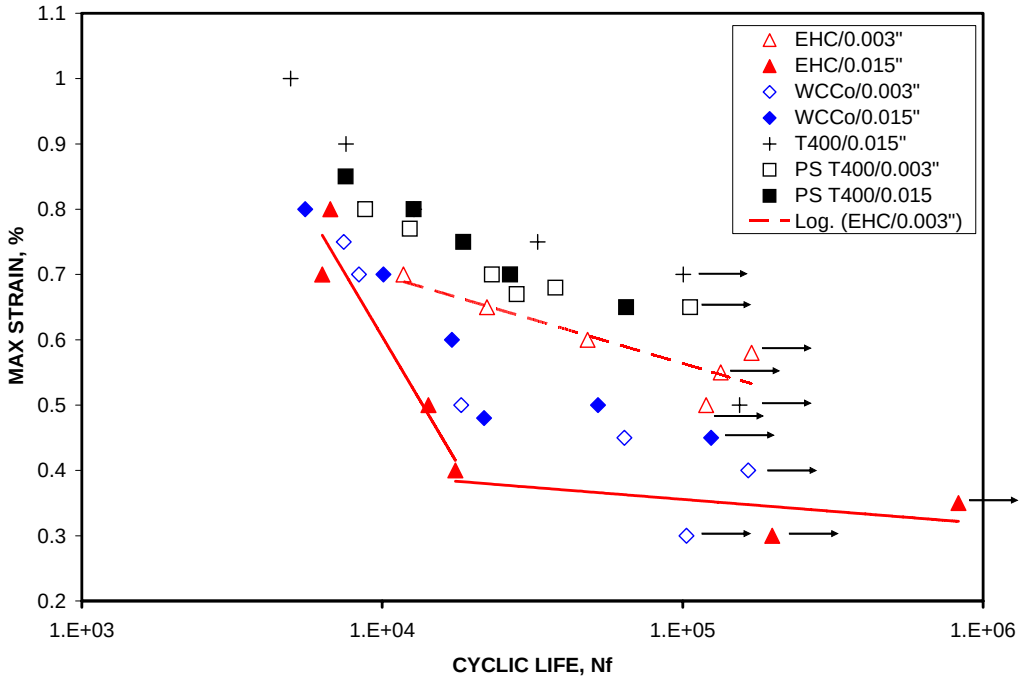


**Figure 4-23 Strain Control A=0.95, AM-355, 750 °F**

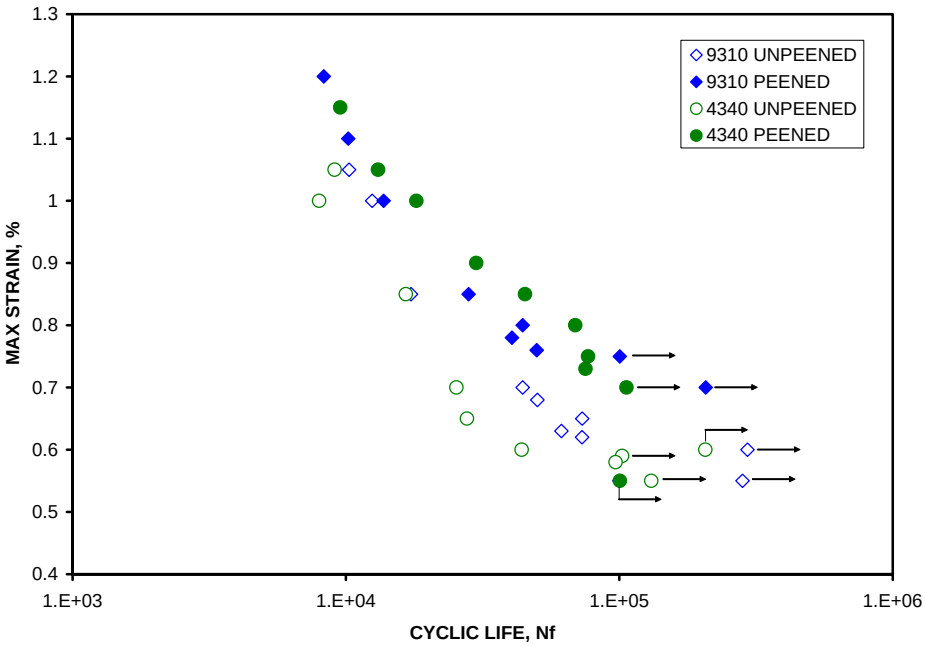


**Figure 4-24 Strain Control A=0.95, 300 °F BARE 9310**

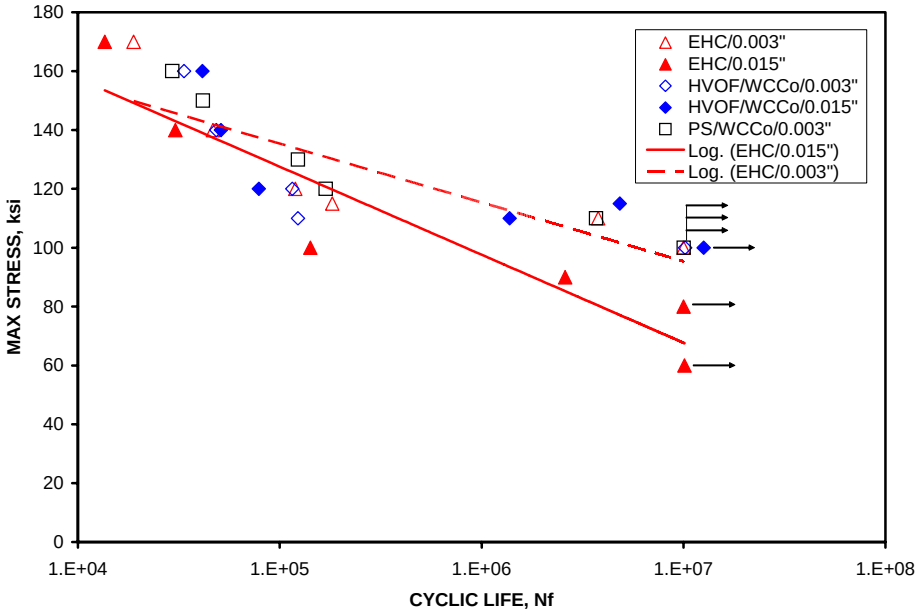


**Figure 4-25 Load Control A=0.5, 9310, 300 °F**

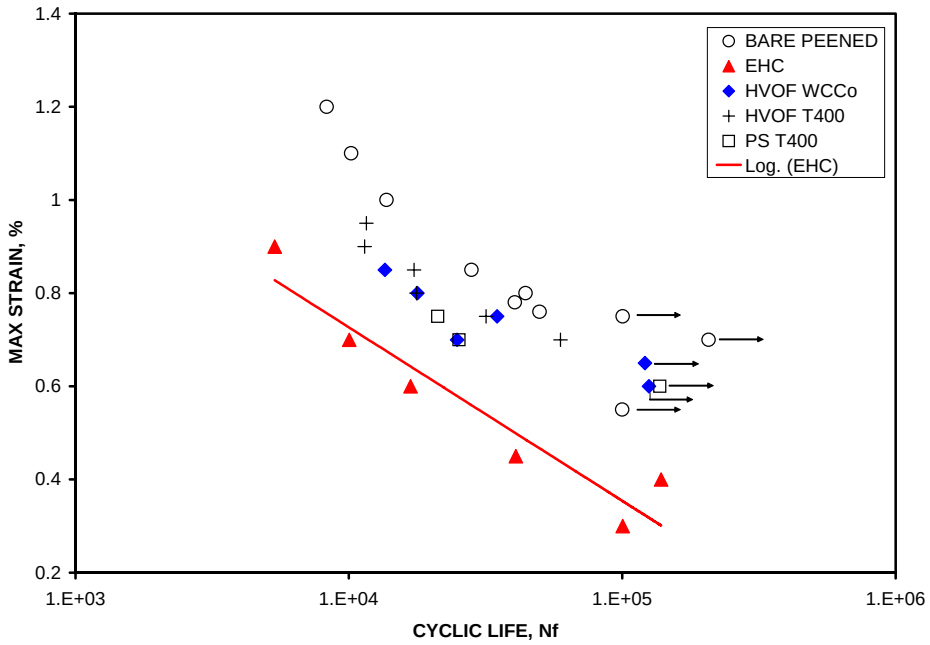


**Figure 4-26 Strain Control A=0.95, 9310/0.015", 300 °F**

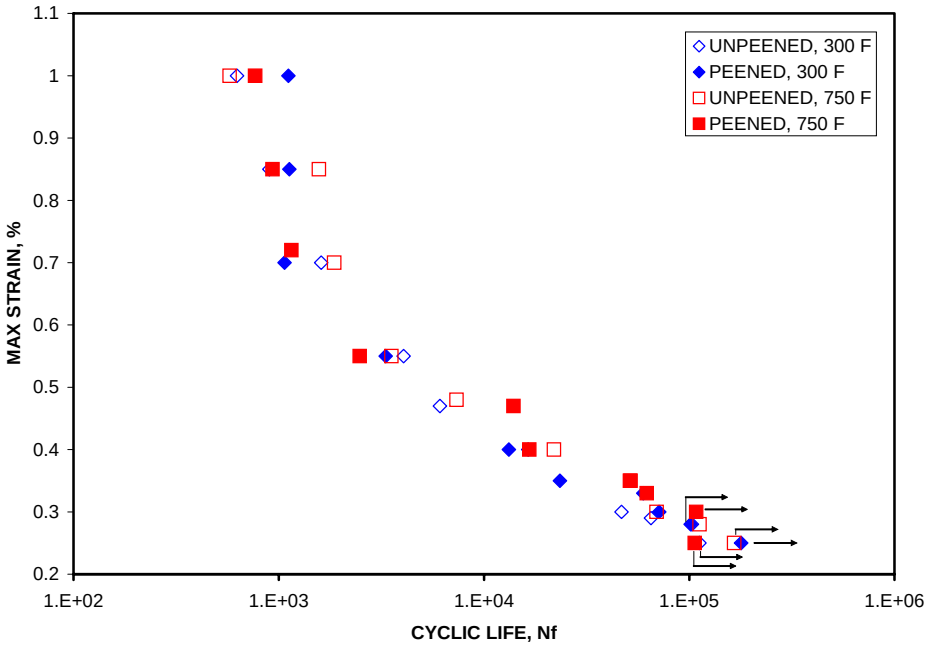


**Figure 4-27 Strain Control A=0.95, IN-901 BARE**

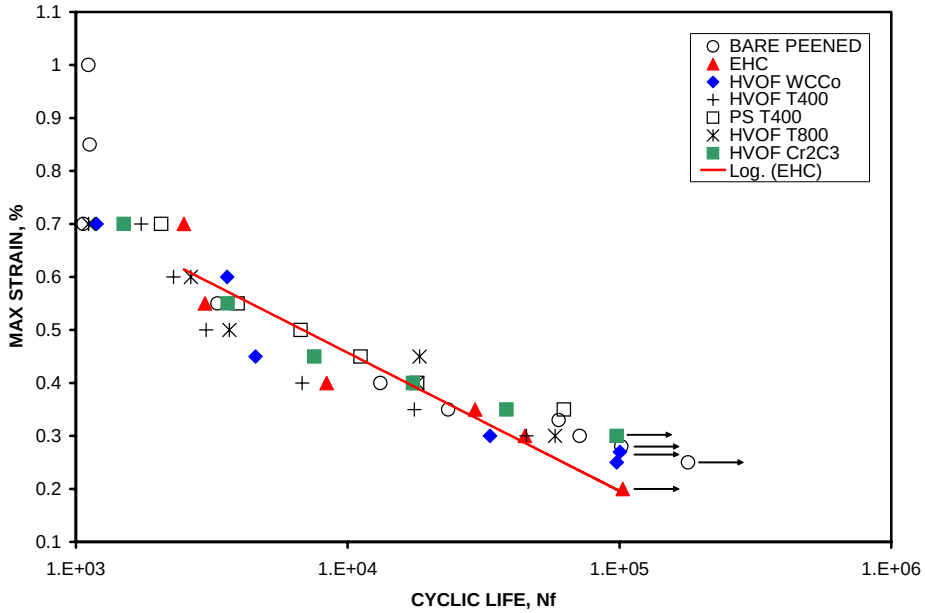


**Figure 4-28 Strain Control A=0.95, IN-901/0.015", 300 °F**

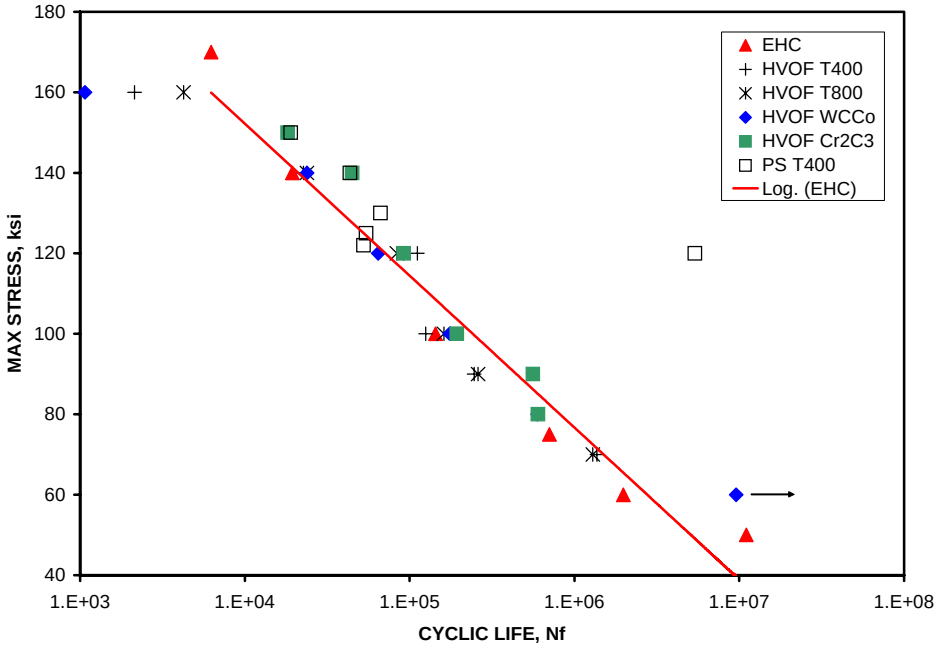


**Figure 4-29 Load Control A=0.5, IN-901/0.015", 300 °F**

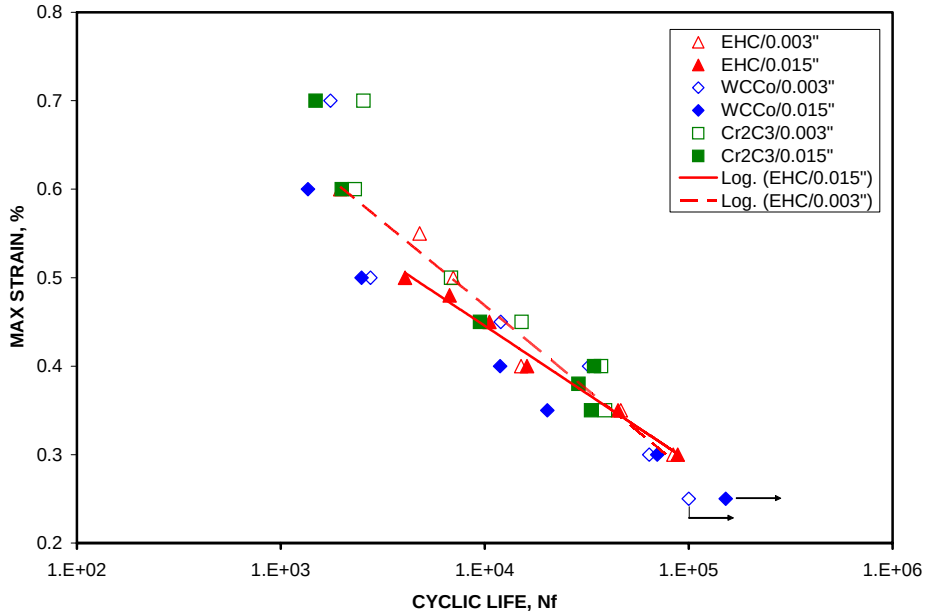


**Figure 4-30 Strain Control A=0.95, IN-901, 750 °F Set 1**

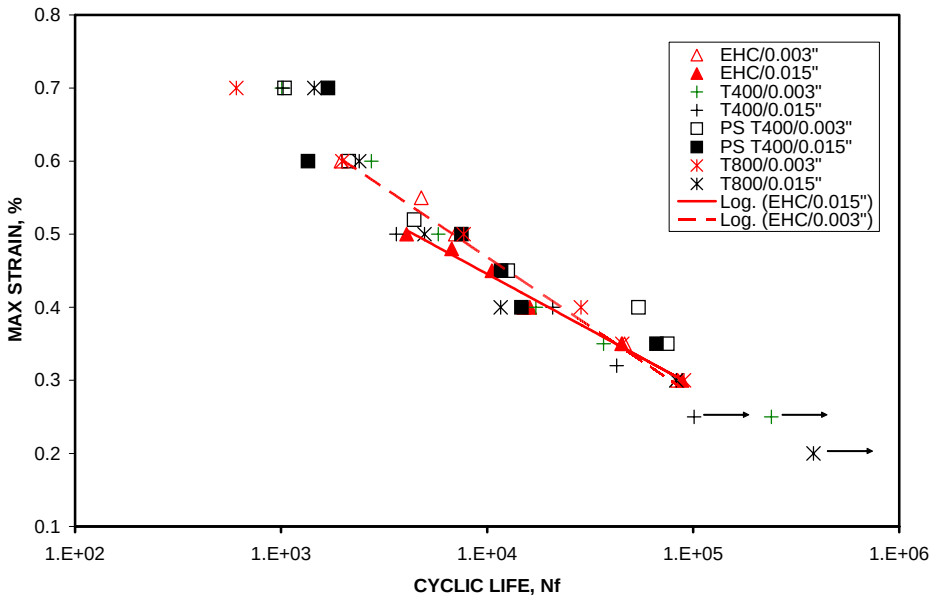


**Figure 4-31 Strain Control A=0.95, IN-901, 750 °F Set 2**

#### 4.5.6.1.6. 4340 Results

The comparisons for 4340 are very similar. When compared to previous HCAT work, it must be noted that the 4340 was heat treated to RC 48-50 in lieu of the RC 52-54 for landing gear applications. General comments on the comparisons are:

- Figure 4-32 shows the comparison of the bare material at the varied elevated temperatures and unpeened vs. peened data.
- Figure 4-33 shows the data for HCF testing at 300 $^{o}$F at both the thickness values of .003 and .015". In this case, all coatings are equal to or better than EHC.
- Figure 4-35 shows the data for LCF testing at 300 $^{o}$F at a thickness of .015". In this case, all coatings are equal to or better than EHC.

#### 4.5.6.1.7. 17-4PH Results

The comparisons for 17-4PH are very similar. General comments on the comparisons are:

- Figure 4-34 shows the comparison of the bare material at the varied elevated temperatures and unpeened vs. peened data.
- Figure 4-36 shows the data for LCF testing at 300 $^{o}$F at a thickness of .015". In this case, all coatings are equal to or better than EHC.
- Figure 4-37 shows the data for HCF testing at 300 $^{o}$F at a thickness of .015". In this case, all coatings are equal to or better than EHC.
- Figure 4-38 and Figure 4-39 show the data for LCF testing at 750 $^{o}$F and compares the thickness values of .003 and .015". In this case, the Set 1 graph shows that .003" thick coatings fall below the EHC curve. For Set 2, all coatings are equal to or better than EHC.

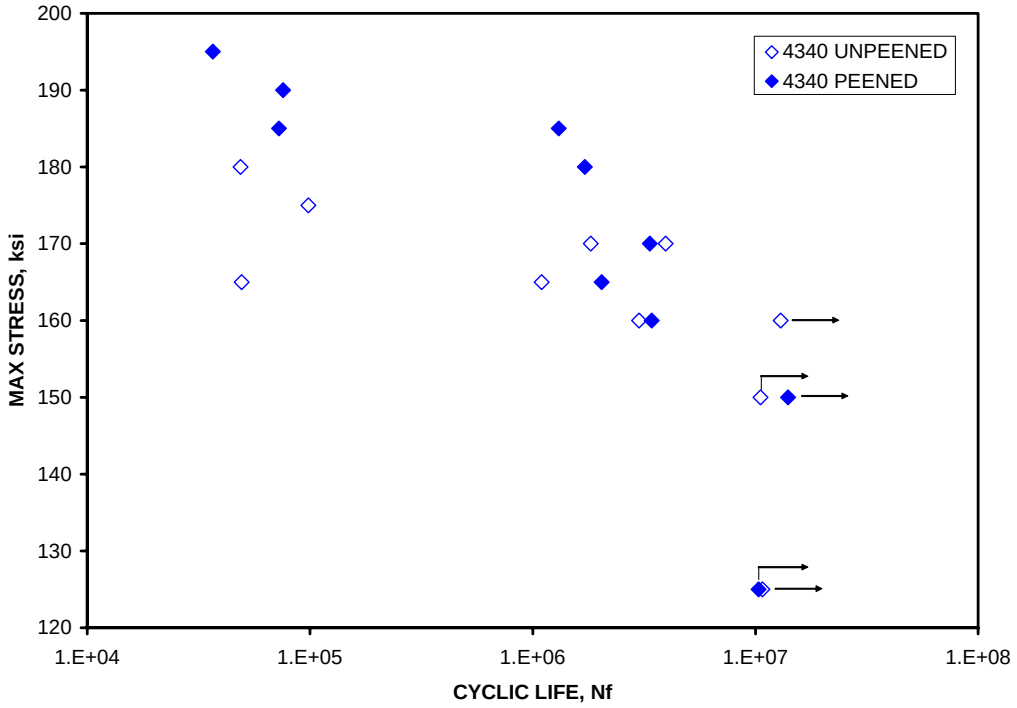


**Figure 4-32 Load Control A=0.5, 4340 BARE, 300 °F**

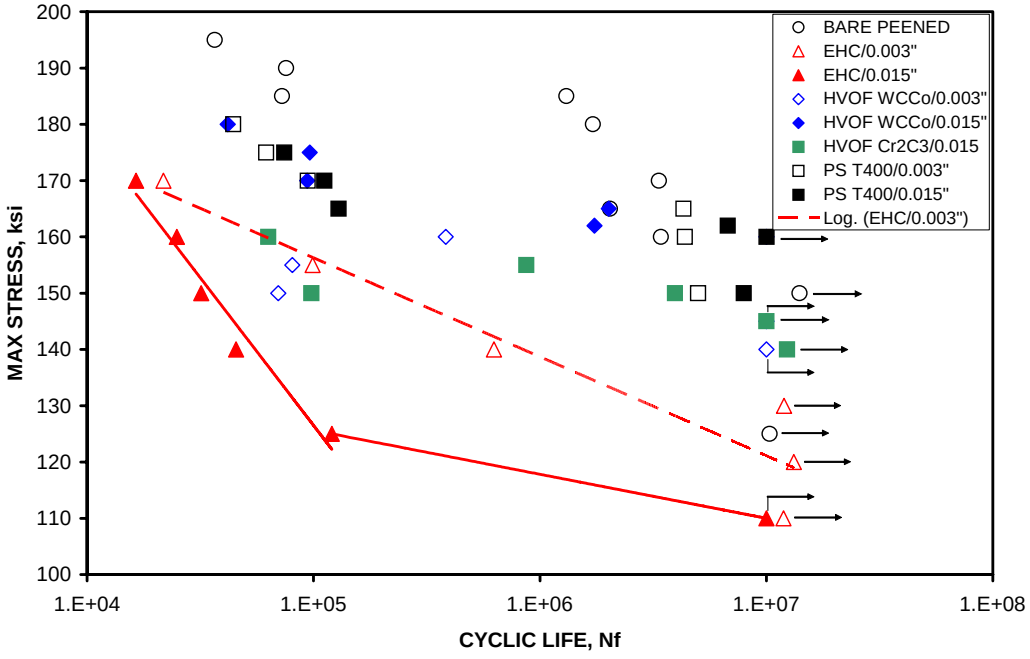


**Figure 4-33 Load Control A=0.5, 4340, 300 °F**

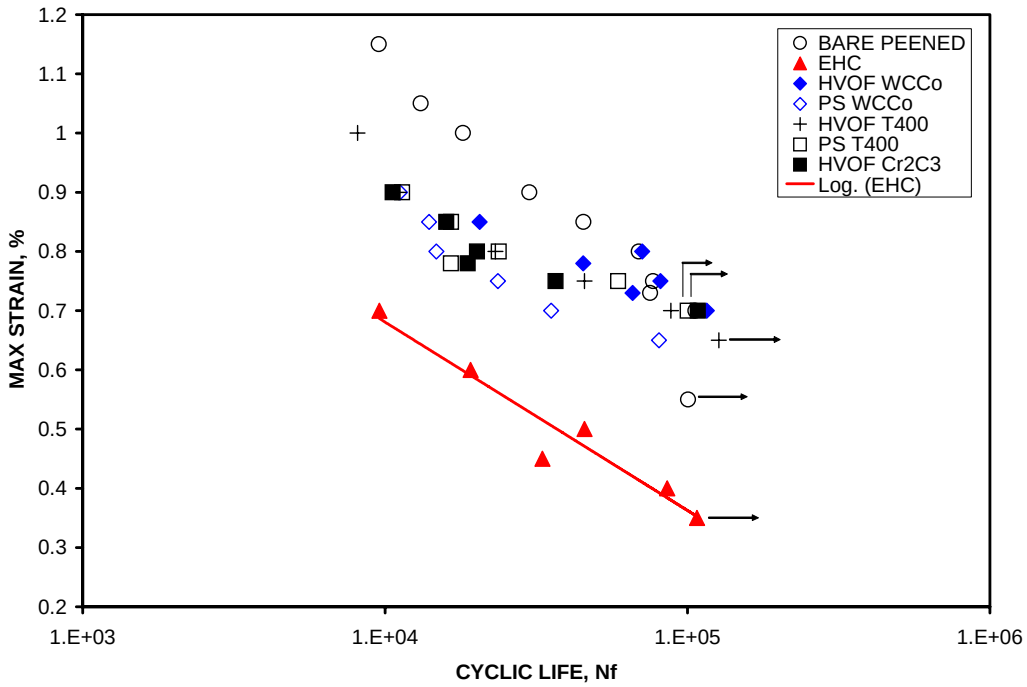


**Figure 4-35 Strain Control A=0.95, 4340/0.015", 300 °F**

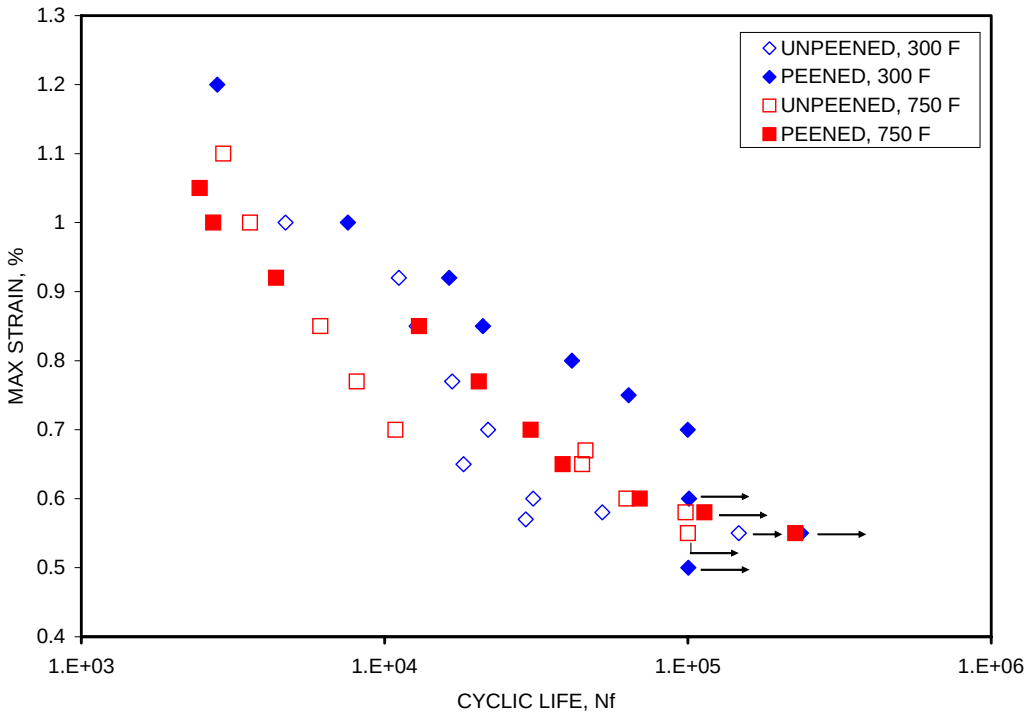


**Figure 4-34 Strain Control A=0.95, 17-4PH BARE**

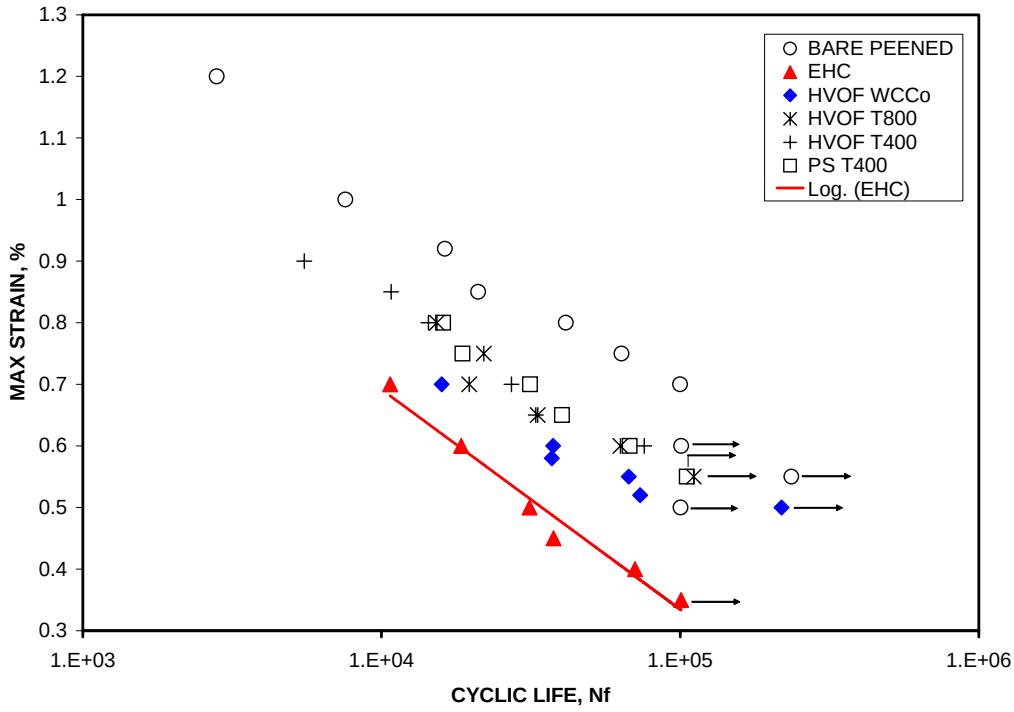


**Figure 4-36 Strain Control A=0.95, 17-4PH/0.015", 300 °F**

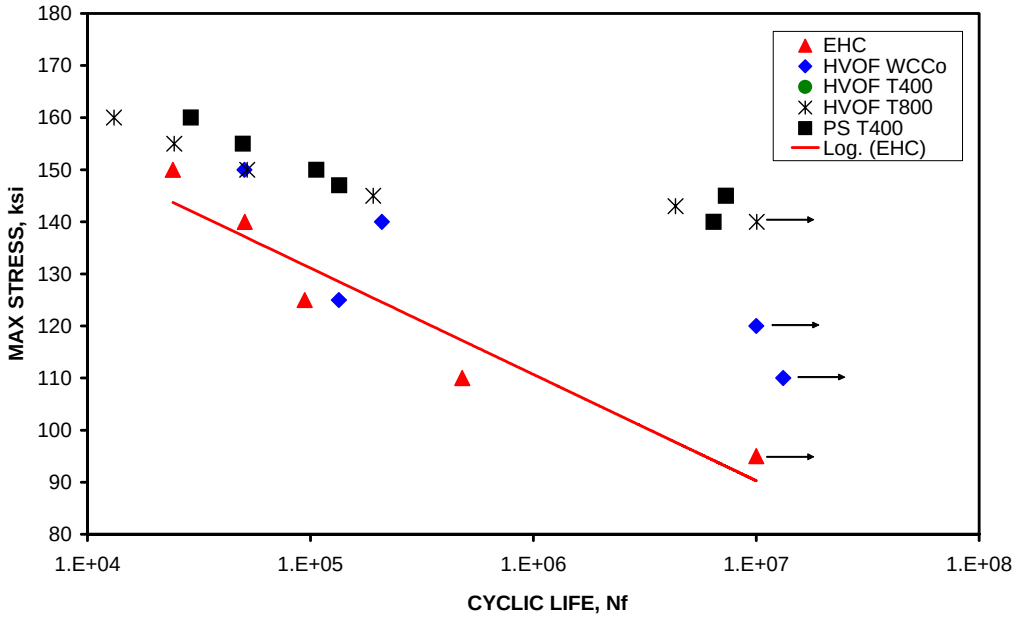


**Figure 4-37 Load Control A=0.5, 17-4PH, 300 °F**

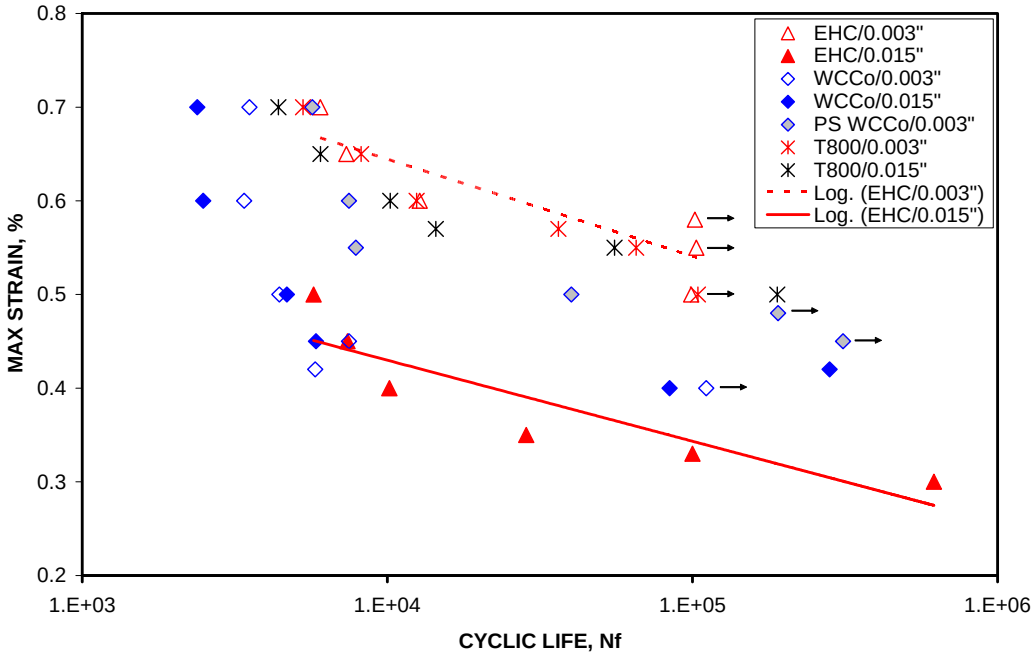


**Figure 4-38 Strain Control A=0.95, 17-4PH, 750 °F, Set 1.**

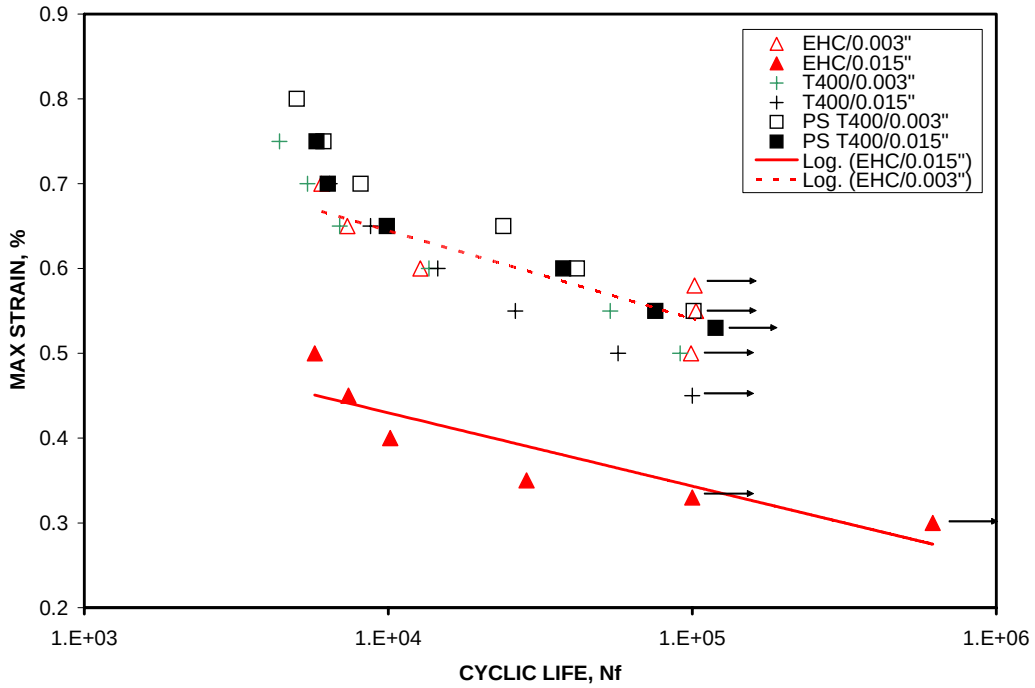


**Figure 4-39. Strain Control A=0.95, 17-4PH, 750 °F, Set 2**

#### 4.5.6.2.Fuel Comparison-Hydrogen vs. Natural Gas

Three alloys and four coatings as listed in Table 4-34 were chosen for the comparison.

**Table 4-34 Alloys and Coating Selected for the Fuel Gas Comparison**

| Alloys | Coatings |
|---|---|
| IN-718 | HVOF WC/17Co |
| AM-355 | HVOF $Cr_3C_2$-NiCr |
| 4340 | HVOF T-800 |
| | HVOF T-400 |

All testing was performed at the thickness of .015". For IN-718, the comparisons were made at both 300 °F and 750 °F. For the AM-355 and 4340 alloys, the testing was only performed at 300 °F. When compared to previous HCAT work, it must be noted that the 4340 was heat treated to Rc 48-50 in lieu of the Rc 52-54 for landing gear applications.

##### 4.5.6.2.1. IN-718 Results

The comparisons for this data involve both the chrome baseline and the previously shown hydrogen fuel data.

- Figure 4-40 shows the LCF comparison at 300 °F with all the coatings equal to or better than chrome.
- Figure 4-41 shows the HCF comparison at 300 °F. The hydrogen HVOF WC/Co data did not meet the equal to better than chrome criteria and the natural gas data is only marginally acceptable.
- Figure 4-42 shows the LCF comparison at 750 °F. As was observed with the hydrogen data both the HVOF WC/Co and Chrome Carbide coatings do not meet the equal to or better than chrome criteria.
- Figure 4-43 shows the HCF comparison at 750 °F. In this case, no real conclusions can be drawn since no baseline testing for this temperature/alloy combination was performed in this protocol.

##### 4.5.6.2.2. AM-355 Results

The comparisons for this data involve both the chrome baseline and the previously shown hydrogen fuel data.

- Figure 4-44 shows the LCF comparison at 300 °F with all the coatings equal to or better than chrome.
- Figure 4-45 shows the HCF comparison at 300 °F with all the coatings equal to or better than chrome.

##### 4.5.6.2.3. 4340 Results

The comparisons for this data involve both the chrome baseline and the previously shown hydrogen fuel data. When compared to previous HCAT work, it must be noted that the 4340 was heat treated to RC 48-50 in lieu of the RC 52-54 for landing gear applications.

- Figure 4-46 shows the LCF comparison at 300 °F with all the coatings equal to or better than chrome.
- Figure 4-47 shows the HCF comparison at 300 °F with all the coatings equal to or better than chrome.

#### 4.5.6.3. Coating Failure Locations

Since this protocol used a patch coating in the test area, there is some likelihood that failure during testing will occur outside the coated area. To ensure that failure location did not adversely affect or skew the fatigue test results or the conclusions drawn from the data, the site for specimen failure was tracked as shown in Table 4-35. As can bee seen, there are no real trends across any alloy/coating combinations that would appear to significantly affect the results.

For comparison, the statistics from the previous Landing Gear JTP are also included. In the Landing Gear JTP, the chrome/coating results were almost identical. In comparison to the GTE JTP, the coating results are comparable but the chrome results for the Landing Gear JTP show more of a tendency for failure under the patch. This may be part of the inherent process variability present with chrome plating as the specimens for the protocols were plated at two different depots.

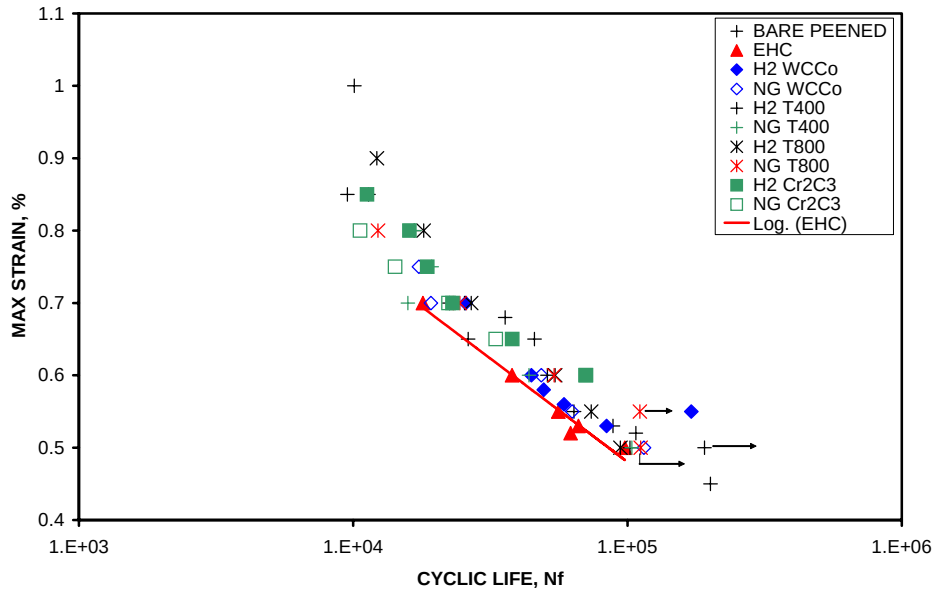


**Figure 4-40 Strain Control A=0.95, IN-718, 300 °F, Comparison Between Hydrogen (H2) and Natural Gas (NG) as Fuel.**

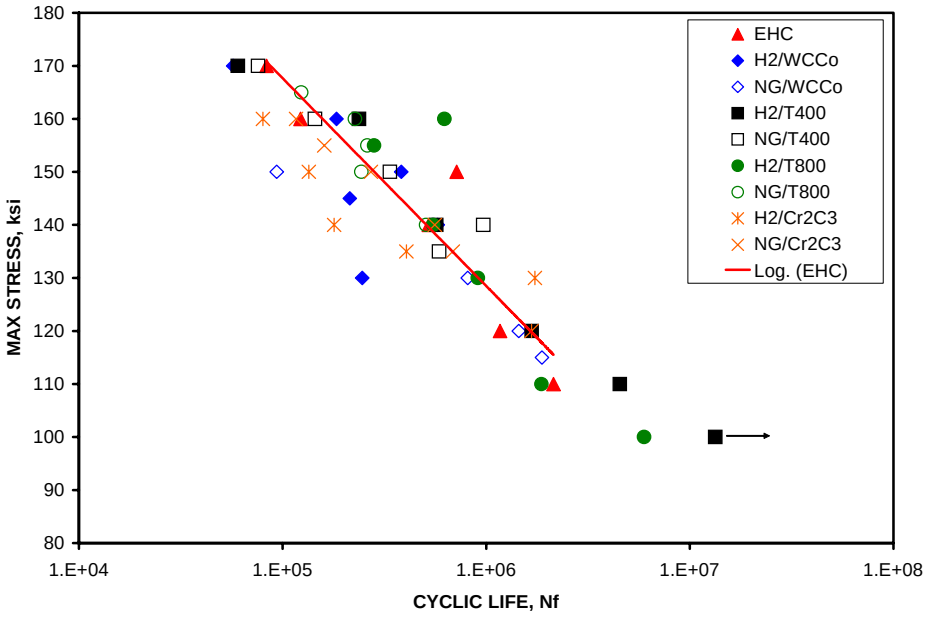


**Figure 4-41 Load control A=0.5, IN-718, 300 °F, Comparison Between Hydrogen (H2) and Natural Gas (NG) as Fuel.**

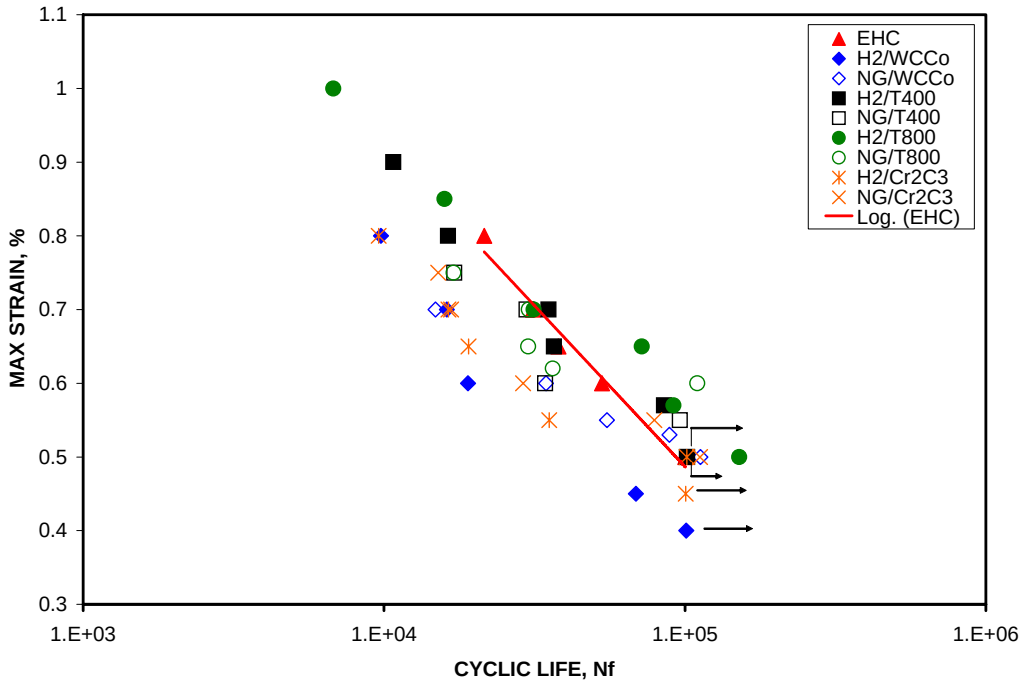


**Figure 4-42 Strain Control A=0.95, IN-718, 750 °F, Comparison Between Hydrogen (H2) and Natural Gas (NG) as Fuel.**

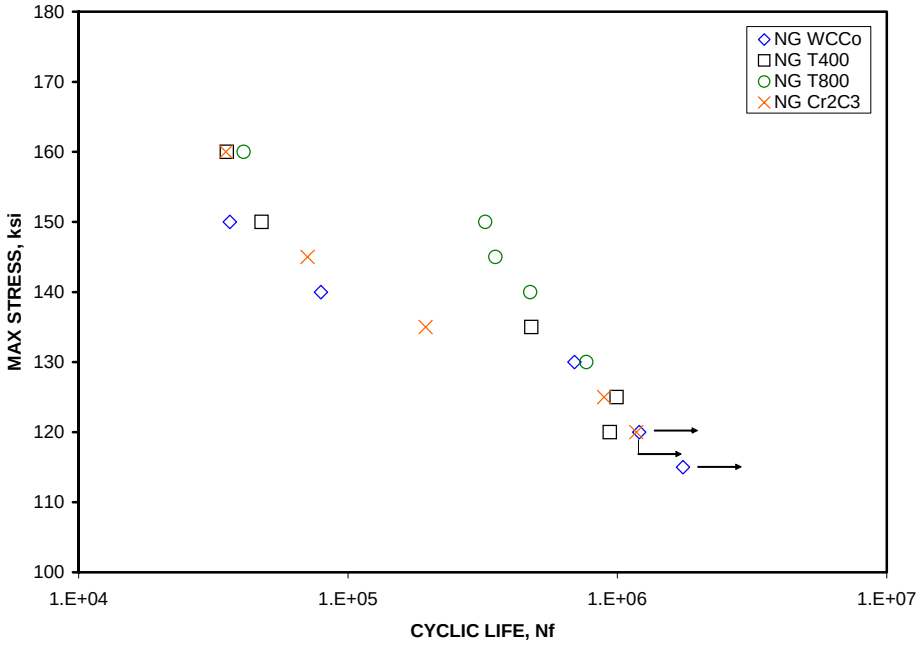


**Figure 4-43 Load control A=0.5, IN-718, 750 °F, Using Natural Gas as Fuel.**

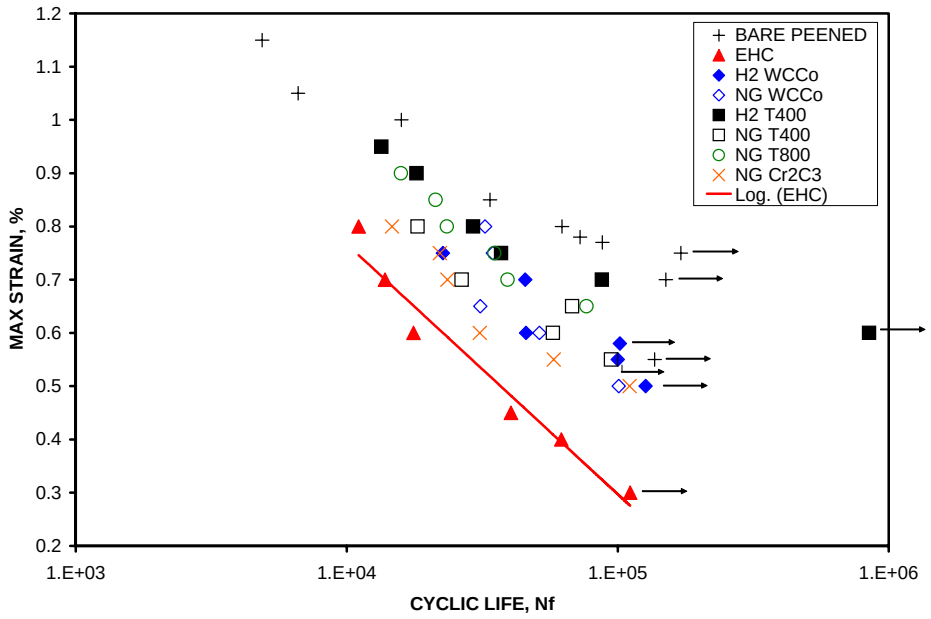


**Figure 4-44 Strain Control A=0.95, AM-355, 300 °F, Comparison Between Hydrogen (H2) and Natural Gas (NG) as Fuel.**

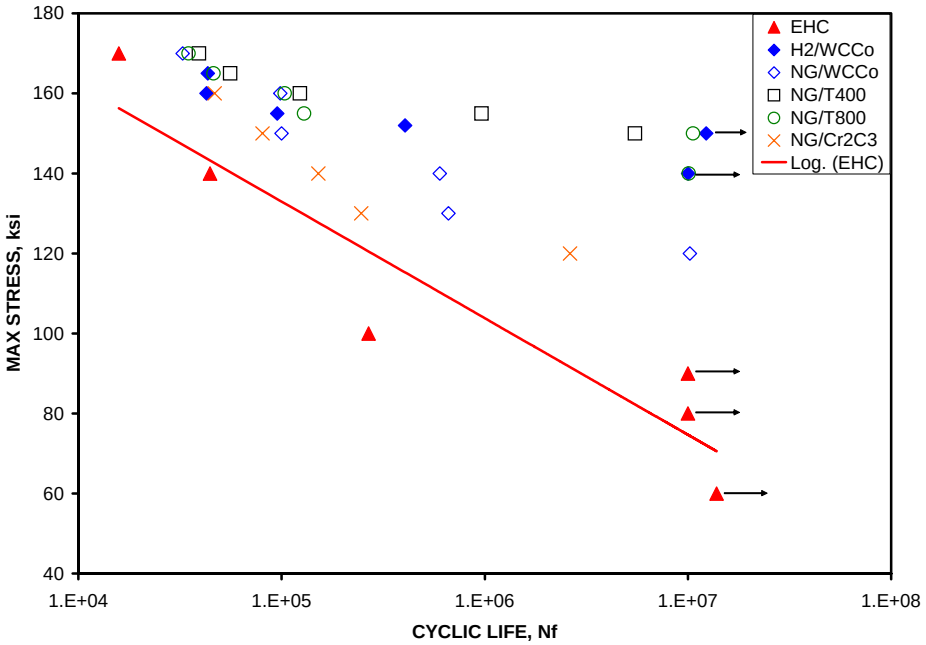


**Figure 4-45 Load control A=0.5, AM-355, 300 °F, Comparison Between Hydrogen (H2) and Natural Gas (NG) as Fuel.**

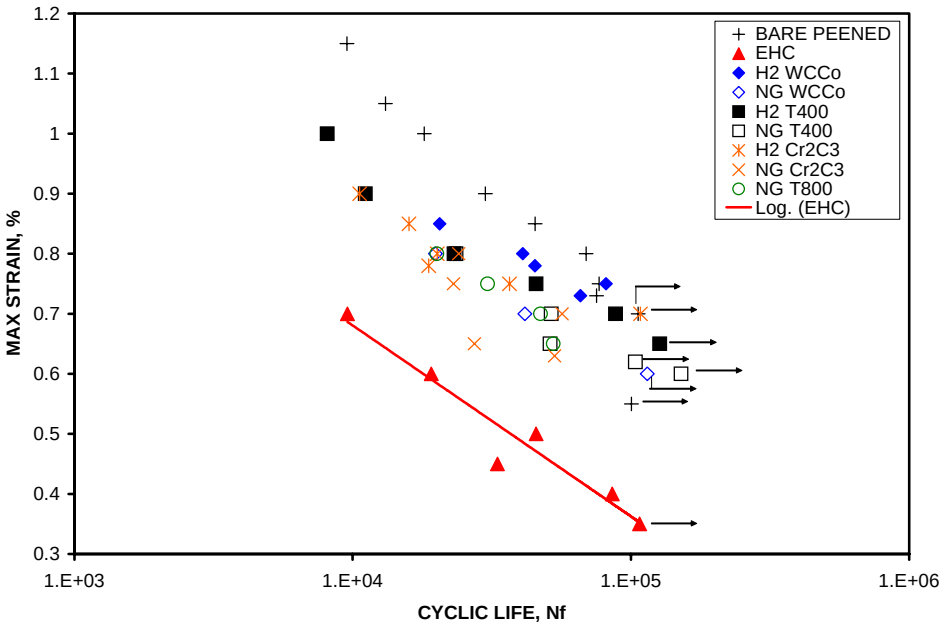


**Figure 4-46 Strain Control A=0.95, 4340, 300 °F, Comparison Between Hydrogen (H2) and Natural Gas (NG) as Fuel.**

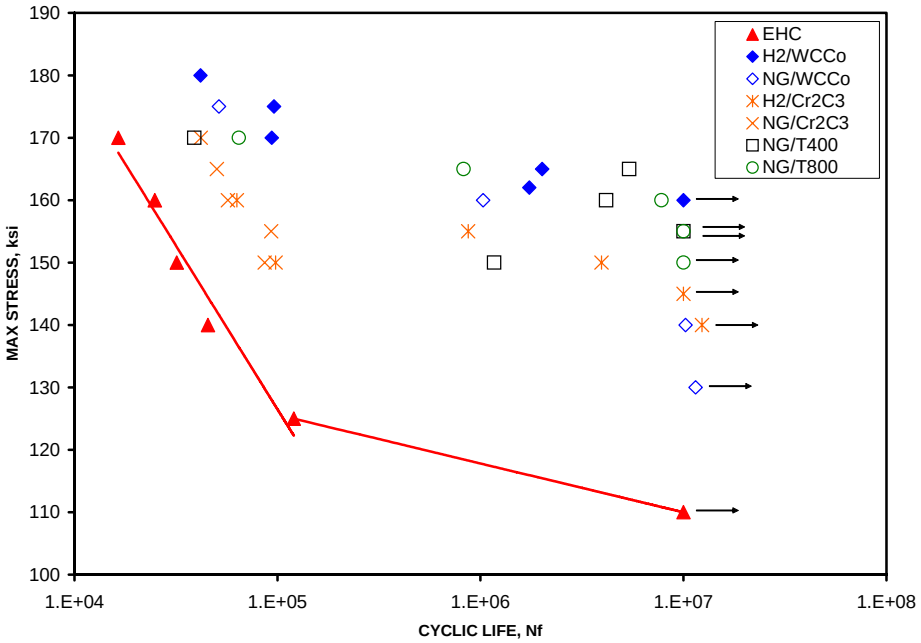


**Figure 4-47 Load control A=0.5, 4340, 300 °F, Comparison Between Hydrogen (H2) and Natural Gas (NG) as Fuel.**

**Table 4-35. Failure Locations for Fatigue Specimens.**

| | EHC | | | HVOF+PS | | | NG/HVOF | | |
|---|---|---|---|---|---|---|---|---|---|
| SUBSTRATE | Runout | Under patch | Edge/ outside patch | Runout | Under patch | Edge/ outside patch | Runout | Under patch | Edge/ outside patch |
| IN178 | 3 | 14<br>67% | 7<br>33% | 10 | 61<br>50% | 60<br>50% | 4 | 38<br>50% | 38<br>50% |
| A-286 | 6 | 15<br>83% | 3<br>17% | 7 | 22<br>42% | 30<br>58% | | | |
| AM-355 | 9 | 9<br>60% | 6<br>40% | 14 | 19<br>41% | 27<br>59% | 4 | 31<br>72% | 12<br>28% |
| 9310 | 4 | 8<br>57% | 6<br>43% | 7 | 15<br>52% | 14<br>48% | | | |
| IN-901 | 1 | 11<br>65% | 6<br>35% | 5 | 28<br>31% | 62<br>69% | | | |
| 4340<br>RC 48-50 | 7 | 16<br>94% | 1<br>6% | 9 | 36<br>57% | 27<br>43% | 11 | 20<br>71% | 8<br>29% |
| 17-4PH | 6 | 14<br>78% | 4<br>22% | 13 | 53<br>60% | 36<br>40% | | | |
| 4340<br>RC 52-54 | | 54% | 46% | | 41% | 59% | | | |
| TOTAL | 36 | 87<br>73% | 33<br>28% | 65 | 234<br>48% | 256<br>52% | 19 | 89<br>61% | 58<br>39% |

### 4.5.7. Coating Integrity Analysis

Coating integrity can be defined as the ability of a coating to continue protecting the underlying material during application of cyclic stresses without significant cracking (that might cause a corrosive medium to penetrate to the substrate) and without delamination or spalling which clearly would result in a loss of protection. The presence of fine cracks does not necessarily imply loss of coating integrity. This issue arose in the landing gear project during axial fatigue testing on smooth gage specimens where spallation of some HVOF coatings occurred. When observed it would quite often result in large sections of the coating being ejected from the substrate, analogous to the action of a spring. The spallation occurred almost exclusively on specimens that were subjected to fully reversed stresses, i.e., the maximum stress was applied in both tension and compression (R = -1). For coatings of approximate thickness 0.003", spallation was observed just below the yield stress of the base material. The stress level for spallation decreased with increasing coating thickness.

HVOF thermal spray coating spallation has been observed to a greater degree (meaning at a wider range of stresses) upon fracture of the fatigue specimen. This is attributed to the significant stresses applied to the coating as the specimen separates into two sections. A correlation between coating spallation at specimen fracture and coating integrity during actual testing has not been established.

The issue of coating integrity has resulted in adding to test protocols the periodic visual examinations of coated fatigue samples during testing. The problem in the GTE fatigue testing is that all tests were conducted with the specimens inside specially designed heating cells to

maintain the elevated temperatures. Thus, it was not possible to inspect the specimens during testing. Runout samples could of course be inspected but these were conducted at relatively low stresses and strains.

With the above caveats related to the ability to inspect the specimens during testing and inconclusive evidence of a correlation of coating spallation after fracture with coating integrity, a few observations can be made. In previous testing, there has been virtually no spallation of EHC coatings either during testing or after fracture. However, in some of these tests, there was spallation of the EHC coatings as indicated in Figure 4-48 which shows IN-718 specimens coated with 0.015" of EHC following LCF testing at 750 ºF. The figure also shows a runout specimen with extensive cracking of the hard chrome.

Spallation of the thermal spray coatings after specimen fracture when failure was inside the coated area was often observed. This is illustrated in Figure 4-49 which shows 4340 specimens coated with 0.015" of HVOF WC/Co following LCF testing at 300 ºF. However, it was observed that when fracture occurred outside of the coated area, spallation of the thermal spray coatings was not observed.

Significant cracking of any of the thermal sprayed coatings was rare. One example where circumferential or ring cracking was observed is indicated in Figure 4-50 which shows a runout IN-718 specimen coated with 0.015" of HVOF WC/Co following LCF testing at 750 ºF. Such cracking occurred on more LCF test specimens than on HCF test specimens, presumably because the stress ratio was greater for the LCF testing.

There was no correlation between thermal spray coating cracking or post-test spallation with substrate material, test temperature, or spray process (HVOF with $H_2$ fuel, HVOF with NG, or plasma spray).

**Figure 4-48 IN-718 Specimens Coated With 0.015" of EHC Following LCF Testing at 750 ºF.**

**Figure 4-49 4340 Specimens Coated With 0.015" of HVOF WC/Co Following LCF Testing at 300 ºF.**

**Figure 4-50 IN-718 Specimens Coated With 0.015" of HVOF WC/Co Following LCF Testing at 750 ºF.**

### 4.5.8. Discussion

Plasma spray WC/Co was dropped from the test matrix since it could not be deposited with the compressive stress required for good fatigue performance. Plasma spray T-400, however, was retained since (as the general fatigue results show) lower modulus Tribaloy coatings do not generally cause as large a fatigue debit.

For most substrate/coating combinations the fatigue of the thermal spray coated materials was better than EHC, as is generally the case for thermal spray (especially HVOF) coatings. However, 13% of the thermal spray curves fell below the hard chrome baseline. Table 4-36 is a statistical summary of those substrate/coating combinations showing fatigue inferior to the hard chrome baseline.

Clearly, the primary fatigue problems are with IN-718, especially at 750 °F (where half the WC-Co and $Cr_3C_2$-NiCr data fell below the baseline) and 17-4PH (where almost 40% of the 750 °F data fell below the baseline). It is not clear why these materials should show a larger debit; their hardness, elastic moduli, and coefficients of thermal expansion are similar to the other alloys and they do not appear to be particularly heat-sensitive so that they would be more strongly affected by the spray temperature. There are a great many factors that influence fatigue crack initiation, and it is not possible to understand why these coated materials are more fatigue-sensitive without extensive materials analysis.

It is known, however, that fatigue may be strongly affected by deposition conditions. The deposition conditions used for coating IN-718 and 17-4PH, as for coating all the other alloys, were determined by optimizing for fatigue of coated 4340 steel. However, it may well be that these alloys demand somewhat different deposition parameters for optimized fatigue. That this may be the case is shown by pre-HCAT data obtained in 1997 for HVOF WC/Co on IN-718 at 800 °F [4]. Both HVOF WC/Co and T-400 were optimized for deposition on IN-718 by a full DOE. While the fatigue curve for the T-400 was well above that of the hard chrome baseline, the curve for WC/Co was only a little above the EHC, and in fact appeared to fall a little below it at the highest stress. Although no prior data are available for 17-4PH, early data on 13-8Mo (another precipitation hardened stainless steel) showed very similar fatigue debits for HVOF carbide and EHC coatings [10]. Thus even a small change in the relative fatigue caused by small differences in the properties of either the thermal spray coating or the hard chrome can move the fatigue curve of the thermal spray coating above or below that of the EHC baseline.

Therefore, if carbides are to be used on IN-718 or 17-4PH the deposition parameters must be properly optimized for those alloys through a DOE analysis, with careful quality control to ensure their reproducibility.

## Table 4-36 Datasets Below Chrome Baseline.

| Alloy | Test condition | Temp F | Coating | Thickness | Fuel | Comments | |
|---|---|---|---|---|---|---|---|
| IN-718 | HCF | 300 | $Cr_3C_2$-NiCr | 0.015 | Hydrogen | | |
| IN-718 | LCF | 750 | $Cr_3C_2$-NiCr | 0.003 | Hydrogen | | |
| IN-718 | LCF | 750 | $Cr_3C_2$-NiCr | 0.015 | Hydrogen | | |
| IN-718 | LCF | 750 | $Cr_3C_2$-NiCr | 0.015 | Nat Gas | | |
| IN-718 | LCF | 750 | WC/Co | 0.003 | Hydrogen | | |
| IN-718 | LCF | 750 | WC/Co | 0.015 | Hydrogen | | |
| IN-718 | LCF | 750 | WC/Co | 0.015 | Nat Gas | | |
| IN-718 | LCF | 750 | T-800 | 0.015 | Nat Gas | | |
| IN-718 | LCF | 750 | T-400 | 0.015 | Nat Gas | | |
| IN-718 | HCF | 300 | T-400 | 0.015 | Hydrogen | | |
| IN-718 | HCF | 300 | WC/Co | 0.015 | Hydrogen | | |
| IN-718 | HCF | 300 | WC/Co | 0.015 | Nat Gas | Marginal | |
| 17-4PH | LCF | 750 | Plasma WC/Co | 0.003 | Hydrogen | | |
| 17-4PH | LCF | 750 | T-400 | 0.003 | Hydrogen | Marginal | |
| 17-4PH | LCF | 750 | T-800 | 0.003 | Hydrogen | Marginal | |
| 17-4PH | LCF | 750 | WC/Co | 0.003 | Hydrogen | | |
| AM-355 | LCF | 750 | WC/Co | 0.003 | Hydrogen | | |
| IN-901 | LCF | 750 | WC/Co | 0.015 | Hydrogen | | |

| Total fatigue tests | | | | Coatings below chrome baseline, by substrate alloy | | | |
|---|---|---|---|---|---|---|---|
| **Alloy** | **Sets** | **300 °F** | **750 °F** | **Below at 300 °F** | **%** | **Below at 750 °F** | **%** |
| IN-718 | 34 | 18 | 16 | 4 | 22% | 8 | 50% |
| 4340 | 19 | 19 | None | 0 | 0% | No test | |
| A-286 | 10 | 5 | 5 | 0 | 0% | 0 | 0% |
| AM-355 | 18 | 13 | 5 | 0 | 0% | 1 | 20% |
| IN-901 | 20 | 10 | 10 | 0 | 0% | 1 | 10% |
| 9310 | 6 | 6 | None | 0 | 0% | No test | |
| 17-4PH | 16 | 8 | 8 | 0 | 0% | 4 | 50% |
| **Totals** | **123** | **79** | **44** | **4** | | **14** | |

| Total fatigue tests | | | | Coatings below chrome baseline, by coating | | | |
|---|---|---|---|---|---|---|---|
| **Coating** | **Sets** | **300 °F** | **750 °F** | **Below at 300 °F** | **%** | **Below at 750 °F** | **%** |
| WC/Co | 33 | 22 | 11 | 2 | 9% | 7 | 64% |
| $Cr_3C_2$-NiCr | 18 | 12 | 6 | 1 | 8% | 3 | 50% |
| T-800 | 19 | 12 | 7 | 0 | 0% | 2 | 29% |
| T-400 | 27 | 17 | 10 | 1 | 6% | 2 | 20% |
| PS T-400 | 25 | 15 | 10 | 0 | 0% | 0 | 0% |
| **Totals** | **123** | **79** | **44** | **4** | | **14** | |
| | | | **Total %** | **Below Chrome** | **13%** | | |

### 4.5.9. Conclusions

The following conclusions can be drawn from the fatigue data:

1. For the majority of the alloy/coatings combinations involving HVOF WC/Co, HVOF $Cr_3C_2$/NiCr , HVOF T-800, HVOF T-400, and plasma spray T-400 in conjunction with AM-355, 4340, IN-901, A-286, and 9310, the fatigue performance was equal to or better than chrome. This encompassed 105/123 (85%) of the total coating evaluations.
2. There was a significant fatigue debit for IN-718 coated with WC-Co and $Cr_3C_2$-NiCr. IN-718 data accounted for 12 of the 18 results below the chrome baseline; 8 of these involved LCF at 750 °F and 4 involved HCF at 300 °F.
3. In all, LCF testing at 750 °F accounted for 14 out of the 18 results below chrome baseline. This is the first time that 750 °F testing has been conducted within the HCAT program.
4. The 17-4PH/coating combinations accounted for 4 out of the 18 below chrome baseline results, again involving 750 °F LCF data, but a variety of coatings. Early 13-8PH elevated temperature work also showed marginal results, indicating a possible issue with the coating of the PH series of materials.

There was no obvious reason for these trends, except for the possibility that the thermal spray parameters were not fully optimized for these materials.

# 4.6. Wear Testing

## 4.6.1. Data Summary

**Table 4-37 Quick Reference to Primary Data. Click Blue Links t o Jump to Data**

| Item | Item Number |
|---|---|
| Wear Test Matrix | Table 4-39 |
| Vickers Microhardness Values of Coatings and Substrates | Table 4-40 |
| Wear Coefficients for Coated Blocks 300 ºF | Figure 4-56 |
| Wear Coefficients for Uncoated Shoes 300 ºF | Figure 4-57 |
| Wear Coefficients for Coated Blocks 750 ºF | Figure 4-58 |
| Wear Coefficients for Uncoated Shoes 750 ºF | Figure 4-59 |

## 4.6.2. Test Rationale and Description

A fretting wear test was selected to simulate the dithering or vibration movement between two mating components that are typical in gas turbine engines. It was believed that there were no standard ASTM wear tests that would accurately reflect conditions of use for GTE components, so a dedicated wear test that is used by GE Aircraft Engines was selected.

The test configuration is shown schematically in Figure 4-51. The coating to be evaluated is applied to one face of a metal block. A metal shoe with a small contact area is placed against the coated block with a uniform load applied. The block is then oscillated in a direction perpendicular to the applied load with a short stroke and fairly high frequency.

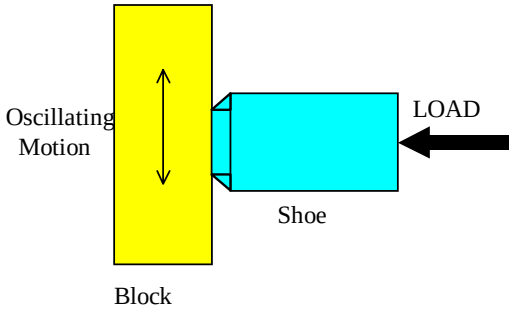


**Figure 4-51 Schematic of Fretting Test**

The wear test plan in the GTE Materials JTP indicated that there would be an extensive series of more than 240 tests carried out under a DOE approach. There were to have been tests with different alloys used for the coated blocks (similar to the alloys used in the fatigue testing), two different loads, two different coating thicknesses (0.003” and 0.015”) and two different surface finishes. All of the planned coated test blocks were prepared. However, due to funding and time constraints, it was not possible to carry out all of the specified wear tests.

Since wear is principally a surface phenomenon, it was decided that the block material was not a critical parameter, so virtually all of the blocks used in the wear tests were fabricated from 4340 steel. Since the principal objective was a comparison of thermal spray wear performance versus hard chrome wear performance, some preliminary wear measurements were taken on hard chrome to verify a measurable wear rate that was capable of discriminating between different

coating materials. Once that load was established, then the same load was used for all subsequent wear tests. In addition, only one surface finish on the coatings was used. The mating alloys (shoes) consisted of IN-718, IN-901, 17-4PH and M50 which are typically used in GTE engines. The M50 was selected because a major application of hard chrome in engines is on bearing journals and these are often fabricated from this alloy.

### 4.6.3. Specimen Fabrication and Preparation

The materials from which the wear test blocks and shoes were fabricated were in the heat-treat condition as specified in Section 4.2. Figure 4-52 and Figure 4-53 are schematics of the shoes and blocks, respectively. The samples were rough machined, stress relieved as necessary, and low-stress ground to final dimension. Grinding was performed in accordance with MIL-STD-866 and GE low stress grind specifications. The final surface finish on the shoes was 6-12 microinches Ra. The one face of the blocks onto which the coating was to be applied was shot peened as specified in Section 4.2. The final surface finish on the face was 6-12 microinches Ra.

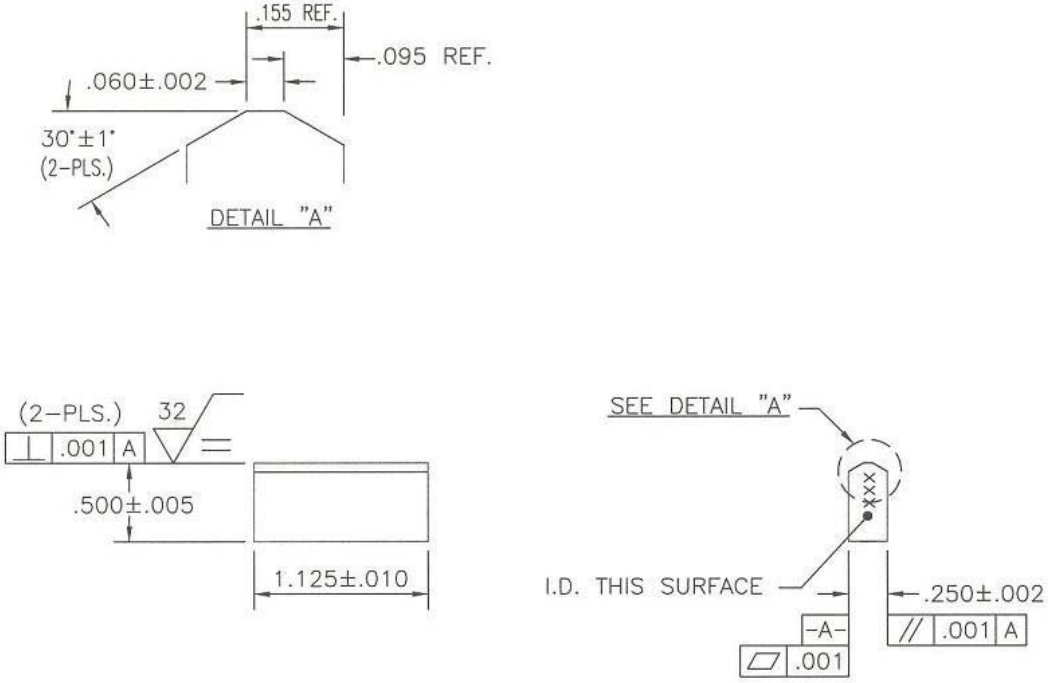


**Figure 4-52 Schematic of the Shoe Used in the Wear Testing**

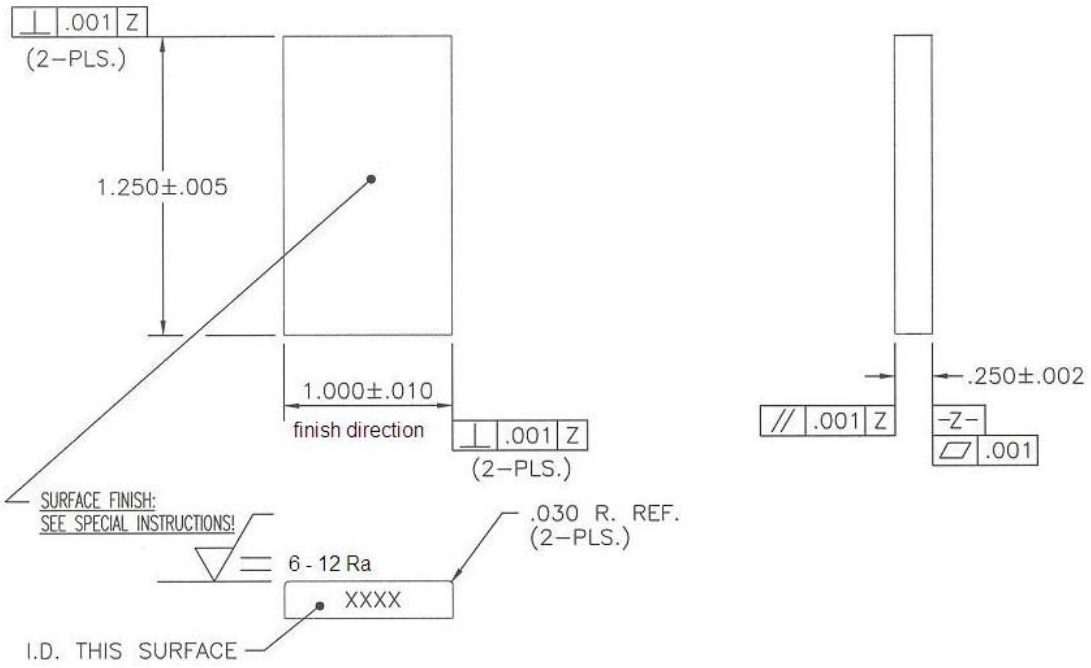


**Figure 4-53 Schematic of the Block onto which the Coating was Applied for the Wear Testing**

### 4.6.4. Coating Deposition

The coatings that were applied to the one prepared face of the blocks were EHC, HVOF WC/17Co, HVOF $Cr_3C_2$/NiCr, HVOF T-800 and plasma spray (PS) T-400. Plasma spray WC-Co was to have been tested, but could not be produced with compressive residual stress, which is required for good fatigue performance, as described in Section 4.4.

The test blocks to be chrome plated were grit blasted with #13 glass bead or 220-grit aluminum oxide per QQ-C-320 not more than 2 hours prior to application of the coating. Then they were solvent wiped with reagent grade acetone and/or isopropyl alcohol. The EHC coatings were deposited on the test blocks at NADEP Jacksonville at a temperature of 130 $^{o}$F in accordance with MIL-STD-1501 Class 1, Type 1 supported by QQ-C-320. No interfacial layer was used between the specimen and EHC coating. Also, no sealer was applied to the EHC. The thickness values were 0.003" and 0.015" ± 0.0005" subsequent to grinding (i.e., coatings were deposited approximately 0.002" to 0.004" thicker than specified and then ground to final dimension). All as-plated specimens were baked 24 hrs at 375 ± 25 $^{o}$F within four hours after plating for hydrogen embrittlement relief prior to grinding to final dimension.

The test blocks to receive the thermal spray coatings were grit blasted with 54 grit aluminum oxide at 60 psi in accordance with MIL-STD-1504 except that a 45-degree angle of impingement was used. The standoff distance was 4-6 inches. The HVOF coatings were deposited at Hitemco using a Sulzer Metco Diamond Jet 2600 hybrid gun with hydrogen as the primary fuel gas and with nitrogen as the secondary gas. The plasma spray T-400 coatings were deposited at Hitemco using a Metco 3M system. Optimized deposition parameters as delineated in Section 4.4 of this report were used.

Air cooling and/or built in pause times off the specimens were utilized to ensure the surface temperature did not exceed 350 $^{o}$F. The thermal spray coatings were deposited directly onto the substrate material with no interfacial layer. The thickness values were 0.003" and 0.015" ± 0.0005" subsequent to grinding (i.e., coatings were deposited approximately 0.002" to 0.004" thicker than specified and then ground to final dimension). All HVOF coatings were deposited with residual compressive stress (Almen N values ranging from 4 to 12). The plasma-sprayed T-400 was deposited with residual tensile stress (Almen N values ranging from 0 to -2).

Subsequent to deposition, each coating was low-stress ground in accordance with MIL-STD-866 and GEAE Word Drawing 4013195-990 to a surface finish of 6-12 microinches Ra. It was decided that only as-ground coating thicknesses of 0.003" would be evaluated so those test blocks designated for wear testing that had the thicker coatings were ground such that the final thickness was 0.003".

### 4.6.5. Wear Test Methodology

As discussed in Section 4.6.2, the initial thrust of the fretting wear test matrix was to use a DOE configuration in which there were a number of variables (base metal alloy, coating material, surface finish, ambient test temperature, mating alloy, and coating thickness). This would have resulted in wear coefficient data that could be analyzed for each type of coating material and shoe type with a minimum number of tests. This would then have allowed for prediction of wear life for combinations not actually included in the wear matrix. However, due to funding and time constraints, it was evident that this work scope could not be accomplished and it was decided to conduct simple relative comparisons between EHC-plated and thermal-sprayed coatings sliding against different materials at two different temperatures. This could be accomplished using just the coated 4340 blocks as specified in the Materials JTP with the exception of those coated with $Cr_3C_2$/NiCr for which there were an insufficient number of samples. In that case, four IN-901 blocks with those coatings were also tested.

A small number of tests were run in initial screening work to determine the proper testing conditions which would allow for definitive ranking of coating performance. Then, a total of 77 fretting wear tests were conducted using the test conditions as specified in Table 4-38. The lower number of cycles for those tests conducted using the IN-901 shoes was because of the higher rate of wear on that material.

The contact area of the shoe on the block was 0.0675 square inches (0.06" x 1.125" – see Figure 4-52). Thus, the contact stress was 53.3 ksi.

**Table 4-38 Wear Test Parameters**

| Parameter | Value |
|---|---|
| Load | 3600 lbs |
| Duration | 25,000 cycles (12,500 cycles for IN-901 shoes) |
| Frequency | 4 Hz |
| Stroke(Total length of travel per cycle) | .060" |
| Temperature | 300$^{o}$/750 $^{o}$F |
| Lubrication | Dry |

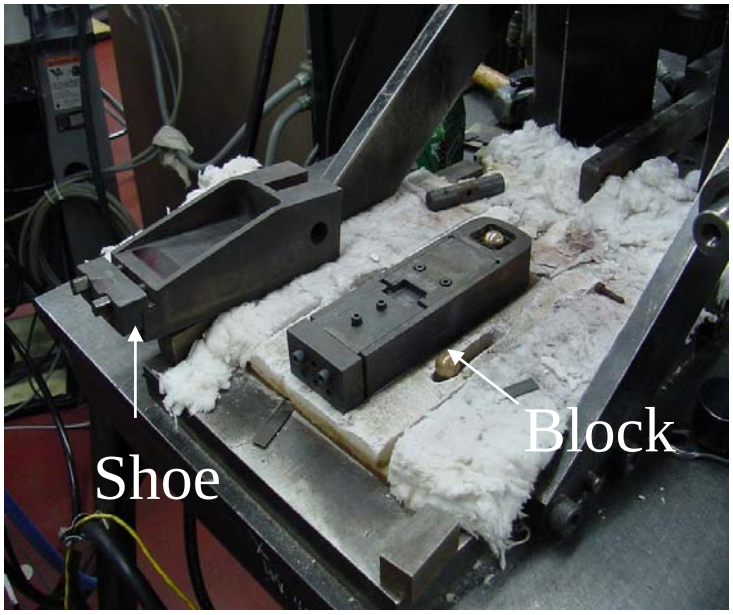


**Figure 4-54 Components of the Wear Test Apparatus Disassembled**

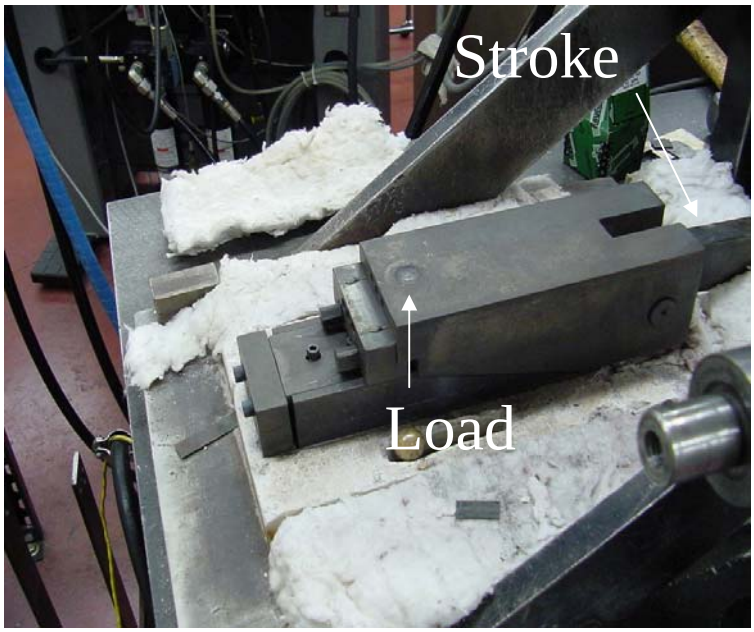


**Figure 4-55 Components of the Wear Test Apparatus Assembled**

Figure 4-54 shows the components of the wear test apparatus disassembled and Figure 4-55 shows the components assembled and ready for testing.

In general, there were two tests conducted for each specific condition of coating/shoe/ temperature. The wear coefficients on the coated blocks were determined by taking the average

of nine equally spaced measurements of the depth relative to the original surface made across the width of the wear scar. The wear coefficients on the shoes were determined by taking nine equally spaced measurements of material removal across the width of the face. In those cases where widely differing values of wear were obtained for the two tests, a third test was conducted for those conditions. Table 4-39 lists all of the individual wear tests that were conducted, indicating the mating shoe material, the block material, the coating on the block and the test temperature.

### 4.6.6. Test Results

Figure 4-56 and Figure 4-57 show the wear coefficients for the coated blocks and shoes, respectively, for testing done at 300 ºF. Figure 4-58 and Figure 4-59 show the wear coefficients for the coated blocks and shoes, respectively, for testing done at 750 ºF. Triplicate data on all graphs has been designated with a cross-hatch pattern. The data is arranged in material hardness order from the M-50 to IN-901 shoes, with the Rockwell C hardness values indicated at the top of each set of data. The coatings are also arranged in hardness order, with the exception of chrome which is shown first for comparative purposes. The hardness values for all the coatings and shoes are summarized in Table 4-40 (with Rockwell C numbers converted to Vickers microhardness numbers for the shoes).

## Table 4-39 Matrix of Fretting Wear Tests Indicating the Shoe and Block Material, the Coating on the Block and the Test Temperature

| Test No. | Shoe | Block | Coating | Temp | Test No. | Shoe | Block | Coating | Temp |
|---|---|---|---|---|---|---|---|---|---|
| 1 | M50 | 4340 | EHC | 300 | 41 | IN718 | 4340 | PS T400 - 66F | 750 |
| 2 | M50 | 4340 | EHC | 300 | 42 | IN718 | 4340 | PS T400 - 66F | 750 |
| 3 | M50 | 4340 | EHC | 750 | 43 | IN901 | 4340 | EHC | 300 |
| 4 | M50 | 4340 | EHC | 750 | 44 | IN901 | 4340 | EHC | 300 |
| 5 | M50 | 4340 | HVOF WCCo - 2005 | 300 | 45 | IN901 | 4340 | EHC | 300 |
| 6 | M50 | 4340 | HVOF WCCo - 2005 | 300 | 46 | IN901 | 4340 | EHC | 750 |
| 7 | M50 | 4340 | HVOF WCCo - 2005 | 750 | 47 | IN901 | 4340 | EHC | 750 |
| 8 | M50 | 4340 | HVOF WCCo - 2005 | 750 | 48 | IN901 | 4340 | HVOF WCCo - 2005 | 300 |
| 9 | M50 | 4340 | HVOF Cr3C2 - 3007 | 300 | 49 | IN901 | 4340 | HVOF WCCo - 2005 | 300 |
| 10 | M50 | 4340 | HVOF Cr3C2 - 3007 | 300 | 50 | IN901 | 4340 | HVOF WCCo - 2005 | 750 |
| 11 | M50 | 4340 | HVOF Cr3C2 - 3007 | 300 | 51 | IN901 | 4340 | HVOF WCCo - 2005 | 750 |
| 12 | M50 | **IN901** | HVOF Cr3C2 - 3007 | 750 | 52 | IN901 | 4340 | HVOF T800 - 3001 | 300 |
| 13 | M50 | **IN901** | HVOF Cr3C2 - 3007 | 750 | 53 | IN901 | 4340 | HVOF T800 - 3001 | 300 |
| 14 | M50 | 4340 | HVOF T800 - 3001 | 300 | 54 | IN901 | 4340 | HVOF T800 - 3001 | 750 |
| 15 | M50 | 4340 | HVOF T800 - 3001 | 300 | 55 | IN901 | 4340 | HVOF T800 - 3001 | 750 |
| 16 | M50 | 4340 | HVOF T800 - 3001 | 300 | 56 | IN901 | 4340 | PS T400 - 66F | 300 |
| 17 | M50 | 4340 | HVOF T800 - 3001 | 750 | 57 | IN901 | 4340 | PS T400 - 66F | 300 |
| 18 | M50 | 4340 | HVOF T800 - 3001 | 750 | 58 | IN901 | 4340 | PS T400 - 66F | 750 |
| 19 | M50 | 4340 | PS T400 - 66F | 300 | 59 | IN901 | 4340 | PS T400 - 66F | 750 |
| 20 | M50 | 4340 | PS T400 - 66F | 300 | 60 | IN901 | 4340 | PS T400 - 66F | 750 |
| 21 | M50 | 4340 | PS T400 - 66F | 750 | 61 | 17-4PH | 4340 | EHC | 300 |
| 22 | M50 | 4340 | PS T400 - 66F | 750 | 62 | 17-4PH | 4340 | EHC | 300 |
| 23 | IN718 | 4340 | EHC | 300 | 63 | 17-4PH | 4340 | EHC | 750 |
| 24 | IN718 | 4340 | EHC | 300 | 64 | 17-4PH | 4340 | EHC | 750 |
| 25 | IN718 | 4340 | EHC | 750 | 65 | 17-4PH | 4340 | HVOF WCCo - 2005 | 300 |
| 26 | IN718 | 4340 | EHC | 750 | 66 | 17-4PH | 4340 | HVOF WCCo - 2005 | 300 |
| 27 | IN718 | 4340 | HVOF WCCo - 2005 | 300 | 67 | 17-4PH | 4340 | HVOF WCCo - 2005 | 300 |
| 28 | IN718 | 4340 | HVOF WCCo - 2005 | 300 | 68 | 17-4PH | 4340 | HVOF WCCo - 2005 | 750 |
| 29 | IN718 | 4340 | HVOF WCCo - 2005 | 300 | 69 | 17-4PH | 4340 | HVOF WCCo - 2005 | 750 |
| 30 | IN718 | 4340 | HVOF WCCo - 2005 | 750 | 70 | 17-4PH | 4340 | HVOF T800 - 3001 | 300 |
| 31 | IN718 | 4340 | HVOF WCCo - 2005 | 750 | 71 | 17-4PH | 4340 | HVOF T800 - 3001 | 300 |
| 32 | IN718 | 4340 | HVOF WCCo - 2005 | 750 | 72 | 17-4PH | 4340 | HVOF T800 - 3001 | 750 |
| 33 | IN718 | **IN901** | HVOF Cr3C2 - 3007 | 750 | 73 | 17-4PH | 4340 | HVOF T800 - 3001 | 750 |
| 34 | IN718 | **IN901** | HVOF Cr3C2 - 3007 | 750 | 74 | 17-4PH | 4340 | PS T400 - 66F | 300 |
| 35 | IN718 | 4340 | HVOF T800 - 3001 | 300 | 75 | 17-4PH | 4340 | PS T400 - 66F | 300 |
| 36 | IN718 | 4340 | HVOF T800 - 3001 | 300 | 76 | 17-4PH | 4340 | PS T400 - 66F | 750 |
| 37 | IN718 | 4340 | HVOF T800 - 3001 | 750 | 77 | 17-4PH | 4340 | PS T400 - 66F | 750 |
| 38 | IN718 | 4340 | HVOF T800 - 3001 | 750 | | | | | |
| 39 | IN718 | 4340 | PS T400 - 66F | 300 | | | Indicates | Triplicate Test | |
| 40 | IN718 | 4340 | PS T400 - 66F | 300 | | | | | |

**Table 4-40. Vickers Microhardness Values for Coatings and Test Shoes.**

| Coating | Microhardness |
|---|---|
| EHC | 950 |
| HVOF WC/Co | 1100 |
| HVOF $Cr_3C_2$/NiCr | 1000 |
| HVOF T-800 | 700 |
| PS T-400 | 550 |
| **Shoe** | |
| M50 | 720 |
| IN-718 | 430 |
| 17-4PH | 380 |
| IN-901 | 340 |

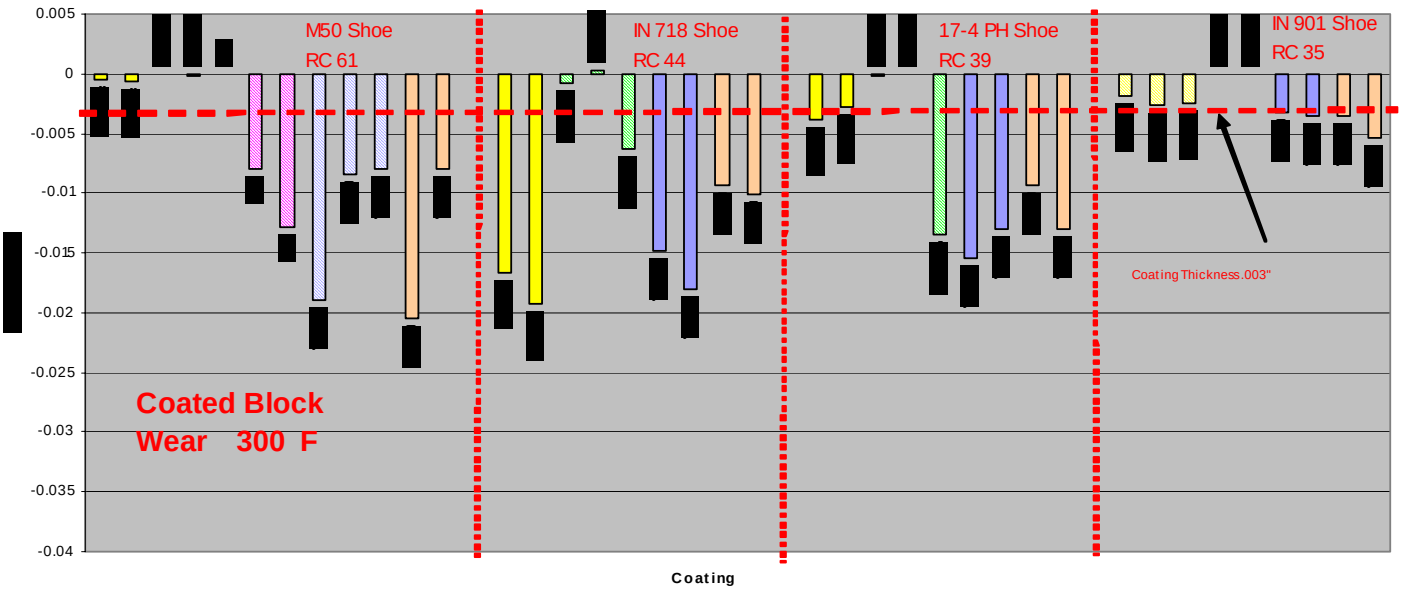


**Figure 4-56 Wear Coefficients (Plotted as Average Wear Depth) for Coated Blocks Against the Four Different Shoe Materials for Testing at 300 ºF.**

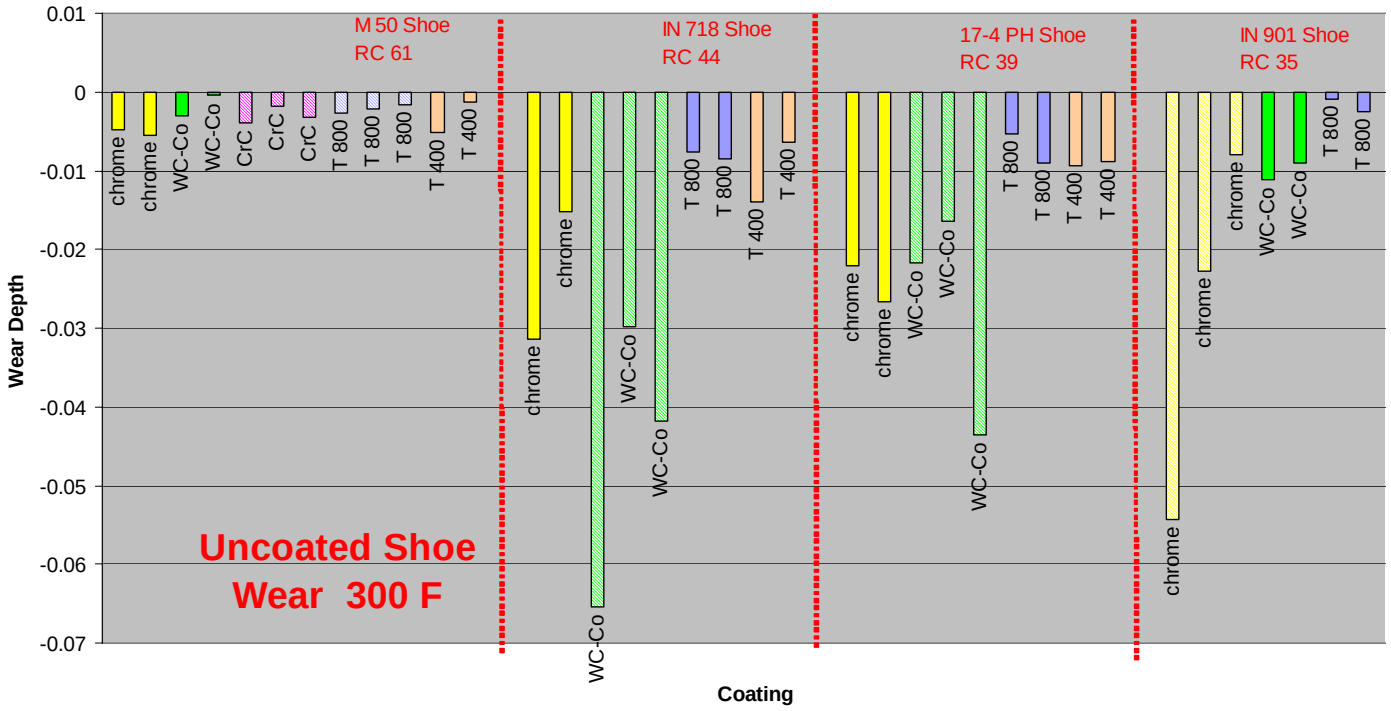


**Figure 4-57 Wear Coefficients (Plotted as Average Wear Depth) for Shoes Sliding Against the Indicated Coatings for Testing at 300 ºF**

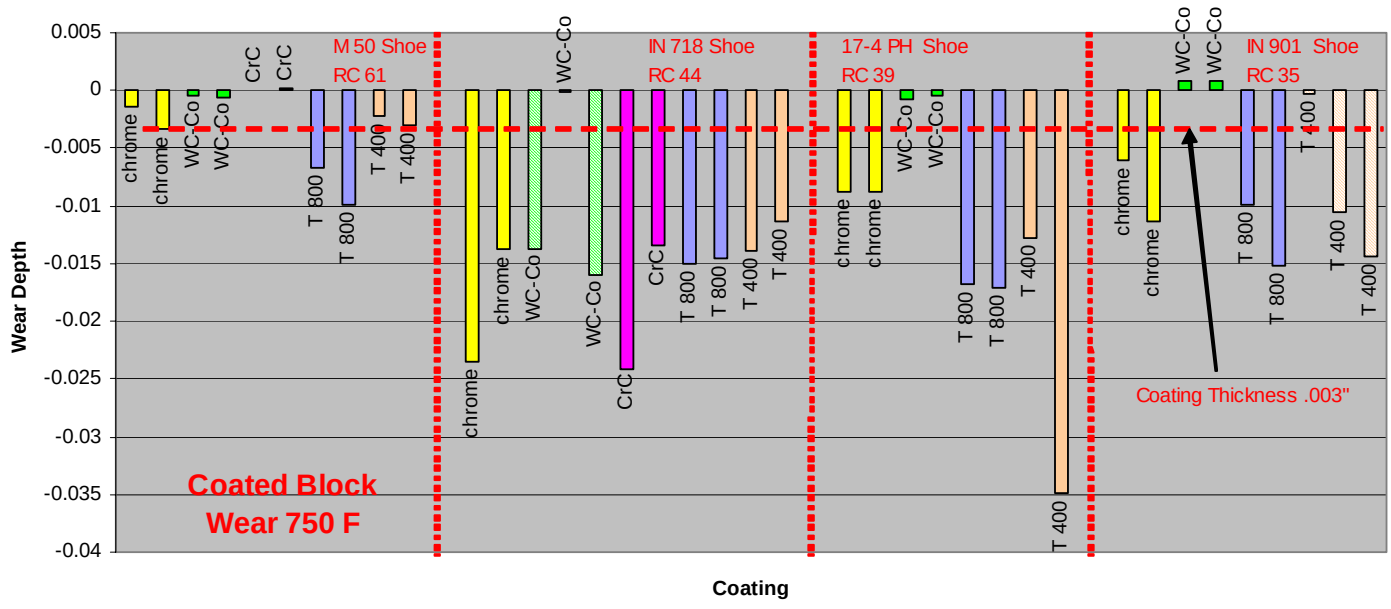


**Figure 4-58 Wear Coefficients (Plotted as Average Wear Depth) for Coated Blocks Sliding Against the Four Different Shoe Materials for Testing at 750 ºF**

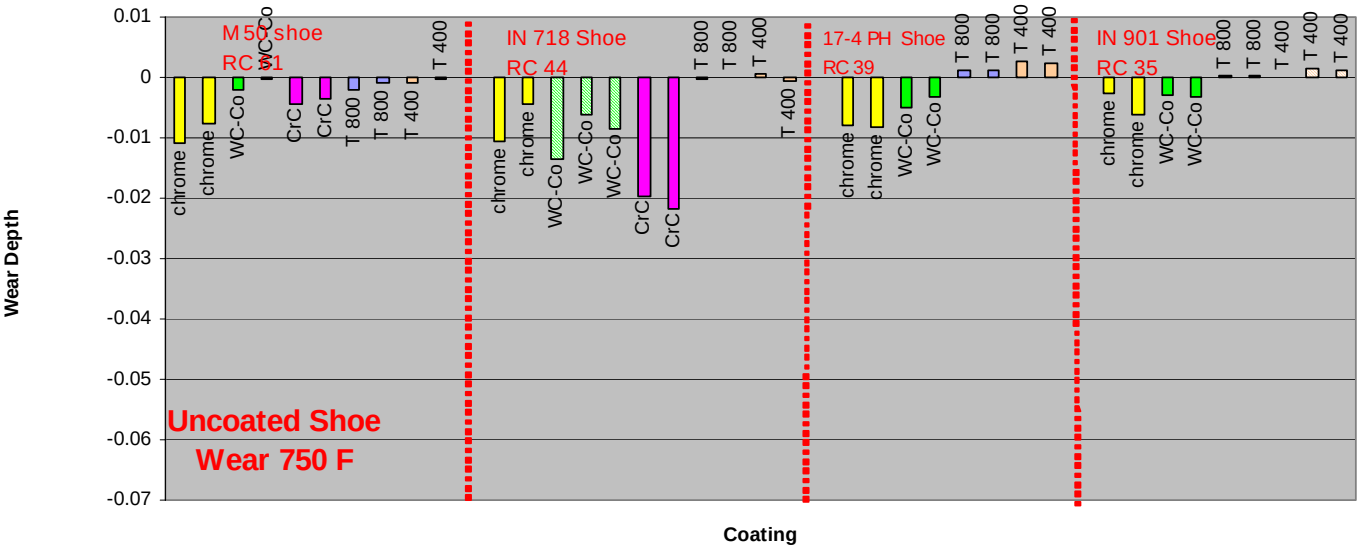


**Figure 4-59 Wear Coefficients (Plotted as Average Wear Depth) for Shoes Sliding Against the Indicated Coatings for Testing at 750 ºF**

Figure 4-60 through Figure 4-65 are photographs of selected samples following wear testing. Figure 4-60 shows the WC/Co-coated block and the mating IN-718 shoe following wear testing at 300 ºF (Test #27). Although it appears that there has been substantial wear to the coating, in fact, as indicated in Figure 4-56, the wear depth was only about 0.002". On the other hand, the wear of the IN-718 was substantial, with approximately 0.065" of material removed (see Figure 4-57).

Figure 4-61 shows the EHC-coated block and the mating IN-718 shoe following wear testing at 300 ºF (Test #23). The amount of wear on the hard chrome was substantial, with an average depth of 0.017" in the wear track as indicated in Figure 4-56. The amount of wear on the IN-718 was likewise substantial, with approximately 0.031" of material removed as indicated in Figure 4-57.

Figure 4-62 shows the $Cr_3C_2$/NiCr-coated block and the mating M50 shoe following wear testing at 300 ºF (Test #9). The amount of wear on the coating was moderate, with an average depth of 0.012" in the wear track as indicated in Figure 4-56. There was very little wear of the M50 shoe as indicated in Figure 4-57.

Figure 4-63 shows the WC/Co-coated block and the mating M50 shoe following wear testing at 750 ºF (Test #7). As indicated in Figure 4-58 and Figure 4-59, there was very little wear on either surface.

Figure 4-64 shows the WC/Co-coated block and the mating IN-718 shoe following wear testing at 750 ºF (Test #30). In this case there was moderate wear on both the coating (0.014") and on the shoe (0.013") as indicated in Figure 4-58 and Figure 4-59.

Figure 4-65 shows the PS T-400-coated block and the mating IN-901 shoe following wear testing at 750 ºF (Test #58). The amount of wear on the coating was moderate, with an average depth of 0.011" in the wear track as indicated in Figure 4-58. There was evidence of material transfer from the block to the shoe as indicated by a net growth in the thickness of the shoe (Figure 4-59).

Figure 4-66 shows the EHC-coated block and the mating 17-4PH shoe following wear testing at 750 ºF (Test #63). There was moderate wear on both the coating (0.009") and on the shoe (0.008") as indicated in Figure 4-58 and Figure 4-59.

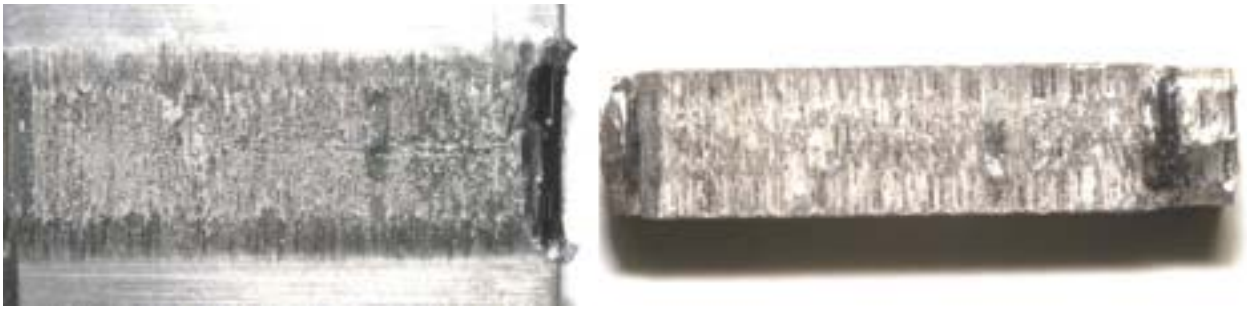

**Figure 4-60 WC/Co-coated Block (left) and the Mating IN-718 Shoe (right) Following Wear Testing at 300 ºF (Test #27)**

**Figure 4-61 EHC-coated Block (left) and the Mating IN-718 Shoe (right) Following Wear Testing at 300 ºF (Test #23)**

**Figure 4-62 WC/Co-coated Block (left) and the Mating IN-718 Shoe (right) Following Wear Testing at 750 ºF (Test #30)**

**Figure 4-63 WC/Co-coated Block (left) and the Mating M50 Shoe (right) Following Wear Testing at 750 ºF**

**Figure 4-64 $Cr_3C_2$/NiCr-coated Block (left) and the Mating M50 Shoe (right) Following Wear Testing at 300 ºF (Test #9)**

**Figure 4-65 PS T-400-coated Block (left) and the Mating IN-901 Shoe (right) Following Wear Testing at 750 ºF (Test #58)**

**Figure 4-66 EHC-coated Block (left) and the Mating 17-4PH Shoe (right) Following Wear Testing at 750 ºF (Test #63)**

### 4.6.7. Discussion

One problem with the wear testing is that in many cases the wear on the coated blocks extended through the coating thickness (0.003") and into the substrate material (in most cases 4340 steel). Therefore, conclusions drawn in these cases based on total amount of wear are tenuous at best. However, relative performance can still be inferred on the assumption that consistent wear rates are obtained for any given shoe material sliding against the 4340 steel. For example, if for one coating/block the total wear was 0.020" (extending 0.017" beyond the coating) whereas for another coating/block the total wear was 0.010" (extending 0.007" beyond the coating), then it can be concluded that it took longer to wear through the second coating than the first.

One general observation that can be made is that, except for the M50 shoe, the coating/block wear is higher at 750 ºF than at 300 ºF whereas for the shoe the opposite is the case. The difference is

particularly noteworthy for the shoes, where the wear is much lower at the higher temperature. It is not clear what is the reason for this, but it could be due to the formation of a thicker oxide film at the higher temperature that would provide a harder and/or more lubricious surface on the shoes.

It is difficult to establish any significant trends related to hardness and wear rates (a correlation that does not necessarily exist in sliding wear). It is apparent that the wear of the hardest shoe material, M50, is much less than for the other shoes at 300 ºF, regardless of the coating against which it is sliding. At 750 ºF, however, the wear of the M50 shoes is comparable to that for the other shoes. The IN-901 shoes generally show less wear than the IN-718 shoes at either temperature and against any coating, even though the IN-901 is softer than the IN-718.

Related to hardness of the coating, the wear of the hardest coating, WC/Co, is less than for any other coating regardless of the shoe material against which it is sliding. However, the wear of the $Cr_3C_2$/NiCr coatings for those cases tested is generally only comparable to the much softer HVOF T-800 and PS T-400.

The general objective of the study was a comparison of the performance of the different thermal spray coatings to hard chrome, both for the wear of the coating and the wear of the mating material. Related to that comparison, the following observations can be made:

300 ºF:

For sliding against the M50 shoe, it is clear that the performance of the WC/Co in terms of both the coating wear and the total system wear (coating + shoe) is superior to hard chrome. The wear performance of the other coatings sliding against the M50 shoe was inferior to that of hard chrome.

For sliding against the IN-718 shoe, the wear of WC/Co was less than for hard chrome, but the wear of the shoe was significantly higher, with total system wear higher for WC/Co than for hard chrome. Coating wear for HVOF T-800 and PS T-400 was comparable to chrome, but the total system wear for these coatings was somewhat less than for hard chrome.

For sliding against the 17-4PH shoes, the results are inconclusive, with the wear of the hard chrome and WC/Co coatings less than for the HVOF T-800 and PS T-400 coatings, but with the wear of the shoes less for the latter two coatings than for the hard chrome and WC/Co. Thus, there was not much difference in total system wear for these combinations.

For sliding against the IN-901 shoes, the wear of the WC/Co coatings was less than for hard chrome, with the wear of the HVOF T-800 and PS T-400 coatings comparable to hard chrome. However, total system wear for all of the thermal spray coatings was significantly less than for chrome.

750 ºF:

For sliding against the M50 shoe, the wear of all of the thermal spray coatings was comparable to hard chrome. In terms of total system wear, all of the thermal spray coatings were superior to hard chrome with the exception of HVOF T-800.

For sliding against the IN-718 shoe, the wear rates for all coatings were comparable (except for one WC/Co coating where there was virtually no wear). The shoe wear was substantially less for the HVOF T-800 and PS T-400 coatings than for the other coatings, thereby indicating that total system wear was less for those coatings.

For sliding against the 17-4PH shoes, the wear rate for WC/Co was significantly lower than for hard chrome and the other thermal spray coatings, with total system wear substantially less as well. The wear rates for the HVOF T-800 and PS T-400 coatings were higher than for hard chrome, but the shoe wear was less, resulting in comparable total system wear rates.

For sliding against the IN-901 shoes, the wear rate for WC/Co was essentially zero, significantly lower than for hard chrome and the other thermal spray coatings, with total system wear substantially less as well. The wear rates for the HVOF T-800 and PS T-400 coatings were slightly higher than for hard chrome, but the shoe wear was less, resulting in comparable total system wear rates.

### 4.6.8. Conclusions

As indicated above, the fact that the wear for the majority of the coated blocks extended beyond the 0.003" coating thickness, with total wear ranging up to 0.021" at 300 ºF and up to 0.035" at 750 ºF, makes quantitative comparisons difficult. However, there are some conclusions than can be inferred from the results.

More definitive conclusions can be drawn from the results at 750 ºF than from the results at 300 ºF. At the higher temperature, WC/Co performed significantly better than hard chrome and the other thermal spray coatings for all mating materials except for the IN-718 shoes where the performance was comparable to hard chrome. This was the case for both coating wear and total system wear. One item of concern is the high rates of wear for all coatings sliding against the IN-718 since this is a common engine material.

The results for testing at 300 ºF are less definitive. For sliding against M50, WC/Co is the superior coating, with slightly lower coating and total system wear rates. The other thermal spray coating wear rates were substantially higher. For sliding against IN-718, the wear rates for the WC/Co were very low, but the mating surface wear was exceptionally high, making total system performance lower than for hard chrome. In this case, HVOF T-800 or PS T-400 provides total system wear performance comparable to hard chrome. For sliding against PH17-4, total system performance for any of the thermal spray coatings is essentially comparable to hard chrome. Finally, for sliding against IN-901, the WC/Co coatings provide substantially lower coating and mating surface wear rates than for hard chrome. Within the thermal spray coatings, the WC/Co coatings had lower wear rates whereas the HVOF T-800 and PS T-400 had lower mating surface wear rates.

Overall, out of the eight combinations of mating surface and temperature, WC/Co is the clear choice for six, with HVOF T-800 or PS T-400 the choice for lower temperature sliding against IN-718 and 17-4PH.

## 4.7. Corrosion

### 4.7.1. Specimen Fabrication and Preparation

The substrate materials onto which the coatings were applied were 4340 steel and Inconel 718 (IN-718). For 4340, two different specimen geometries were used for the corrosion studies – rod and plate. For IN-718, only rods were used. The rods were 1" diameter and 6" in length, and the plates were 3" x 4" x ¼" thick. The curved surface on the rods and one face on the plates were ground to a 32 micro-inch Ra finish. Each specimen was heat treated as indicated in Table 4-3.

The curved surface of the rods and the flat surface of the plates onto which the coatings were applied were shot-peened with cut wire in accordance with AMS-2432 under computer control. The shot peening was conducted over the entire surface with a 100% surface coverage.

Subsequent to shot peening, the curved surface of the rods and the flat surface of the plates onto which the coatings were applied were grit blasted not more than 2 hours prior to application of the coating. Standard surface preparation for the chrome-plated specimens involved grit blasting with #13 glass bead or 220 grit aluminum oxide per QQ-C-320. Standard surface preparation for the surfaces to receive the thermal spray coatings involved grit blasting with 54 grit aluminum oxide at 60 psi at a 45 degree angle of impingement in accordance with MIL-STD-1504 (except angle). A uniform standoff distance of 4-6 inches was used.

### 4.7.2. Application of Coatings to Specimens

Table 4-41 indicates the coatings that were deposited onto the different specimens.

EHC was deposited on the samples in accordance with MIL-STD-1501, supported by QQ-C-320. The thicknesses were 0.003" and 0.015" ± 0.0005" subsequent to grinding (i.e., coatings were deposited approximately 0.002" to 0.004" thicker than specified and then ground to final dimension). A sulfamate Ni underlayer was applied to a minimum thickness of 0.0015" in accordance with specification QQ-N-290 on some of the specimens as indicated in Table 4-41. No sealer was applied to any of the coatings. The coatings were applied to the curved surface of the rods except for a 1.25" length at one end which is the portion that was inside the specimen holder in the corrosion cabinet. The coatings were applied to the one face of the plates except for a 1"-wide area at one end that was inside the specimen holder in the corrosion cabinet. All as-plated specimens were baked at 375 °F ± 25 °F within four hours after plating for a total of 24 hours prior to grinding to final dimension for hydrogen embrittlement relief and to enhance coating adhesion.

The thermal spray coatings identified in Table 4-41 were deposited onto the specimens using the exact same equipment, powders, gases, and deposition parameters as specified in Section 4.4. Air cooling and/or built-in pause times off the specimen as required were utilized to ensure the specimen surface temperature did not exceed 350 °F. The coating thicknesses were 0.003" and 0.015" ± 0.0005" subsequent to grinding (i.e., the coatings were deposited approximately 0.002" to 0.004" thicker than specified and then ground to final dimension).

**Table 4-41 Type of Coatings, Thicknesses and Number of Specimens for Each Material and Specimen Geometry that were Subjected for Corrosion Testing**

| Specimen Geometry | Material | Coating | Thickness (inches) | Ni under-Layer | No. of Specimens |
|---|---|---|---|---|---|
| Rod | 4340 | EHC | 0.003 | No | 3 |
| Rod | 4340 | EHC | 0.003 | Yes | 3 |
| Plate | 4340 | EHC | 0.003 | No | 3 |
| Rod | 4340 | EHC | 0.015 | No | 3 |
| Rod | 4340 | EHC | 0.015 | Yes | 3 |
| Plate | 4340 | EHC | 0.015 | No | 3 |
| Rod | 4340 | HVOF Tribaloy 400 | 0.003 | No | 3 |
| Plate | 4340 | HVOF Tribaloy 400 | 0.003 | No | 3 |
| Rod | 4340 | HVOF Tribaloy 400 | 0.015 | No | 3 |
| Plate | 4340 | HVOF Tribaloy 400 | 0.015 | No | 3 |
| Rod | 4340 | HVOF Tribaloy 800 | 0.003 | No | 3 |
| Plate | 4340 | HVOF Tribaloy 800 | 0.003 | No | 3 |
| Rod | 4340 | HVOF Tribaloy 800 | 0.015 | No | 3 |
| Plate | 4340 | HVOF Tribaloy 800 | 0.015 | No | 3 |
| Rod | 4340 | HVOF $Cr_3C_2$/NiCr | 0.003 | No | 3 |
| Plate | 4340 | HVOF $Cr_3C_2$/NiCr | 0.003 | No | 3 |
| Rod | 4340 | HVOF $Cr_3C_2$/NiCr | 0.015 | No | 3 |
| Plate | 4340 | HVOF $Cr_3C_2$/NiCr | 0.015 | No | 3 |
| Rod | 4340 | PS Tribaloy 400 | 0.003 | No | 3 |
| Plate | 4340 | PS Tribaloy 400 | 0.003 | No | 3 |
| Rod | 4340 | PS Tribaloy 400 | 0.015 | No | 3 |
| Plate | 4340 | PS Tribaloy 400 | 0.015 | No | 3 |
| Rod | IN-718 | EHC | 0.003 | No | 3 |
| Rod | IN-718 | EHC | 0.003 | Yes | 3 |
| Rod | IN-718 | EHC | 0.015 | No | 3 |
| Rod | IN-718 | EHC | 0.015 | Yes | 3 |
| Rod | IN-718 | HVOF Tribaloy 400 | 0.003 | No | 3 |
| Rod | IN-718 | HVOF Tribaloy 400 | 0.015 | No | 3 |
| Rod | IN-718 | HVOF Tribaloy 800 | 0.003 | No | 3 |
| Rod | IN-718 | HVOF Tribaloy 800 | 0.015 | No | 3 |
| Rod | IN-718 | HVOF $Cr_3C_2$/NiCr | 0.003 | No | 3 |
| Rod | IN-718 | HVOF $Cr_3C_2$/NiCr | 0.015 | No | 3 |
| Rod | IN-718 | PS Tribaloy 400 | 0.003 | No | 3 |
| Rod | IN-718 | PS Tribaloy 400 | 0.015 | No | 3 |
| | | | | **TOTAL** | **102** |

No sealer was applied to the thermal spray coatings. The coatings were applied to the curved surface of the rods except for a 1.25" length at one end which is the portion that was inside the specimen holder in the corrosion cabinet. The coatings were applied to the one face of the plates except for a 1"-wide area at one end that was inside the specimen holder in the corrosion cabinet.

Subsequent to deposition, each coating was ground in accordance with MIL-STD-866 and GEAE Word Drawing 4013195-9990. Subsequent to grinding of the coatings, an epoxy sealer was applied to all non-coated areas of the specimens. On the rod specimens, on the end with the 1.25" uncoated area, the epoxy extended at least ¼" onto the coating. On the opposite end, the epoxy extended over the edge and covered at least ¼" of the coating. On the plate specimens, the epoxy was placed around the edges such that it extended at least ¼" onto the coating.

### 4.7.3. Corrosion Testing Procedures

ASTM B117 salt fog tests were conducted in a Q-Fog Model CCT600 salt spray chamber. The salt fog test is an accelerated corrosion test by which samples exposed to the same condition can be compared, thereby providing a means of ranking the relative corrosion resistance. For these tests, the mounting of the plate specimens in the chamber followed the B117 protocol. Since rod-shaped specimens are not in the B117 protocol, specimen holders (made from an inert material such as teflon) were fabricated in which the rods were placed, with 4.25 inches of the specimen extending out from the holder. The holders were constructed such that the rods sat at an angle of 45 degrees to the vertical.

As specified in the B117 protocol, the samples were exposed to a salt fog generated from a 5% sodium chloride solution with a pH between 6.5 and 7.2. The temperature in the chamber was maintained at 35 ºC.

Samples for each coating/substrate combination were placed in the salt fog chamber for a total exposure time of 1000 hours. Photographs were taken before and subsequent to exposure to document the surface conditions. Samples were monitored and ratings based on the appearance of the samples were measured at 125-hour intervals. However, these ratings were misleading. In some cases, the coatings were undercut and the appearance rating underestimated the degree of corrosion. In other cases, the corrosion products accumulated on the surface making the surface appear more highly corroded than was actually the case. Thus, as discussed below, only protection ratings based on samples that were cleaned after 1000 hours of testing are presented.

Specimens were cleaned with a Scotch 3M abrasive pad to remove loosely adherent corrosion products, then dried. After cleaning, it was possible to identify surface defects such as blisters and/or coating degradation. Removing the blisters and portions of the coating that were undercut by corrosion provided a better representation of the area that was affected by corrosion. A protection rating for the coating was then determined based on the area of the sample that had undergone corrosion as a result of cracks and/or defects in the coating, i.e. how well the coating protected the substrate. The replicate samples were examined and given a protection rating (0-10 with 0 being worst) in accordance with ASTM B537 which is summarized in Table 4-42. The arithmetic average of the replicate samples was computed and used for all data analysis. It was also observed that many of the coatings themselves appear to have undergone degradation, and that is also reported here. This degradation appeared as a general or localized discoloration of the surface. In general, the discoloration was easily removed using the abrasive pad.

### 4.7.4. Corrosion Testing Results and Discussion

While several trends were apparent between all base metal/coating combinations, some significant differences were also found. The discussion will focus first on the results for each base metal with a summary of the overall results presented at the end.

4340 plates

**Table 4-42 Protection Rating Versus Area of Defect from ASTM B 537-70.**

| Area of Defect (in percent) | Rating |
|---|---|
| 0 | 10 |
| to 0.1 | 9 |
| 0.1 to 0.25 | 8 |
| 0.25 to 0.5 | 7 |
| 0.5 to 1.0 | 6 |
| 1.0 to 2.5 | 5 |
| 2.5 to 5.0 | 4 |
| 5 to 10 | 3 |
| 10 to 25 | 2 |
| 25 to 50 | 1 |
| greater than 50 | 0 |

The results for the coating/4340 steel plate combinations are presented in Figure 4-67 through Figure 4-69 and Table 4-43. In general, the 0.003”-thick EHC coating outperformed the 0.003”-thick HVOF and PS coatings in every direct comparison. The best performance of the other coatings was the HVOF T-400. However the protection rating for this coating was only 4.3. As the photographs in Figure 4-67 and Figure 4-68 show, the HVOF and PS coatings experienced significant blistering. It is important to note that the HVOF T-400 and T-800 and the PS T-400 coatings also experienced general corrosion, i.e. degradation of the coating. These samples were given a relative ranking in regard to the degradation of the coating surface with the HVOF T-400 being best and the PS T-400 being worst. In many cases it appeared as if the epoxy mask failed and in addition many samples experienced crevice corrosion, i.e. corrosion beneath the epoxy mask. It was not possible to determine if the epoxy failure was related to the crevice corrosion.

For the 0.0015”-thick coatings, the EHC, HVOF T-400 and HVOF T-800 had an average protection rating of 9 while the rating for PS T-400 was 8.8. The HVOF $Cr_3C_2$/NiCr had a protection rating of 0. The HVOF T-400 and T-800 and the PS T-400 coatings experienced

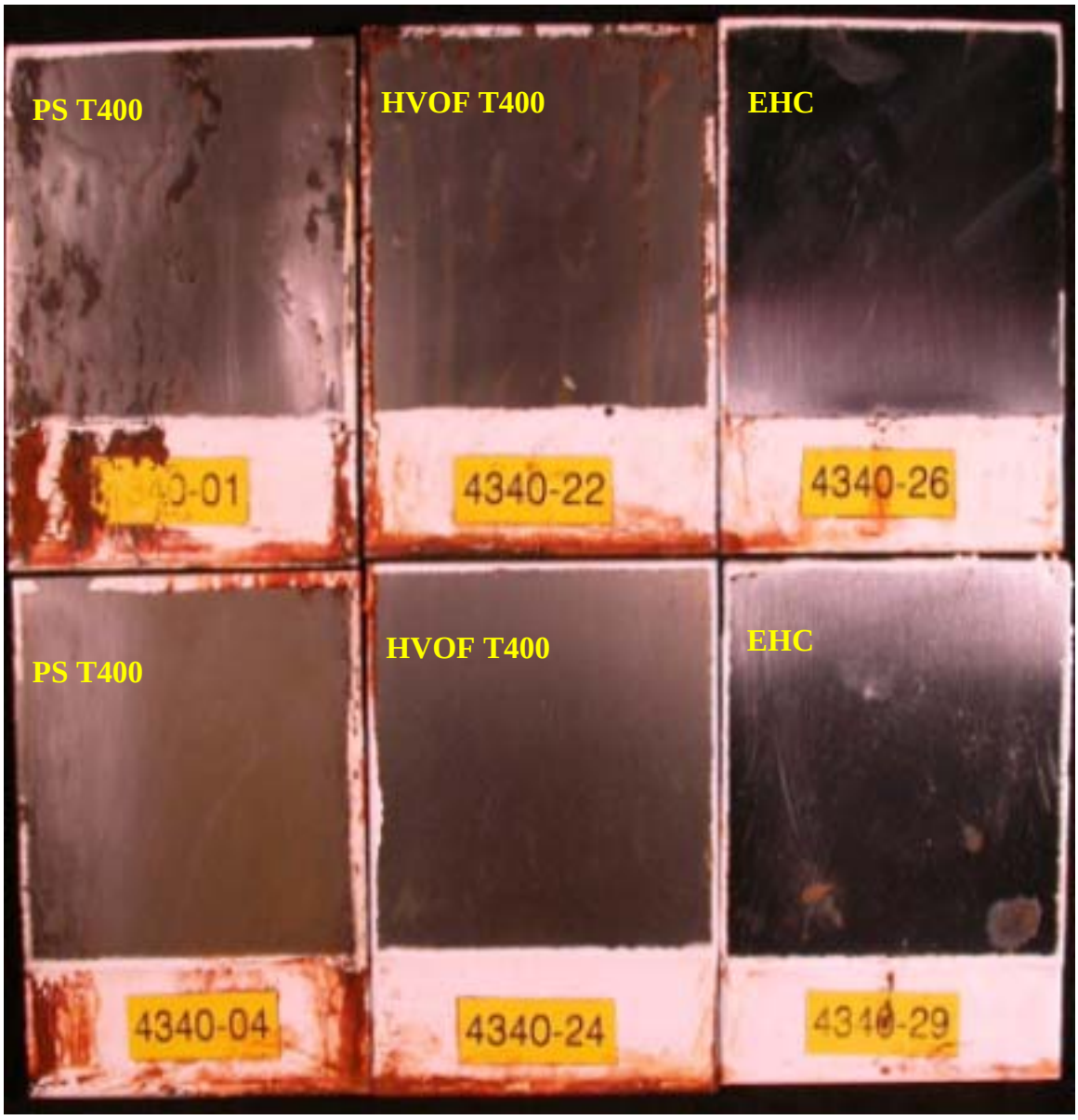


**Figure 4-67 Coated 4340 Steel Plates After 1000 Hours Salt Fog Exposure. (Top row: 0.003”-thick coatings; bottom row: 0.015”-thick coatings)**

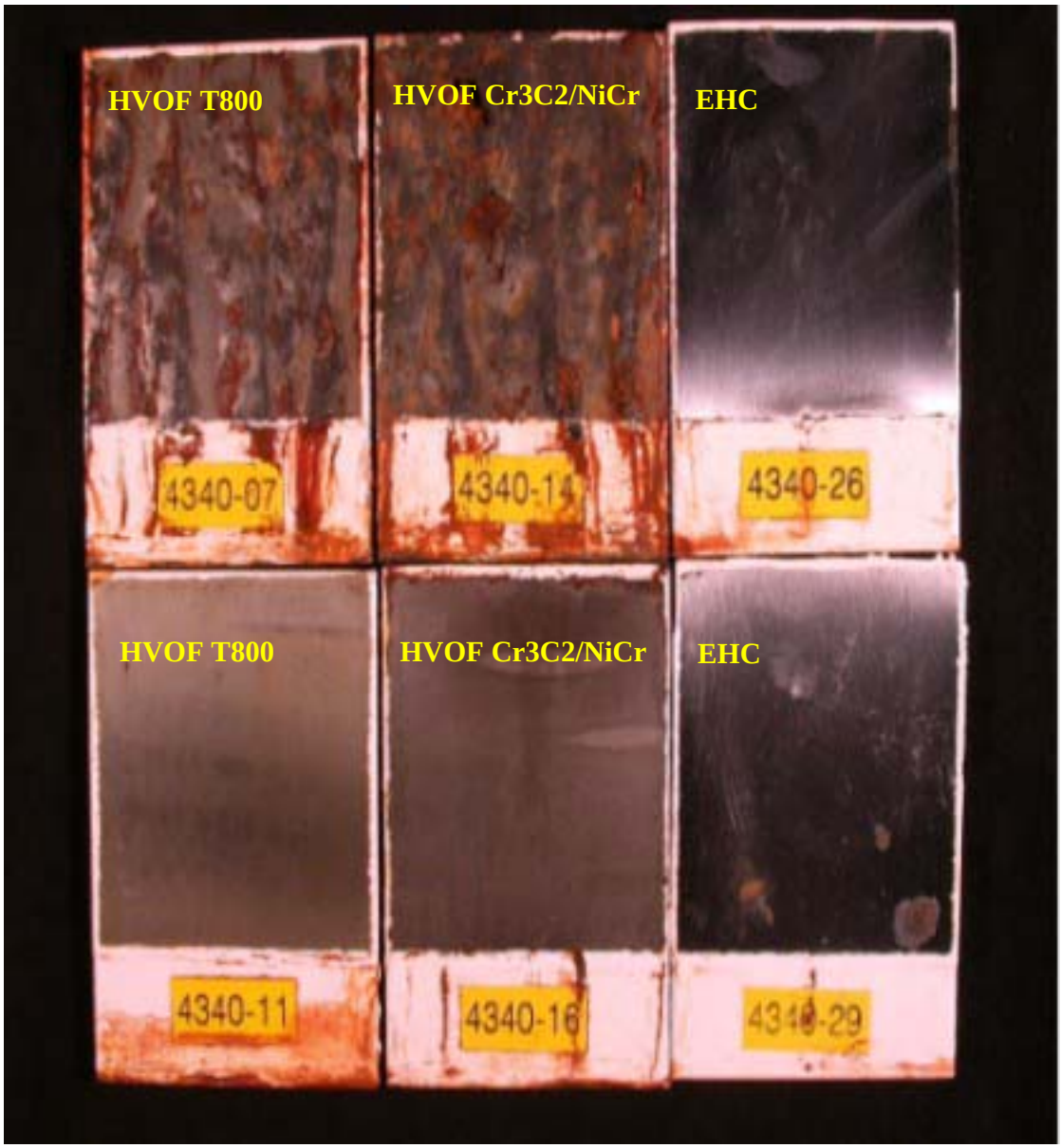


**Figure 4-68 Coated 4340 Steel Plates After 1000 Hours Salt Fog Exposure. (Top row: 0.003”-thick coatings; bottom row: 0.015”-thick coatings)**

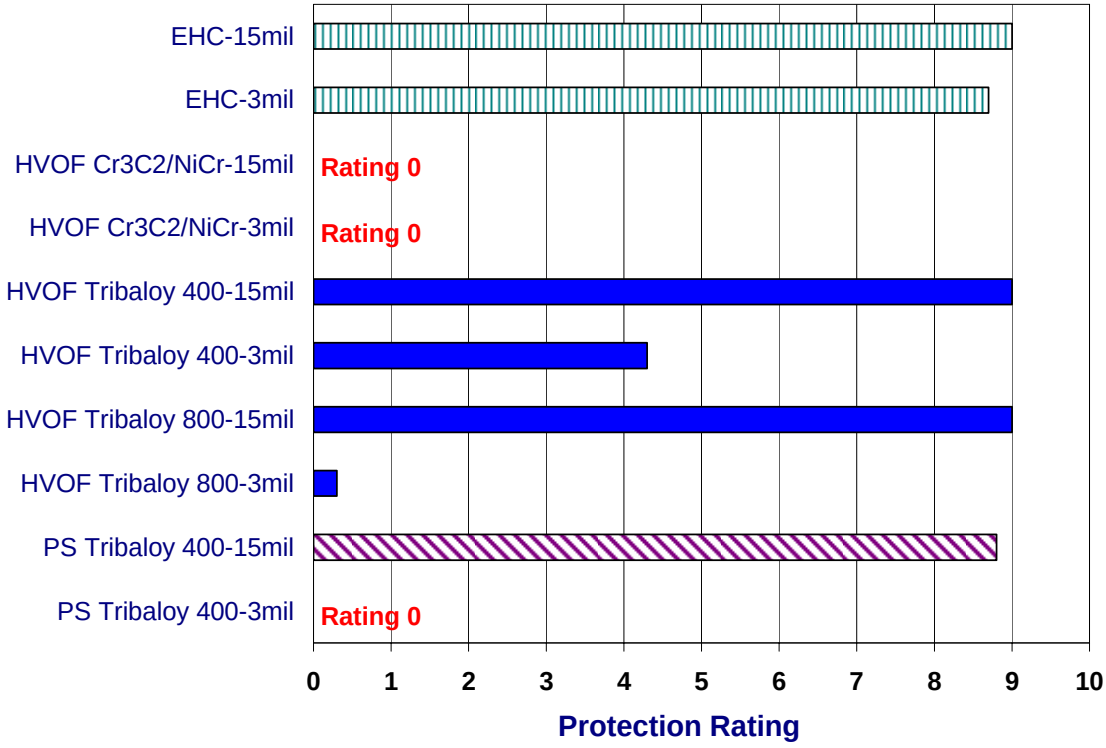


**Figure 4-69 Protection Ratings for Coated 4340 Steel Plates After 1000 Hours Salt Fog Exposure**

**Table 4-43 4340 steel Plate/Coating Combinations After 1000 Hours of B117 Testing**

| Coating - Coating thickness | Protection Rating | Range | Coating Corrosion |
|---|---|---|---|
| PS Tribaloy 400 – 0.003” | 0 | - | yes |
| PS Tribaloy 400 – 0.015” | 8.8 | 8.5 - 9 | yes |
| HVOF Tribaloy 800 – 0.003” | 0.3 | 0 - 1 | yes |
| HVOF Tribaloy 800 – 0.015” | 9 | - | yes |
| HVOF Tribaloy 400 – 0.003” | 4.3 | 4 - 5 | yes |
| HVOF Tribaloy 400 – 0.015” | 9 | - | yes |
| HVOF Cr3C2/NiCr – 0.003” | 0 | - | ? |
| HVOF Cr3C2/NiCr – 0.015” | 0 | - | ? |
| EHC – 0.003” | 8.7 | 8 - 9 | no |
| EHC – 0.015” | 9 | - | no |

**?** Not enough of the HVOF $Cr_3C_2$/NiCr coating was intact to determine whether coatings corrosion had occurred

general corrosion. As above, these samples were given a relative ranking in regard to the degradation of the coating surface with the HVOF T-400 being best and the PS T-400 being worst. There was not enough of the HVOF $Cr_3C_2$/NiCr coating intact to determine whether coating corrosion had occurred. As with the 0.003"-thick coatings, in many cases it appeared as if the epoxy mask failed. These samples also showed signs of crevice corrosion.

Taking the protection rating and coating corrosion into consideration, the EHC coatings had the best performance for both coating thicknesses followed by HVOF T-400 and HVOF T-800. In general the 0.015"-thick coatings performed significantly better than the 0.003"-thick coatings.

4340 rods

The results for the coating/4340 steel rod combinations are presented in Figure 4-70 to Figure 4-72 and Table 4-44. The 0.003"-thick EHC coatings outperformed the 0.003"-thick HVOF and PS coatings in every direct comparison. The best performance for the thermal spray coatings was the HVOF T-400 and $Cr_3C_2$/NiCr. However the protection rating for these coatings was only 2. The photographs in Figure 4-70 and Figure 4-71 show that the HVOF and PS coatings experienced significant blistering and cracking. The HVOF T-400 and T-800 and the PS T-400 coatings experienced general corrosion. There was no apparent general corrosion of the HVOF $Cr_3C_2$/NiCr coating. These samples were given a relative ranking in regard to the degradation of the coating surface. The ranking from best to worst is HVOF $Cr_3C_2$/NiCr (no apparent corrosion), HVOF T-800, HVOF T-400 and PS T-400. In many cases the epoxy mask failed and, as with the plate samples, crevice corrosion was occurring underneath the epoxy. The crevice corrosion was observed on all of the HVOF and PS coated samples. One EHC sample without the Ni underlayer and two EHC samples with the Ni underlayer experienced crevice corrosion. It was not possible to determine if the epoxy failure was related to the crevice corrosion.

For the 0.0015"-thick coatings, the EHC with the nickel underlayer performed best and had a rating of 9.5. The HVOF T-400 and PS T-400 had an average protection rating of 9. The HVOF T-800 and HVOF $Cr_3C_2$/NiCr had protection ratings of 3.7 and 2.3, respectively. The HVOF T-400 and T-800 and the PS T-400 coatings experienced general corrosion. There was no apparent corrosion of the HVOF $Cr_3C_2$/NiCr coating. These samples were given a relative ranking in regard to the degradation of the coating surface. The ranking from best to worst is HVOF $Cr_3C_2$/NiCr (no apparent corrosion), HVOF T-800, HVOF T-400 and PS T-400. In some cases the epoxy mask failed and crevice corrosion was occurring underneath the epoxy. The crevice corrosion was seen on all of the HVOF and PS coated samples. One EHC sample in each of the sets (with and without Ni underlayers) experienced crevice corrosion and the other two samples in each set showed signs of surface etching. It was not possible to determine if the epoxy failure was related to the crevice corrosion and there were cases of crevice corrosion where the epoxy coating remained intact.

Taking the protection rating and coating corrosion into consideration, the EHC coatings with the nickel underlayer had the best performance for both coating thicknesses. For the 0.003"-thick coatings the second best performance was exhibited by the EHC coating without the nickel underlayer with the other coatings performing very poorly. For the 0.015"-thick coatings, the HVOF T-400 and PS T-400 coatings had protection ratings of 9 that were slightly better than the EHC coating without the nickel underlayer. However, coating corrosion was noted for both the HVOF T-400 and PS T-400 coatings. The thicker coatings performed better than the 0.003"-thick coatings.

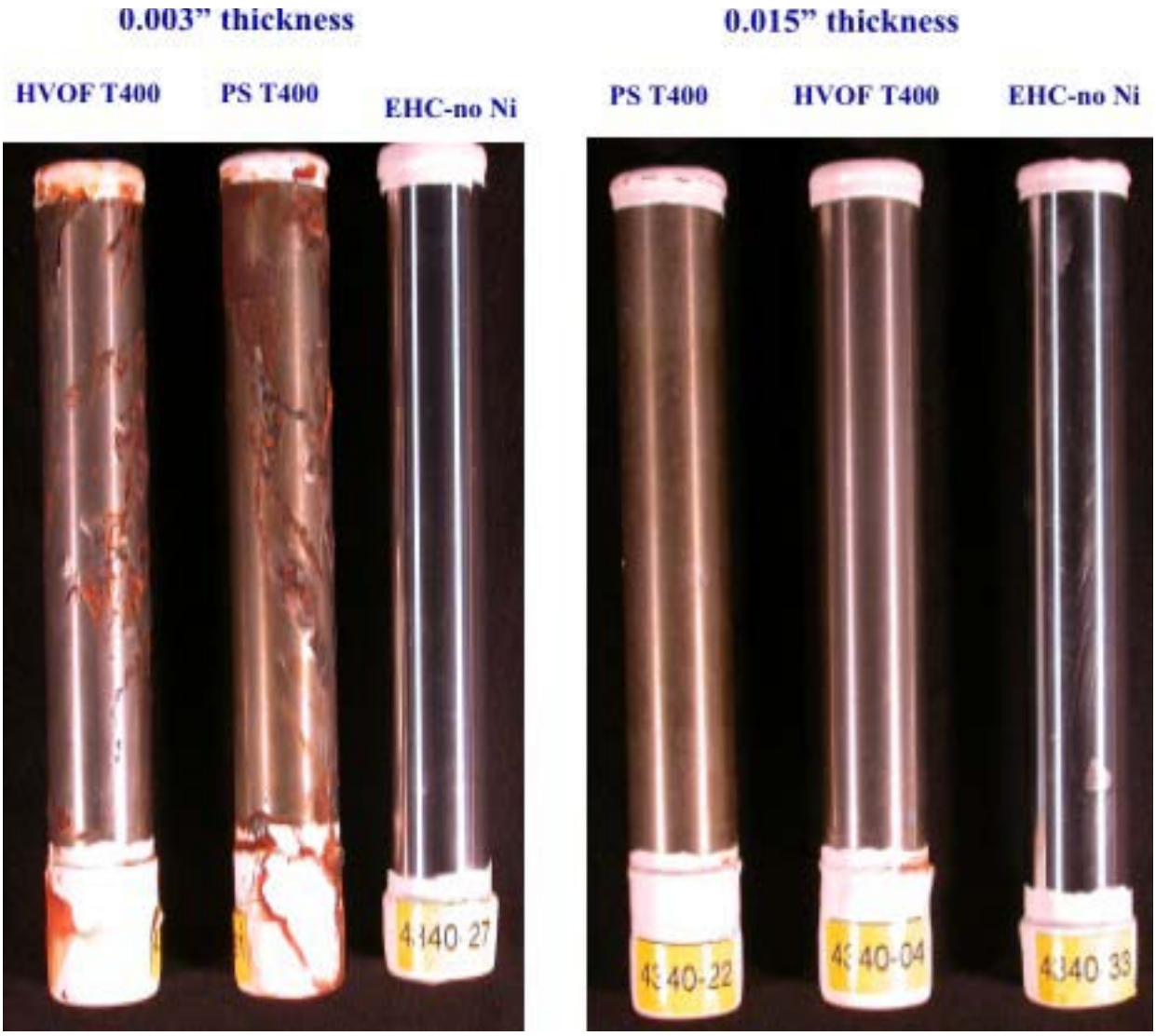


**Figure 4-70 Coated 4340 Steel Rods After 1000 Hours Salt Fog Exposure**

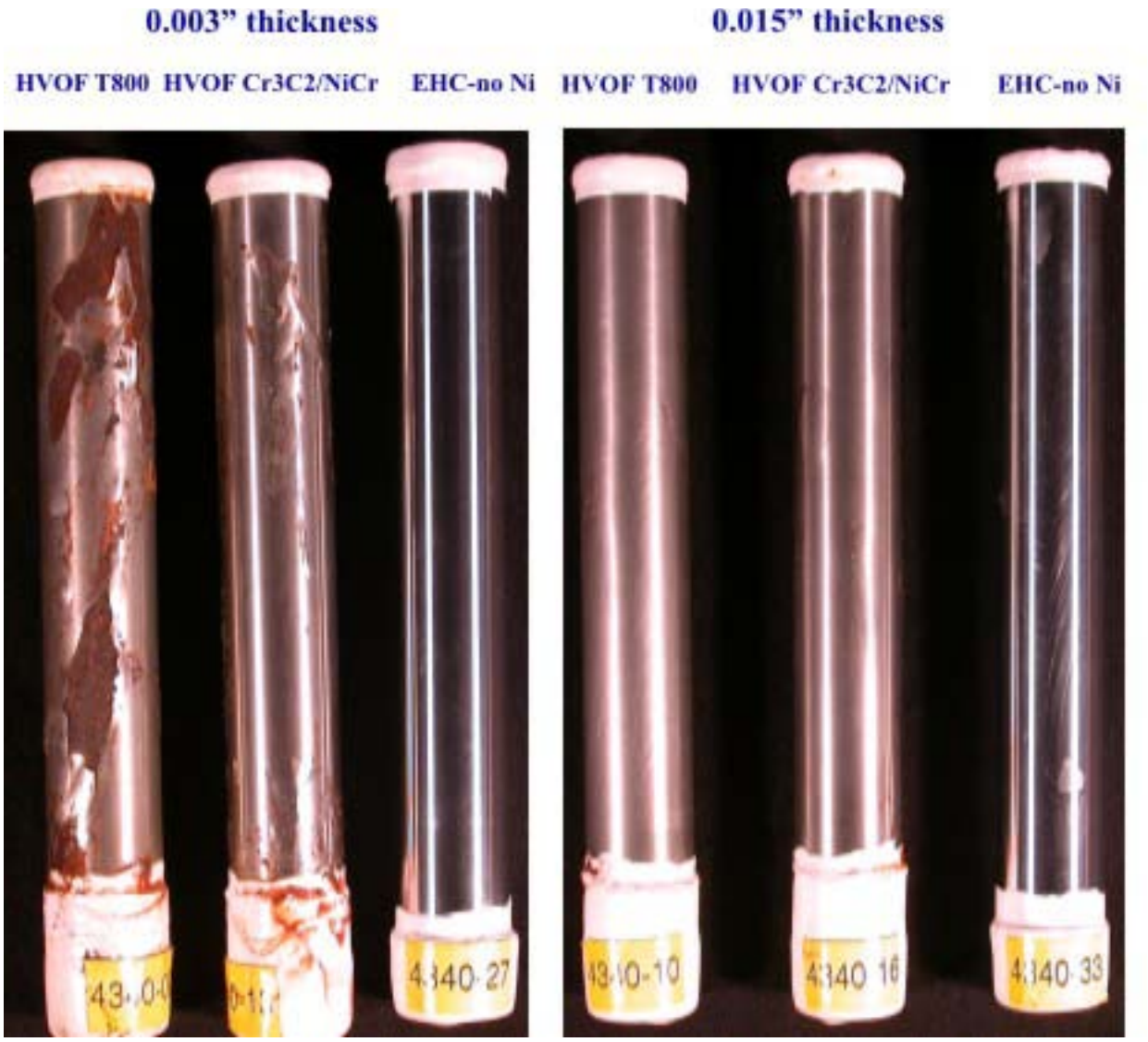


**Figure 4-71 Coated 4340 Steel Rods After 1000 Hours Salt Fog Exposure**

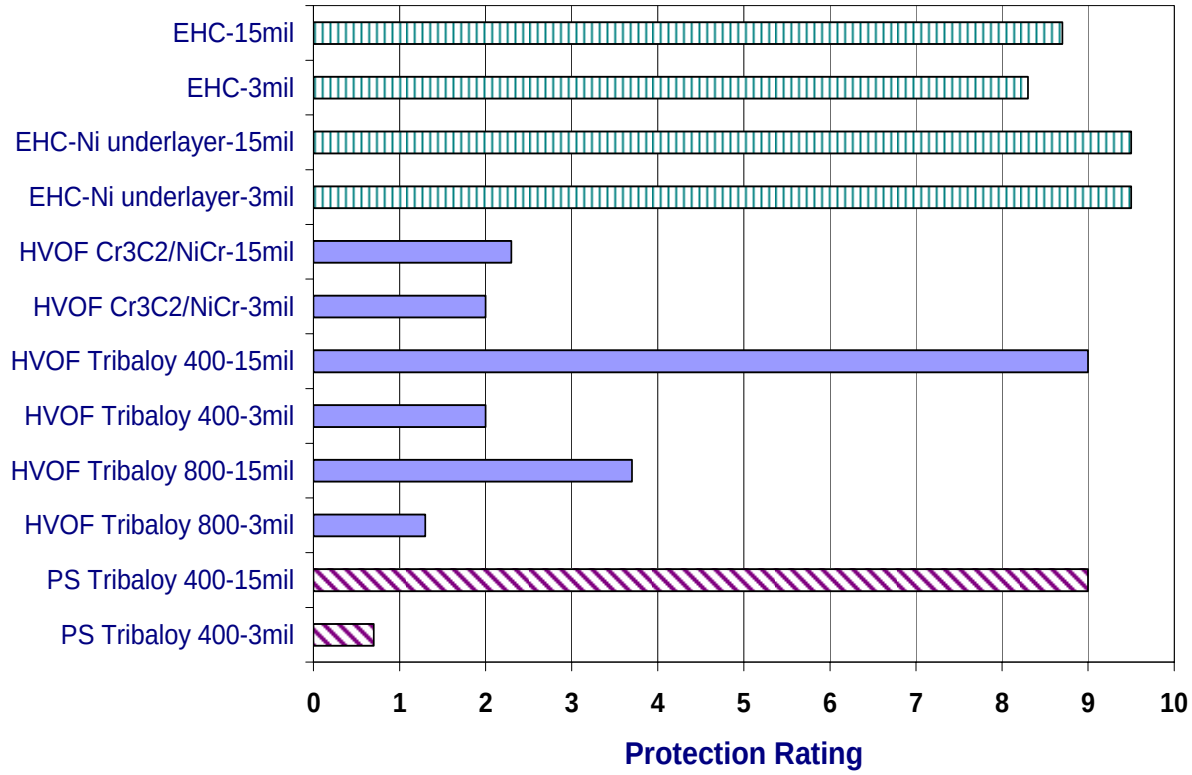


**Figure 4-72 Protection Ratings for Coated 4340 Steel Plates After 1000 Hours Salt Fog Exposure**

**Table 4-44 4340 Steel Rod/Coating Combinations After 1000 Hours of B117 Testing**

| Coating - Coating thickness | Protection Rating | Range | Coating Corrosion |
|---|---|---|---|
| PS Tribaloy 400 – 0.003” | 0.7 | 0 - 1 | Yes |
| PS Tribaloy 400 – 0.015” | 9 | - | Yes |
| HVOF Tribaloy 800 – 0.003” | 1.3 | 1 - 2 | Yes |
| HVOF Tribaloy 800 – 0.015” | 3.7 | | Yes |
| HVOF Tribaloy 400 – 0.003” | 2 | 1 - 3 | Yes |
| HVOF Tribaloy 400 – 0.015” | 9 | 8.5 - 9.5 | Yes |
| HVOF $Cr_3C_2$/NiCr – 0.003” | 2 | 0 - 3 | Yes |
| HVOF $Cr_3C_2$/NiCr – 0.015” | 2.3 | 1 - 3 | Yes |
| EHC-Ni underlayer – 0.003” | 9.5 | - | No |
| EHC-Ni underlayer – 0.015” | 9.5 | - | No |
| EHC – 0.003” | 8.3 | 6 - 9.5 | No |
| EHC – 0.015” | 8.7 | 8 - 9 | No |

IN-718 rods

The results for the coating/IN-718 rod combinations are presented in Figure 4-73 through Figure 4-75 and Table 4-45. For the 0.003”-thick coatings, EHC without the nickel underlayer (9.3 rating) performed best followed closely by EHC with the nickel underlayer (9), HVOF T-800 (9) and PS T-400 (9). The HVOF T-400 had a rating of 7.7 while the HVOF $Cr_3C_2$/NiCr had a rating of 7.3. The HVOF and PS coatings experienced corrosion of the coating. These samples were given a relative ranking in regard to the degradation of the coating surface. The ranking from best to worst is HVOF T-800, HVOF T-400, HVOF $Cr_3C_2$/NiCr, and PS T-400. As with the 4340 samples, crevice corrosion was occurring underneath the epoxy. Crevice corrosion was noted for the EHC, the HVOF T-800 and T-400, and the PS T-400 coatings. The HVOF $Cr_3C_2$/NiCr showed signs of etching beneath the epoxy.

For the 0.0015”-thick coatings, the EHC without the nickel underlayer, the HVOF T-800, the HVOF T-400 and the PS T-400 all had a protection rating value of 9.5. The HVOF $Cr_3C_2$/NiCr (one sample in this set) and EHC with the Ni underlayer had protection ratings of 8.5 and 7 respectively. The HVOF and PS coatings experienced general corrosion. These samples were given a relative ranking in regard to the degradation of the coating surface. The ranking from best to worst is HVOF T-800, HVOF T-400, HVOF $Cr_3C_2$/NiCr, and PS T-400. The epoxy mask failed on some samples and crevice corrosion was noted underneath the epoxy. Crevice corrosion was noted for the EHC, the HVOF T-800 and T-400 and the PS T-400 coatings. The HVOF $Cr_3C_2$/NiCr showed signed of etching beneath the epoxy.

Taking the protection rating and coating corrosion into consideration, the EHC without the Ni underlayer performed best followed by the HVOF T-800. The thicker coatings (0.015”) performed better than the 0.003”-thick coatings.

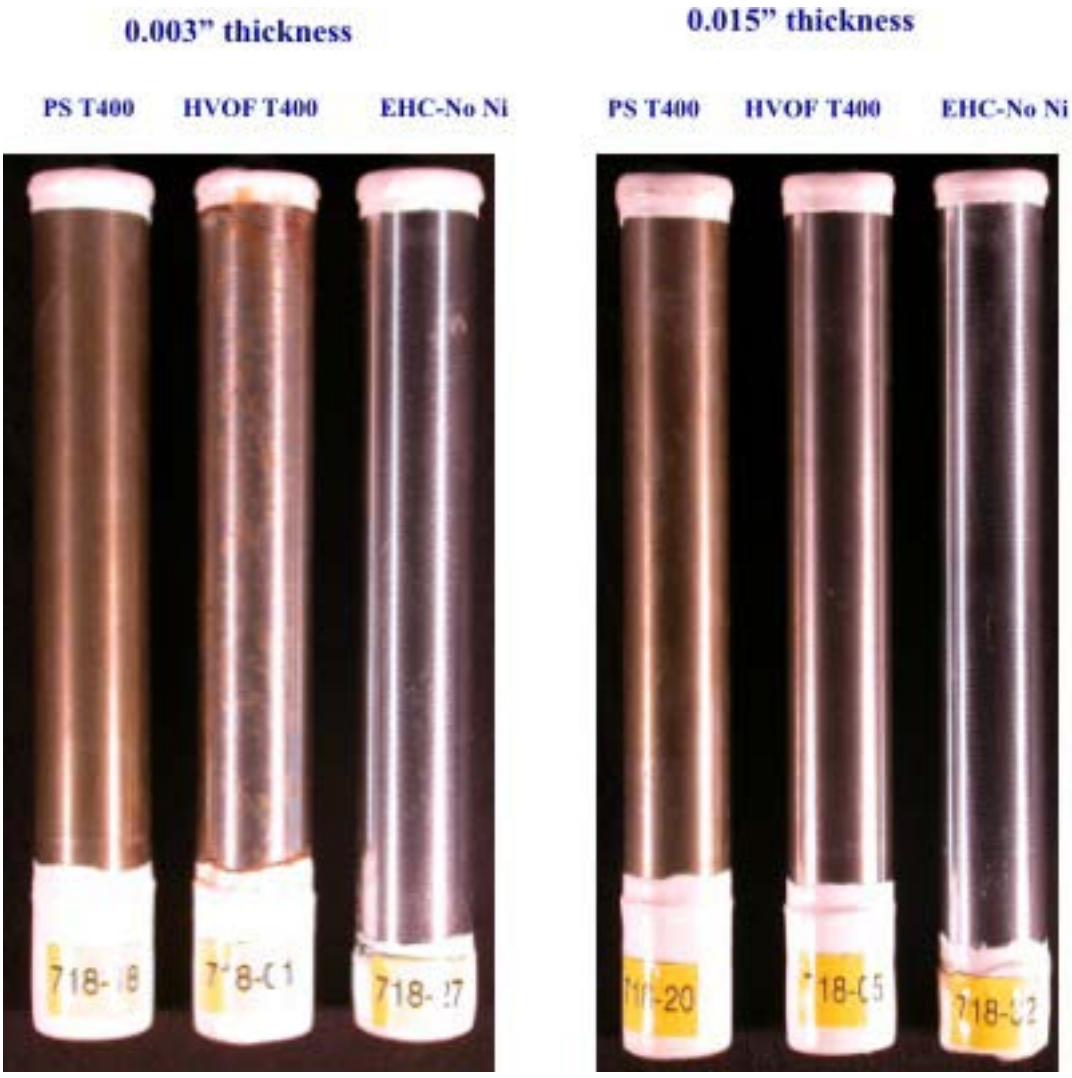


**Figure 4-73 Coated IN-718 Rods After 1000 Hours Salt Fog Exposure**

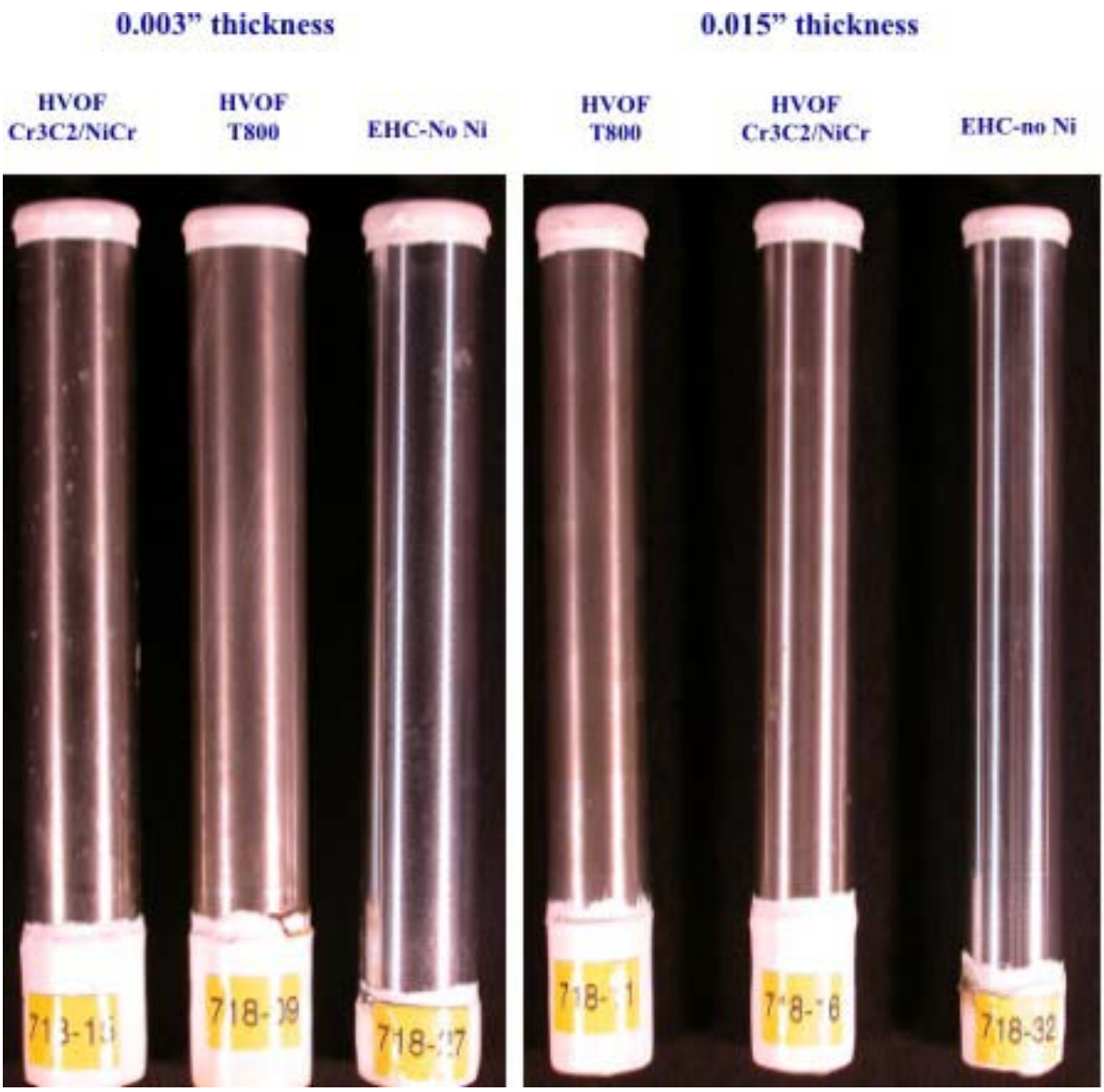


**Figure 4-74 Coated IN-718 Rods After 1000 Hours Salt Fog Exposure**

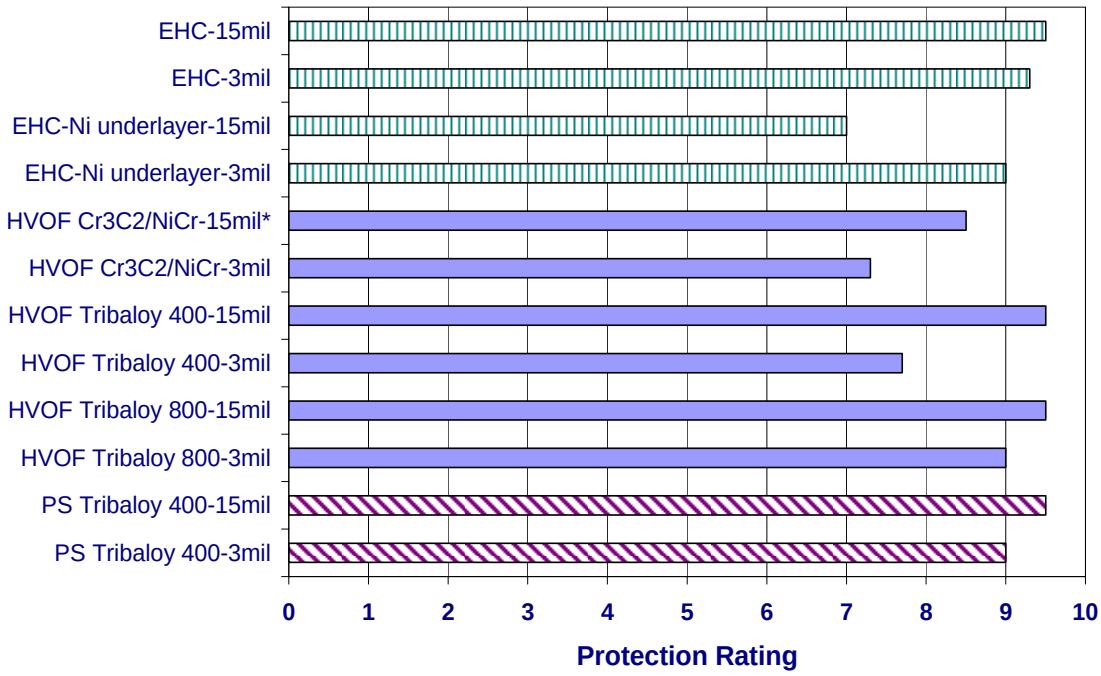


**Figure 4-75 Protection Ratings for Coated IN-718 Rods After 1000 Hours Salt Fog**

**Table 4-45 IN-718 rod/coating combinations after 1000 hours of B117 Testing**

| Coating - Coating Thickness | Protection Rating | Range | Coating Corrosion |
|---|---|---|---|
| PS Tribaloy 400 – 0.003” | 9 | - | yes |
| PS Tribaloy 400 – 0.015” | 9.5 | - | yes |
| HVOF Tribaloy 800 – 0.003” | 9 | - | yes |
| HVOF Tribaloy 800 – 0.015” | 9.5 | - | yes |
| HVOF Tribaloy 400 – 0.003” | 7.7 | 7 - 8 | yes |
| HVOF Tribaloy 400 – 0.015” | 9.5 | - | yes |
| HVOF $Cr_3C_2$/NiCr – 0.003” | 7.3 | 7 - 8 | yes |
| HVOF $Cr_3C_2$/NiCr – 0.015” | 8.5 | one sample | yes |
| EHC-Ni underlayer – 0.003” | 9 | - | no |
| EHC-Ni underlayer – 0.015” | 7 | none | no |
| EHC – 0.003” | 9.3 | 9 to 9.5 | no |
| EHC – 0.015” | 9.5 | none | no |

### 4.7.5. Summary and discussion

1. When the protection rating and coating corrosion (or lack thereof) were taken into consideration, the EHC coatings (with and without the Ni underlayer) had the best performance for both coating thicknesses on the 4340 steel plates, followed by HVOF T-400 and HVOF T-800.
2. In the case of the 4340 rods, the EHC coatings with the nickel underlayer had the best performance for both coating thicknesses (again taking the protection rating and coating corrosion into consideration). For the 0.003"-thick coatings the second best performance was exhibited by the EHC coating without the nickel underlayer with the other coatings performing very poorly. For the 0.015"-thick coatings, the HVOF T-400 and PS T-400 had protection ratings of 9 that were slightly better than the EHC coating without the nickel underlayer. However, coating corrosion was noted for both the HVOF T-400 and PS T-400 coatings.
3. For the IN-718 substrate, all of coatings performed very similarly. The EHC without the Ni underlayer performed best followed by the HVOF T-800. Better corrosion performance without a Ni barrier layer is probably due to variation in the chrome layer. This variation in EHC performance is not at all uncommon, and has been seen in other testing reported to HCAT (ref to Steve Gaydos, 20th HCAT, Orlando [11].
4. In general, the 0.015"-thick HVOF coatings performed better than the 0.003"-thick coatings. Since these coatings serve as barrier coatings to corrosion, that result was expected.
5. The HVOF $Cr_3C_2$-NiCr did not perform well, especially on plates. Why there should be significant differences between the two geometries in unclear. However, the results suggest that this material should not be used for applications in severe corrosion environments.
6. As seen in prior work HVOF coatings themselves corrode, whereas EHC coatings do not. EHC coatings fail by corrosion of the substrate and undercutting of the plating. EHC coatings therefore tend to corrode, blister and spall. HVOF coatings can fail in the same manner by slow dissolution and roughening. The EHC specimens showed remarkably little corrosion for a 1,000 hr B117 test.
7. The results indicate that HVOF and PS coatings have a greater susceptibility than EHC to crevice corrosion. However, since this was not designed as a crevice corrosion test, this conclusion needs to be confirmed by proper crevice corrosion testing (which was not incorporated in the JTP).

### 4.7.6. Conclusions

In general the HVOF and PS coatings failed the acceptance criterion of being equal to or better than chrome. However, in each group some of the thermal sprayed specimens had performance equivalent to chrome. At the same time these hard chrome specimens showed significantly less corrosion than is commonly seen in this type of test. This level of variability is not unexpected.

# 4.8. Carbon Seal Testing

## 4.8.1. Data Summary

Table 4-46 provides a quick reference to the primary data and its location in this section.

**Table 4-46 Primary Data Quick Reference Guide**

| ITEM | ITEM NUMBER | PAGE |
|---|---|---|
| Materials Evaluated | Table 4-47 | 128 |
| Test Matrix | Table 4-48 | 129 |
| Carbon & Coated Rotor Specimens | Figure 4-77 and Figure 4-78 | 123,124 |
| Isometric Solid Model of Test Rig | Figure 4-81 | 126 |
| Summary Table - Wear Data | Table 4-49 | 133 |
| Wear Summary Charts | Figure 4-85 - Figure 4-88 | 134 – 138 |
| Wear of Carbon Seals | Figure 4-89 - Figure 4-92 | 138 – 141 |
| Wear of Runner Coatings | Figure 4-93 - Figure 4-96 | 142 – 145 |
| Statistical Analysis of Wear Data | Table 4-51 - Table 4-53 | 149 - 151 |

## 4.8.2. Test Rationale

Carbon seal wear tests were performed due to their unique requirements in gas turbine engines. Carbon seal systems operate at the engine rpm and therefore have high sliding speeds. The rotating part, commonly called the runner, is usually fabricated from steel and coated with EHC. The opposing stationary part holds the carbon seal material and a spring assembly behind it provides the seal contact pressure. The purpose of the tests conducted under the JTP was to evaluate the performance of alternative thermal spray coatings applied to runners by measuring both the wear on the carbon seals and the wear on the coatings in contact with the carbon seals. A test rig, described in Section 4.8.3.3, was utilized for these studies which simulated the loads and sliding speeds encountered in GTEs.

Within GTEs, carbon seals can be used with two different design intents. In the first design, the carbon seal seldom makes contact with the runner, but does occasionally come into rubbing contact during transient events during which the heat generation can cause unstable mechanical responses if the carbon seal and runner are incompatible. In the second design, the carbon seal is in continuous rubbing contact and is intended to be a sacrificial material. There are also two configurations of carbon seals, face seals and radial seals, as seen in the illustrations of Figure 4-76. A carbon face seal operating under continuous sliding contact was selected for the test configuration in the JTP because face seals tend to be more sensitive to sliding contact effects and therefore this was deemed the most appropriate configuration for a materials evaluation of the effects due to changing the runner coating from EHC to an alternative material.

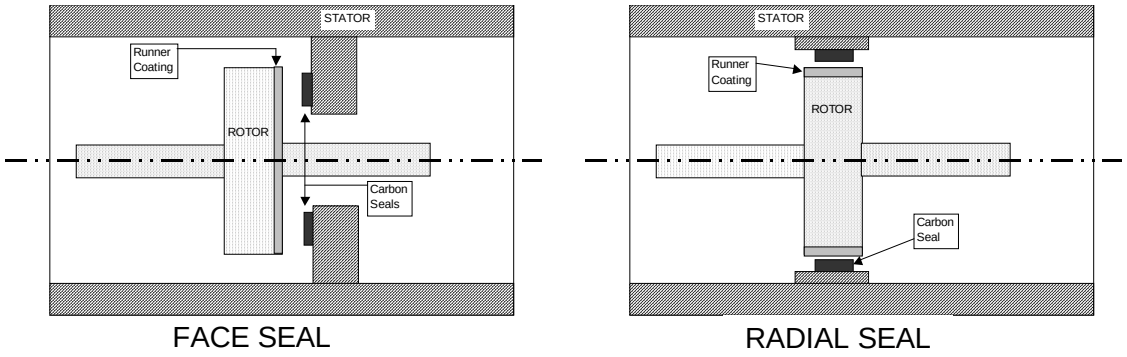


**Figure 4-76 Illustration of Two Different Types of Carbon Seal Configurations.**

## 4.8.3. Specimen Fabrication and Test Rig Description

### 4.8.3.1. Carbon Seals

The carbon seals used in GTEs are typically very soft compared to metallic surfaces and come in a variety of grades. Two carbon seal materials were selected for the tests under the JTP – Graphitar 67 which is one of the softer grades and Graphitar 39 which is one of the harder grades in actual use with components identified for carbon seal use. Selection of these two grades of carbon seals was based on the realization that while the carbon usually wears, there has been field experience in which some wear of the runner coating has occurred. The intended approach was to test one soft and one hard grade of carbon to assure maximum discernment between the candidate alternative coatings. In general, hardness values for carbon seal materials are measured using a Scleroscope in accordance with ASTM C886, "Standard Test Method for Scleroscope Hardness Testing of Fine-Grained Carbon and Graphite Materials." A dimensionless Shore Hardness number is obtained which is based upon the height of rebound of a diamond-tipped hammer dropped from a fixed height onto the material. The Shore Hardness values obtained on carbon materials should not be confused with Shore hardness values obtained on steels which can be correlated with hardness values obtained by other methods such as Vickers or Brinell. For Graphitar 39, the specified minimum Shore hardness value was 100 with an actual value of 100 for the materials used in the tests, and for Graphitar 67 the specified minimum Shore hardness value was 62 with an actual value of 87 for the materials used in the tests. Therefore, the difference in hardnesses between the two carbon seal materials was not as great as it could have been.

The carbon seal nose specimens were manufactured by US Graphite to a standard one-piece carbon ring cartridge assembly which conformed to the requirements of GE P/N 9541M72P01, Rev. D, which required a Graphitar 39 carbon grade. The second carbon grade, Graphitar 67, was manufactured to the same dimensions and substituted in the 9541M72 cartridge assembly to permit testing against the second carbon grade. All carbon rings were finished to a flatness requirement of 3 helium light bands. The carbon seals met requirements of GE material specification A50TF96-S8. A schematic of the carbon seal nose specimen is shown in Figure 4-77.

### 4.8.3.2. Seal Runners

The seal runners were fabricated from 9310 steel since it is the most commonly used parent metal alloy for these components in GTEs. The seal runners were designed by Rexnord Corporation to enable use of the standard carbon seal cartridges GE P/N 9541M72P01, Rev. D, described above and adapted to an existing carbon seal test rig at Rexnord. A schematic of the seal runner

specimen is shown in Figure 4-78. Coatings were applied to selected areas on both faces of each runner as indicated in Figure 4-79.

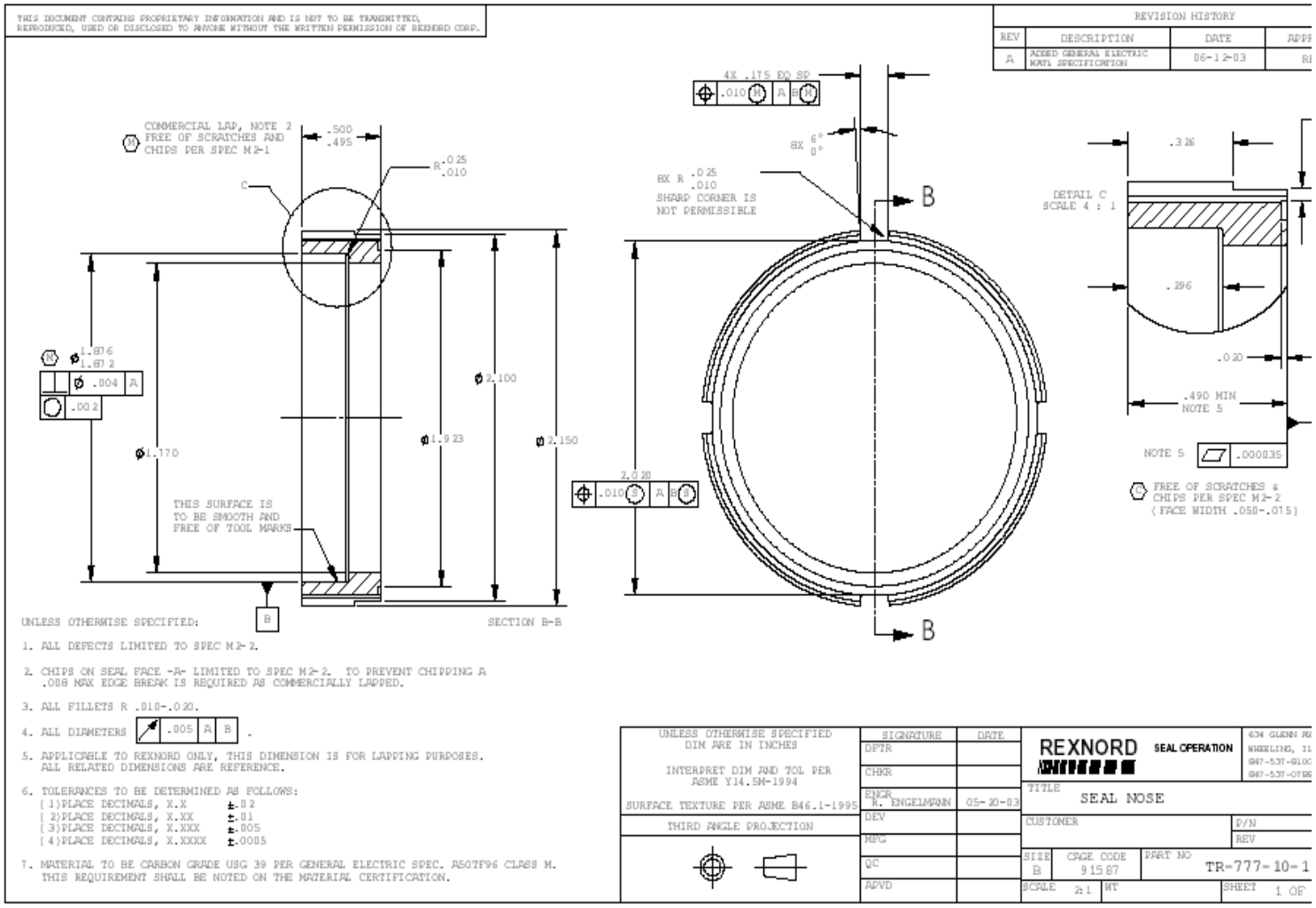


**Figure 4-77 Schematic of Carbon Seal Nose Specimen**

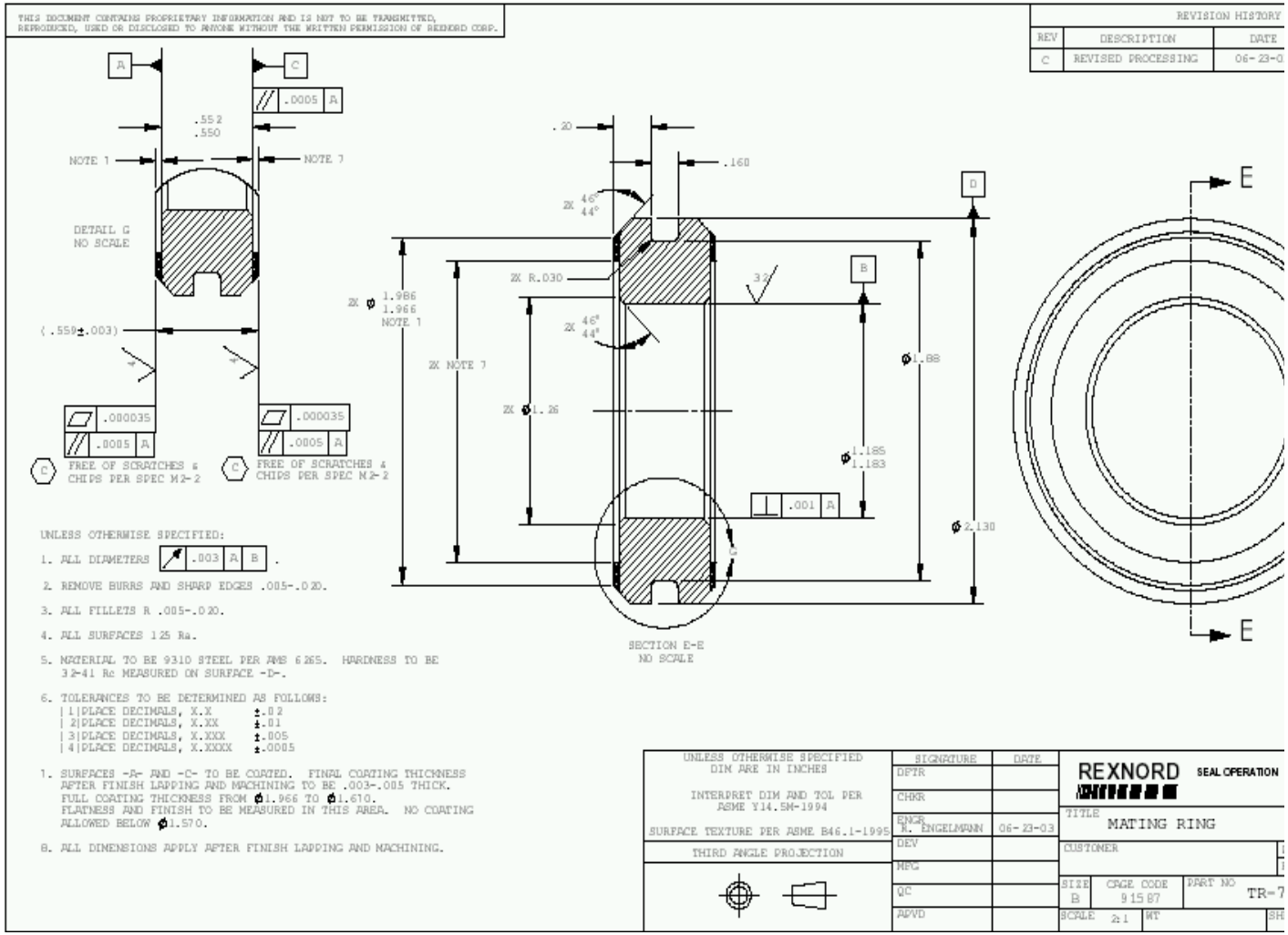


**Figure 4-78 Schematic of the Coated Seal Runner Ring**


**Figure 4-79 Photograph of Seal Runner Ring Indicating Location of Coating**

#### 4.8.3.3. Description of Test Rig

Figure 4-80 is a photograph of the Rexnord Corporation carbon seal test rig used in these studies. Figure 4-81 is a three-dimensional cross-sectional diagram and Figure 4-82 is a two-dimensional cross-sectional diagram of the test rig. The rig was designed such that four carbon-seal/coating tests could be performed in each test run. Two seal runner rings with coatings on each side (indicated in yellow in Figure 4-81 and as items 12 in Figure 4-82) were attached to the high-speed spindle (item 2 in Figure 4-82) that was belt driven by a motor that was controlled by a variable frequency electrical drive. Four cartridges, the boxlike structure with an upward-extending arm, held the grey-colored annular carbon seals (items 4 in Figure 4-82). The four cartridges were installed into the green stator holder plates (items 3, 7, 9, and 11 in Figure 4-82). A wave spring in each cartridge (indicated as items 13 in Figure 4-82) provided the axial load on the carbon seal holding it against the seal runner ring. Thus, the seal runner rings rotated against the spring-loaded carbon seals. Each ring was cooled by an oil jet stream impinging into the groove on its circumference.

The loads applied by the springs were equivalent to those encountered in actual GTEs and were intended to be constant for each test. However, the actual loads of the carbon seals on the runner rings varied due to slight variations in position each time the unit was assembled. Because of this, each carbon cartridge was calibrated for load versus deflection prior to each test. This was accomplished by placing the cartridge in an Instron Model 1122 mechanical test stand and measuring the deflection versus load. Thus, position of the deflected carbon seal in the test rig was used to measure the normal load as wear occurred. A position variation of only 0.06 inches resulted in a load change of about 3 pounds (2.5 to 5.5 pounds). As a result, small variations in final seal position during rig assembly gave unintended variations in the wear load from test to test.

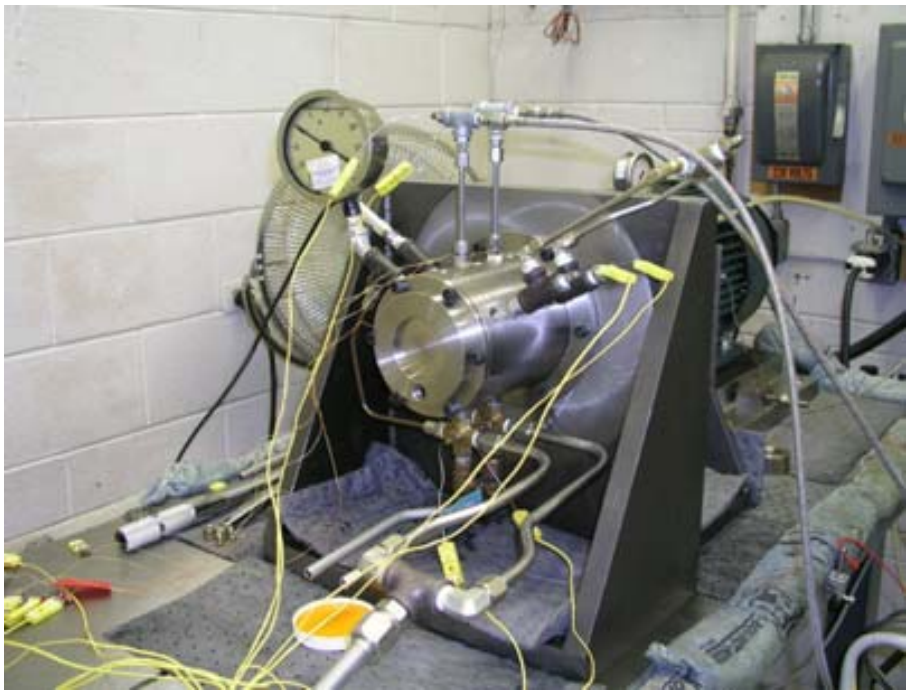

**Figure 4-80 Photograph of Rexnord Corporation Four-Station Carbon Seal Test Rig**

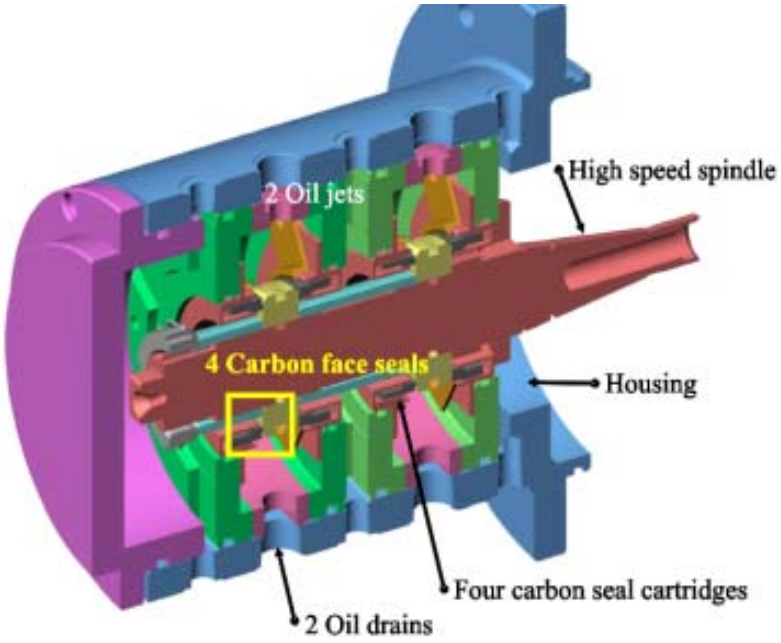


**Figure 4-81 Three-dimensional Cross-Sectional Diagram of Carbon Seal Test Rig**

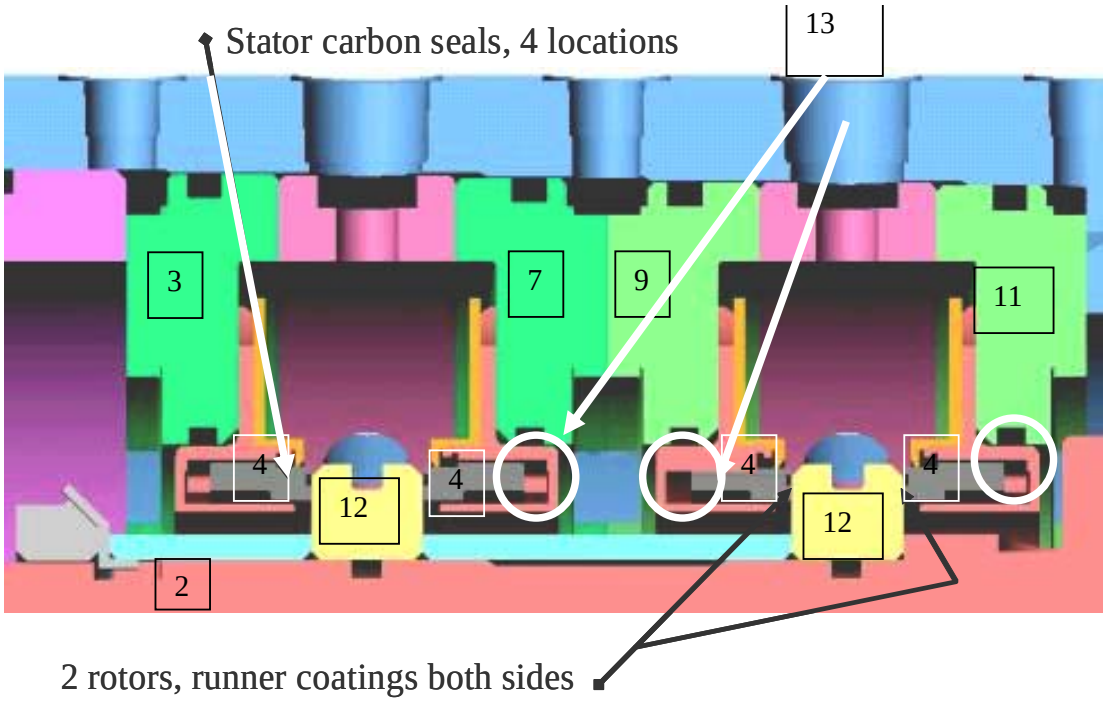


**Figure 4-82 Two-dimensional Cross-Sectional Diagram of Carbon Seal Test Rig**

## 4.8.4. Coating Deposition

### 4.8.4.1. Electrolytic Hard Chrome

EHC was deposited on the seal runner rings by Fountain Plating, an approved aerospace vendor, in accordance with MIL-STD-1501, supported by QQ-C-320. There was no interfacial layer between the runner and EHC coating and no sealer was applied to the EHC. The thickness was 0.003" to 0.005" subsequent to grinding (i.e., coatings were deposited to approximately 0.002" to 0.004" thicker than specified and then ground to final dimension). Subsequent to deposition, each coating was low-stress ground and final lapped by Westfield Gage (an aerospace supplier of seal runners) to a nominal Ra surface finish of either 8 or 4 microinches and to a flatness of 3 helium light bands.

### 4.8.4.2. Thermal Spray Coatings

The thermal spray coatings evaluated in the carbon seal tests included HVOF WC/17Co, $Cr_3C_2$/NiCr, Tribaloy 400 and Tribaloy 800, and PS WC/17Co and Tribaloy 400. The HVOF coatings were deposited using a Sulzer Metco Diamond Jet 2600 hybrid gun with hydrogen as the fuel gas and the PS coatings were deposited using a Metco 3M system. Deposition parameters were those identified in Section 4.4 and were the same as used for other materials studies with the exception of the PS WC/17Co which was not evaluated in other materials tests. Deposition parameters for that coating were identified in Table 4-19 using the run parameters (settings) that provided a minimum tensile residual stress in the coating.

A combination of air cooling and built-in pause times off the specimen were utilized to ensure the specimen surface temperature did not exceed 300 °F. The thermal spray coatings were deposited directly onto the substrate material with no interfacial layer. The thickness was 0.003" to 0.005" subsequent to grinding (i.e. coatings were deposited to approximately 0.002" to 0.004" thicker

than specified and the ground to final dimension). Subsequent to deposition, each coating was low-stress ground and final lapped by Westfield Gage (an aerospace supplier of seal runners) to a nominal Ra surface finish of either 8 or 4 microinches and to a flatness of 3 helium light bands. It was noted that the surface of the PS coatings contained some pores that were deeper than the measured surface finish, but there were no protrusions above the lapped surface.

Table 4-47 provides a summary of all of the coatings evaluated in this study including the type of powder used for the thermal spray coatings and their average diamond pyramidal hardness. The table also provides information on the carbon seal materials used in the tests.

**Table 4-47 Summary of the Runner Coatings, the Powder Used for Application of the Thermal Spray Coatings, the Diamond Pyramidal Hardness of the Thermal Spray Coatings, and the Grades, Shore Hardness Values and Porosity of the Carbon Seals**

| Runner Coatings: | | | |
|---|---|---|---|
| Composition, Weight % | Process | Powder | Avg. DPH [$kg/mm^2$] |
| Hard chrome | Electrolytic plating | Not applicable | ------ |
| WC-17 Co | HVOF [3] | Diamalloy 2005 | 1088 |
| $Cr_3C_2$-20 (Ni,Cr) | HVOF | Diamalloy 3007 | 987 |
| Co-28 Mo-17 Cr-3 Si [1] | HVOF | Diamalloy 3001 | 532 |
| Co-28 Mo-8 Cr-2 Si [2] | HVOF | Diamalloy 3002 | 609 |
| WC-17 Co | APS [4] | Metco 73F-NS-1 | 1038 |
| Co-28 Mo-8 Cr-2 Si [2] | APS [4] | Metco 66F-NS | ----- |
| **Carbon Grades:** | | | |
| Grade | Specified Shore Hardness Number | Delivered Carbons' Avg. Shore Hardness No. | Porosity % Spec-----Delivered |
| Graphitar 39 | 100 minimum | 100 | 1 max--------0.3% |
| Graphitar 67 | 62 minimum | 87 | 3 to 16--------7.2 % |

NOTES: [1] Tribaloy 800 [3] High Velocity Oxy-Fuel, thermal sprayed
[2] Tribaloy 400 [4] Air Plasma Spray, thermal sprayed

### 4.8.5. Test Description and Parameters

Tests were performed using spindle rotational velocities of either 7000 or 13,500 rpm which provided surface velocities of the carbon seals against the coated runners representative of the range encountered in actual GTEs. The test sequence consisted of four 12-hour segments for a total test time of 48 hours. Prior to initiating each test, the oil was preheated to a temperature of 300 °F and this temperature was maintained constant throughout the duration of the test. Table 4-48 presents the entire test matrix, indicating the number of tests conducted for each condition of coating, surface finish, carbon seal material and rotational speed. This test matrix differed slightly from that presented in the JTP due to the need for some additional tests of EHC with an Ra surface finish of 4 microinches. The different coated runner rings and carbon seals were

randomly distributed throughout the test rig to ensure there were no effects due to location in the rig. Since the rig tested four carbon seals vs. runners simultaneously, 19 actual test runs were performed for the 76 individual tests.

**Table 4-48 Final Carbon Seal Test Matrix**

| Shaft Material | Runner Coating | Ctg Finish (micro-inch) | Seal Material | Oil Temp. (Deg. F) | Speed (rpm) | Time (hours) | No. Tests |
|---|---|---|---|---|---|---|---|
| 9310 | EHC | 8 | Grade 39 | 300 | 13,500 | 4 x 12 | 2 |
| 9310 | EHC | 8 | Grade 67 | 300 | 13,500 | 4 x 12 | 2 |
| 9310 | EHC | 4 | Grade 39 | 300 | 13,500 | 4 x 12 | 2 |
| 9310 | EHC | 4 | Grade 67 | 300 | 13,500 | 4 x 12 | 2 |
| 9310 | HVOF WC-17Co | 8 | Grade 39 | 300 | 13,500 | 4 x 12 | 3 |
| 9310 | HVOF WC-17Co | 4 | Grade 39 | 300 | 13,500 | 4 x 12 | 1 |
| 9310 | HVOF WC-17Co | 8 | Grade 67 | 300 | 13,500 | 4 x 12 | 3 |
| 9310 | HVOF WC-17Co | 4 | Grade 67 | 300 | 13,500 | 4 x 12 | 1 |
| 9310 | HVOF $Cr_3C_2$-NiCr | 8 | Grade 39 | 300 | 13,500 | 4 x 12 | 2 |
| 9310 | HVOF $Cr_3C_2$-NiCr | 4 | Grade 67 | 300 | 13,500 | 4 x 12 | 2 |
| 9310 | HVOF T800 | 4 | Grade 39 | 300 | 13,500 | 4 x 12 | 2 |
| 9310 | HVOF T800 | 4 | Grade 67 | 300 | 13,500 | 4 x 12 | 2 |
| 9310 | HVOF T400 | 8 | Grade 39 | 300 | 13,500 | 4 x 12 | 2 |
| 9310 | HVOF T400 | 8 | Grade 67 | 300 | 13,500 | 4 x 12 | 4 |
| 9310 | PS WC-17Co | 8 | Grade 39 | 300 | 13,500 | 4 x 12 | 2 |
| 9310 | PS WC-17Co | 4 | Grade 67 | 300 | 13,500 | 4 x 12 | 2 |
| 9310 | PS T400 | 4 | Grade 39 | 300 | 13,500 | 4 x 12 | 2 |
| 9310 | PS T400 | 8 | Grade 67 | 300 | 13,500 | 4 x 12 | 4 |
| TOTAL HIGH SPEED TESTS | | (4 seals per rig set-up; 1.0-5.5 lbs load) | | | | | 40 |
| 9310 | EHC | 8 | Grade 39 | 300 | 7,000 | 4 x 12 | 2 |
| 9310 | EHC | 8 | Grade 67 | 300 | 7,000 | 4 x 12 | 2 |
| 9310 | EHC | 4 | Grade 39 | 300 | 7,000 | 4 x 12 | 1 |
| 9310 | EHC | 4 | Grade 67 | 300 | 7,000 | 4 x 12 | 1 |
| 9310 | HVOF WC-17Co | 8 | Grade 39 | 300 | 7,000 | 4 x 12 | 2 |
| 9310 | HVOF WC-17Co | 4 | Grade 39 | 300 | 7,000 | 4 x 12 | 2 |
| 9310 | HVOF WC-17Co | 8 | Grade 67 | 300 | 7,000 | 4 x 12 | 2 |
| 9310 | HVOF WC-17Co | 4 | Grade 67 | 300 | 7,000 | 4 x 12 | 2 |
| 9310 | HVOF $Cr_3C_2$-NiCr | 8 | Grade 39 | 300 | 7,000 | 4 x 12 | 2 |
| 9310 | HVOF $Cr_3C_2$-NiCr | 4 | Grade 67 | 300 | 7,000 | 4 x 12 | 2 |
| 9310 | HVOF T800 | 4 | Grade 39 | 300 | 7,000 | 4 x 12 | 3 |
| 9310 | HVOF T800 | 4 | Grade 67 | 300 | 7,000 | 4 x 12 | 3 |
| 9310 | HVOF T400 | 8 | Grade 39 | 300 | 7,000 | 4 x 12 | 2 |
| 9310 | HVOF T400 | 8 | Grade 67 | 300 | 7,000 | 4 x 12 | 2 |
| 9310 | PS WC-17Co | 8 | Grade 39 | 300 | 7,000 | 4 x 12 | 2 |
| 9310 | PS WC-17Co | 4 | Grade 67 | 300 | 7,000 | 4 x 12 | 2 |
| 9310 | PS T400 | 4 | Grade 39 | 300 | 7,000 | 4 x 12 | 2 |
| 9310 | PS T400 | 8 | Grade 67 | 300 | 7,000 | 4 x 12 | 2 |
| TOTAL LOW SPEED TESTS | | (4 seals per rig set-up; 1.0-5.5 lbs load) | | | | | 36 |

Since heat generation during testing can play a critical role in how carbon seals perform, a number of temperature measurements were collected to allow for thermal analysis of the results. These included measurement of the temperature in the carbon nose seals using embedded thermocouples, measurement of the input and output temperature of the oil, and measurement of the seal cavity air temperature. In general, all temperatures remained within the allowable limits during all test runs and therefore it was concluded there were no temperature effects on the results.

A stylus type Taylor Hobson Talysurf 10 surface profilometer was used to measure wear. The carbon seal cartridge and the seal runner were mounted to precision jigs for the measurements. Reference planes on the carbon seal and on the seal runner allowed accurate differential heights to be measured as the amount of wear. Figure 4-83 shows the measurement set-ups used for the carbon seals and coated seal runners. Three chord traverses at 120 degrees apart gave 6 measurement locations on the carbon seals. The runner rings had two diametrical traces made at 90 degrees to each other for four measurements of the coatings. Figure 4-84 shows a representative series of profilometer traverses taken on a carbon seal prior to testing and after 12, 24, 36 and 48 hours of testing. It is clear from the traverses that material was lost from the carbon seal during the test. The profilometer results for all traverses on each carbon seal or coated runner were averaged to give a value for total thickness of material removed (or, in a few cases, material gained).


**Figure 4-83 Carbon Seal (left) and Seal Runner (right) Mounted on Wear Measurement Jigs for Use in Talysurf Surface Profilometer**

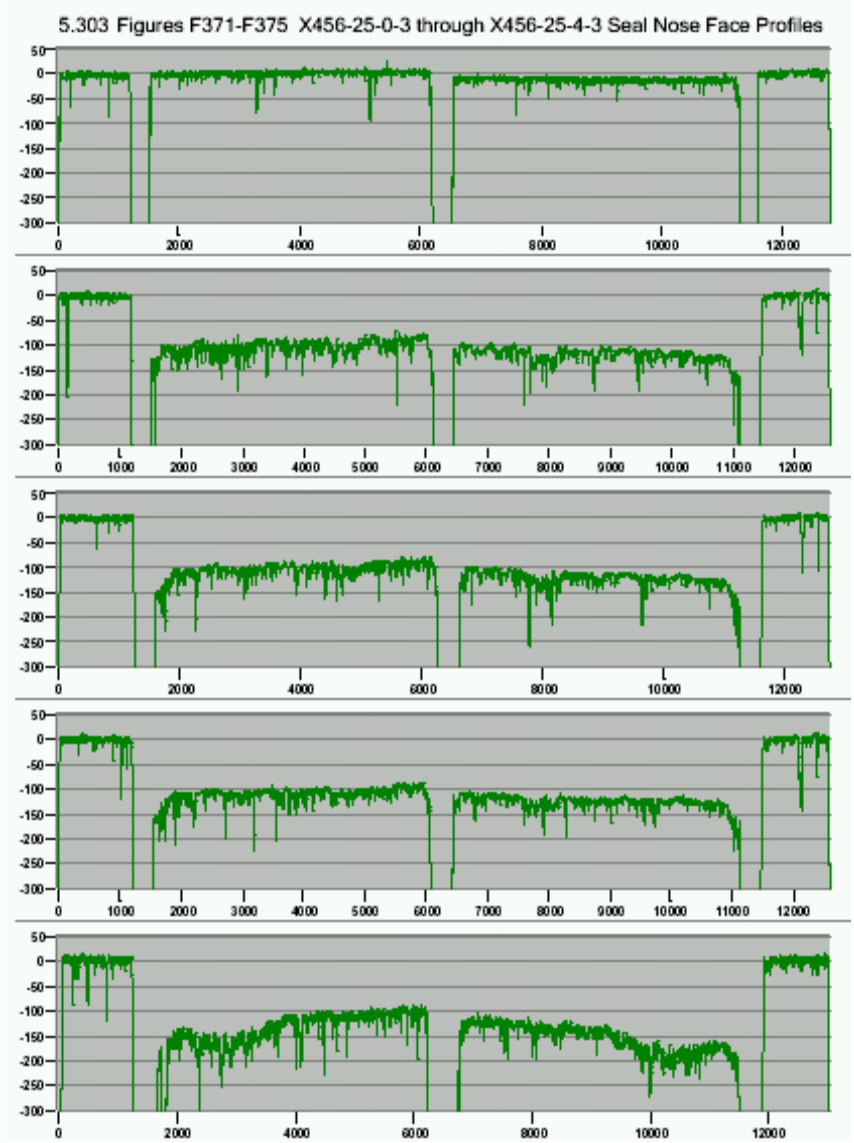


**Figure 4-84 Example of Profilometer Wear Measurements on a Carbon Seal Taken Prior to Testing and After 12, 24, 36 and 48 Hours of Testing (numbers on vertical axis are in units of microinches)**

## 4.8.6. Test Results and Discussion

### 4.8.6.1. Wear Values and General Observations

Table 4-49 provides the actual wear data for the 76 tests that were conducted by Rexnord, with Figure 4-85 and Figure 4-86 providing a graphical representation of the data as a function of time for the carbon seals and coated runners, respectively. The numbers in the table are in microinches, with a negative number indicating loss of material and a positive number indicating an increase in thickness. It is apparent from Figure 4-85 that most of the wear on the carbon seals occurred during the first 12 hours of testing. This is a common occurrence in sliding wear tests and the initial high-wear period is often referred to as run-in or break-in wear. Thus, the first 12-hour time segment will be referred to as break-in wear. Based on this analysis, it was considered appropriate to separate the break-in wear values from the amount of wear that occurred from 12

to 48 hours (designated the continuous wear period) and these numbers are indicated separately in Table 4-49. Note that the overall average wear on the carbon seals was 113 microinches, with 96 microinches of that occurring during the break-in period. It is apparent from the data in Figure 4-86 that a break-in wear period is not as evident for the coatings as it was for the carbon seals, but the values of wear for the coatings for the first 12 hours of testing and for the remaining 36 hours of testing are also given in Table 4-49.

An analysis of the wear data indicated that the average amount of wear on the carbon seals was approximately an order of magnitude greater than the average amount of wear on the coatings, with the total wear on the latter ranging from less than 10 to several 10's of microinches, indicating extremely low wear rates. This result was not unexpected because of the fact that all of the coatings were considerably harder than the carbon seals. The fluctuations in the wear values for the coatings as indicated in Figure 4-86, in some cases showing a gain in material, are most likely the result of the very small amount of wear that has occurred and the accuracy of the profilometer in this range.

## Table 4-49 Values of Total Wear, Break-in Wear, and Wear From 12-48 Hours for Carbon Seals and Coated Runners for Each Test Run (values expressed in microinches)

| Test # X456- | Mating Ring Coating | Coating Finish Ra [micro-inches] | USG Carbon Grade | Carbon Scleroscope Hardness | Speed [rpm] | Seal Load, [lbs] | Carbon Total Wear | Coating Total Wear | Total Wear Ratio | Carbon Break-in wear | Coating Break-in Wear | Break-in Wear Ratio | Carbon Wear, 12-48 Hrs | Coating Wear 12-48 Hours | Wear Ratio,12-48 Hrs |
|---|---|---|---|---|---|---|---|---|---|---|---|---|---|---|---|
| 1 | HVOF Tribaloy 400 | 8 | 39 | 100 | 13,500 | 4.18 | -95 | -9 | 11 | ND | ND | ND | ND | ND | ND |
| 2 | HVOF Tribaloy 400 | 8 | 67 | 87 | 13,500 | 2.72 | -99 | -22 | 4 | ND | ND | ND | ND | ND | ND |
| 3 | HVOF Tribaloy 800 | 4 | 39 | 100 | 13,500 | 4.51 | -231 | -14 | 16 | ND | ND | ND | ND | ND | ND |
| 4 | HVOF Tribaloy 800 | 4 | 67 | 87 | 13,500 | 2.90 | -185 | -18 | 10 | ND | ND | ND | ND | ND | ND |
| 5 | HVOF Cr3C2-20NiCr | 8 | 39 | 100 | 7,000 | 4.30 | -20 | -2 | 12 | 0 | -1 | 0 | -20 | -1 | 22 |
| 6 | HVOF Cr3C2-20NiCr | 8 | 39 | 100 | 7,000 | 3.46 | 0 | -3 | 0 | 5 | -1 | -5 | -5 | -2 | 2 |
| 7 | PS WC-17Co | 4 | 67 | 87 | 7,000 | 4.97 | -81 | -12 | 7 | -74 | -9 | 9 | -7 | -3 | 3 |
| 8 | PS WC-17Co | 4 | 67 | 87 | 7,000 | 2.88 | -58 | -8 | 7 | -52 | -7 | 7 | -7 | -1 | 7 |
| 9 | PS Tribaloy 400 | 4 | 39 | 100 | 7,000 | 4.19 | -23 | -7 | 4 | -11 | -1 | 12 | -13 | -6 | 2 |
| 10 | PS Tribaloy 400 | 4 | 39 | 100 | 7,000 | 3.01 | -3 | 3 | -1 | 4 | 0 | 11 | -7 | 3 | -2 |
| 11 | HVOF WC-17Co | 4 | 39 | 100 | 7,000 | 5.07 | -5 | -4 | 1 | -3 | -3 | 1 | -2 | -2 | 1 |
| 12 | HVOF WC-17Co | 4 | 67 | 87 | 7,000 | 3.49 | -13 | -4 | 3 | -9 | -2 | 4 | -4 | -2 | 2 |
| 13 | HVOF WC-17Co | 8 | 39 | 100 | 13,500 | 4.23 | -25 | -3 | 9 | -26 | -4 | 7 | 1 | 1 | 1 |
| 14 | HVOF WC-17Co | 8 | 67 | 87 | 13,500 | 3.65 | -14 | -1 | 10 | -11 | 0 | -29 | -4 | -2 | 2 |
| 15 | PS WC-17Co | 8 | 39 | 100 | 13,500 | 4.52 | -74 | -4 | 21 | -27 | -3 | 8 | -47 | 0 | 705 |
| 16 | PS WC-17Co | 8 | 39 | 100 | 13,500 | 2.81 | -52 | 1 | -69 | -43 | -1 | 49 | -9 | 2 | -6 |
| 17 | HVOF WC-17Co | 4 | 39 | 100 | 13,500 | 3.96 | -49 | -4 | 14 | -59 | -3 | 21 | 11 | -1 | -15 |
| 18 | HVOF WC-17Co | 4 | 67 | 87 | 13,500 | 3.50 | -209 | -17 | 12 | -169 | -16 | 11 | -40 | -1 | 32 |
| 19 | HVOF Cr3C2-20NiCr | 4 | 67 | 87 | 13,500 | 4.78 | -28 | -9 | 3 | -23 | -7 | 3 | -5 | -1 | 3 |
| 20 | HVOF Cr3C2-20NiCr | 4 | 67 | 87 | 13,500 | 3.33 | -18 | -15 | 1 | -16 | -13 | 1 | -3 | -1 | 2 |
| 21 | HVOF Tribaloy 800 | 4 | 67 | 87 | 7,000 | 4.21 | -35 | -10 | 3 | -27 | -6 | 5 | -8 | -4 | 2 |
| 22 | HVOF Tribaloy 800 | 4 | 39 | 100 | 7,000 | 3.34 | -108 | -14 | 7 | -103 | -12 | 9 | -5 | -2 | 2 |
| 23 | EHC | 8 | 39 | 100 | 7,000 | 4.60 | -261 | -7 | 36 | -199 | -6 | 34 | -62 | -1 | 42 |
| 24 | EHC | 8 | 67 | 87 | 7,000 | 2.76 | -138 | -11 | 12 | -102 | -8 | 12 | -36 | -3 | 13 |
| 25 | PS Tribaloy 400 | 8 | 67 | 87 | 13,500 | 4.29 | -154 | -14 | 11 | -119 | -8 | 14 | -34 | -6 | 6 |
| 26 | PS Tribaloy 400 | 8 | 67 | 87 | 13,500 | 2.90 | -415 | -37 | 11 | -350 | -25 | 14 | -65 | -11 | 6 |
| 27 | HVOF WC-17Co | 8 | 67 | 87 | 13,500 | 4.74 | -72 | -14 | 5 | -69 | -9 | 8 | -3 | -5 | 1 |
| 28 | HVOF WC-17Co | 8 | 39 | 100 | 13,500 | 2.81 | -45 | -2 | 19 | -27 | -2 | 13 | -19 | 0 | 52 |
| 29 | EHC | 8 | 39 | 100 | 7,000 | 4.23 | -399 | -14 | 29 | -342 | -8 | 44 | -57 | -6 | 10 |
| 30 | EHC | 8 | 67 | 87 | 7,000 | 3.26 | -103 | -11 | 9 | -86 | -7 | 12 | -17 | -4 | 4 |
| 31 | HVOF Tribaloy 400 | 8 | 67 | 87 | 7,000 | 4.64 | -24 | -11 | 2 | -10 | -4 | 2 | -14 | -7 | 2 |
| 32 | HVOF Tribaloy 400 | 8 | 39 | 100 | 7,000 | 2.92 | -32 | -9 | 4 | -24 | -5 | 5 | -7 | -4 | 2 |
| 33 | PS WC-17Co | 4 | 67 | 87 | 13,500 | 4.03 | -68 | -2 | 32 | -62 | -3 | 23 | -6 | 1 | -11 |
| 34 | PS WC-17Co | 4 | 67 | 87 | 13,500 | 2.97 | -100 | -6 | 17 | -95 | -6 | 17 | -5 | 0 | 33 |
| 35 | EHC | 8 | 39 | 100 | 13,500 | 4.87 | -422 | -4 | 110 | -305 | -8 | 36 | -118 | 5 | -26 |
| 36 | EHC | 8 | 67 | 87 | 13,500 | 2.85 | -287 | -15 | 19 | -251 | -8 | 30 | -36 | -7 | 5 |
| 37 | HVOF WC-17Co | 8 | 39 | 100 | 7,000 | 4.04 | -26 | 0 | -87 | -18 | -2 | 8 | -8 | 3 | -3 |
| 38 | HVOF WC-17Co | 8 | 67 | 87 | 7,000 | 2.86 | -17 | 2 | -10 | -8 | -1 | 10 | -9 | 3 | -3 |
| 39 | HVOF Tribaloy 400 | 8 | 67 | 87 | 7,000 | 4.79 | -121 | -7 | 18 | -117 | -15 | 8 | -3 | 8 | 0 |
| 40 | HVOF Tribaloy 400 | 8 | 39 | 100 | 7,000 | 2.79 | -123 | -4 | 27 | -116 | -10 | 12 | -7 | 5 | -1 |
| 41 | HVOF Tribaloy 800 | 4 | 67 | 87 | 13,500 | 4.29 | -145 | -20 | 7 | -136 | -20 | 7 | -9 | 0 | 23 |
| 42 | HVOF Tribaloy 800 | 4 | 39 | 100 | 13,500 | 2.93 | -173 | -8 | 22 | -152 | -6 | 24 | -21 | -1 | 14 |
| 43 | HVOF Tribaloy 400 | 8 | 67 | 87 | 13,500 | 4.62 | -97 | -25 | 4 | -93 | -25 | 4 | -4 | 0 | 9 |
| 44 | HVOF Tribaloy 400 | 8 | 39 | 100 | 13,500 | 2.70 | -170 | -8 | 23 | -165 | -6 | 28 | -5 | -2 | 3 |
| 45 | HVOF Cr3C2-20NiCr | 4 | 67 | 87 | 7,000 | 3.84 | -11 | -2 | 4 | -8 | -1 | 6 | -3 | -1 | 2 |
| 46 | HVOF Cr3C2-20NiCr | 4 | 67 | 87 | 7,000 | 2.83 | -18 | -4 | 5 | -16 | -2 | 6 | -2 | -1 | 2 |
| 47 | HVOF Tribaloy 800 | 4 | 39 | 100 | 7,000 | 4.76 | -83 | -7 | 13 | -77 | -8 | 10 | -6 | 1 | -6 |
| 48 | HVOF Tribaloy 800 | 4 | 67 | 87 | 7,000 | 2.79 | -41 | -8 | 5 | -33 | -6 | 6 | -7 | -2 | 4 |
| 49 | HVOF WC-17Co | 8 | 39 | 100 | 7,000 | 4.05 | -13 | -4 | 3 | -12 | -4 | 3 | -1 | 0 | -19 |
| 50 | HVOF WC-17Co | 8 | 67 | 87 | 7,000 | 2.94 | -32 | -12 | 3 | -14 | -6 | 2 | -18 | -6 | 3 |
| 51 | PS WC-17Co | 8 | 39 | 100 | 7,000 | 4.61 | -34 | 0 | 2354 | -28 | -3 | 8 | -6 | 3 | -2 |
| 52 | PS WC-17Co | 8 | 39 | 100 | 7,000 | 2.52 | -49 | 2 | -27 | -50 | 2 | -20 | 1 | -1 | -1 |
| 53 | PS Tribaloy 400 | 8 | 67 | 87 | 13,500 | 4.23 | -286 | -44 | 7 | -299 | -35 | 9 | 13 | -9 | -1 |
| 54 | PS Tribaloy 400 | 8 | 67 | 87 | 13,500 | 2.90 | -166 | -31 | 5 | -159 | -30 | 5 | -7 | 0 | 15 |
| 55 | HVOF Cr3C2-20NiCr | 8 | 39 | 100 | 13,500 | 4.61 | -100 | -9 | 11 | -114 | -7 | 15 | 14 | -2 | -8 |
| 56 | HVOF Cr3C2-20NiCr | 8 | 39 | 100 | 13,500 | 2.63 | -58 | -6 | 10 | -61 | -4 | 14 | 3 | -2 | -2 |
| 57 | PS Tribaloy 400 | 4 | 39 | 100 | 13,500 | 4.27 | -86 | -1 | 128 | -54 | -5 | 11 | -32 | 4 | -7 |
| 58 | PS Tribaloy 400 | 4 | 39 | 100 | 13,500 | 3.15 | -80 | -2 | 34 | -75 | 5 | -14 | -6 | -8 | 1 |
| 59 | EHC | 8 | 39 | 100 | 13,500 | 4.76 | -646 | -4 | 164 | -486 | -6 | 86 | -160 | 2 | -93 |
| 60 | EHC | 8 | 67 | 87 | 13,500 | 2.67 | -199 | -9 | 21 | -182 | -11 | 17 | -17 | 1 | -13 |
| 61 | PS Tribaloy 400 | 8 | 67 | 87 | 7,000 | 3.93 | -811 | -63 | 13 | -797 | -72 | 11 | -14 | 9 | -2 |
| 62 | PS Tribaloy 400 | 8 | 67 | 87 | 7,000 | 2.90 | -283 | -11 | 26 | -276 | -20 | 14 | -7 | 9 | -1 |
| 63 | HVOF WC-17Co | 4 | 39 | 100 | 7,000 | 4.46 | -14 | -2 | 7 | -5 | -2 | 2 | -9 | 0 | -353 |
| 64 | HVOF WC-17Co | 4 | 67 | 87 | 7,000 | 2.85 | 1 | -7 | 0 | -1 | -4 | 0 | 1 | -3 | 0 |
| 65 | HVOF Tribaloy 800 | 4 | 67 | 87 | 7,000 | 4.34 | -87 | -11 | 8 | -79 | -10 | 8 | -8 | -1 | 8 |
| 66 | HVOF Tribaloy 800 | 4 | 39 | 100 | 7,000 | 2.84 | -219 | -11 | 20 | -213 | -11 | 19 | -6 | 0 | -43 |
| 67 | EHC | 4 | 39 | 100 | 7,000 | 4.57 | -9 | -3 | 3 | -9 | -2 | 4 | 0 | -1 | 0 |
| 68 | EHC | 4 | 67 | 87 | 7,000 | 2.58 | -7 | 1 | -6 | -4 | -3 | 1 | -3 | 3 | -1 |
| 69 | HVOF Tribaloy 400 | 8 | 67 | 87 | 13,500 | 4.08 | -90 | -4 | 20 | -69 | -4 | 17 | -20 | 0 | 52 |
| 70 | HVOF Tribaloy 400 | 8 | 67 | 87 | 13,500 | 2.98 | -155 | -14 | 11 | -147 | -12 | 12 | -8 | -2 | 4 |
| 71 | HVOF WC-17Co | 8 | 67 | 87 | 13,500 | 4.74 | -47 | -11 | 4 | -29 | -9 | 3 | -18 | -2 | 11 |
| 72 | HVOF WC-17Co | 8 | 39 | 100 | 13,500 | 2.97 | -72 | -6 | 11 | -68 | -6 | 12 | -4 | 0 | 9 |
| 73 | EHC | 4 | 67 | 87 | 13,500 | 4.02 | 2 | -1 | -2 | -1 | -3 | 0 | 3 | 2 | 2 |
| 74 | EHC | 4 | 39 | 100 | 13,500 | 3.09 | -42 | 2 | -26 | -42 | -1 | 43 | 0 | 3 | 0 |
| 75 | EHC | 4 | 67 | 87 | 13,500 | 4.63 | -4 | 0 | -28 | 0 | -2 | 0 | -4 | 2 | -2 |
| 76 | EHC | 4 | 39 | 100 | 13,500 | 3.04 | -22 | -1 | 15 | -17 | -4 | 4 | -4 | 3 | -2 |
| | | | | Wear | Min | | -811 | -63 | -87 | -797 | -72 | -29 | -160 | -11 | -353 |
| | | | | | Avg | | -113 | -9 | 42 | -96 | -8 | 11 | -15 | -1 | 7 |
| | | | | Ratios of | Min | | | 13 | | | 11 | | | 14 | |
| | | | | | Avg | | | 13 | | | 12 | | | 19 | |

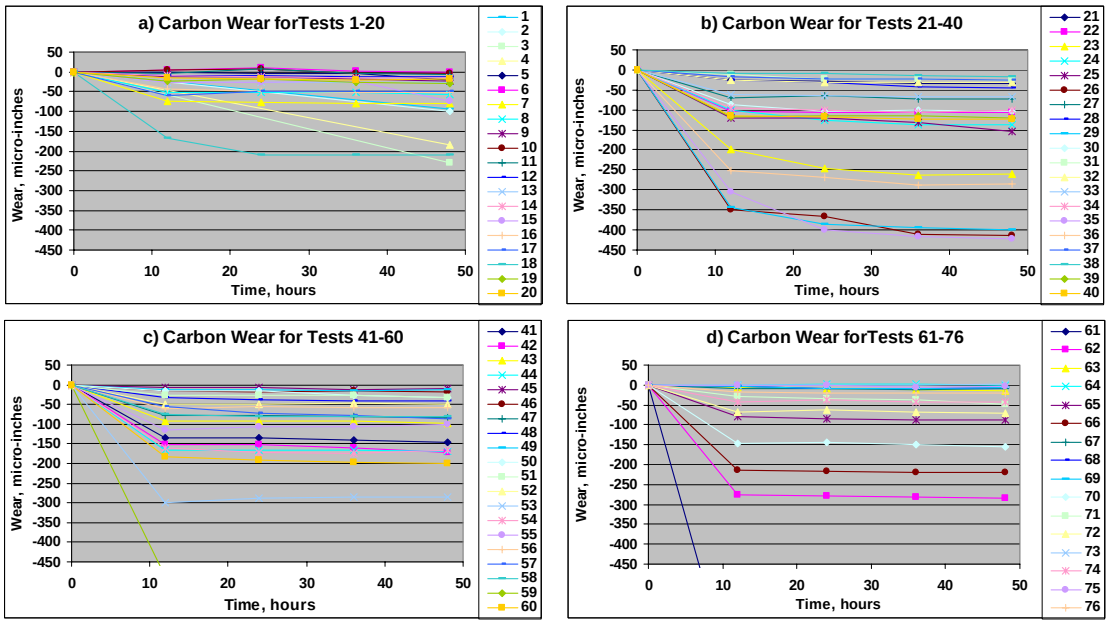


**Figure 4-85 Graphs of the Amount of Wear as a Function of Time for Carbon Seals for Each Test Run**

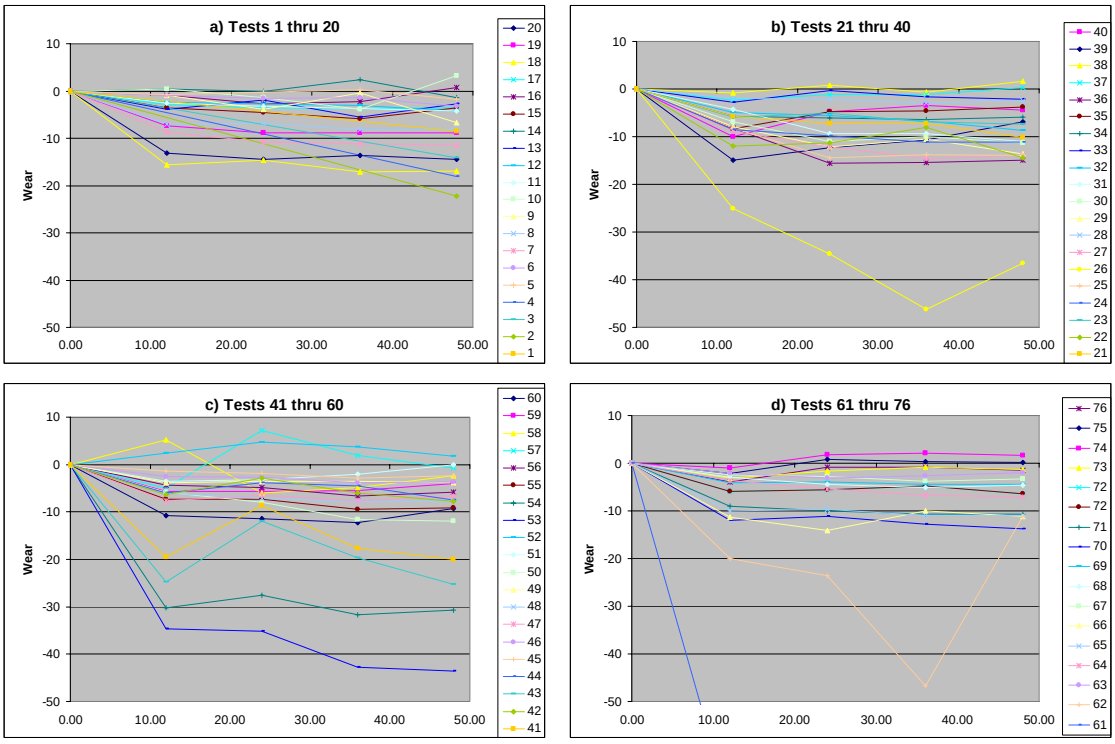


**Figure 4-86 Graphs of the Amount of Wear as a Function of Time for Coated Runners for Each Test Run**

Figure 4-87**Error! Reference source not found.** and Figure 4-88 present all the wear results in bar chart form in test sequence order. There do not seem to be any systematic upward or downward trends. The total wear and break-in wear charts mirror each other fairly closely while the continuous wear period values were much more random, particularly for the coating wear. Note the order of magnitude difference for the wear values on the vertical axis between the charts for the carbon seals in Figure 4-87**Error! Reference source not found.** and those for the coatings in Figure 4-88. The vertical-axis values for the total wear, break-in wear and continuous wear were kept the same within the carbon seal charts and the coating charts to emphasize the degree of difference between them. Subsequent coating comparison charts will expand the wear axis scale to facilitate comparisons.

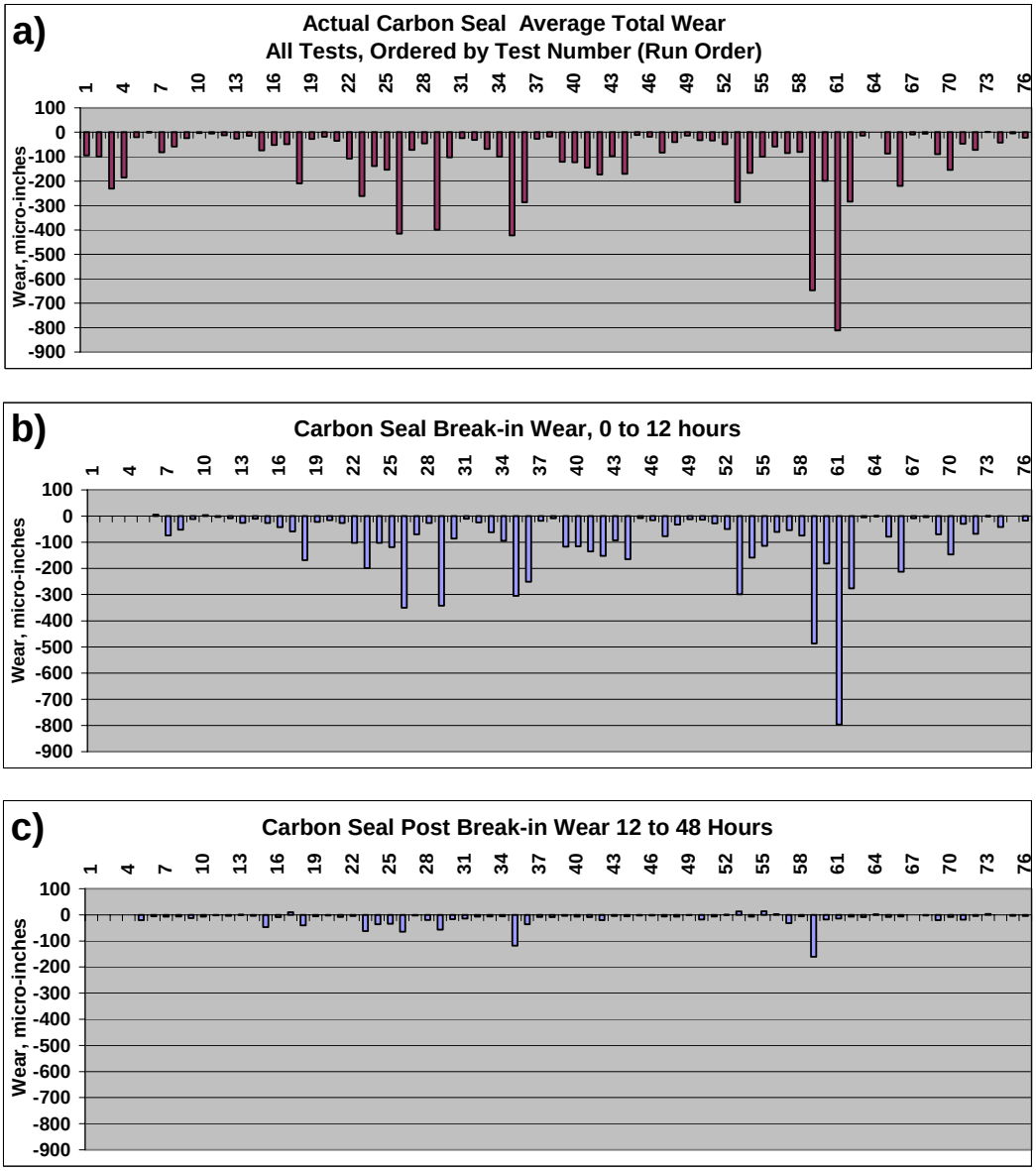


**Figure 4-87. Wear of the Carbon Seals for Each Test Run (a) Average Total Wear, (b) Break-in Wear, (c) Average Continuous (Post Break-in) Wear**

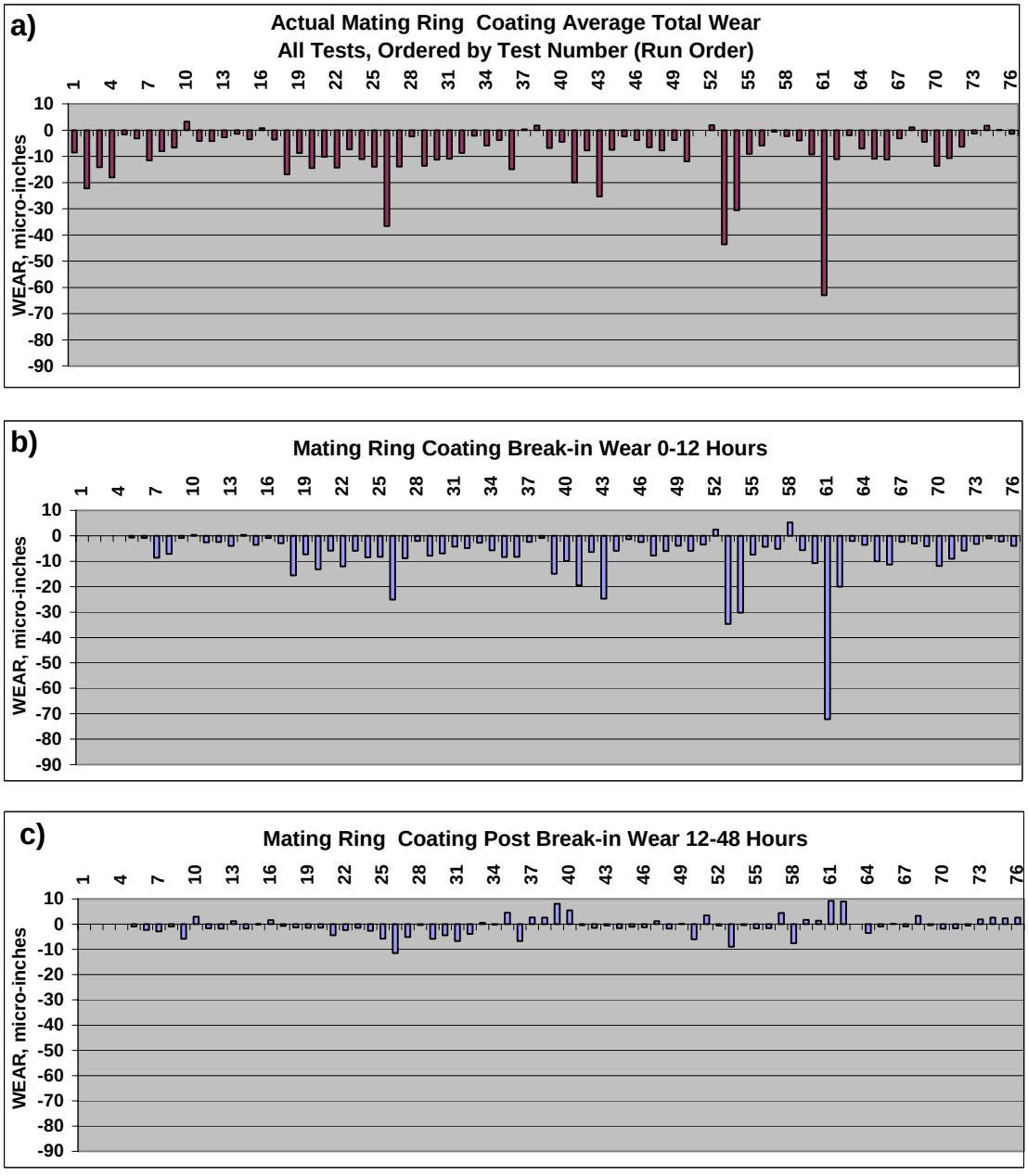


**Figure 4-88 Wear of the Coatings on the Runners for Each Test Run (a) Average Total Wear, (b) Break-in Wear, (c) Average Continuous (Post Break-in) Wear**

#### 4.8.6.2. Comparison of Results

The primary purpose for the carbon seal wear tests was to determine if the alternative coatings give wear performance equivalent to electroplated hard chrome (EHC), both for the coatings themselves and for the mating carbon seals. Therefore, the wear data was sorted according to the main variables included in the study which included the carbon grade, the rotor speed in RPM, and the surface finish of the EHC and alternative coatings. Figure 4-89 through Figure 4-96 contain bar charts of results for the total wear, the break-in wear period, and the continuous post break-in wear so that the overall coating effects and those for each portion of the test may be examined separately. The figures are organized as follows:

Figure 4-89: Wear for GR39 carbon seals when sliding against the coatings at 13,500 rpm
Figure 4-90: Wear for GR39 carbon seals when sliding against the coatings at 7000 rpm
Figure 4-91: Wear for GR67 carbon seals when sliding against the coatings at 13,500 rpm
Figure 4-92: Wear for GR67 carbon seals when sliding against the coatings at 7000 rpm
Figure 4-93: Wear for the coatings when sliding against GR39 carbon seals at 13,500 rpm
Figure 4-94: Wear for the coatings when sliding against GR39 carbon seals at 7000 rpm
Figure 4-95: Wear for the coatings when sliding against GR67 carbon seals at 13,500 rpm
Figure 4-96: Wear for the coatings when sliding against GR67 carbon seals at 7000 rpm

For convenience, the test number followed by the type of coating has been used on the horizontal axis to identify the data. Each individual chart has the results for the two surface finishes separated and labeled as 4 Ra or 8 Ra. The EHC baseline data is given by the blue bars and the alternative coatings data by the purple bars. Examination of Figure 4-89 and Figure 4-90 for the higher hardness GR39 carbon seals shows that the EHC consistently gave higher carbon seal wear when the EHC had an 8 Ra surface finish, but gave low carbon seal wear when the EHC had a 4 Ra surface finish. All of the alternative coatings with 8 Ra finishes gave lower carbon seal wear than the EHC with an 8 Ra finish in these tests. When the coatings had a 4 Ra finish, only the carbide coatings consistently approached the performance levels of the EHC. The accompanying coating wear for these tests seen in Figure 4-93 and Figure 4-94 is uniformly low, with the Tribaloy coatings showing somewhat more wear than EHC and the thermal spray carbides.

The wear results for the softer GR67 carbon seals are given in Figure 4-91 and Figure 4-92. Again, the wear of the carbon seals was considerably higher when sliding against the EHC with an 8 Ra finish than against EHC with a 4 Ra finish. The overall trend is for the EHC and thermal spray carbides to cause similar amounts of carbon seal wear for equivalent surface finishes while the Tribaloy coatings tended to cause higher carbon seal wear, particularly the PS Tribaloy 400 in some of the tests. There was also one instance of somewhat higher carbon seal wear for HVOF WC/Co at the 4 Ra finish. The coating wear for these same tests is seen in Figure 4-95 and Figure 4-96. The coating wear tends to be somewhat higher when sliding against the soft carbon seal than against the hard carbon seal. At the 8 Ra finish, the wear of the EHC and carbide coatings is comparable, with the Tribaloy coatings experiencing about twice the wear at the high speed. At the lower speed, the Tribaloy coatings were comparable to the EHC except for Test 61. At the 4 Ra finish the EHC performed somewhat better. The overall trend for all the tests suggests that the carbide coatings are better alternatives to EHC than the Tribaloy coatings. It also suggests that when EHC with an 8 Ra (or higher) finish is used in a current design carbon seal, the use of the alternative carbides coatings is acceptable. For seal designs that require a 4 Ra EHC, the alternatives may well still be acceptable since the wear of any of the coatings is so low, but care should be taken for such applications.

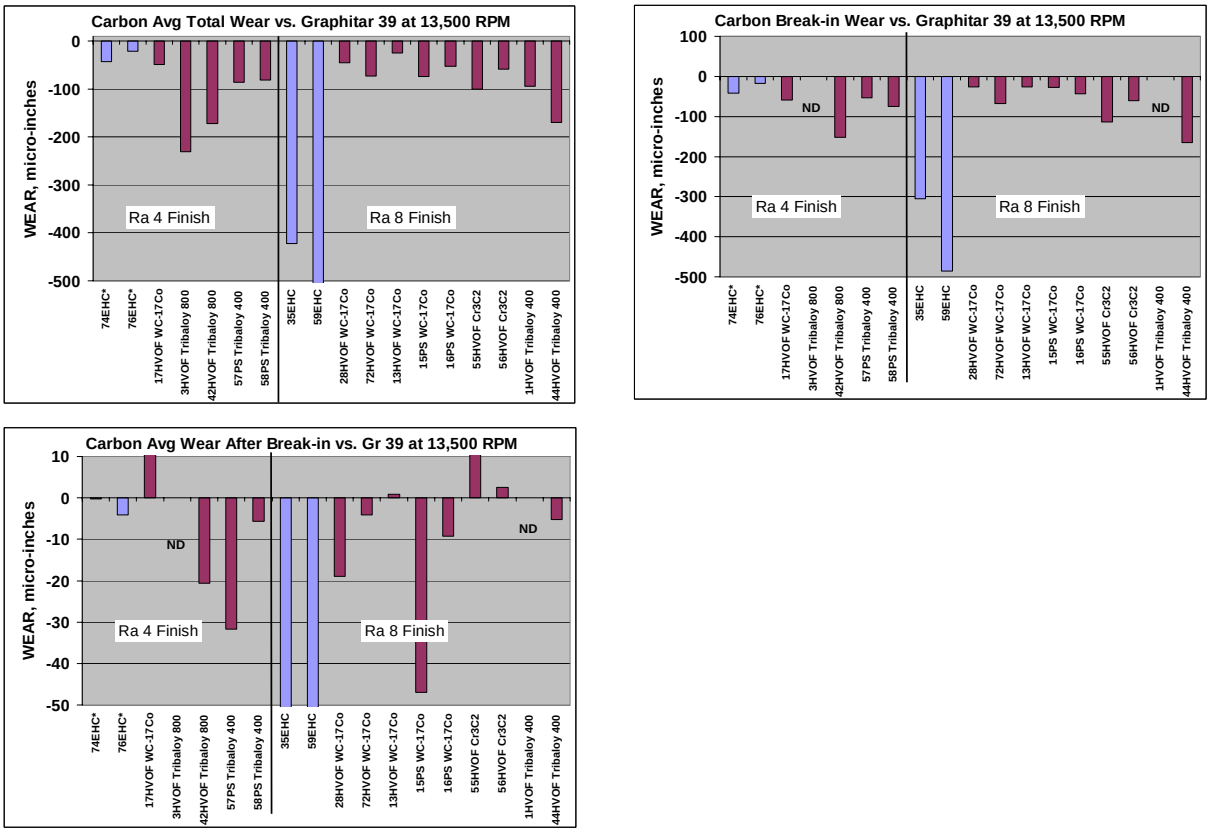


**Figure 4-89 Wear for GR39 Carbon Seals when Sliding Against the Indicated Coatings at 13,500 rpm**

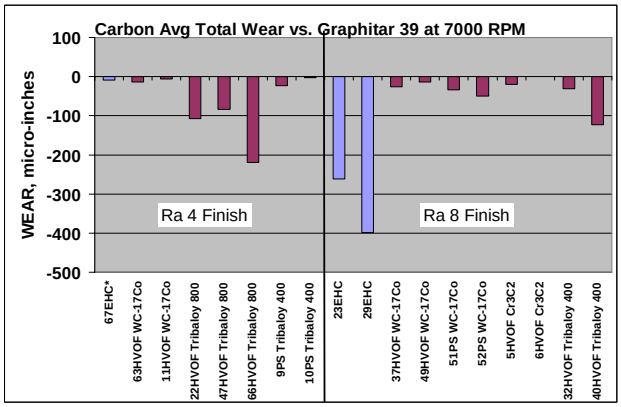


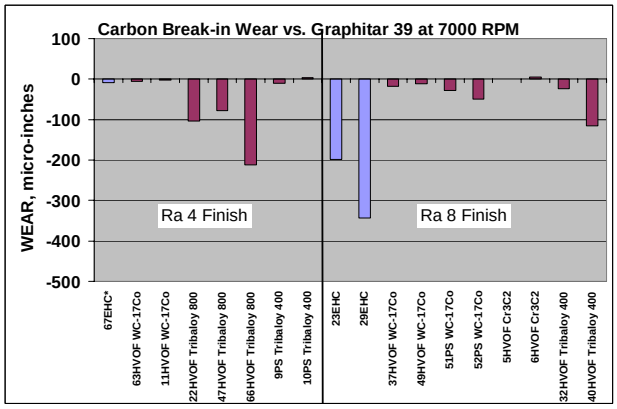


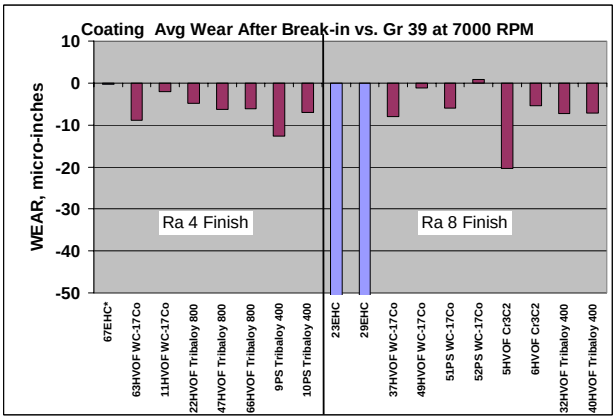


**Figure 4-90 Wear for GR39 Carbon Seals when Sliding Against the Indicated Coatings at 7000 rpm**

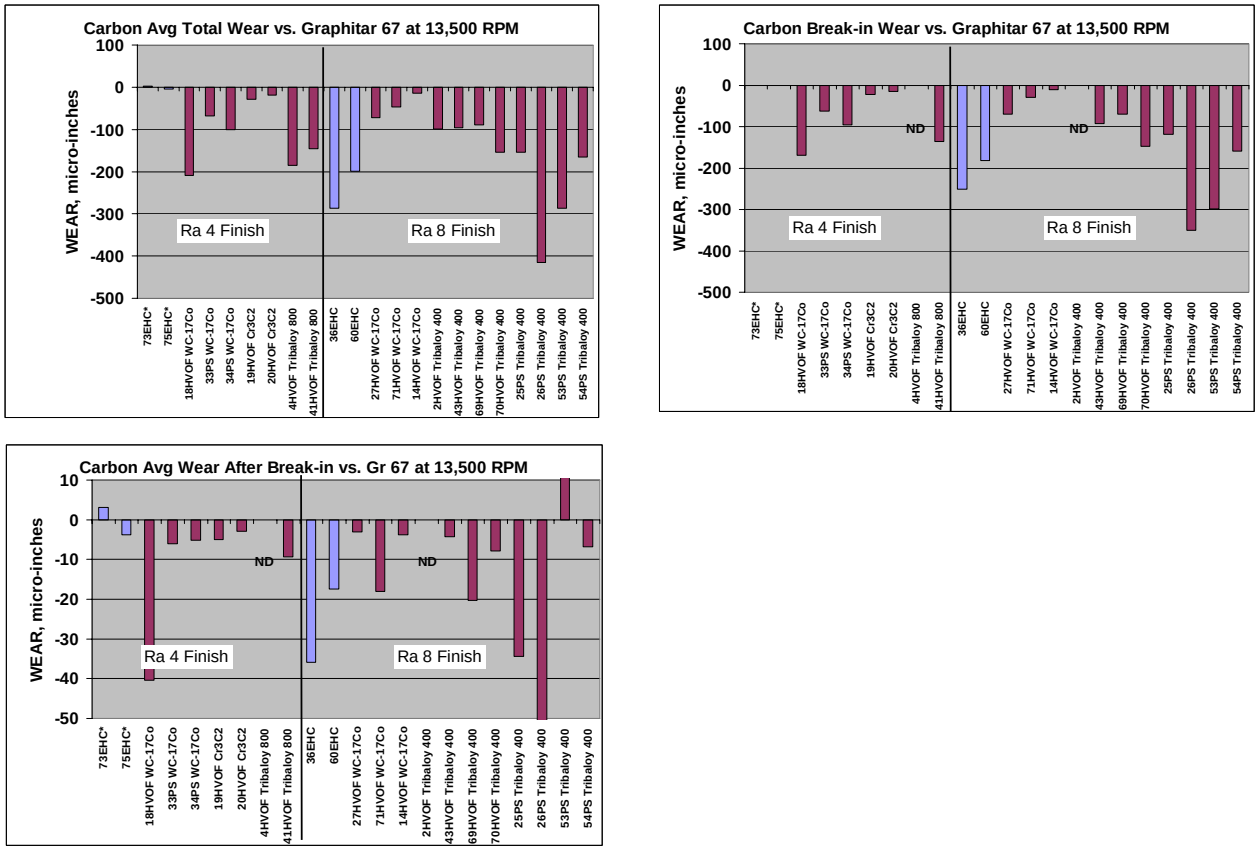


**Figure 4-91 Wear for GR67 Carbon Seals when Sliding Against the Indicated Coatings at 13,500 rpm**

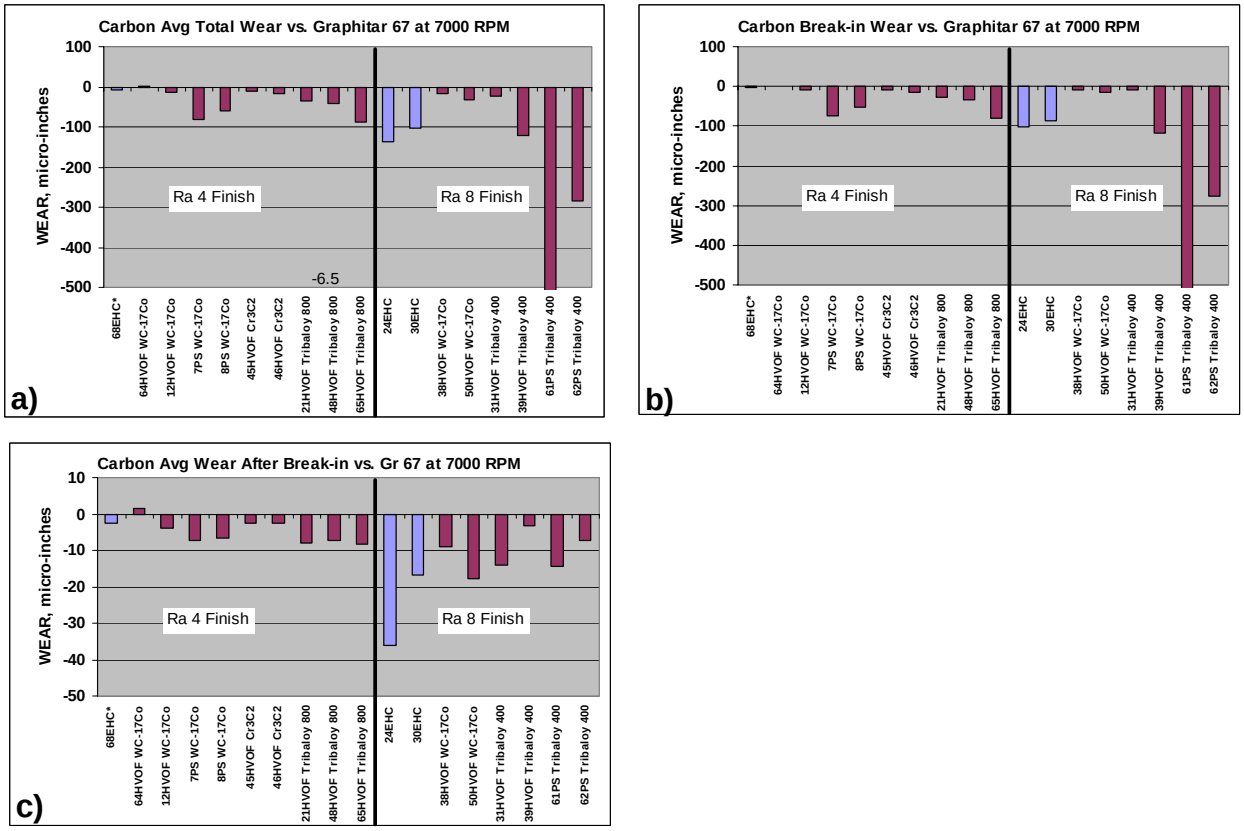


**Figure 4-92 Wear for GR67 Carbon Seals when Sliding Against the Indicated Coatings at 7000 rpm**

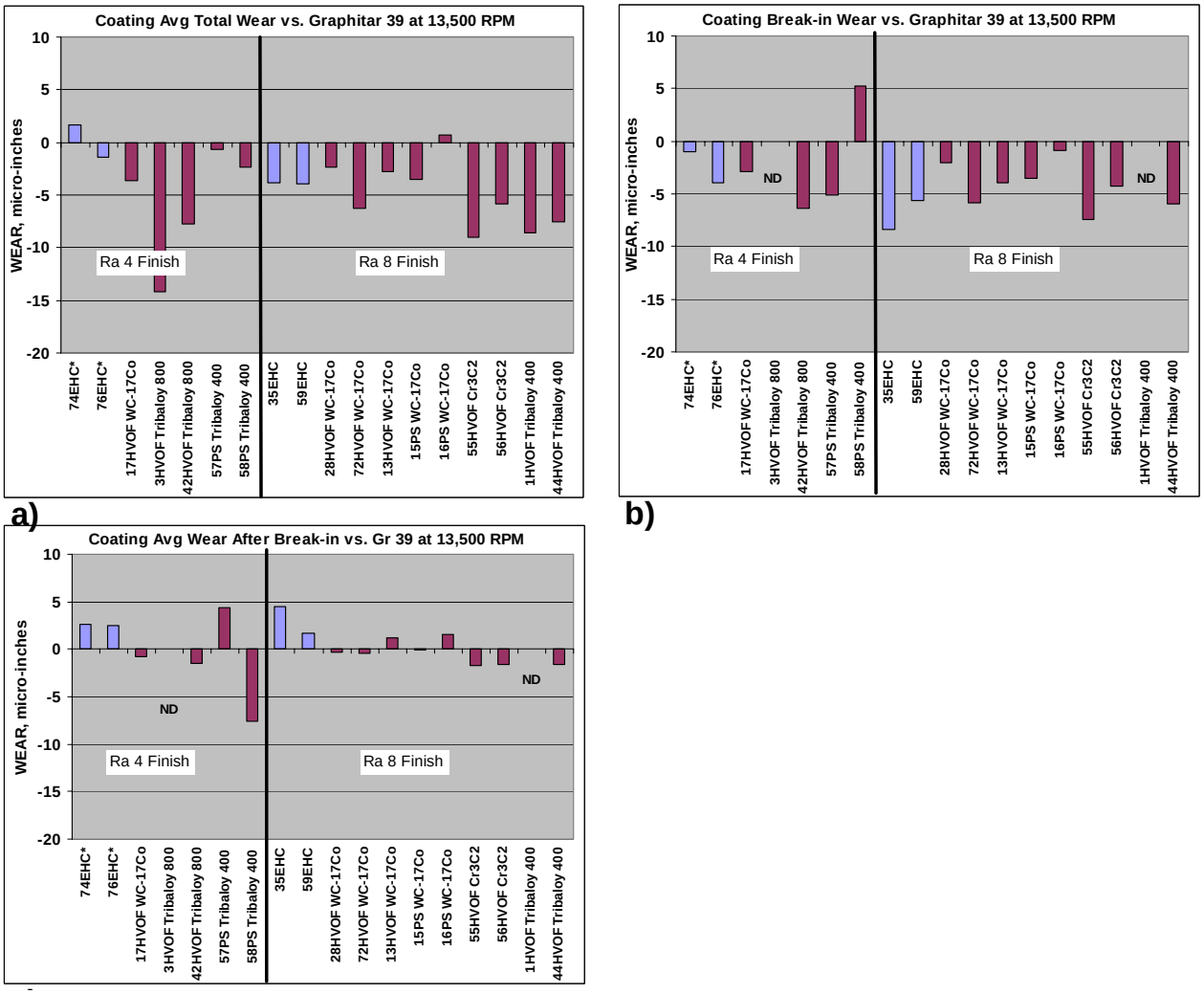


**Figure 4-93 Wear for the Indicated Coatings on the Runner Rings when Sliding Against GR39 Carbon Seals at 13,500 rpm**

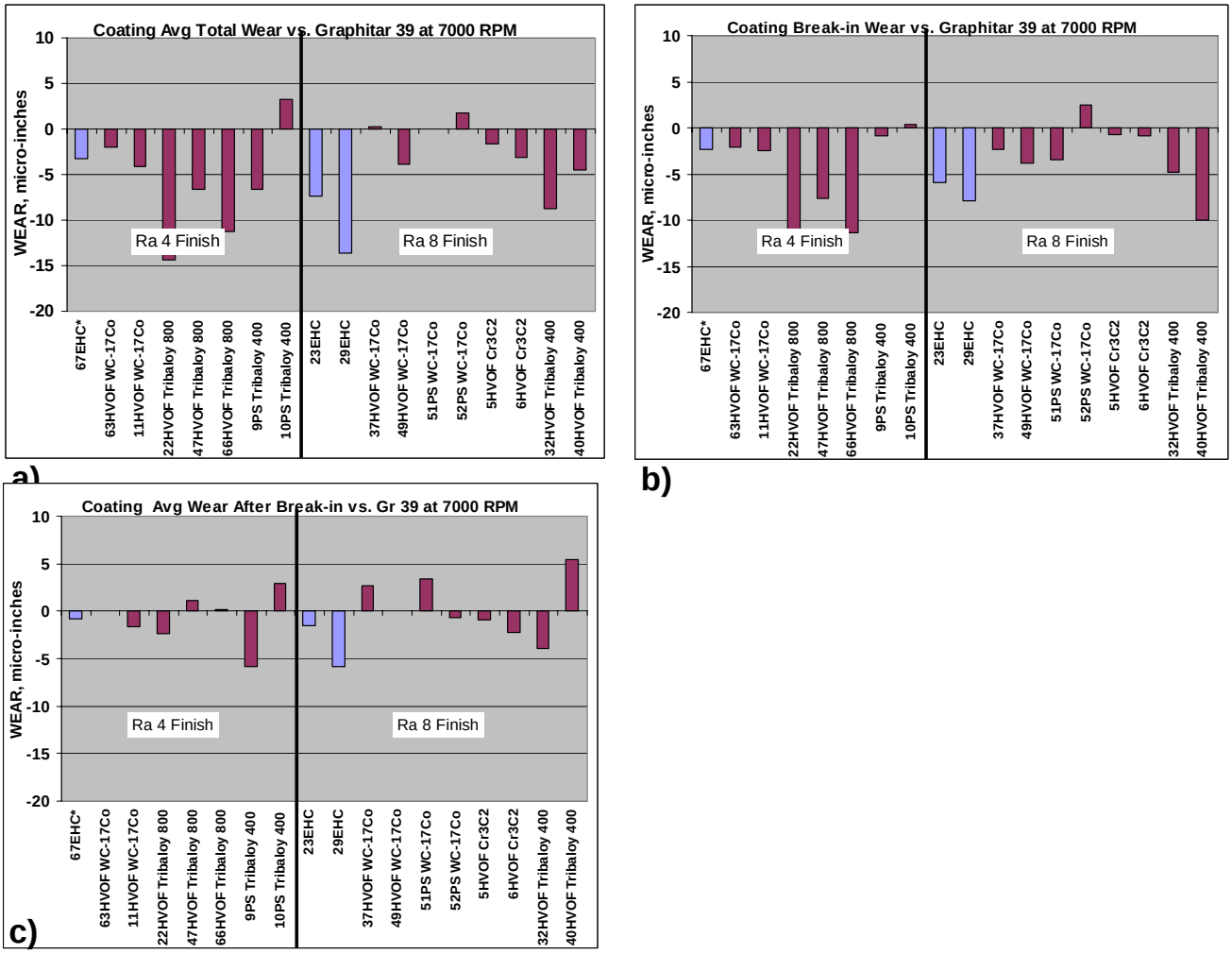


**Figure 4-94 Wear for the Indicated Coatings on the Runner Rings when Sliding Against GR39 Carbon Seals at 7000 rpm**

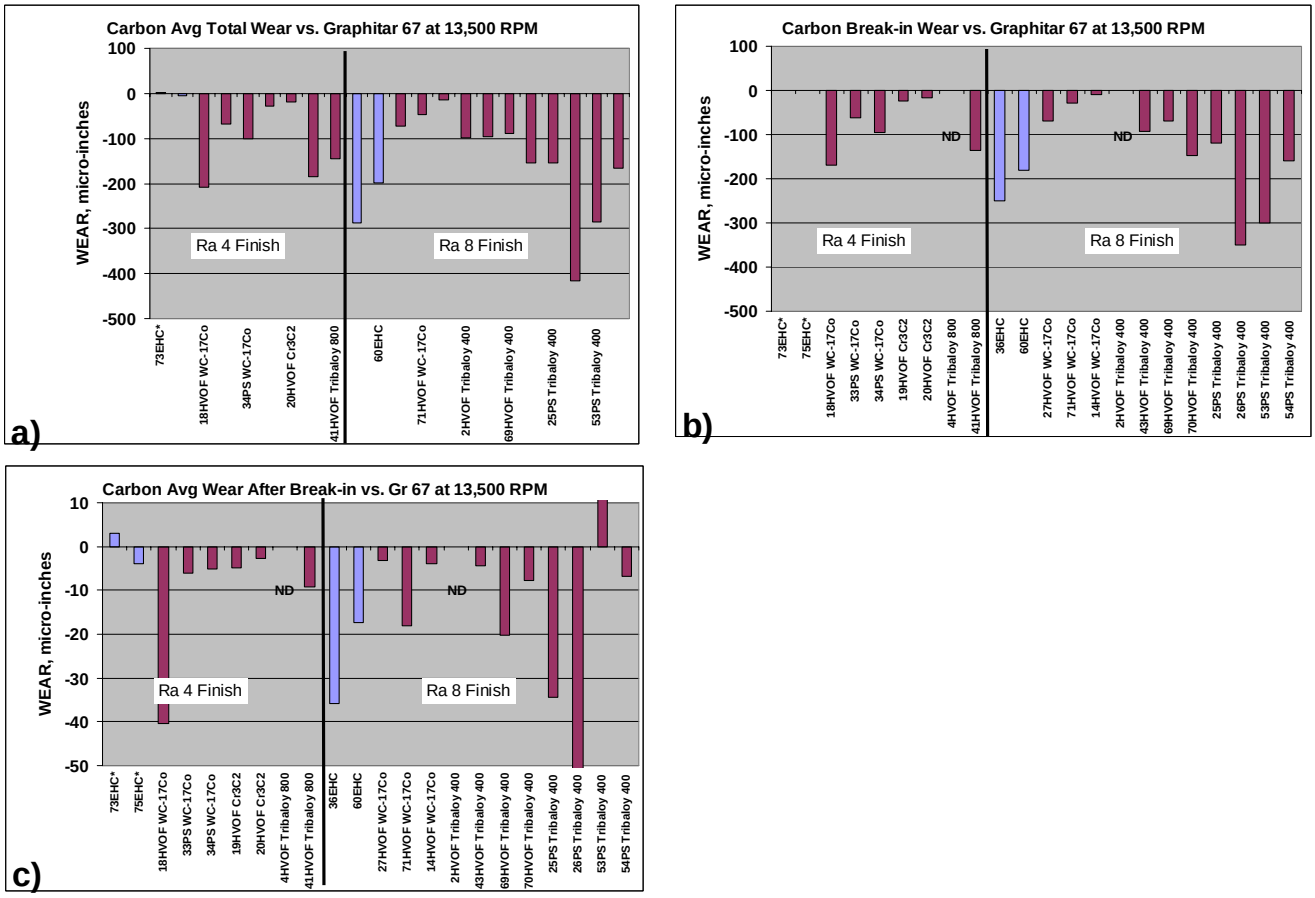


**Figure 4-95 Wear for the Indicated Coatings on the Runner Rings when Sliding Against GR67 Carbon Seals at 13,500 rpm**

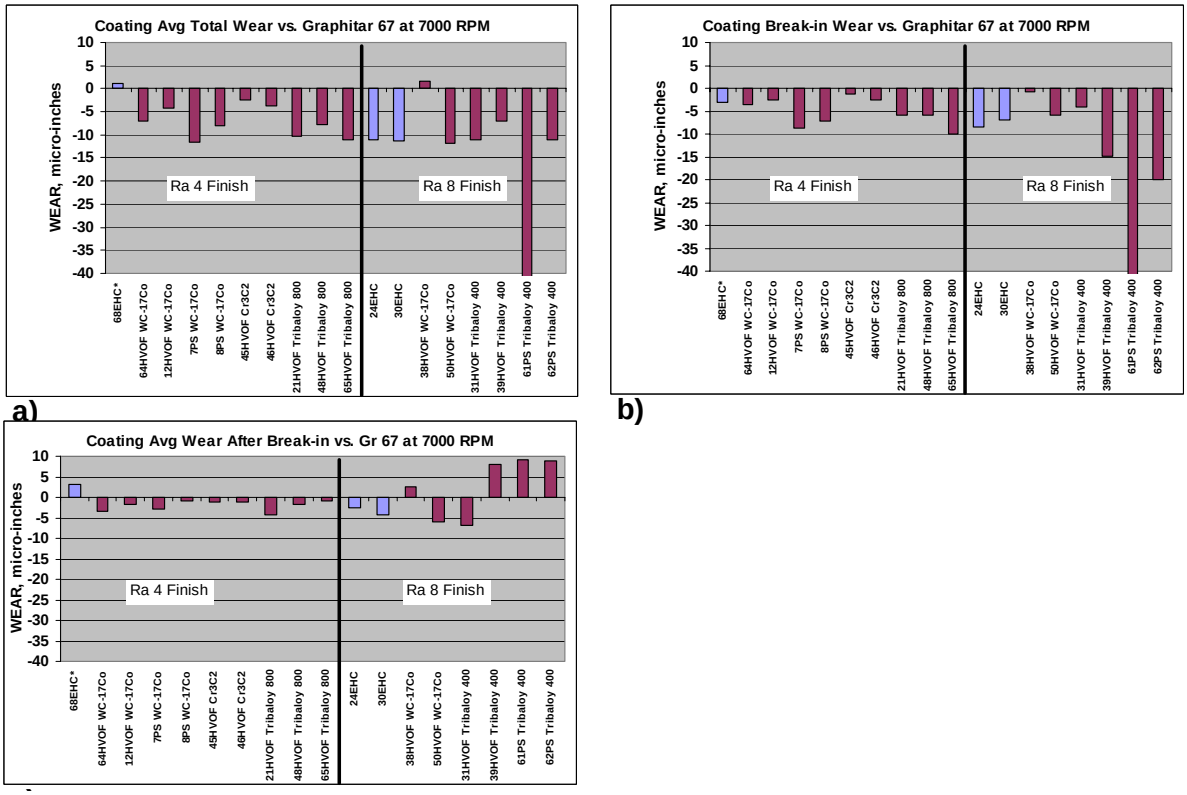


**Figure 4-96 Wear for the Indicated Coatings on the Runner Rings when Sliding Against GR67 Carbon Seals at 7000 rpm**

### 4.8.6.3. Analysis of Results

As indicated in Section 4.8.3.3, it was not possible to precisely re-position the spring-loaded cartridges containing the carbon seals for each test run. The position varied by a maximum of only 0.06 inches, but this resulted in a load change variation of 2.5 to 5.5 pounds (see Table 4-49). If the wear of the carbon seals follows Archard's Law [12], which assumes a linear process, i.e., wear is proportional to the applied load and distance, and inversely proportional to hardness, then it is possible to take into account these variations in load. Archard's Law can be expressed as:

$$W = \frac{kLD}{H}$$

Where W is the wear volume, L is the normal load, D is the distance of sliding, H is hardness, and k is the proportionality factor, also called the wear coefficient. In order to make direct comparisons between wear data with varying load, the wear coefficient is determined since that normalizes out the differences in load. Solving for k in the above equation gives:

$$k = \frac{WH}{LD}$$

In the studies reported here, the average diameter of the contact area was 1.85 inches and therefore the average circumference was 5.8 inches. For 7000 rpm the sliding velocity was

40,600 inches/minute and for 13,500 rpm the sliding velocity was 78,300 inches/minute. Therefore, for the complete 48-hour tests, the total sliding distances were $1.17 \times 10^8$ inches and $2.25 \times 10^8$ inches for 7000 and 13,500 rpm, respectively. The contact area on the carbon seals was 0.444 square inches, so the wear volume is obtained by multiplying that number by the average wear depths measured by the profilometer.

Normally, k is dimensionless but that only occurs when hardness can be expressed in terms of load per unit area (Vickers hardness values are commonly expressed in $kg/mm^2$). However, in these studies, the values for hardness of the carbon seals were only relative numbers obtained from a Scleroscope and therefore they have no dimensional units. Therefore, the values for k calculated for these tests using the above equation have units of $in^2/lb$. Although this does not rigorously follow Archard's analysis, it still provides a means for removing the load variations and making direct comparisons of wear data.

The values for the wear coefficients for the carbon seals materials for each run are provided in Table 4-50. The table follows the format of Table 4-49 and also includes the wear coefficients for the break-in period and for the continuous wear period of 12-48 hours. For completeness, the wear ratios from Table 4-49 were applied to the carbon seal wear coefficients to derive numbers for wear coefficients for the coatings. Although these numbers are not rigorously correct because they do not take into account the hardness values for the coatings, they still allow for normalization of the coating wear to take into account the variations in load.

# Table 4-50 Calculated Wear Coefficients for Total Wear, Break-in Wear, and Continuous Wear for the Carbon Seals and Coatings for Each Test

| Test # X456- | Mating Ring Coating | Coating Finish Ra [micro-inches] | USG Carbon Grade | Carbon Scleroscope Hardness | Speed [rpm] | Seal Load, [lbs] | Carbon Total Wear | Coating Total Wear | Total Wear Ratio | Carbon Break-in wear | Coating Break-in Wear | Break-in Wear Ratio | Carbon Wear, 12-48 Hrs | Coating Wear 12-48 Hours | Wear Ratio,12-48 Hrs |
|---|---|---|---|---|---|---|---|---|---|---|---|---|---|---|---|
| 1 | HVOF Trib | 8 | 39 | 100 | 13,500 | 4.18 | -4.5E-12 | -4.0E-13 | 1.1E+01 | ND | ND | ND | ND | ND | ND |
| 2 | HVOF Trib | 8 | 67 | 87 | 13,500 | 2.72 | -6.2E-12 | -1.4E-12 | 4.4E+00 | ND | ND | ND | ND | ND | ND |
| 3 | HVOF Trib | 4 | 39 | 100 | 13,500 | 4.51 | -1.0E-11 | -6.2E-13 | 1.6E+01 | ND | ND | ND | ND | ND | ND |
| 4 | HVOF Trib | 4 | 67 | 87 | 13,500 | 2.90 | -1.1E-11 | -1.1E-12 | 1.0E+01 | ND | ND | ND | ND | ND | ND |
| 5 | HVOF Cr3( | 8 | 39 | 100 | 7,000 | 4.30 | -1.8E-12 | -1.5E-13 | 1.2E+01 | 2.1E-15 | -6.6E-14 | -3.2E-02 | -1.8E-12 | -8.2E-14 | 2.2E+01 |
| 6 | HVOF Cr3( | 8 | 39 | 100 | 7,000 | 3.46 | -5.2E-14 | -3.5E-13 | 1.5E-01 | 5.4E-13 | -1.0E-13 | -5.4E+00 | -5.9E-13 | -2.5E-13 | 2.4E+00 |
| 7 | PS WC-17( | 4 | 67 | 87 | 7,000 | 4.97 | -5.4E-12 | -7.7E-13 | 7.0E+00 | -4.9E-12 | -5.7E-13 | 8.5E+00 | -4.9E-13 | -1.9E-13 | 2.5E+00 |
| 8 | PS WC-17( | 4 | 67 | 87 | 7,000 | 2.88 | -6.7E-12 | -9.2E-13 | 7.3E+00 | -5.9E-12 | -8.1E-13 | 7.3E+00 | -7.6E-13 | -1.1E-13 | 6.8E+00 |
| 9 | PS Tribaloy | 4 | 39 | 100 | 7,000 | 4.19 | -2.1E-12 | -6.0E-13 | 3.5E+00 | -9.8E-13 | -7.9E-14 | 1.2E+01 | -1.1E-12 | -5.2E-13 | 2.2E+00 |
| 10 | PS Tribaloy | 4 | 39 | 100 | 7,000 | 3.01 | -4.3E-13 | 4.1E-13 | -1.1E+00 | 4.5E-13 | 4.2E-14 | 1.1E+01 | -8.9E-13 | 3.6E-13 | -2.4E+00 |
| 11 | HVOF WC- | 4 | 39 | 100 | 7,000 | 5.07 | -3.9E-13 | -3.1E-13 | 1.3E+00 | -2.4E-13 | -1.9E-13 | 1.3E+00 | -1.6E-13 | -1.2E-13 | 1.3E+00 |
| 12 | HVOF WC- | 4 | 67 | 87 | 7,000 | 3.49 | -1.2E-12 | -4.0E-13 | 3.0E+00 | -8.1E-13 | -2.3E-13 | 3.5E+00 | -3.8E-13 | -1.7E-13 | 2.2E+00 |
| 13 | HVOF WC- | 8 | 39 | 100 | 13,500 | 4.23 | -1.2E-12 | -1.3E-13 | 9.1E+00 | -1.2E-12 | -1.8E-13 | 6.6E+00 | 3.8E-14 | 5.4E-14 | 7.0E-01 |
| 14 | HVOF WC- | 8 | 67 | 87 | 13,500 | 3.65 | -6.8E-13 | -6.7E-14 | 1.0E+01 | -5.0E-13 | 1.7E-14 | -2.9E+01 | -1.8E-13 | -8.4E-14 | 2.2E+00 |
| 15 | PS WC-17( | 8 | 39 | 100 | 13,500 | 4.52 | -3.2E-12 | -1.5E-13 | 2.1E+01 | -1.2E-12 | -1.5E-13 | 7.8E+00 | -2.0E-12 | -2.9E-15 | 7.1E+02 |
| 16 | PS WC-17( | 8 | 39 | 100 | 13,500 | 2.81 | -3.6E-12 | 5.3E-14 | -6.9E+01 | -3.0E-12 | -6.1E-14 | 4.9E+01 | -6.5E-13 | 1.1E-13 | -5.7E+00 |
| 17 | HVOF WC- | 4 | 39 | 100 | 13,500 | 3.96 | -2.4E-12 | -1.8E-13 | 1.4E+01 | -3.0E-12 | -1.4E-13 | 2.1E+01 | 5.3E-13 | -3.6E-14 | -1.5E+01 |
| 18 | HVOF WC- | 4 | 67 | 87 | 13,500 | 3.50 | -1.0E-11 | -8.2E-13 | 1.2E+01 | -8.3E-12 | -7.6E-13 | 1.1E+01 | -2.0E-12 | -6.3E-14 | 3.2E+01 |
| 19 | HVOF Cr3( | 4 | 67 | 87 | 13,500 | 4.78 | -1.0E-12 | -3.1E-13 | 3.2E+00 | -8.2E-13 | -2.6E-13 | 3.1E+00 | -1.8E-13 | -5.2E-14 | 3.4E+00 |
| 20 | HVOF Cr3( | 4 | 67 | 87 | 13,500 | 3.33 | -9.5E-13 | -7.5E-13 | 1.3E+00 | -8.0E-13 | -6.8E-13 | 1.2E+00 | -1.5E-13 | -7.0E-14 | 2.1E+00 |
| 21 | HVOF Trib | 4 | 67 | 87 | 7,000 | 4.21 | -2.7E-12 | -8.0E-13 | 3.4E+00 | -2.1E-12 | -4.5E-13 | 4.6E+00 | -6.3E-13 | -3.4E-13 | 1.8E+00 |
| 22 | HVOF Trib | 4 | 39 | 100 | 7,000 | 3.34 | -1.2E-11 | -1.6E-12 | 7.5E+00 | -1.2E-11 | -1.4E-12 | 8.6E+00 | -5.4E-13 | -2.7E-13 | 2.0E+00 |
| 23 | EHC | 8 | 39 | 100 | 7,000 | 4.60 | -2.2E-11 | -6.1E-13 | 3.6E+01 | -1.6E-11 | -4.9E-13 | 3.4E+01 | -5.2E-12 | -1.2E-13 | 4.2E+01 |
| 24 | EHC | 8 | 67 | 87 | 7,000 | 2.76 | -1.7E-11 | -1.3E-12 | 1.2E+01 | -1.2E-11 | -1.0E-12 | 1.2E+01 | -4.3E-12 | -3.2E-13 | 1.3E+01 |
| 25 | PS Tribaloy | 8 | 67 | 87 | 13,500 | 4.29 | -6.1E-12 | -5.6E-13 | 1.1E+01 | -4.8E-12 | -3.3E-13 | 1.4E+01 | -1.4E-12 | -2.3E-13 | 6.0E+00 |
| 26 | PS Tribaloy | 8 | 67 | 87 | 13,500 | 2.90 | -2.4E-11 | -2.2E-12 | 1.1E+01 | -2.1E-11 | -1.5E-12 | 1.4E+01 | -3.8E-12 | -6.8E-13 | 5.6E+00 |
| 27 | HVOF WC- | 8 | 67 | 87 | 13,500 | 4.74 | -2.6E-12 | -5.0E-13 | 5.2E+00 | -2.5E-12 | -3.2E-13 | 7.8E+00 | -1.1E-13 | -1.8E-13 | 6.0E-01 |
| 28 | HVOF WC- | 8 | 39 | 100 | 13,500 | 2.81 | -3.2E-12 | -1.7E-13 | 1.9E+01 | -1.9E-12 | -1.4E-13 | 1.3E+01 | -1.3E-12 | -2.6E-14 | 5.2E+01 |
| 29 | EHC | 8 | 39 | 100 | 7,000 | 4.23 | -3.6E-11 | -1.2E-12 | 2.9E+01 | -3.1E-11 | -7.1E-13 | 4.4E+01 | -5.1E-12 | -5.2E-13 | 9.8E+00 |
| 30 | EHC | 8 | 67 | 87 | 7,000 | 3.26 | -1.0E-11 | -1.1E-12 | 9.1E+00 | -8.7E-12 | -7.0E-13 | 1.2E+01 | -1.7E-12 | -4.4E-13 | 3.8E+00 |
| 31 | HVOF Trib | 8 | 67 | 87 | 7,000 | 4.64 | -1.7E-12 | -7.8E-13 | 2.2E+00 | -7.2E-13 | -3.0E-13 | 2.4E+00 | -9.9E-13 | -4.8E-13 | 2.1E+00 |
| 32 | HVOF Trib | 8 | 39 | 100 | 7,000 | 2.92 | -4.1E-12 | -1.1E-12 | 3.6E+00 | -3.2E-12 | -6.3E-13 | 5.0E+00 | -9.5E-13 | -5.0E-13 | 1.9E+00 |
| 33 | PS WC-17( | 4 | 67 | 87 | 13,500 | 4.03 | -2.9E-12 | -9.2E-14 | 3.2E+01 | -2.6E-12 | -1.2E-13 | 2.3E+01 | -2.6E-13 | 2.4E-14 | -1.1E+01 |
| 34 | PS WC-17( | 4 | 67 | 87 | 13,500 | 2.97 | -5.8E-12 | -3.4E-13 | 1.7E+01 | -5.5E-12 | -3.3E-13 | 1.7E+01 | -2.9E-13 | -9.0E-15 | 3.3E+01 |
| 35 | EHC | 8 | 39 | 100 | 13,500 | 4.87 | -1.7E-11 | -1.5E-13 | 1.1E+02 | -1.2E-11 | -3.4E-13 | 3.6E+01 | -4.8E-12 | 1.8E-13 | -2.6E+01 |
| 36 | EHC | 8 | 67 | 87 | 13,500 | 2.85 | -1.7E-11 | -9.0E-13 | 1.9E+01 | -1.5E-11 | -5.0E-13 | 3.0E+01 | -2.2E-12 | -4.0E-13 | 5.3E+00 |
| 37 | HVOF WC- | 8 | 39 | 100 | 7,000 | 4.04 | -2.5E-12 | 2.9E-14 | -8.7E+01 | -1.7E-12 | -2.2E-13 | 7.8E+00 | -7.5E-13 | 2.5E-13 | -3.0E+00 |
| 38 | HVOF WC- | 8 | 67 | 87 | 7,000 | 2.86 | -2.0E-12 | 2.0E-13 | -1.0E+01 | -9.7E-13 | -1.0E-13 | 9.5E+00 | -1.0E-12 | 3.0E-13 | -3.4E+00 |
| 39 | HVOF Trib | 8 | 67 | 87 | 7,000 | 4.79 | -8.3E-12 | -4.7E-13 | 1.8E+01 | -8.1E-12 | -1.0E-12 | 7.9E+00 | -2.3E-13 | 5.5E-13 | -4.1E-01 |
| 40 | HVOF Trib | 8 | 39 | 100 | 7,000 | 2.79 | -1.7E-11 | -6.1E-13 | 2.7E+01 | -1.6E-11 | -1.4E-12 | 1.2E+01 | -9.7E-13 | 7.4E-13 | -1.3E+00 |
| 41 | HVOF Trib | 4 | 67 | 87 | 13,500 | 4.29 | -5.8E-12 | -8.0E-13 | 7.3E+00 | -5.4E-12 | -7.8E-13 | 7.0E+00 | -3.7E-13 | -1.6E-14 | 2.3E+01 |
| 42 | HVOF Trib | 4 | 39 | 100 | 13,500 | 2.93 | -1.2E-11 | -5.2E-13 | 2.2E+01 | -1.0E-11 | -4.2E-13 | 2.4E+01 | -1.4E-12 | -9.8E-14 | 1.4E+01 |
| 43 | HVOF Trib | 8 | 67 | 87 | 13,500 | 4.62 | -3.6E-12 | -9.4E-13 | 3.8E+00 | -3.4E-12 | -9.2E-13 | 3.7E+00 | -1.6E-13 | -1.8E-14 | 8.6E+00 |
| 44 | HVOF Trib | 8 | 39 | 100 | 13,500 | 2.70 | -1.2E-11 | -5.5E-13 | 2.3E+01 | -1.2E-11 | -4.3E-13 | 2.8E+01 | -3.9E-13 | -1.1E-13 | 3.4E+00 |
| 45 | HVOF Cr3( | 4 | 67 | 87 | 7,000 | 3.84 | -9.0E-13 | -2.1E-13 | 4.4E+00 | -6.8E-13 | -1.1E-13 | 5.9E+00 | -2.3E-13 | -9.2E-14 | 2.5E+00 |
| 46 | HVOF Cr3( | 4 | 67 | 87 | 7,000 | 2.83 | -2.1E-12 | -4.4E-13 | 4.8E+00 | -1.8E-12 | -2.9E-13 | 6.3E+00 | -2.8E-13 | -1.5E-13 | 1.9E+00 |
| 47 | HVOF Trib | 4 | 39 | 100 | 7,000 | 4.76 | -6.6E-12 | -5.2E-13 | 1.3E+01 | -6.2E-12 | -6.1E-13 | 1.0E+01 | -5.0E-13 | 8.9E-14 | -5.6E+00 |
| 48 | HVOF Trib | 4 | 67 | 87 | 7,000 | 2.79 | -4.8E-12 | -9.2E-13 | 5.2E+00 | -3.9E-12 | -7.1E-13 | 5.6E+00 | -8.6E-13 | -2.1E-13 | 4.0E+00 |
| 49 | HVOF WC- | 8 | 39 | 100 | 7,000 | 4.05 | -1.2E-12 | -3.6E-13 | 3.5E+00 | -1.1E-12 | -3.6E-13 | 3.1E+00 | -1.1E-13 | 6.0E-15 | -1.9E+01 |
| 50 | HVOF WC- | 8 | 67 | 87 | 7,000 | 2.94 | -3.6E-12 | -1.3E-12 | 2.7E+00 | -1.6E-12 | -6.6E-13 | 2.4E+00 | -2.0E-12 | -6.8E-13 | 3.0E+00 |
| 51 | PS WC-17( | 8 | 39 | 100 | 7,000 | 4.61 | -2.8E-12 | -1.2E-15 | 2.4E+03 | -2.3E-12 | -2.8E-13 | 8.0E+00 | -5.0E-13 | 2.8E-13 | -1.8E+00 |
| 52 | PS WC-17( | 8 | 39 | 100 | 7,000 | 2.52 | -7.4E-12 | 2.7E-13 | -2.7E+01 | -7.5E-12 | 3.7E-13 | -2.0E+01 | 1.3E-13 | -9.7E-14 | -1.3E+00 |
| 53 | PS Tribaloy | 8 | 67 | 87 | 13,500 | 4.23 | -1.2E-11 | -1.8E-12 | 6.6E+00 | -1.2E-11 | -1.4E-12 | 8.6E+00 | 5.1E-13 | -3.6E-13 | -1.4E+00 |
| 54 | PS Tribaloy | 8 | 67 | 87 | 13,500 | 2.90 | -9.8E-12 | -1.8E-12 | 5.4E+00 | -9.4E-12 | -1.8E-12 | 5.3E+00 | -4.0E-13 | -2.7E-14 | 1.5E+01 |
| 55 | HVOF Cr3( | 8 | 39 | 100 | 13,500 | 4.61 | -4.3E-12 | -3.9E-13 | 1.1E+01 | -4.9E-12 | -3.2E-13 | 1.5E+01 | 5.8E-13 | -7.2E-14 | -8.2E+00 |
| 56 | HVOF Cr3( | 8 | 39 | 100 | 13,500 | 2.63 | -4.4E-12 | -4.4E-13 | 9.9E+00 | -4.6E-12 | -3.2E-13 | 1.4E+01 | 1.9E-13 | -1.2E-13 | -1.6E+00 |
| 57 | PS Tribaloy | 4 | 39 | 100 | 13,500 | 4.27 | -3.9E-12 | -3.1E-14 | 1.3E+02 | -2.5E-12 | -2.3E-13 | 1.1E+01 | -1.5E-12 | 2.0E-13 | -7.2E+00 |
| 58 | PS Tribaloy | 4 | 39 | 100 | 13,500 | 3.15 | -5.0E-12 | -1.5E-13 | 3.4E+01 | -4.7E-12 | 3.3E-13 | -1.4E+01 | -3.5E-13 | -4.7E-13 | 7.4E-01 |
| 59 | EHC | 8 | 39 | 100 | 13,500 | 4.76 | -2.7E-11 | -1.6E-13 | 1.6E+02 | -2.0E-11 | -2.3E-13 | 8.6E+01 | -6.6E-12 | 7.1E-14 | -9.3E+01 |
| 60 | EHC | 8 | 67 | 87 | 13,500 | 2.67 | -1.3E-11 | -6.0E-13 | 2.1E+01 | -1.2E-11 | -6.9E-13 | 1.7E+01 | -1.1E-12 | 8.6E-14 | -1.3E+01 |
| 61 | PS Tribaloy | 8 | 67 | 87 | 7,000 | 3.93 | -6.8E-11 | -5.3E-12 | 1.3E+01 | -6.7E-11 | -6.1E-12 | 1.1E+01 | -1.2E-12 | 7.7E-13 | -1.6E+00 |
| 62 | PS Tribaloy | 8 | 67 | 87 | 7,000 | 2.90 | -3.2E-11 | -1.3E-12 | 2.6E+01 | -3.1E-11 | -2.3E-12 | 1.4E+01 | -8.5E-13 | 1.0E-12 | -8.4E-01 |
| 63 | HVOF WC- | 4 | 39 | 100 | 7,000 | 4.46 | -1.2E-12 | -1.7E-13 | 6.8E+00 | -4.2E-13 | -1.8E-13 | 2.4E+00 | -7.6E-13 | 2.1E-15 | -3.5E+02 |
| 64 | HVOF WC- | 4 | 67 | 87 | 7,000 | 2.85 | 9.3E-14 | -8.2E-13 | -1.1E-01 | -7.6E-14 | -4.1E-13 | 1.8E-01 | 1.7E-13 | -4.0E-13 | -4.2E-01 |
| 65 | HVOF Trib | 4 | 67 | 87 | 7,000 | 4.34 | -6.6E-12 | -8.3E-13 | 8.0E+00 | -6.0E-12 | -7.6E-13 | 7.9E+00 | -6.2E-13 | -7.4E-14 | 8.4E+00 |
| 66 | HVOF Trib | 4 | 39 | 100 | 7,000 | 2.84 | -2.9E-11 | -1.5E-12 | 2.0E+01 | -2.8E-11 | -1.5E-12 | 1.9E+01 | -8.3E-13 | 1.9E-14 | -4.3E+01 |
| 67 | EHC | 4 | 39 | 100 | 7,000 | 4.57 | -7.5E-13 | -2.7E-13 | 2.8E+00 | -7.3E-13 | -2.0E-13 | 3.7E+00 | -2.3E-14 | -6.9E-14 | 3.3E-01 |
| 68 | EHC | 4 | 67 | 87 | 7,000 | 2.58 | -8.4E-13 | 1.4E-13 | -5.9E+00 | -4.9E-13 | -3.8E-13 | 1.3E+00 | -3.4E-13 | 4.1E-13 | -8.2E-01 |
| 69 | HVOF Trib | 8 | 67 | 87 | 13,500 | 4.08 | -3.8E-12 | -1.9E-13 | 2.0E+01 | -2.9E-12 | -1.7E-13 | 1.7E+01 | -8.5E-13 | -1.6E-14 | 5.2E+01 |
| 70 | HVOF Trib | 8 | 67 | 87 | 13,500 | 2.98 | -8.9E-12 | -7.9E-13 | 1.1E+01 | -8.4E-12 | -6.8E-13 | 1.2E+01 | -4.5E-13 | -1.0E-13 | 4.3E+00 |
| 71 | HVOF WC- | 8 | 67 | 87 | 13,500 | 4.74 | -1.7E-12 | -3.9E-13 | 4.4E+00 | -1.1E-12 | -3.3E-13 | 3.3E+00 | -6.5E-13 | -6.0E-14 | 1.1E+01 |
| 72 | HVOF WC- | 8 | 39 | 100 | 13,500 | 2.97 | -4.8E-12 | -4.2E-13 | 1.1E+01 | -4.5E-12 | -3.9E-13 | 1.2E+01 | -2.8E-13 | -3.2E-14 | 8.6E+00 |
| 73 | EHC | 4 | 67 | 87 | 13,500 | 4.02 | 9.6E-14 | -5.5E-14 | -1.8E+00 | -3.7E-14 | -1.3E-13 | 2.7E-01 | 1.3E-13 | 8.0E-14 | 1.7E+00 |
| 74 | EHC | 4 | 39 | 100 | 13,500 | 3.09 | -2.7E-12 | 1.0E-13 | -2.6E+01 | -2.7E-12 | -6.2E-14 | 4.3E+01 | -1.5E-14 | 1.7E-13 | -8.9E-02 |
| 75 | EHC | 4 | 67 | 87 | 13,500 | 4.63 | -1.5E-13 | 5.3E-15 | -2.8E+01 | -9.1E-15 | -8.0E-14 | 1.1E-01 | -1.4E-13 | 8.6E-14 | -1.7E+00 |
| 76 | EHC | 4 | 39 | 100 | 13,500 | 3.04 | -1.4E-12 | -9.2E-14 | 1.5E+01 | -1.1E-12 | -2.6E-13 | 4.4E+00 | -2.7E-13 | 1.6E-13 | -1.6E+00 |
| | | | | **Wear** | Min | | -6.8E-11 | -5.3E-12 | -8.7E+01 | -6.7E-11 | -6.1E-12 | -2.9E+01 | -6.6E-12 | -6.8E-13 | -3.5E+02 |
| | | | | | Avg | | -7.8E-12 | -6.2E-13 | 4.2E+01 | -6.8E-12 | -5.5E-13 | 1.1E+01 | -9.7E-13 | -4.9E-14 | 7.0E+00 |
| | | | | **Ratios of** | Min | | | 12.9 | | | 11.0 | | | 9.8 | |
| | | | | | Avg | | | 12.6 | | | 12.3 | | | 19.6 | |

Since scatter in wear data is expected, a significant number of tests for a given condition must usually be conducted. However, in the tests conducted here, because of the large number of variables, it was not possible to perform many tests for each condition. It was still possible, however, to perform a statistical analysis of the results to more clearly delineate the relative effects of the various factors investigated: carbon hardness, different coatings, rotor speed, and coating surface finish. For comparison purposes, the direct wear results from Table 4-49, the wear coefficient data from Table 4-50, plus a third category where the direct wear was simply normalized to a 3-lb load, were statistically analyzed at the same time to determine if the results were consistent or if any additional conclusions could be made from the different data sets.

The wear data, load-normalized wear data, and wear coefficients (k) data were input to Minitab® Software and the statistical analyses performed. The General Linear Model feature of the software using the ANOVA method was utilized to provide maximum flexibility in making the analyses. The output of the model has been tabulated for total wear, break-in wear and continuous wear in Table 4-51 through Table 4-53, respectively. The table portion lists the details of the analysis results and the charts below show the magnitudes of the main effects for the factors considered. Both the carbon wear and coating wear results are presented. The wear period and the specimen (carbon or coating) are at the far left with the Design Factors under consideration immediately to their right. The highlighted values in the results are the only meaningful results. The results are presented as % Effects and p-values. The % Effects indicate what percentage of the data set are accounted for by the given factor and the result is statistically significant only when the p-value is less than 0.05. The analysis also calculates an error term that shows what percentage of the data set is not accounted for by the selected design factors, and identifies unusual results that do not fit with the rest of the data. Three tests in particular were identified multiple times in the nine statistical analyses of complete data sets covered in the tables as being unusually high. These were tests 61 and 26 (PS Tribaloy 400) and test 59 (EHC). Several other tests were also flagged at least once as unusually high results, the most noticeable of which was test 18 (HVOF WC/Co).

Results in Table 4-51 show that for the carbon wear, the coating surface finish and the type of coating account for about 90% of the variation in the data set. This holds true for all three methods of examining the data, directly by measured wear, by normalized wear adjusted for the load variations from test to test, and by the wear coefficient method. Wear of the runner ring coating was most influenced by the carbon hardness (50+ %) and the coating surface finish (~30%). The type of coating also played a statistically significant role, but to a much lesser extent (~15%). This confirms that the alternative coatings can be substituted for EHC with a relatively high confidence as long as their surface finish is controlled and attention is paid to the carbon hardness.

## Table 4-51 Statistical Analysis Results for Total Wear Data and Main Effects Charts

| Wear Period / Specimen | Design Factors | Measured Wear [micro-inches] % Effects | Measured Wear [micro-inches] p(1) | Normalized Wear [to 3 Lb load, micro-inches] % Effects | Normalized Wear [to 3 Lb load, micro-inches] p | Wear Coefficient, K % Effects | Wear Coefficient, K p |
|---|---|---|---|---|---|---|---|
| **Total Wear (0-48 hrs)** | | | | | | | |
| **Carbon** | Carbon Hardness | 1.6 | 0.596 | 3.9 | 0.336 | 1.1 | 0.637 |
| | Type Coating | 21.9 | 0.001 | 21.7 | 0.000 | 20.6 | 0.001 |
| | Coating Surface Finish | 69.0 | 0.000 | 67.0 | 0.000 | 62.5 | 0.001 |
| | Rotor Speed | 2.6 | 0.462 | 3.2 | 0.382 | 11.1 | 0.131 |
| | Error | 4.8 | ----- | 4.1 | ----- | 4.7 | ----- |
| | | | | | | Ctg Load(4) | Noise Factor |
| | | | | | | 23.3 | 0.079 |
| **Coating(2)** | Carbon Hardness | 52.0 | 0.000 | 50.7 | 0.000 | 13.6 | 0.154 |
| | Type Coating | 14.8 | 0.000 | 14.9 | 0.000 | 12.9 | 0.172 |
| | Coating Surface Finish | 29.4 | 0.002 | 30.5 | 0.001 | 27.2 | 0.075 |
| | Rotor Speed | 0.9 | 0.591 | 1.1 | 0.523 | 19.2 | 0.110 |
| | Error | 2.9 | ----- | 2.7 | ----- | 3.8 | ----- |

Footnotes:
(1) Statistically significant effect only if $p < 0.050$
(2) Coating is on the mating ring of the rotor
(3) Wear Ratio = Carbon Wear ÷ Coating Wear. On average, the wear ratios were about 12 for Total Wear and Break-in Wear and about 20 for Continuous Wear.
(4) Due to low wear, coating wear coefficient had high error when analyzed without the variations in Load as a noise factor. For this reason, the data presented here includes Load as a noise factor to reduce the error, but Load itself remains a statistically insignificant factor.

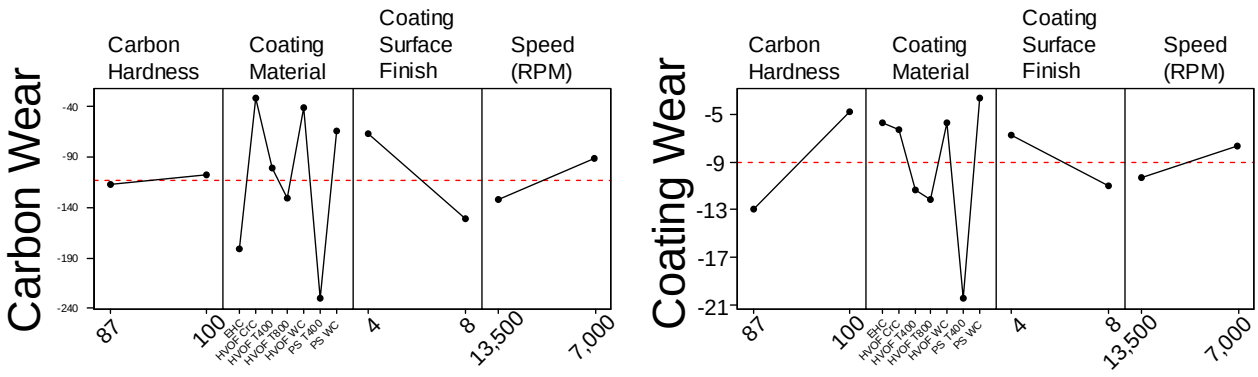


Order of coatings are, left to right:
EHC, HVOF CrC, HVOF T400,
HVOF T800, HVOF WC,
PS T400, PS WC

## Table 4-52 Statistical Analysis Results for Break-in Wear Data and Main Effects Charts

| Wear Period / Specimen | Design Factors | Measured Wear [micro-inches] % Effects | Measured Wear p(1) | Normalized Wear [to 3 Lb load, micro-inches] % Effects | Normalized Wear p | Wear Coefficient, K % Effects | Wear Coefficient, K p |
|---|---|---|---|---|---|---|---|
| **Break-in (0-12 hrs)** | | | | | | | |
| **Carbon** | Carbon Hardness | 3.6 | 0.407 | 5.7 | 0.268 | 2.9 | 0.452 |
| | Type Coating | 22.5 | 0.001 | 22.5 | 0.000 | 22.7 | 0.001 |
| | Coating Surface Finish | 66.9 | 0.001 | 64.7 | 0.000 | 63.4 | 0.001 |
| | Rotor Speed | 1.9 | 0.544 | 2.6 | 0.449 | 6.0 | 0.282 |
| | Error | 5.1 | ----- | 4.5 | ----- | 5.1 | ----- |
| | | | | | | Ctg Load(4) Noise Factor 2.7 | 0.446 |
| **Coating** | Carbon Hardness | 48.8 | 0.001 | 48.5 | 0.001 | 25.8 | 0.035 |
| | Type Coating | 16.2 | 0.002 | 16.6 | 0.001 | 6.6 | 0.170 |
| | Coating Surface Finish | 30.7 | 0.008 | 31.2 | 0.005 | 30.4 | 0.028 |
| | Rotor Speed | 0.1 | 0.853 | 0.1 | 0.850 | 32.5 | 0.026 |
| | Error | 4.1 | ----- | 3.6 | ----- | 1.9 | ----- |

Footnotes:
(1) Statistically significant effect only if $p < 0.050$
(2) Coating is on the mating ring of the rotor
(3) Wear Ratio = Carbon Wear ÷ Coating Wear. On average, the wear ratios were about 12 for Total Wear and Break-in Wear and about 20 for Continuous Wear.
(4) Due to low wear, coating wear coefficient had high error when analyzed without the variations in Load as a noise factor. For this reason, the data presented here includes Load as a noise factor to reduce the error, but Load itself remains a statistically insignificant factor.

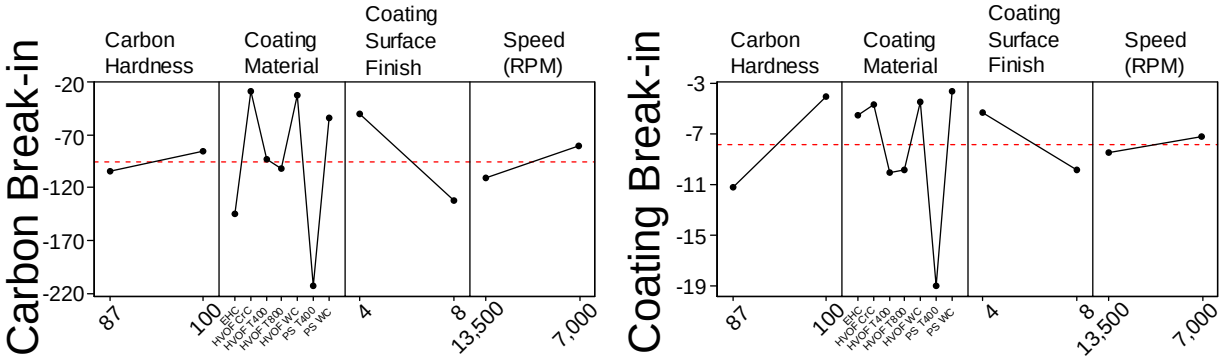


Order of coatings are, left to right:
EHC, HVOF CrC, HVOF T400,
HVOF T800, HVOF WC,
PS T400, PS WC

## Table 4-53 Statistical Analysis Results for Continuous Wear Data and Main Effects Charts

| Wear Period / Specimen | Design Factors | Measured Wear [micro-inches] % Effects | Measured Wear p[(1)] | Normalized Wear [to 3 Lb load, micro-inches] % Effects | Normalized Wear p | Wear Coefficient, K % Effects | Wear Coefficient, K p |
|---|---|---|---|---|---|---|---|
| **Continuous (12-48 hrs)** | | | | | | | |
| **Carbon** | Carbon Hardness | 6.9 | 0.356 | 1.0 | 0.702 | 1.9 | 0.556 |
| | Type Coating | 22.8 | 0.016 | 22.4 | 0.008 | 21.4 | 0.002 |
| | Coating Surface Finish | 54.9 | 0.011 | 62.5 | 0.004 | 59.8 | 0.002 |
| | Rotor Speed | 7.5 | 0.336 | 7.0 | 0.319 | 11.4 | 0.153 |
| | Error | 7.9 | ----- | 7.0 | ----- | 5.5 | ----- |
| | | | | | | Ctg Load[(4)] Noise Factor | |
| | | | | | | 20.2 | 0.517 |
| **Coating** | Carbon Hardness | 40.8 | 0.225 | 35.5 | 0.246 | 1.6 | 0.777 |
| | Type Coating | 10.0 | 0.896 | 8.7 | 0.914 | 55.7 | 0.176 |
| | Coating Surface Finish | 8.5 | 0.578 | 10.9 | 0.519 | 4.4 | 0.645 |
| | Rotor Speed | 13.4 | 0.486 | 19.0 | 0.395 | 1.3 | 0.802 |
| | Error | 27.2 | ----- | 25.9 | ----- | 16.8 | ----- |

Footnotes:
(1) Statistically significant effect only if $p < 0.050$
(2) Coating is on the mating ring of the rotor
(3) Wear Ratio = Carbon Wear ÷ Coating Wear. On average, the wear ratios were about 12 for Total Wear and Break-in Wear and about 20 for Continuous Wear.
(4) Due to low wear, coating wear coefficient had high error when analyzed without the variations in Load as a noise factor. For this reason, the data presented here includes Load as a noise factor to reduce the error, but Load itself remains a statistically insignificant factor.

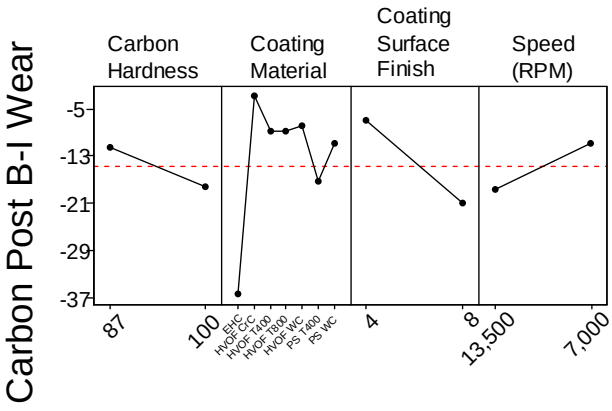


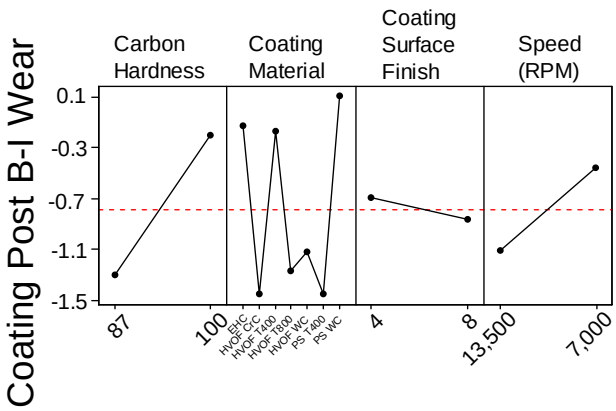


Order of coatings are, left to right:
EHC, HVOF CrC, HVOF T400,
HVOF T800, HVOF WC,
PS T400, PS WC

The Main Effects charts in the lower half of each table show the average wear values by the factor levels. Looking at the factors identified as meaningful, for carbon wear, the three carbide coatings gave the lowest overall average wear while EHC and APS Tribaloy 400 caused the highest wear. The coating wear was lowest for EHC and the three carbide coatings. The 4 micro-inch Ra coating surface finish was preferred for both low carbon wear and low coating wear. A point worth noting is the low error values, which showed that ignoring the test-to-test load variations was justifiable for two of the three approaches to looking at the data. However, for the Wear Coefficient method this was not the case. When the load was not included as a factor, the analysis gave 52% error. Therefore, this particular analysis was repeated with load included as a noise factor since it was not intentionally varied. This reduced the error, but resulted in a more nearly equal distribution of the % Effects. Due to the more nearly even distribution of % effects across the different factors, the outcome was that none of the individual factors were statistically significant for the Wear Coefficients method when total wear was examined. When separated into break-in wear and continuous wear, several factors showed significance for break-in wear, but load was not one of them. No significant factors stood out for continuous wear even though the type of coating accounted for 55% of the wear variation. This undoubtedly is due to the very low values of wear seen during the continuous wear process.

The total wear and break-in wear statistical analyses gave very similar results (with the one exception discussed above for Coating Wear Coefficients), as expected based on the earlier observations that break-in wear accounted for the majority of the wear. The continuous wear results were also similar to the total wear results for the carbon wear, but showed no significant results for the coating wear, probably due to the very low amounts of wear seen for most of the data set.

### 4.8.7. Conclusions

An extensive test matrix of carbon seal component rig wear tests have been conducted to evaluate the potential of alternative thermal spray coatings to replace EHC coatings on the rotor running surfaces where the carbon seal pieces make contact, either continuously or as transient rub events, depending on the design of the carbon seal. The wear data were analyzed by several methods with particular attention to differences between:

a) break-in wear and continuous wear effects, and

b) effects of unintended seal load variations from test to test on the wear results.

Overall the HVOF WC/Co and $Cr_3C_2$/NiCr coatings performed comparable to EHC in terms of both wear on the mating carbon seals and wear of the coatings themselves. The performance of the other thermal spray coatings was somewhat inferior to EHC in terms of wear of the carbon seals.

Surface finish of the coatings plays a vital role in the carbon seal system wear with the 4 microinch Ra finish being preferred. The 8 microinch Ra EHC performed poorly in these tests, whereas the 4 microinch Ra EHC coatings demonstrated excellent performance with both low carbon seal and coating wear. The engineer from GE Aircraft Engines who helped coordinate these tests could not explain the disparity in performance of the EHC coatings with the two surface finishes. He indicated that a surface finish of 8 microinches is most commonly used and that is why most of the thermal spray coatings had a surface finish of 8 microinches. It is not know why the carbon seals were more sensitive to surface finish for the chrome than for the thermal spray coatings and to definitively address the issue would require additional testing that was no possible in this project.

In general, the wear rate on all the coatings was very low, especially for the EHC with an Ra

surface finish of 4 microinches and for all of the HVOF WC/Co coatings. The average wear depth on the WC/Co coatings for all tests (including both surface finishes) was approximately 6 microinches over the 48-hour test period. This equates to a removal rate of 0.12 microinches per hour. Assuming the speeds and loads in these tests were representative of real-life gas turbine engine conditions, then it would take approximately 8000 hours of operation before even 0.001" of coating thickness had been removed. This is equivalent to many years of operation. Therefore, the principal consideration in replacing EHC with HVOF WC/Co (or the other thermal spray coatings) is the wear on the carbon seals.

This page intentionally left blank.

# 5. Component Testing on TF33 Gas Turbine Engine

## 5.1. Engine and Components Selection

The evaluation of components in rig tests that simulate real-life operating conditions is an integral part in the process of qualifying thermal spray coatings as an alternative to EHC coatings. As discussed in Section 2, an analysis was conducted of the extent of hard chrome plating within the propulsion community. Table 2-2 listed the DOD gas turbine engines onto which hard chrome is currently being applied to at least one component based on an assessment by the stakeholders in the project. In conjunction with the materials testing described in Section 4, it was decided that each DOD service and GTE manufacturer would evaluate the hardware under consideration for thermal spray coating and decide if additional component or engine testing beyond the materials JTP would be necessary. Such additional testing could be required due to the critical nature of the mechanical system response for some specific GTE components.

There are more than 3000 TF33 gas turbine engines in service throughout the Air Force on the B-52H, C-141, E-3 and KC-135 aircraft, and repair of components from this engine represents the largest chrome plating workload at Oklahoma City Air Logistics Center (OC-ALC). Therefore, testing of selected HVOF-coated components that are normally EHC-plated in a TF33 engine test, designated Advanced Mission Test (AMT) was viewed as a high priority and essential to move toward qualification of the HVOF coatings. Process and materials engineers from OC-ALC and Pratt & Whitney (P&W), the manufacturer of the TF33, identified the engine part classes that were high-volume HVOF repair candidates and then they participated in the selection of components to be coated and tested in a TF33 AMT engine.

From all of the chrome-plated parts on the TF33, the following seven components were selected for actual qualification in the AMT.

Housing, No. 1 Bearing, P/N 437486, with HVOF WC/Co on inner bearing journal

Housing, No. 5 Bearing, P/N 488476, with HVOF WC/Co on inner bearing journal

Housing, No. 6 Bearing, P/N 415711, with HVOF WC/Co on inner bearing journal

Low-Pressure Turbine (LPT) Shaft, P/N 506966, with HVOF WC/Co on No. 4-1/2 bearing and spacer outer journals

High-Pressure Turbine (HPT) Shaft, P/N 638326, with HVOF WC/Co on No. 5 bearing and spacer outer journals

Rear Compressor Rear Hub (#4) , P/N 727616, with HVOF WC/Co on No. 2, No. 2-1/2, and No. 3 bearing outer journals

Front Compressor Rear Hub (#2), P/N 530073, with HVOF WC/Co on No. 4 bearing outer journal

Based on the operating temperatures of the components and previous P&W commercial experience, it was decided that HVOF WC/17Co coatings would be applied on the areas of the components on which EHC is currently applied. The deposition parameters used for the WC/Co coatings were the same as for the coupons used in the materials testing described in Section 4.

Figure 5-1 through Figure 5-7 are photographs of the components showing the particular areas onto which the HVOF WC/17Co coatings were applied.

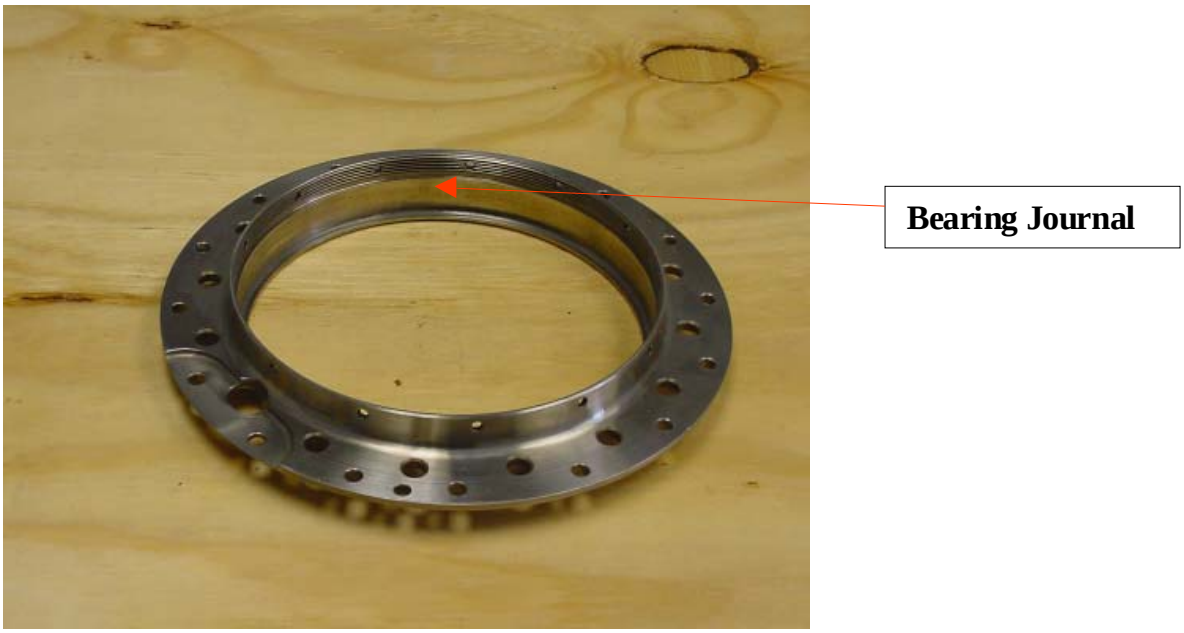


**Figure 5-1 #1 Bearing Housing, Indicating Area Onto Which WC/Co Was Applied.**

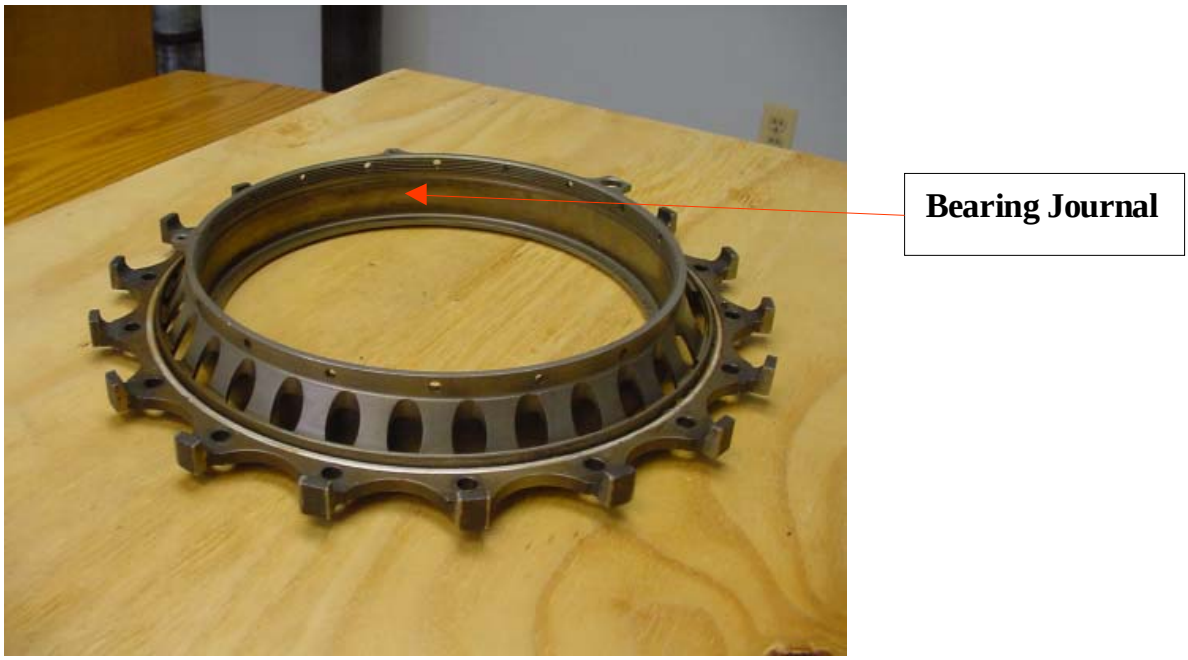


**Figure 5-2 #5 Bearing Housing, Indicating Area Onto Which WC/Co Was Applied.**

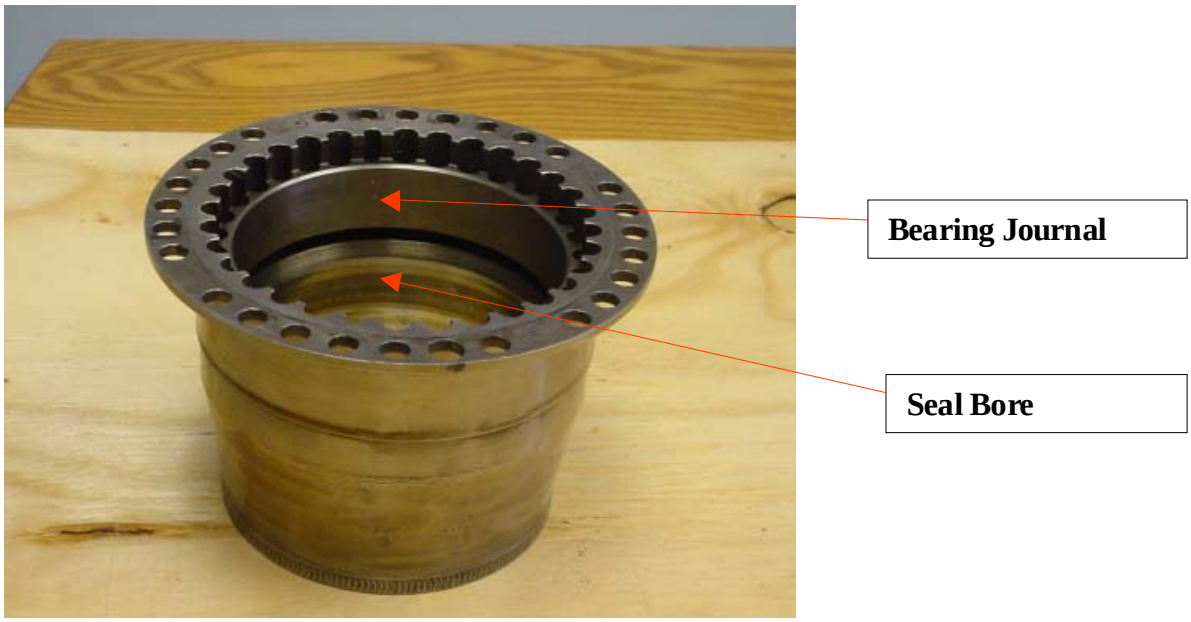


**Figure 5-3 #6 Bearing Housing, Indicating Areas Onto Which WC/Co Was Applied.**


**Figure 5-4 Low-Pressure Turbine Shaft, Indicating Areas Onto Which WC/Co Was Applied.**

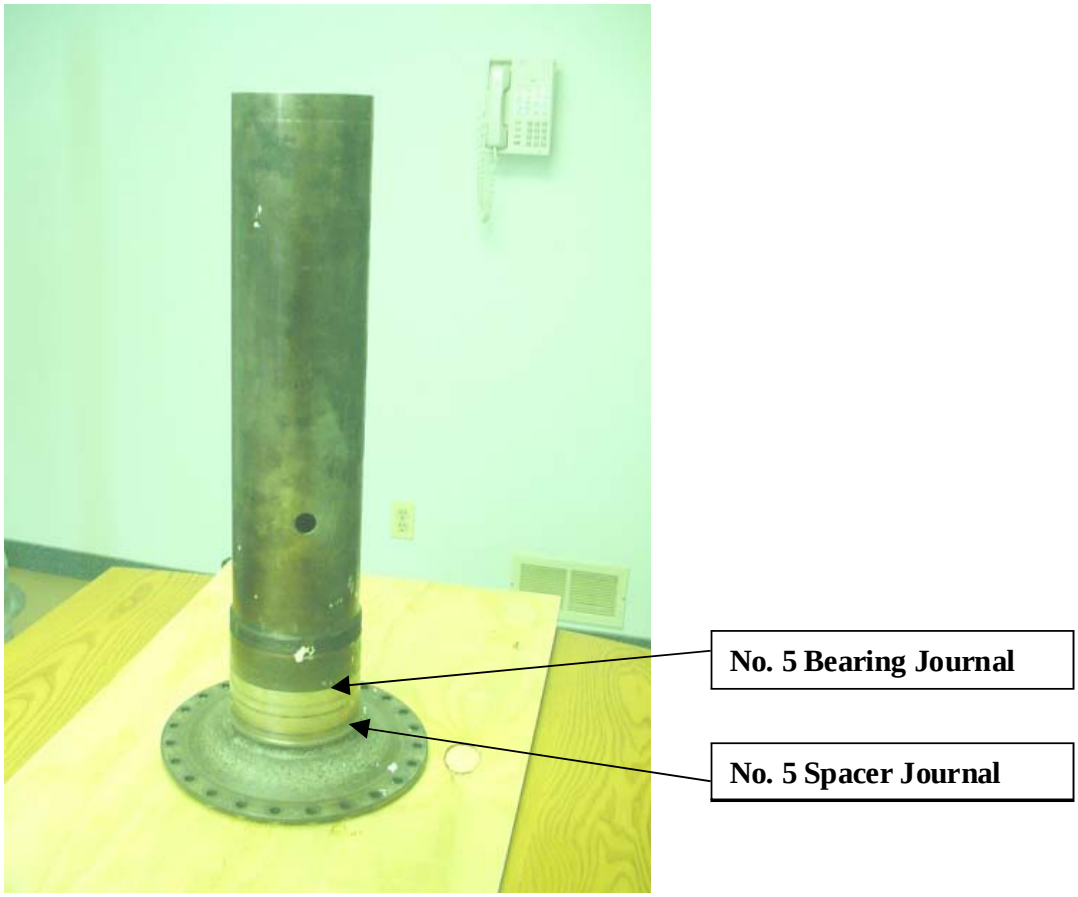


**Figure 5-5 High-Pressure Turbine Shaft, Indicating Areas Onto Which WC/Co Was Applied.**

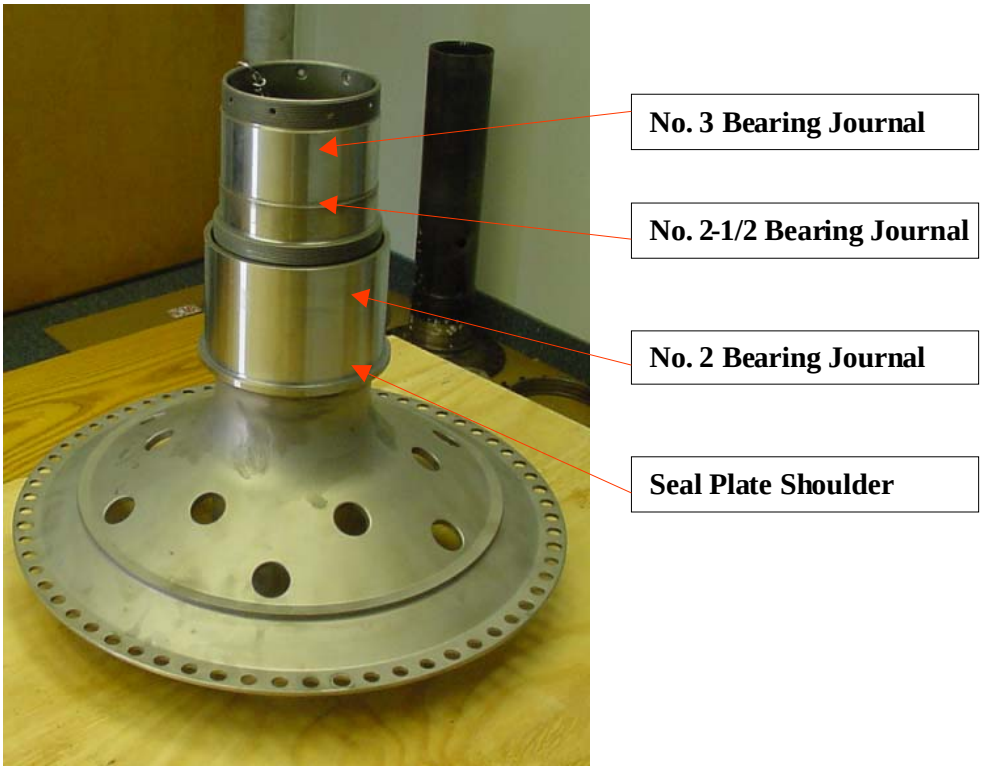


**Figure 5-6 Front Compressor Rear Hub (#2), Indicating Areas Onto Which WC/Co Was Applied.**


**Figure 5-7 Rear Compressor Rear Hub (#4), Indicating Areas Onto Which WC/Co Was Applied.**

Figure 5-8 is a schematic of the TF33 engine showing the location of the demonstration components.

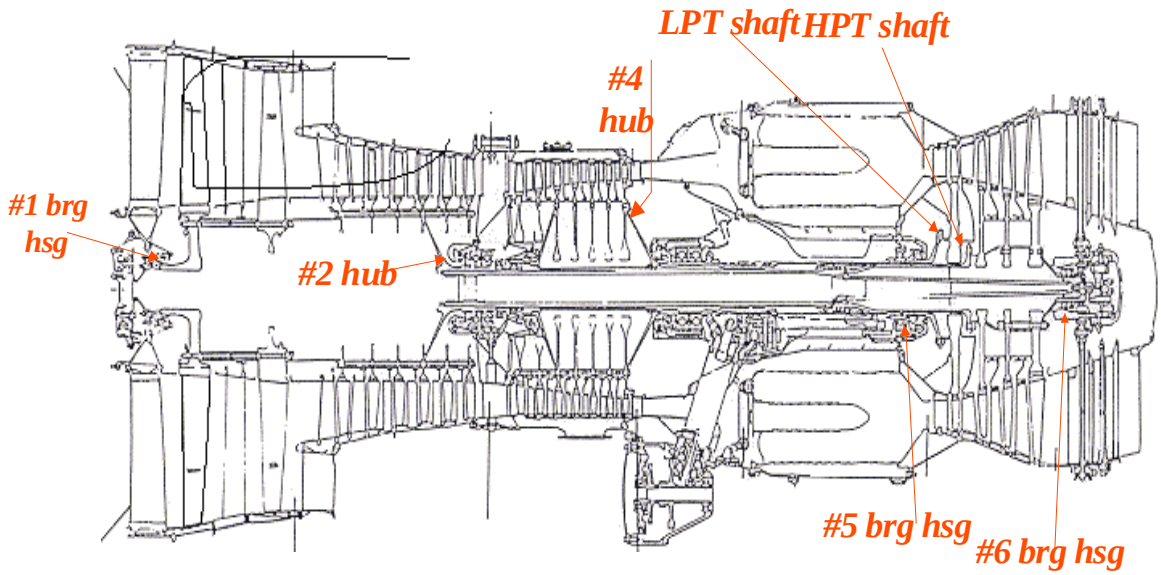


**Figure 5-8 Schematic of TF33 Engine Showing Location of Components Onto Which the WC/Co Coatings Were Applied**

It was decided that two complete sets of components would be coated with the HVOF WC/Co, the first set being designated for functional testing and the second for the actual AMT endurance testing.

## 5.2. Functional Testing of Coated Components

The purpose of the functional test components was to demonstrate that coatings with acceptable properties could be deposited uniformly onto the designated areas on each component and that they could withstand several assembly/disassembly procedures in the engine without sustaining any damage.

The deposition of the coatings onto the components involved several developmental steps:

- Design operation sheets
- Design tooling for holding the components
- Build tooling
- Write computer programs for robot holding HVOF spray gun for each component
- Complete spray trials
- Complete grinding trials
- Process functional components

Engelhard Corporation was tasked with executing the developmental steps, including the coating of the functional components. In order to ensure that functional test components would have acceptable coatings, Engelhard made dummy TF33 components and inserted test coupons, at selected locations, to provide component representative coating specimens. The dummy components were made to the approximate configuration and size of the engine hardware and a slot was cut into each one. A coupon was inserted into the slot and the entire coupon surface was

coated using parameters that would be used on the component. The coupon was removed and used as the coating metallographic specimen. Engelhard's metallographic analyses showed that the coating met acceptance standards in terms of porosity, oxide content and hardness. On the coupons from the three bearing housings, representative of an internal-diameter (ID)-coated surface, the measured Vickers hardness values on the coatings were 1188, 1190, and 1187HV which satisfied the minimum hardness requirements of 1150HV. Surface smoothness measurements performed at Duval Precision, as well as Engelhard, met the Technical Order (T.O.) requirements of 8Ra maximum.

Following the coating and analysis of the coupons, coatings of approximate thickness 0.006" were applied to the functional components. Then the coatings were ground using low-stress grinding techniques to a final thickness of 0.003" and with a nominal Ra surface finish of 8 microinches. All components were then shipped to the Phoenix Air National Guard engine shop for execution of the functional tests which consisted of pressing bearings onto and into the HVOF-coated components a total of five times. The following is a description of the actual functional test procedures performed on each component which included a visual and fluorescent penetrant inspection (FPI) after each assembly/disassembly procedure:

**#1 Bearing Housing**

1. Install #1 bearing per T O 2J-TF33-76 WP 504 paragraph 10
2. Remove #1 bearing per T O 2J-TF33- 76 WP 106 paragraph 12
3. Visually inspect HVOF journal area for any signs of chipping, flaking and check mating surfaces for material transfer
4. Repeat step 1-3 four times
5. Local FPI HVOF journal

**#5 Bearing Housing**

1. Install #5 bearing per T O 2J-TF33-76 WP 405 paragraph 13
2. Remove #5 bearing per T O 2J-TF33- 76 WP 205 paragraph 9
3. Visually inspect HVOF journal area for any signs of chipping, flaking and check mating surfaces for material transfer
4. Repeat step 1-3 four times
5. Local FPI HVOF journal

**#6 Bearing Housing**

1. Install #6 bearing per T O 2J-TF33-76 WP401 paragraph 10
2. Remove #6 bearing per T O 2J-TF33- 76 WP 201 paragraph 16
3. Visually inspect HVOF journal area for any signs of chipping, flaking and check mating surfaces for material transfer
4. Repeat step 1-3 four times
5. Local FPI HVOF journal

**Low-Pressure Turbine Shaft**

1. Install #4 1/2 bearing per T O 2J-TF33-76 WP402 paragraph 9
2. Remove #4 1/2 bearing per T O 2J-TF33- 76 WP 202 paragraph 9
3. Visually inspect HVOF journal area for any signs of chipping, flaking and check mating surfaces for material transfer
4. Repeat step 1-3 four times

5. Local FPI HVOF journal

**High-Pressure Turbine Shaft**

1. Install #5 bearing per T O 2J-TF33-76 WP404 paragraph 16
2. Remove #5 bearing per T O 2J-TF33- 76 WP 204 paragraph 10
3. Visually inspect HVOF journal area for any signs of chipping, flaking and check mating surfaces for material transfer
4. Repeat step 1-3 four times
5. Local FPI HVOF journal

**Rear Compressor Rear Hub**

1. Install #2 bearing per T O 2J-TF33-66 WP 410 paragraph 19
2. Remove #2 bearing per T O 2J-TF33-66 WP 210 paragraph 14
3. Alternate assembly and disassembly check is to use slave bearing and fixture available through rotor balance shop at Tinker AFB
4. Visually inspect HVOF journal area for any signs of chipping, flaking and check mating surfaces for material transfer
5. Repeat step 1-4 four times
6. Local FPI HVOF journal

**Front Compressor Rear Hub**

1. Install #4 bearing per T O 2J-TF33-66 WP 408 paragraph 14
2. Remove #4 bearing per T O 2J-TF33-66 WP 208 paragraph 10
3. Alternate assembly and disassembly check is to use slave bearing and fixture available through rotor balance shop at Tinker AFB
4. Visually inspect HVOF journal area for any signs of chipping, flaking and check mating surfaces for material transfer
5. Repeat step 1-4 four times
6. Local FPI HVOF journal

Following completion of the test matrix, the #6 bearing housing was re-tested utilizing an interference fit between the bearing housing and the mating part. This was accomplished by chilling the #6 bearing housing and heating the #6 bearing in direct violation of T.O. 2J-TF33-76 WP401 paragraph 10. The purpose of this test was to simulate extremely abusive maintenance techniques. With the exception of this one extremely abusive test that showed some small chipping on the #6 bearing housing, all parts passed functional testing.

The components were subsequently shipped to P&W for additional FPI analysis and destructive evaluation of the coatings. There were no FPI indications of cracks or other defects on the coatings on any of the components with the exception of the #6 bearing housing that underwent the abusive test. The components were then cut up and metallographic specimens of the coating, including the coating/substrate interface, were made. The metallurgical assessment included determination of coating hardness, thickness, interface condition, oxide level and porosity. Figure 5-9 is a photomicrograph of the WC/Co coating on the ID surface of the #6 bearing housing showing low porosity and good interface integrity. Coatings on all of the components passed the acceptance criteria and therefore it was decided to proceed with the application of the coatings onto components for the AMT endurance test.

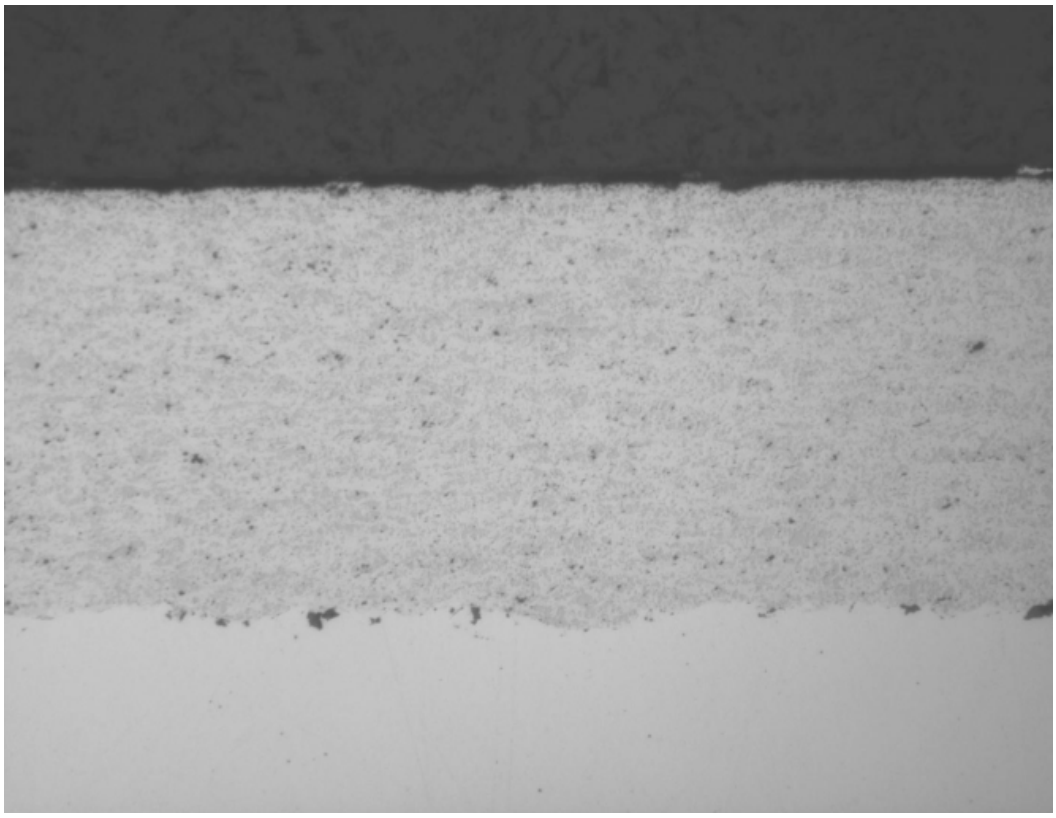

**Figure 5-9 Photomicrograph of HVOF WC/Co Coating on the ID Surface of the #6 Bearing Housing Following Functional Testing**

## 5.3. AMT Endurance Testing of Coated Components

The AMT components were processed by Engelhard using the same deposition parameters for the HVOF WC-Co coatings as used for the functional components, with the coatings ground to a final thickness of 0.003" and an Ra surface finish of 8 microinches. Control coupons were processed, along with the engine components, and evaluated by Engelhard to ensure quality control.

The metallographic examination of the control coupons showed that the coatings were acceptable in terms of porosity and oxide content, and met the minimum hardness requirement. Coating hardness was equivalent or greater than hardnesses measured on the functional component control coupons. The coated components were then shipped to the U.S. Air Force, Phoenix Air National Guard engine shop, and assembled into the AMT engine for testing.

The endurance portion of the AMT test began on October 30, 2001, with the engine running for 4500 equivalent flight hours (EFH). Upon completion of the test, the engine was shipped to the Air Force base at Phoenix for disassembly and inspection, which indicated that there was no visible damage to any of the coated components. A Pratt & Whitney engineer was present for the teardown and inspection. The coated components were subsequently crated and shipped to Pratt & Whitney in East Hartford, CT for destructive evaluations.

At P&W, a dirty inspection of the AMT coated components revealed oil coke but no chipped or worn coating. The components were cleaned using acetone. A second visual inspection, after the acetone clean, did not indicate any cracking or chipping of the coating on any of the engine

components. Additional cleaning was performed, using a caustic cleaner, to remove the coke deposits prior to dimensional inspection. Visual inspection after caustic cleaning did not reveal any coating deterioration.

Typical overhaul of thermal sprayed engine components entails coating removal and examination of the substrate; thus coatings are not normally FPI evaluated. However, to help support the evaluation of HVOF coatings in the TF33, in addition to dimensional and metallographic inspections, the AMT components were inspected with FPI. It should be pointed out that the AMT engine schedule did not permit post grind FPI inspections of the HVOF coated components prior to shipment to Phoenix for installation into the engine. Therefore, pre-test FPI data is not available. However, prior to shipping, the components were visually inspected, without the use of magnification, and no defects were identified.

P&W believed that in order to justify the use of this coating for extended overhaul cycles it would be prudent to evaluate the coated areas with both normal FPI and ultra high sensitivity FPI. Of the seven TF33 components evaluated, many with multiple coated surfaces, using standard FPI, only two components displayed indications in the HVOF coated areas. On one of these components, ultra-high-sensitivity FPI inspection found one additional indication, but no additional indications on any of the other components.

Figure 5-10 shows the front compressor rear hub and the FPI indications on the No.2 Bearing Journal. The indications (A) are not crack-like and appeared to be the loss of local coating. There was no indication of secondary damage to the coating as would be expected if the coating was scraped across the mating part. The lack of secondary damage indicated that the coating might have been missing at the time of engine assembly. However, in the area of coating loss, there appeared to be indications of chattering which extended for 120 degrees around the circumference. The indications in the location of the seal plate shoulder (B) are typical of the indications found near the taper grinds and do not indicate defects.

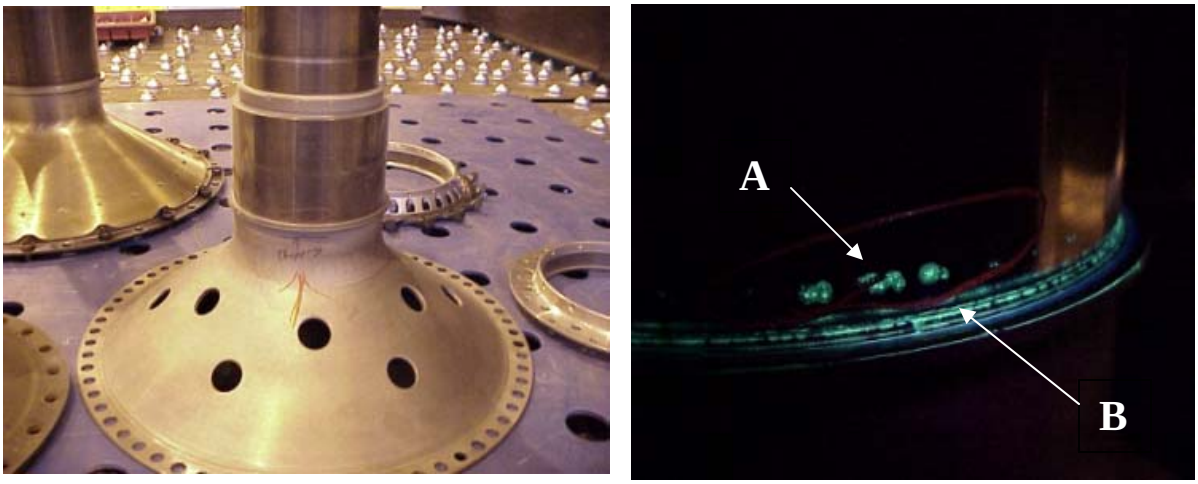


**Figure 5-10 Front Compressor Rear Hub (left) Following AMT Test and Standard FPI Indications (right) on No. 2 Bearing Journal on the Hub**

The ultra-high-sensitivity FPI found an additional group of indications as shown in Figure 5-11. The intermittent indications near the flange correspond to what appeared to be chatter marks. The small scattered indications appeared to be carbide pullout.

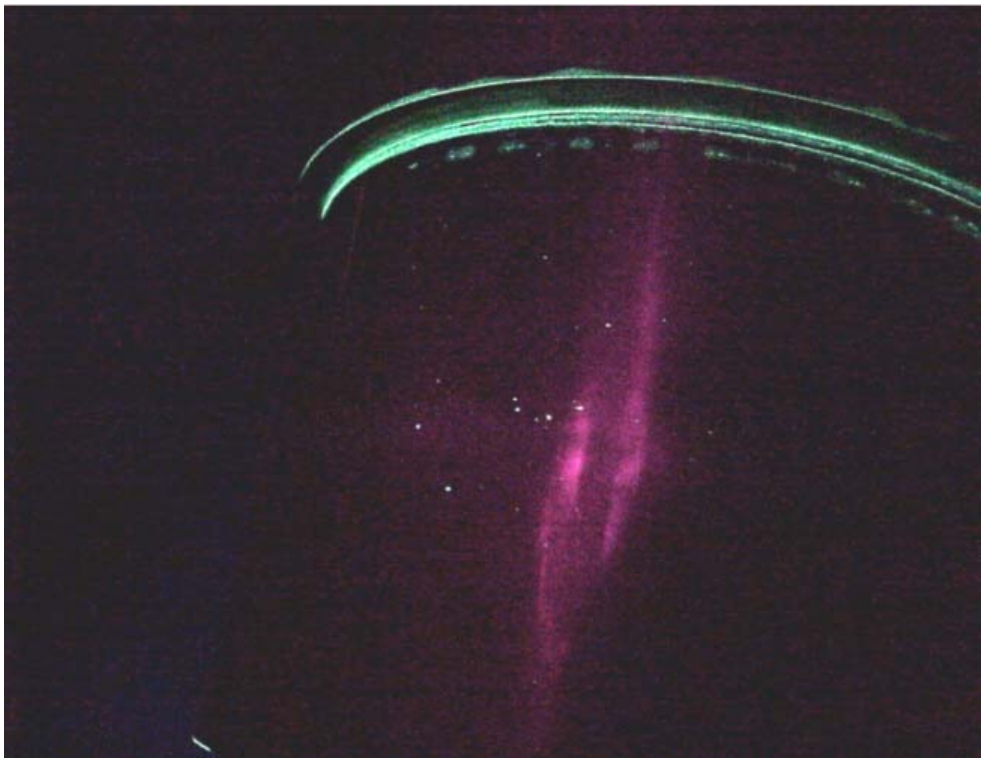

**Figure 5-11 Ultra-High-Sensitivity FPI Indications on No. 2 Bearing Journal on the Front Compressor Rear Hub**

Figure 5-12 shows a standard FPI indication on the No. 5 bearing journal on the high-pressure turbine shaft. This was extremely small and occurred on the step between the diameter change of the No. 5 spacer and the No. 5 bearing journal.

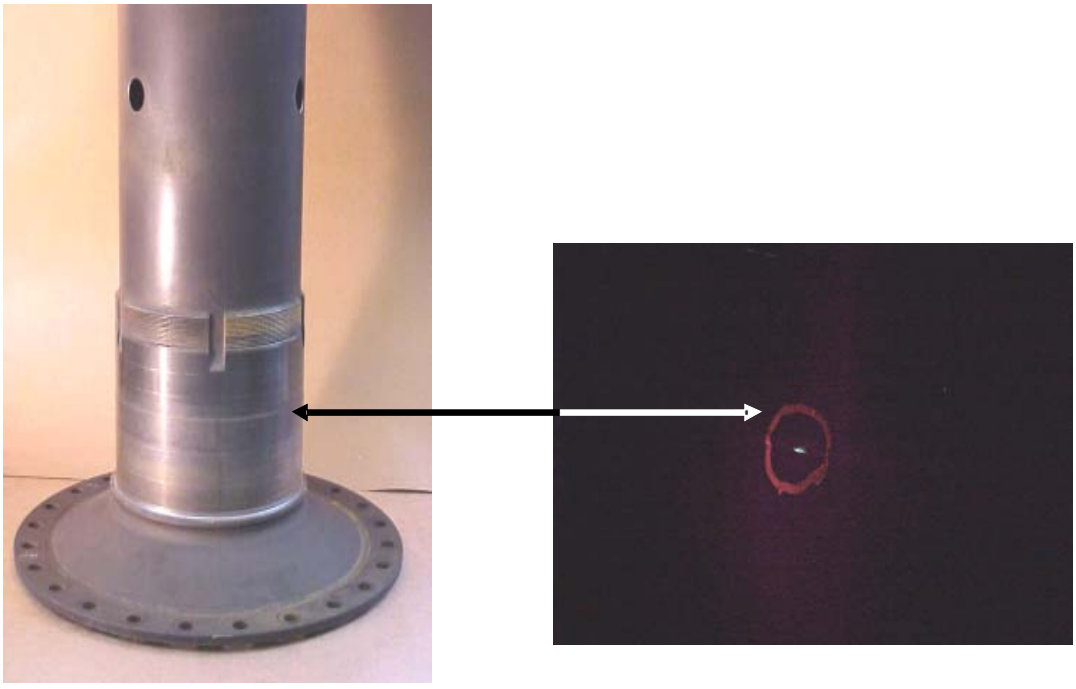

**Figure 5-12 Standard FPI Indication on No. 5 Bearing Journal on the High-Pressure Turbine Shaft**

Dimensional inspections were performed on coated areas and mating components. These data indicated that coated areas changed in dimension by a maximum of 0.0002". This small dimensional change is indicative of material transfer, coating wear and/or measurement accuracy. All coated components met the dimensional requirements for continued engine service.

Metallographic examinations were performed on three of the tested components, (1) #6 Bearing Housing, (2) #2 Front Compressor Rear Hub, and (3) High-Pressure Turbine Shaft. The #6 Bearing Housing was selected to be representative of a coating on an ID surface while the other two components were examined as a result of the FPI data. As the coatings on all other components were acceptable, there was no need to perform destructive evaluation on them. The WC/Co coating on the #6 Bearing Housing was found to be in excellent condition with no coating defects. Coating hardness was measured at two locations and found to average 1012 and 1028HV; this hardness was below the specified target range of 1150-1300HV. The hardness of the functionally tested #6 Bearing Housing component was 1096HV. Therefore, although the test component hardness was below requirements, the coating performance was not compromised.

The #2 Front Compressor Rear Hub was examined in the areas which exhibited FPI indications. These were chatter-like in appearance, adjacent to the front flange, and extended approximately 120° around the shaft. Metallographic examination of theses areas indicated no loss of coating integrity.

A metallographic examination of the High-Pressure Turbine Shaft in the location of the FPI indication failed to identify any coating defects associated with the indication as shown in Figure 5-13. The coating in this area was in excellent condition as was the coating on the adjacent surfaces that contacted seal and bearing journals.

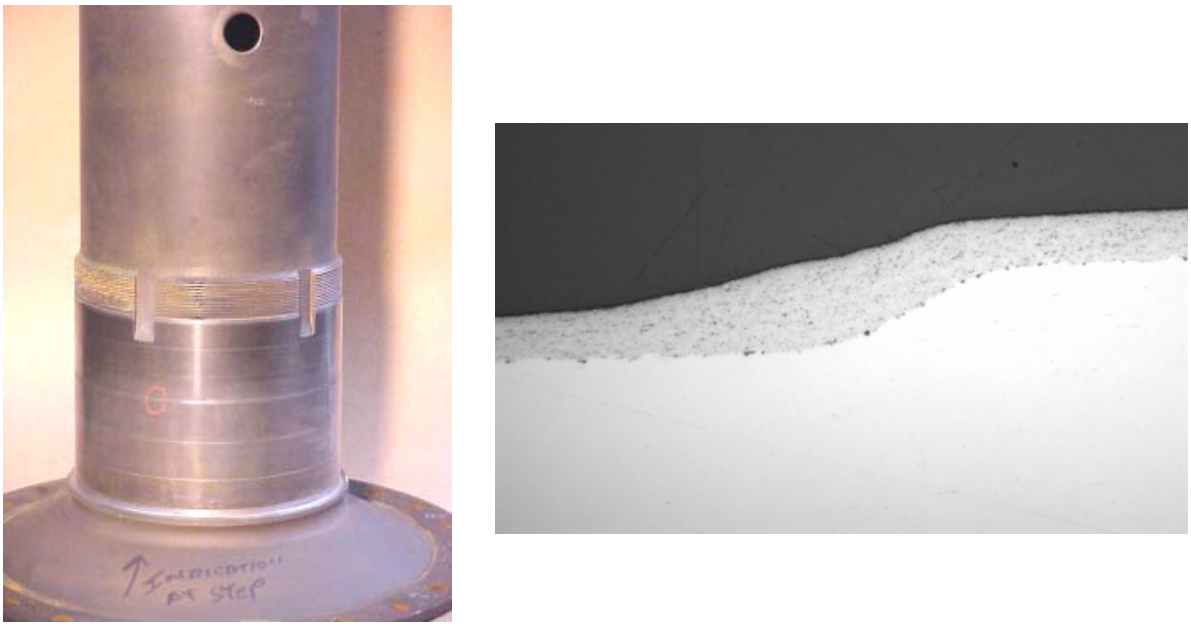

**Figure 5-13 Bearing Journal Area on the High-Pressure Turbine Shaft in Area of FPI Indication (left) and Metallographic Cross-Section of WC/Co Coating (right)**

There was a concern that coating particulates could get into the oil system and result in bearing compartment wear if the HVOF WC/Co coating were to wear or spall. Therefore, the AMT incorporated filter debris and oil analysis to examine for the presence of the coating elements tungsten and cobalt.

Periodically, oil samples were extracted from the engine and were sent to P&W in East Hartford for analysis using inductively-coupled plasma-mass spectrometry. Neither tungsten nor cobalt was detected in any of the oil samples.

At every 476 EFH (approximately every 91 run hours) the 15 micron main oil filter was removed and flushed. Collected debris was analyzed to determine the presence of tungsten or cobalt using Energy Dispersive X-Ray Fluorescence Analysis (ED-XRF). A total of nine oil filters were removed from the engine during the AMT. Results indicated that lead (most likely from anti-seize materials which contain lead compounds) was the major oil filter debris component of the last 8 filters. The first filter contained molybdenum as the primary element (some anti-seize materials also contain molybdenum disulfide). Some tungsten was found in all of the oil filters, although it was a minimal portion of the overall materials. Cobalt was not found in the first five filters analyzed, but was detected in the remaining four filters. As the coating material is 83WC - 17Co and since the levels of tungsten were very low, there was difficulty detecting Co using this technique.

After ED-XRF analysis, the debris from each oil filter was analyzed using scanning electron microscopy to isolate the tungsten- and cobalt-containing materials and determine if they were consistent with the HVOF coating. The isolated W-Co materials were generally fine-grained (less than 10 micrometers) and littered the surface of organic, coke-like (carbon-oxygen phosphorus) material. In three of the filters, pieces (approximately 50 micrometers) were found that had a flake-like appearance. Subsequent examination found these pieces to be weak and easily broken. Additionally, the W-Co material was found to be a thin "icing layer" of agglomerated particles on the coke-like material. A fourth filter was found to contain a few pieces of material similar in composition to M-50 bearing alloy which appeared similar to a machining chip. Analyses of the other filters did not detect any bearing-like material.

## 5.4. Conclusions

It was concluded that all seven WC/Co-coated components performed successfully in the AMT and that the few FPI indications were not of enough significance to indicate a problem with the coating in terms of performance. According to OC-ALC and P&W engineers, had EHC coatings been used in this test, they would have had to have been overhauled at 4500 EFH by stripping and re-applying the EHC. The analysis of the seven WC/Co-coated components (including the destructive metallurgical analysis of the three components that had FPI indications) showed that they all were capable of continued service. It is currently planned to take the four remaining intact components from the AMT and install them in another AMT engine to determine if they can survive up to 9000 EFH.

Based on the results of the TF33 AMT, it appears that the HVOF WC/Co coatings will be able to remain in service through more than one overhaul cycle, thereby reducing life-cycle costs.

This page intentionally left blank.

# 6. Cost Benefit Analysis

## 6.1. Introduction

A detailed cost/benefit analysis (CBA) for replacement of EHC plating with HVOF thermal spray was conducted at a facility that performs repair and overhaul of military gas turbine engines. This CBA was performed using the Environmental Cost Analysis Methodology (ECAM$^{SM}$) [13]. The ECAM was developed to provide users with a consistent and accurate tool for conducting economic analyses, especially where new environmental technologies are being considered. It integrates activity-based costing concepts and provides standard economic indicators, including Net Present Value (NPV), Payback Period, and Internal Rate of Return (IRR).

As shown in Figure 6-1, the ECAM uses a four-step approach that may be applied at both the facility and the process level:

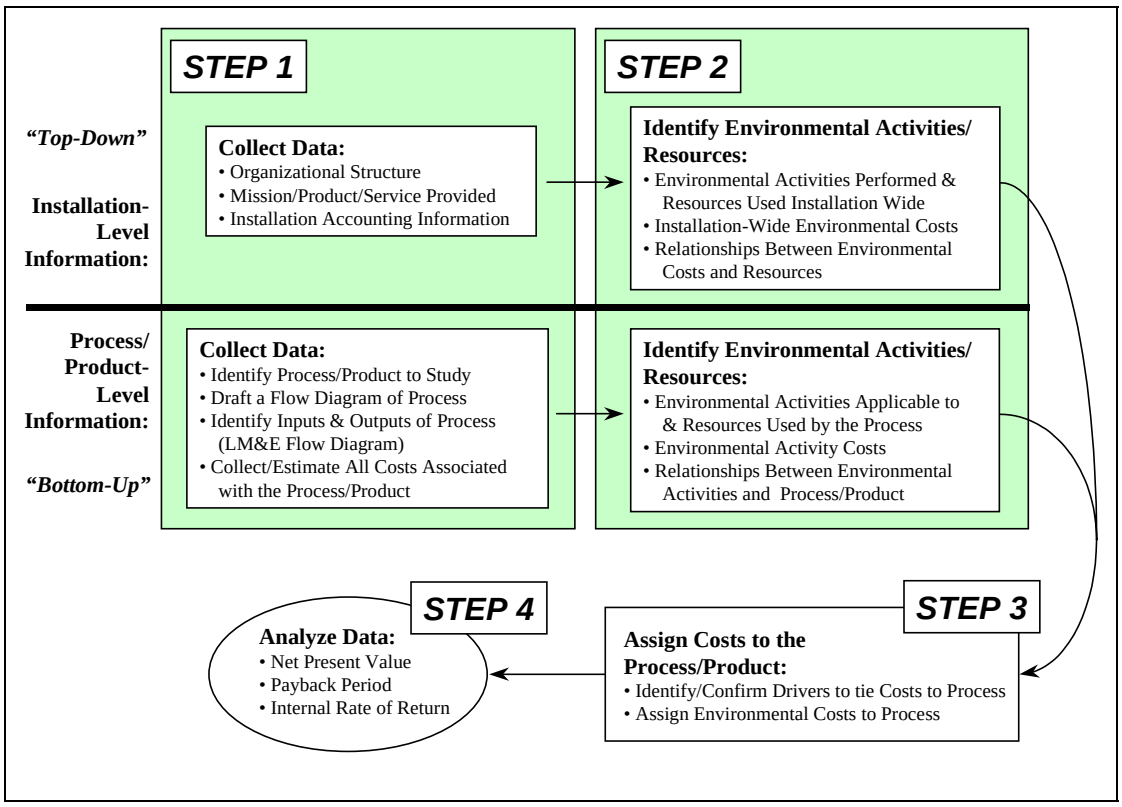


**Figure 6-1 Methodology Flow Diagram**

## 6.2. Cost Benefit Analysis scope

Six different scenarios, referred to as cases, were evaluated for this cost benefit analysis. The first case evaluates the replacement of hard chrome with HVOF for select TF33 turbine engine components, which represents 47% of the current throughput. Case 2 considers the enhanced component life that is expected with the HVOF coating. Since the component life is expected to increase, the maintenance cycle would consequently increase resulting in a declining throughput for the maintenance process.

Case 3 identifies and quantifies the additional environmental cost avoidance that can only be accounted for if all chrome plating is eliminated from the repair facility.

OSHA has proposed a new standard for occupational exposure to hexavalent chromium in response to evidence that occupational exposure to Cr (VI) poses a significant risk of lung cancer and nasal septum ulcerations and perforations. To protect exposed workers from these effects, OSHA has proposed a Permissible Exposure Limit (PEL) of 1 $\mu g/m^3$ measured as an 8-hour time weighted average. Since the baseline process contains hexavalent chromium, it is expected that additional measures will need to be taken by the facility to meet these regulations. Therefore, to ensure a complete analysis, a scenario was created where the baseline materials continue to be used after the new regulations come into effect. This increased cost of using the baseline process was compared to the alternative process that is chromium free.

Cases 4-6 evaluate the impact on plating of the proposed OSHA regulations for chromium exposure; this impact was applied to the first 3 cases.

## 6.3. BASELINE PROCESS

### 6.3.1. Process Description

Hard chrome is applied to turbine engine components to restore dimensions on worn or repaired parts. For most components, a 0.015"-thick coating is deposited, which is then machined down to a dimensional thickness of approximately 0.010". The current chrome plating process at the repair facility includes five chrome-plating tanks and two rinse tanks. To prepare parts for plating, several other activities are also performed, including stripping, shot peening, blasting, and masking. Masking typically consists of the use of lead tape and plating wax. Post-processing steps include demasking, cleaning (using a perchloroethylene degreaser), baking, grinding, and inspection. Specific activities, their frequency and sequence, vary depending on part geometry, condition, and other parameters.

The baseline process flow diagram for the current hard chrome electroplating process at the repair facility is provided in Figure 6-2.

### 6.3.2. Data Collection

A site visit was performed on March 4-7, 2002 to collect baseline data on the hard chrome plating process at the repair facility. During the site visit, interviews were held with process engineers, plating operators, plating supervisors, turbine engine program managers, environmental staff, and other employees throughout the facility. The information gathered during the site visit was supplemented with additional correspondence following the visit.

To calculate the cost to continue the baseline chromium plating process, data from recently published OSHA's studies on the cost to industry of the proposed standards were used. A *large plating - general industry sector establishment* model was developed by OSHA and the cost to achieve the alternative PELS was estimated for this model facility. These expected costs include the cost factors listed below:

- Engineering Controls
- Exposure Monitoring
- Respirator Fit-Testing
- Respirator protection
- Personal Protective Equipment
- Hygiene Areas and Practices
- Housekeeping – Additional Control Using Wet or HEPA Vacuums

- Medical Surveillance
- Communications of Chromium (VI) hazards to Employees
- Recordkeeping

These cost factors were evaluated for the repair facility and resulting estimates were used to capture the increase in baseline costs that would be expected after implementation of the regulation.

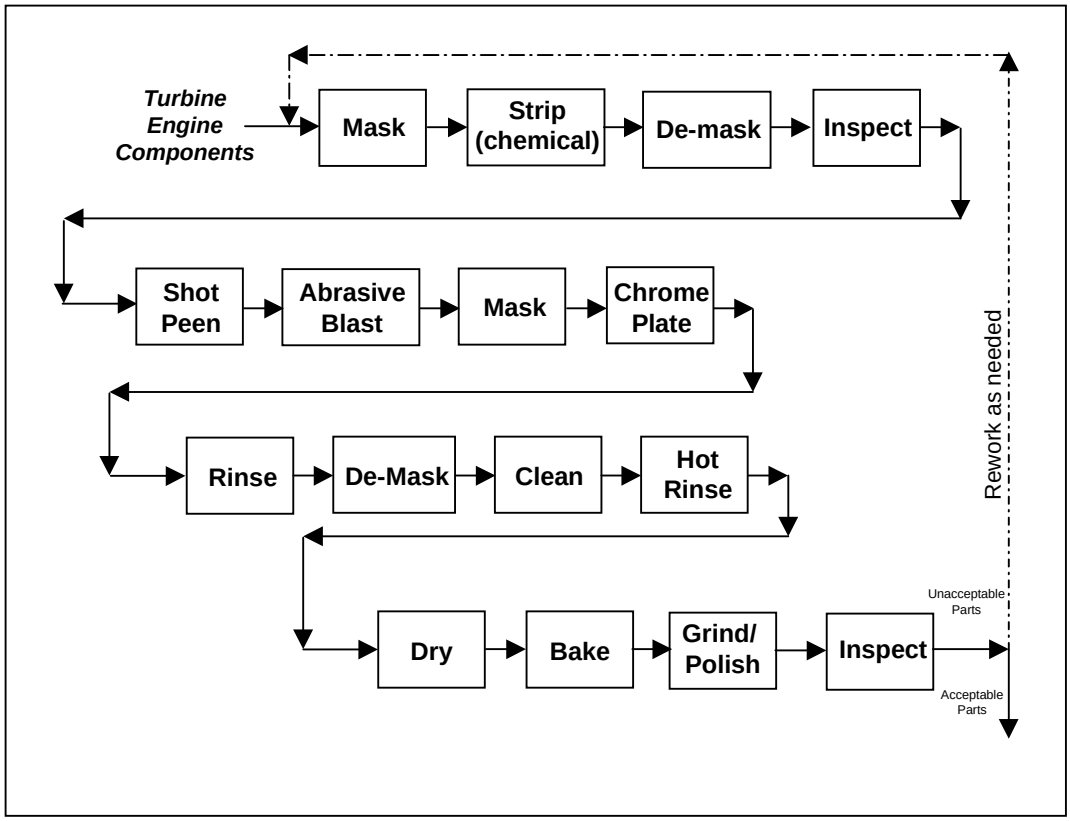


**Figure 6-2 Process Flow of Hard Chrome Electroplating at Repair Facility**

### 6.3.3. Assumptions

The following engineering assumptions were used in evaluating the baseline hard chrome plating process:

- Transition of selected TF33 components to HVOF will result in the repair facility shutting down 2 of 5 plating tanks and 1 of 2 rinse tanks. Therefore, utility costs for the affected TF33 components are based on operation of 2 plating tanks and 1 rinse tank.
- The chrome plating shop is operated 50 weeks per year.
- The rework rate for chrome plating is 10%.
- Chrome plating tank concentrations are tested weekly at a cost of $640/week.
- The cost to manage perchloroethylene emissions and waste is approximately nine times the material cost of perchloroethylene.

- Approximately 500 labor hours are required for the management of chrome plating waste associated with affected TF33 components.
- The labor rate used in this analysis is $65 per hour; this is considered a fully-burdened rate and is often used as a default rate for DOD cost benefit analyses.

### 6.3.4. Capital Costs

Decommissioning of the three process tanks (two plating and one rinse tank) will be limited to emptying the tanks. No deconstruction will take place in the near future; therefore, this cost was not captured in this analysis.

### 6.3.5. Operating Costs

Table 6-1 provides a summary of annual labor, material, utility, and waste disposal costs for the baseline hard chrome plating process (for affected TF33 components only; refer to Table 6-2 for list of candidate HVOF components).

- A reduced OSHA PEL could require additional engineering controls, and increased operating costs related to additional environmental, safety, and occupational health (ESOH) requirements and reduced worker productivity. The cost factors identified in the OSHA report and listed in Section 6.3.2 above were evaluated for application at the repair facility. Since actual costs are unknown, a range of values was used. A best-case scenario assumed that minimal costs would be required; a most-likely scenario includes only those costs that were determined to have a high probability of being incurred by the facility after implementation of the regulation. And for a complete analysis, all costs that may potentially be incurred by the facility were included in the worst-case scenario. The range of values used for each cost factor and the rationale used to determine these for each of these scenarios is given below. Any expected capital costs were annualized into operating costs.

**Table 6-1 Annual Operating Costs for Hard Chrome Plating Process**

| Resource | Annual Cost ($/yr) |
|---|---|
| Labor | |
| Process operations | $52,933 |
| Testing (QA/QC) | $12,800 |
| Contract maintenance [a] | $17,600 |
| Environmental management | $43,994 |
| Materials | |
| Chromium trioxide | $5,565 |
| Perchloroethylene | $1,277 |
| Utilities | |
| Electricity | $9,841 |
| Water | $893 |
| Waste for Disposal | |
| Hazardous Waste | $5,401 |
| **Total Annual Operating Cost** | **$150,304** |

*a. Contract maintenance for environmental controls in plating shop.. .*

*Engineering Controls:* The repair facility maintains a state-of-the-art plating shop (recently upgraded at a cost of $7M); therefore it is expected that no additional engineering controls will be necessary to meet the proposed OSHA regulations. It is anticipated that the current engineering controls will be sufficient to maintain acceptable worker exposure levels. Therefore a value of $0 was included for engineering controls for both the best-case and the most-likely scenario. However, the possibility exists that additional engineering controls will be required. The OSHA reports estimate that a model plating facility will spend $18,775 per year on engineering controls. This value is used as a worst-case scenario for the facility.

*Exposure Monitoring:* The facility has completed some monitoring in the past, however the results were not available while completing this analysis. The best case was considered to be that in which monitoring was conducted within 12 months of the regulation being implemented with the results indicating that the exposure level is below the action level. Therefore no additional monitoring would be required; best-case annual cost for this category was set at $0. The most likely scenario that is expected with the state-of-the-art facility is that initial monitoring would be required, but the results would indicate that exposure was below the action level; most-likely case annual cost for this category was set at $475. The worst-case scenario for this category is that initial monitoring would indicate exposure above the action level requiring quarterly monitoring from that point on: worst-case annual cost for this category was set at $9,478.

*Respirator Fitting and Protection:* The facility presently equips the solution maintenance personnel with respirators to use while adding or maintaining chrome solution. Eight of the twenty chrome-plating personnel conduct solution maintenance. Therefore, it is assume that all 8 of these people will need to meet the requirements for respirator fitting and protection and the annual cost for all three scenarios would be the same value: $1,210 for respirator fitting and $429 for respirator protection.

*Personal protection equipment (PPE):* Since the alternative process, HVOF, would also require PPE, no additional costs were considered for this category.

*Hygiene Areas and Practices:* The best-case scenario would be that no additional showers, hand washing facilities or change rooms would be needed; therefore the best-case annual cost for this category was set at $0. However, based on the OSHA report, it is assumed that these items will need to be purchased and maintained; therefore both the most-likely and worst-case annual costs for this category was set at $7,925.

*Housekeeping – Additional Control Using Wet or HEPA Vacuums:* It is assumed, based on the OSHA report, that HEPA vacuums will be needed for housekeeping. Therefore, all three scenarios are expected to have the same value: an annual cost of $10,026.

*Medical Surveillance:* Potentially exposed employees would require additional medical testing. The best-case scenario is that no employees would need additional testing; therefore best-case annual cost for this category was set at $0. It is assumed that at most only 1 employee per year would need this additional testing; therefore both the most-likely and worst-case annual cost for this category was set at $1,409.

*Communication:* Additional communication to the employees about the hazards of chromium exposure would be required with the new regulation. Therefore the annual cost for all three scenarios would be the same: $1,678 per year.

*Recordkeeping:* Additional recordkeeping on potentially exposed employees would be required. Therefore the annual cost for all three scenarios would be the same: $328 per year.

Due to the difficulties associated with predicting the economic impact of a proposed regulation,

Monte Carlo simulation was used to forecast the potential impact using the variable costs described above.

Monte Carlo simulation is an analytical method meant to imitate a real-life system. Since it is not known what actual costs will be incurred for each of these cost factors, it was assumed that the costs could range from the minimum best-case scenario to the maximum worst-case scenario. For these uncertain variables (cost factors that have a range of possible values), the possible values were defined with a probability distribution. A triangular distribution was used to model this system as shown in Figure 6-3. The potential annual cost impact ranges from a low value of $13,671 (sum of the best-case for all cost factors) to a high value of $51,259 (sum of the worst-case for all cost factors). Based on this analysis, the most-likely value was set $23,481 per year. This probability distribution indicates that the annual costs will vary from $13,671 to $51,259, however those values closest to the most-likely value of $23,481 have a higher probability of occurring; this distribution is shown below. This annualized cost distribution was added to the baseline costs beginning in year 1 even though the implementation date for the regulation is not yet known.

**Assumption: Expected OSHA Compliance Costs** **Cell**

Triangular distribution with parameters:

| | |
|---|---|
| Minimum | $13,671 |
| Likeliest | $23,481 |
| Maximum | $51,259 |

Selected range is from $13,671 to $51,259

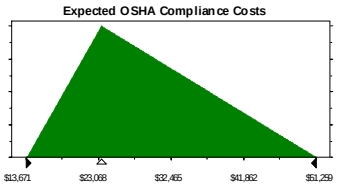


**Figure 6-3 Probability Distribution Assumption for Expected OSHA Compliance Costs**

# 6.4. HVOF Process

## 6.4.1. Process Description

A process flow diagram of the application of tungsten carbide cobalt (WC/Co) by HVOF thermal spraying was developed to aid in the collection of data for the HVOF process alternative. A generic process flow diagram for HVOF is shown in Figure 6-4. Note that five process steps, other than the plating (coating application) step, are expected to be eliminated when transitioning from hard chrome electroplating to HVOF thermal spraying: (Rinse, Clean, Hot Rinse, Dry, and Bake). Specifically related to the cleaning step, there are significant environmental and worker safety benefits associated with elimination of perchloroethylene as a cleaner. In addition, the masking required for HVOF consists of tape and hard fixturing, as opposed to the lead tape and wax dip process used for hard chrome plating.

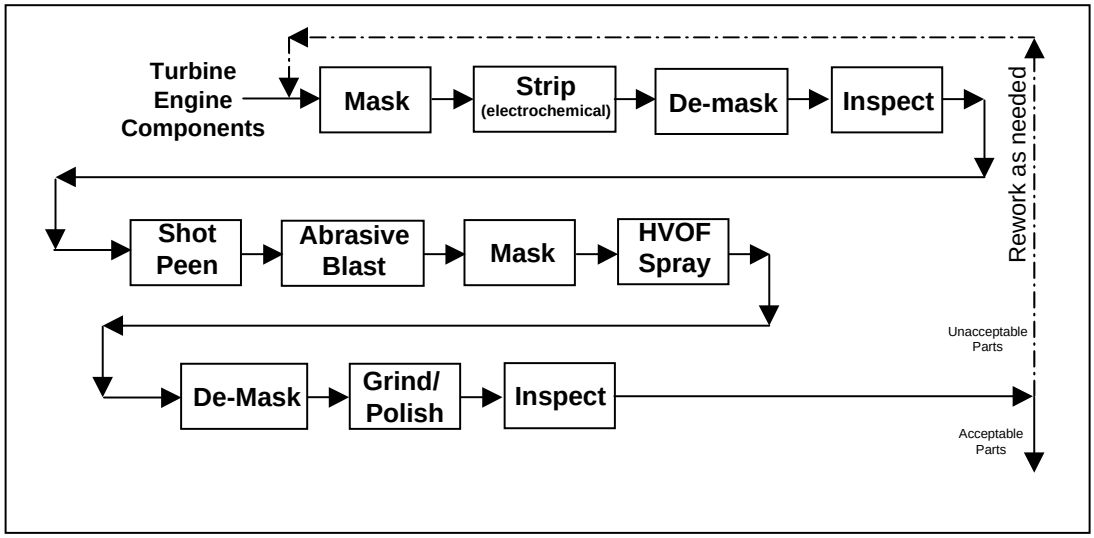


**Figure 6-4 Projected Process Flow of HVOF Thermal Spraying**

The candidate TF33 components to be transitioned to HVOF and their annual throughput rates are listed in Table 6-2.

**Table 6-2 Candidate TF33 Components for HVOF**

| Component | Plated Surface Area ($in^2$) | # Processed (FY01) |
|---|---|---|
| #1 Bearing Housing | 11.1 | 11 |
| #2 Bearing Housing | 56.6 | 16 |
| #2 ½ Bearing Housing | 11.3 | 208 |
| #4 Bearing Housing | 45.9 | 21 |
| #5 Bearing Housing | 39.9 | 15 |
| #2 Hub | 105.4 | 123 |
| #3 Hub | 16.7 | 80 |
| #4 Hub | 68.4 | 73 |
| #6 Hub | 28.0 | 49 |
| Low-Pressure Turbine Shaft | 65.9 | 50 |
| High-Pressure Turbine Shaft | 110.5 | 32 |
| | | |
| **Annual Throughput** | **678 parts/yr** | |
| **Annual Plated Surface Area**[a] | **225 $ft^2$/yr** | |

*a Not including rework*

## 6.4.2. Assumptions

The following engineering assumptions were used in evaluating the HVOF thermal spray coating process:

- Approximately 47% of the parts that are currently chrome plated will be transitioned to HVOF (refer to Table 6-2 for candidate TF33 components for HVOF).

- All operating parameters are based on Sultzer Metco specifications for a Diamond Jet DJ2600 system.
- WC/Co is deposited to a thickness of 0.015" and ground down to the final thickness of 0.010", as is presently done with the current chromium coating.
- The rework rate for HVOF thermal spray is 5%.
- The HVOF spray process has a 40% (deposited to sprayed) coating efficiency.
- Hydrogen ($H_2$) gas will be used as the fuel gas.
- HEPA filters in the dust collection system will be replaced every 5 years at a cost of $20,000, plus $250 for disposal of spent filters.
- The cost of WC/Co powder coating is $32 per lb.
- Initially (in the first few months), all components (up to 10% of annual throughput) will have a sample coupon coated and sent to the lab for testing to assure the process is operating within specifications.
- Upon obtaining a controlled spray process, a sample coupon will be coated and tested once per month.
- Lab cost to perform QA/QC test on coated panel is $350 per panel.
- To assure compliance with specifications, the repair facility will test all WC/Co powder lots to verify composition at a cost of $150 per lot.
- Water and electricity usage is based on 125% of the hourly use of HVOF thermal spray equipment.
- The air filtration system operates 40 hrs/week, 50 weeks/year.
- Ventilation electricity costs are based on a 15 hp (11.19 kW) motor in the air filtration system.
- The ratio of labor for masking (HVOF vs. hard chrome) is 1:1.
- The ratio of labor for coating (HVOF vs. hard chrome) is 1.5:1.
- The ratio of labor for demasking/cleaning (HVOF vs. hard chrome) is 0.27:1.
- The ratio of labor for grinding (HVOF vs. hard chrome) is 0.75:1.
- The cost of stripping chrome is comparable to the cost of stripping HVOF.
- Maintenance to clean spray booths is performed quarterly; 8 hr per booth.
- Maintenance to clean hard masking fixtures is performed monthly; 6 hrs per booth.
- The cost of waste disposal for HVOF overspray and filters is $0.25 per pound.

### 6.4.3. Capital Costs

The repair facility has already installed one HVOF spray booth, which consisted of the purchase of a robot, turntable, controller, feeder, and the retrofit of an existing spray booth and dust collection system. The new equipment cost $200,000 and an additional $275,000 will be spent to move and reinstall the dust collection system and make necessary safety modifications. The purchase of an additional HVOF thermal spray system is anticipated to cost $500,000. Thus, the total capital equipment cost is estimated at $975,000. However, for the purposes of this analysis, only one booth at $500,000 was input as a capital investment since it is sufficient to handle the throughput of the TF33 components.

In addition to the initial equipment costs, the following capital costs have also been considered during the preparation of this CBA. The testing that will initially need to be performed on sample

coupons for all components until the process is determined to be running within tolerance. It is estimated that this testing will be performed on approximately 10% of the annual throughput of TF33 components at a cost of $36,368.

Training for the operators on the safety, and operational procedures of the HVOF spray equipment is estimated to cost $2,000.

### 6.4.4. Operating Costs

Table 6-3 provides a summary of annual labor, material, utility, and waste disposal costs for the HVOF thermal spray process for the affected TF33 components assuming a constant throughput of 678 parts per year (Case 1). This does not include the periodic maintenance costs for replacing the filters in the dust collection system, which is estimated to be $20,250 every five years (includes new filters and disposal of old filters).

**Table 6-3 Annual Operating Costs for HVOF Thermal Spray Process**

| Resource | Annual Cost ($/yr) |
|---|---|
| Labor | |
| Process operations | $52,774 |
| Testing (QA/QC) | $6,759 |
| Maintenance | $6,760 |
| Materials | |
| WC/Co powder | $19,907 |
| Hydrogen | $7,621 |
| Oxygen | $1,365 |
| Nitrogen | $105 |
| Replacement parts [a] | $1,970 |
| Utilities | |
| Electricity | $2,489 |
| Water | $23 |
| Waste for Disposal | |
| Solid waste (overspray) | $93 |
| **Total Annual Operating Cost [b]** | **$99,866** |

*a. Includes nozzles, hoses, o-rings, electrodes, and powder feeder restrictors.*

*b. Does not include the periodic maintenance costs for replacing the filters in the dust collection system, which is estimated to be $20,250 every five years (includes new filters and disposal of old filters).*

It is estimated that a constant throughput of chrome-plated parts will come in for repair and will be recoated using HVOF for a minimum of five years. However, based on the anticipated extension in service life that HVOF is expected to provide, components previously coated with HVOF that return to the depot may not necessarily be processed. If the turbine engine manufacturers agree that HVOF thermal sprayed components do not have to be stripped for inspection upon return to the depot (unless required for repair purposes), the number of TF33 parts processed annually will decrease over time. The following assumptions were used to

analyze the cost benefit of this scenario (Case 2):

- Years 1-5: All TF33 components coming into the depot have chrome plating that is stripped for inspection and repair purposes. Applicable TF33 components are recoated using HVOF thermal spray at the current throughput rate of 678 parts per year.
- Years 6-10: 50% of the TF33 components processed are chrome-plated parts, which are stripped, inspected, repaired, and recoated using HVOF thermal spray. It is assumed that the remaining 50% of the parts were previously coated using HVOF. It is estimated that 25% of these components (12.5% of the total throughput) will be stripped, inspected/repaired, and recoated using HVOF. The remaining components (37.5% of the total throughput) will require no processing. Thus, the total number of parts processed annually will be 424 components.
- Years 11-15: All TF33 components coming into the depot were previously coated using HVOF. Of these, 25% will be stripped, inspected/repaired, and recoated using HVOF thermal spray. The total number of parts processed annually will be 170 components.

Table 6-4 provides a summary of annual labor, material, utility, and waste disposal costs for the declining throughput rate scenario (Case 2) for the affected TF33 components. Again, this does not include the periodic maintenance costs for replacing the filters in the dust collection system, which is estimated to be $20,250 every five years (includes new filters and disposal of old filters).

A third case analysis was also performed to consider the additional savings that could be attributed to HVOF thermal spray if hard chrome plating was completely eliminated at the repair facility. Until chrome plating is completely eliminated, permitting, record keeping, training, and other management costs associated with the use of hexavalent chromium are not likely to change. However, assuming that the facility does eliminate the hard chrome plating process through implementation of alternative technologies, an additional $150,000 environmental management burden will be avoided. Of that cost avoidance, $70,500 can be attributed to the transition of candidate TF33 components to HVOF thermal spray. Assuming the same operating costs for declining TF33 throughput as Case 2, a cost benefit analysis factoring in this additional cost avoidance (accounted for as an additional environmental management burden on the baseline hard chrome plating process) was performed as Case 3.

**Table 6-4 Annual Operating Costs for HVOF Thermal Spray Process**

| Resource | Annual Cost ($/yr) | | |
|---|---|---|---|
| | Years 1-5 | Years 6-10 | Years 11-15 |
| Labor | | | |
| Process operations | $52,774 | $32,988 | $13,195 |
| Testing (QA/QC) | $6,759 | $6,009 | $5,409 |
| Maintenance | $6,760 | $4,254 | $1,748 |
| Materials | | | |
| WC/Co powder | $19,907 | $12,719 | $5,528 |
| Hydrogen | $7,621 | $4,764 | $1,905 |
| Oxygen | $1,365 | $853 | $341 |
| Nitrogen | $105 | $65 | $26 |
| Replacement parts | $1,970 | $1,231 | $492 |
| Utilities | | | |
| Electricity | $2,489 | $2,448 | $2,407 |
| Water | $23 | $15 | $6 |
| Waste for Disposal | | | |
| Solid waste (overspray) | $93 | $60 | $26 |
| **Total Annual Operating Cost [a]** | **$99,866** | **$65,406** | **$31,083** |

*a. Does not include the periodic maintenance costs for replacing the filters in the dust collection system, which is estimated to be $20,250 every five years (includes new filters and disposal of old filters)*

## 6.5. COST BENEFIT ANALYSIS

The ECAM includes a financial analysis that was performed using the Pollution Prevention Financial Analysis and Cost Evaluation System (P2/FINANCE) software. The P2/FINANCE software generates financial indicators that describe the expected performance of a capital investment. A brief explanation on interpreting these financial indicators is provided, as are the results of the financial analyses for the implementation of HVOF thermal spray for TF33 turbine engine components at the repair facility.

To measure the financial viability of this project, three performance measures for investment opportunities were used: net present value (NPV), internal rate of return (IRR), and payback period. The NPV is the difference between capital investments and the present value of future annual cost benefits associated with the alternatives. The IRR is the discount rate at which NPV is equal to zero. NPV and IRR account for the time value of money, and discount the future capital investments or annual cost benefits to the current year. For NPV and IRR, a 3.5% discount rate was used for this financial evaluation, which is consistent with the OMB Circular Number A-94 and the ECAM. The payback period is the time period required to recover all of the capital investment with future cost savings. Guidelines for these performance measures are listed in Table 6-5.

**Table 6-5 Summary of Investment Criteria**

| Criteria | Recommendations/Conclusions |
|---|---|
| NPV > 0 | Investment return acceptable |
| NPV < 0 | Investment return not acceptable |
| Highest NPV | Maximum value to the facility |
| IRR > discount rate | Project return acceptable |
| IRR < discount rate | Project return not acceptable |
| Shortest payback period | Fastest investment recovery and lowest risk |

Adapted from *ECAM Handbook.*

A summary of the financial evaluation for implementing HVOF to replace hard chrome electroplating of TF33 turbine engine components is shown in Table 6-6, Table 6-7, and Table 6-8 for Cases 1, 2, and 3, respectively. This financial evaluation includes the annual operating costs reported in Section 6.3.3 and 6.3.5 and the initial investment costs reported in Section 6.3.4. The evaluation does not include the costs of qualification testing.

**Table 6-6 Results of Financial Evaluation for Constant Throughput (Case 1)**

| Financial Indicator | 5-yr | 10-yr | 15-yr |
|---|---|---|---|
| **Net Present Value** | ($327,688) | ($150,301) | $11,142 |
| Internal Rate of Return | NA | NA | 3.8% |
| Discounted Payback | 14.6 years | | |

**Table 6-7 Results of Financial Evaluation for Declining Throughput (Case 2)**

| Financial Indicator | 5-yr | 10-yr | 15-yr |
|---|---|---|---|
| **Net Present Value** | ($327,688) | ($19,299) | $362,304 |
| Internal Rate of Return | NA | NA | 10.2% |
| Discounted Payback | 10.2 years | | |

**Table 6-8 Results of Financial Evaluation Accounting for Additional Cost Avoidance Realized with the Total Elimination of Chromium Plating (Case 3)**

| Financial Indicator | 5-yr | 10-yr | 15-yr |
|---|---|---|---|
| **Net Present Value** | ($9,377) | $567,022 | $1,174,282 |
| Internal Rate of Return | 2.9% | 19.9% | 23.6% |
| Discounted Payback | 5.1 years | | |

Cases 1, 2, and 3 above were used as the basis of three additional analyses that account for the additional cost avoidance that may be realized if OSHA reduces the PEL for hexavalent chromium in the near future. Due to the difficulties associated with predicting the economic impact of a proposed regulation, Monte Carlo simulation was used to forecast the potential impact using variable capital and operating costs. Using Monte Carlo simulation, key variables are defined within a given range and distribution profile instead of a single (uncertain) value. The output shows the range of possible results and degree of certainty that any desired outcome can be

achieved. During the Monte Carlo simulation, 1,000 trials were run for each case study.

Figure 6-5 shows the results of the Monte Carlo simulation for the 15-year NPV for a PEL of 1.0 µg/m$^3$ (Case 4). For the constant throughput scenario, the 15-year NPV ranges from $ 176K to $593K, with a mean value of $350K. For a declining throughput scenario, the 15-year NPV ranges from $528K to $944K, with a mean value of $702K.

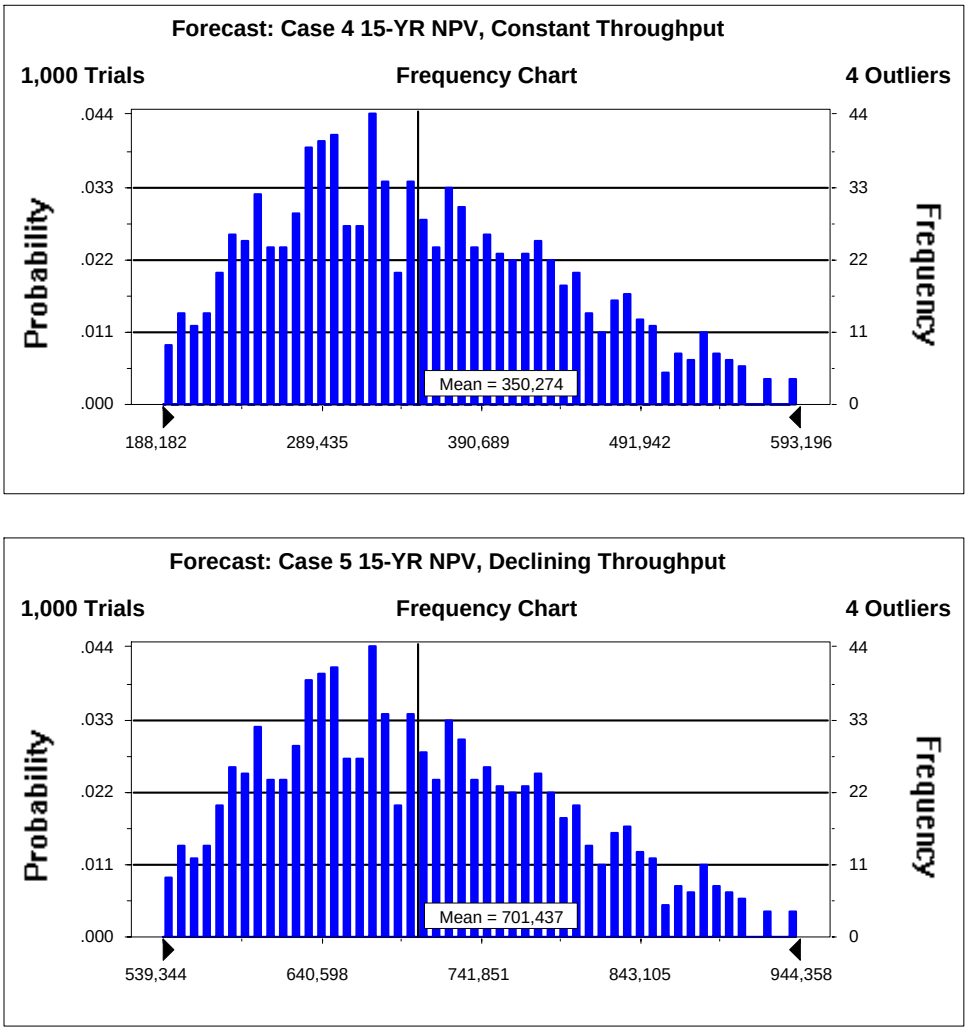


**Figure 6-5 15-Yr NPV for PEL of 1.0 µg/m3 (Cases 4 and 5)**

A summary of the cost benefit indicators for Case 4 is presented in Table 6-9 below. All data are mean values.

**Table 6-9 Results of Financial Evaluation for PEL of 1.0 µg/m3**

| Financial Indicator | Continuous Throughput | Declining Throughput |
|---|---|---|
| **15-Year Net Present Value** | $350,274 | $701,437 |
| Internal Rate of Return | 11.5% | 15.9% |
| Discounted Payback | 8.3years | 7.28.5 years |

A final cost analysis was also performed to consider the additional savings that could be attributed to HVOF thermal spray if hard chrome plating was completely eliminated at the repair facility. Based on Case 3, which consists of declining throughput scenario with an additional environmental management burden for the baseline process, Case 6 includes an additional ESOH burden if the OSHA PEL is reduced to 1.0 µg/m$^3$.

Figure 6-6 shows the results of the Monte Carlo simulation for the 15-year NPV including the additional ESOH burden (Case 6). For a PEL of 1.0 µg/m$^3$, the 15-year NPV ranges from $2.7M to $3.1M, with a mean value of $2.9M.

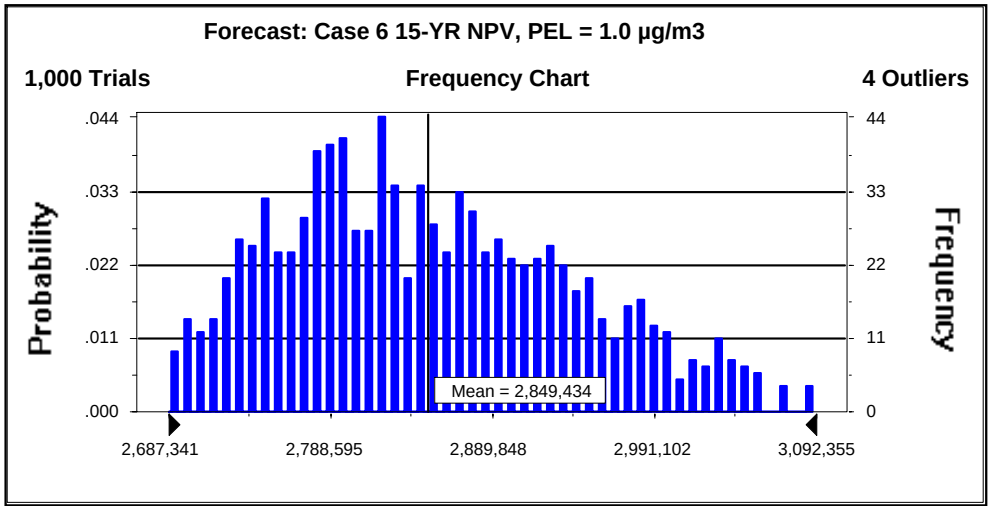


**Figure 6-6 15-Yr NPV Including Additional ESOH Burden (Case 6)**

A summary of the cost benefit indicators for Case 6 is presented in Table 6-10 below. All data are mean values.

**Table 6-10 Results of Financial Evaluation Including ESOH Burden (Case 6) Mean Values**

| Financial Indicator | **PEL = 1.0** µg/m$^3$ |
|---|---|
| **15-Year Net Present Value** | $2,849,400 |
| Internal Rate of Return | 50% |
| Discounted Payback | 2.1 years |

## 6.6. Summary and Conclusions

HVOF application of WC/Co is being investigated as an alternative to hard chrome electroplating for repairing/overhauling aircraft turbine engine components. A cost benefit analysis was performed to identify the potential financial impact of implementing the HVOF coating process at a repair facility for application to TF33 turbine engine components. Data were collected at this facility and the potential economic effects were calculated in accordance with the ECAM.

It was estimated that the use of HVOF on TF33 turbine engine components would result in a net decrease in annual operating costs at the facility of approximately $50K. At this rate, it would take over 14-years to pay back the capital investment costs of implementing HVOF. Accounting for the potential economic impact of a reduced OSHA PEL for chromium, the average 15-year NPV would be $350,000. The payback period would be 8.3 years.

Additional savings will be realized if the requirement to strip HVOF for component inspection is waived based on the increased service life that HVOF is anticipated to provide. In this case, the number of parts processed will decrease over time once all chrome-plated parts have been coated with HVOF WC/Co. For this scenario, the potential savings (NPV) over 15 years is over $362K with a payback period of just over 10 years. Accounting for the potential economic impact of a reduced OSHA PEL for chromium, the average 15-year NPV would be $701,400. The payback period would be 7.2 years.

Further cost savings (through reduced environmental management burden) will be realized and should be attributed to the HVOF thermal spray process once the repair facility completely eliminates all hard chrome plating operations. Considering this additional cost benefit, the potential savings are greater than $1M over the 15-year study period, and the payback period is just over 5 years. Accounting for the potential economic impact of a reduced OSHA PEL for chromium, the average 15-year NPV would range between $2.9M. The payback period would be 2.1years.

This analysis was conducted using recently published OSHA data; the results are given above. The original analysis described in the July 2002 report, resulted in a mean 15-year NPV from $156,000 to $5.4 Million. The range of values has been reduced considerably over the original report due to the better accuracy of data used.

Obviously, the potential economic impact of having to upgrade facilities and assume a greater ESOH burden to comply with a reduced PEL for chromium is significant.

Economic studies of HVOF implementation at other facilities have shown a range of results, indicating that the economic feasibility of HVOF implementation is highly dependent on site-specific details. The actual economic effects at OC-ALC or other facilities will vary depending on the number of actual applications converted, future workloads, and other factors specific to each facility.

This page intentionally left blank.

# 7. Implementation

The implementation of thermal spray coatings as a replacement for electrolytic hard chrome on gas turbine engine components at military repair depots involved the following principal three task areas: (1) demonstration of equivalent or superior performance through materials and component rig testing, (2) demonstration of equivalent or reduced life-cycle costs, and (3) installation of thermal spray equipment and its incorporation into the depot environment, which includes development of fixturing for components, personnel training, and availability of standards and specifications. These will be discussed in the following sections.

## 7.1. Coatings Performance

In general, the fatigue performance of A-286, AMS-355, 9310, IN-901 and 4340 alloy samples coated with the thermal spay coatings was equivalent to or exceeded that of equivalent samples coated with EHC. However, for approximately 50% of the IN-718 and 40% of the 17-4PH samples, the fatigue performance of the thermal spray coatings was inferior to that of EHC. The reason for this could not be definitively determined. One possible explanation is that for coatings such as WC/Co, the deposition parameters used were those developed in the landing gear project for high-strength steels [7]. As discussed in Section 4.5.8, initial fatigue studies performed prior to the initiation of this project on IN718 showed that it was possible to deposit WC/Co such that the fatigue performance was equivalent to that for EHC on IN718. There is a high level of confidence that if a full DOE study were to be performed for optimization of fatigue properties, it would be possible to identify HVOF deposition parameters that would provide performance at least equivalent to that of EHC. Because of the successful rig test on IN718 TF33 components, HVOF WC/Co coatings are being implemented on those types of components regardless of the fatigue results on IN718.

For fretting wear tests conducted at 750º F, HVOF WC/Co coatings performed significantly better than EHC and the other thermal spray coatings when sliding against all of the mating materials, except IN-718 where the coating performance was equivalent to EHC. For fretting wear tests conducted at 300º F, the results were less definitive but in the majority of cases, WC/Co performance was equivalent or superior to EHC. In B117 salt fog corrosion testing, the performance of all of the 0.003”-thick thermal spray coatings was inferior to EHC whereas the performance of the 0.015”-thick thermal spray coatings was generally equivalent to EHC on 4340 steel substrates. (Note that B117 test performance of thermal spray coatings always has very poor correlation with service performance.) For all coatings on IN-718, very little corrosion was observed at either thickness. For the carbon seal tests, in general the performance of the HVOF WC/Co coatings was equivalent to EHC in terms of both the wear of the coating and the mating carbon seal material.

Coating integrity can be defined as the ability of a coating to continue protecting the underlying material during application of cyclic stresses without significant cracking (that might cause a corrosive medium to penetrate to the substrate) and without delamination or spalling, which clearly would result in a loss of protection. This was an issue in the landing gear project where delamination of HVOF WC/Co coatings was observed under certain fatigue test conditions involving high levels of alternating stress [7]. For the GTE project, the levels of alternating stress or strain were generally less than in the landing gear project and therefore delamination during the running of the tests was not encountered. Delamination was observed, however, after failure of the fatigue specimen, with the coating spalling in the vicinity of the fracture. Significant cracking of any of the thermal spray coatings during fatigue testing was rare. On a few samples with 0.015”-thick WC/Co coatings undergoing LCF testing, circumferential or ring cracking was observed, presumably because there was a larger difference between the minimum and maximum

stress for LCF (R = 0.026) than for HCF (R = 0.33) testing. As was observed in the materials tests for the landing gear project [7], there is a greater potential for cracking of the coatings as the difference between minimum and maximum stress is increased. However, the presence of cracks does not mean that the coatings would be rejected in service (consider the extensive cracking in EHC coatings), as long as delamination is not observed.

The seven HVOF WC/Co-coated components evaluated in the TF33 AMT demonstrated significantly better performance than what would be expected for EHC-coated components. Virtually no degradation of the coatings were observed in subsequent visual and FPI analyses as well as in oil analyses conducted during the AMT. As a result of the successful TF33 AMT engine test, the four remaining HVOF WC/Co-coated components will be installed in another AMT to determine if they can survive up to 9000 EFH. It appears that, unlike EHC, the HVOF WC/Co coatings will be able to remain in service through more than one overhaul cycle, thereby reducing life-cycle costs. Keeping the coating on the components over more than one maintenance cycle will require a change in the present overhaul method, which requires that EHC always be stripped and the substrate examined for cracks at each overhaul.

Outside of the scope of this project, the Navy conducted a 50-hour accelerated TF34 engine test in which six components that are normally EHC-coated were instead coated with 0.003”-thick HVOF WC/Co. These components were the B-Sump Housing, Axis-B Bevel Gearshaft, High-Pressure Turbine Rear Shaft, and the #5, #6 and #7 Carbon Seal Runners. Oil analyses conducted during the engine test indicated no loss of coating. Based on visual inspection the appearance of the coatings was identical to before the test and FPI testing gave no indications of defects subsequent to the engine test.

## 7.2. Cost/Benefit Analysis

A cost benefit analysis was performed to identify the potential financial impact of implementing the HVOF coating process at a military gas turbine engine repair facility for application to the components from the engine that provided the largest chrome plating workload. Data were collected at this facility and the potential economic effects were calculated in accordance with the ECAM. It was estimated that the use of HVOF on the turbine engine components would result in a net decrease in annual operating costs at the depot of approximately $50K. At this rate, it would take over 14-years to pay back the capital investment costs of implementing HVOF. Additional savings will be realized if the requirement to strip HVOF for component inspection is waived based on the increased service life that HVOF is anticipated to provide. In this case, the number of parts processed will decrease over time once all chrome-plated parts have been coated with HVOF WC/Co. For this scenario, the potential savings (NPV) over 15 years is over $362K with a payback period of just over 10 years. Further cost savings (through reduced environmental management burden) will be realized and should be attributed to the HVOF thermal spray process once the depot completely eliminates all hard chrome plating operations. Considering this additional cost benefit, the potential savings are greater than $1M over the 15-year study period, and the payback period is just over 5 years.

The CBA also took into account the proposed decrease in the hex-Cr PEL to 1 $\mu g/m^3$. For this analysis a recently released OSHA report was used to estimate future baseline operating costs at the repair facility. From this data it was determined that annual operating costs could increase by up to 34%. Due to the uncertainty associated with predicting the economic impact of the proposed regulation, a Monte Carlo simulation was used. The results showed that if the new proposed hex-Cr PEL is implemented, then the 15-year net present value for the constant-throughput, declining-throughput and chrome-elimination cases would increase to $350,000, $700,000 and $2.9 million, respectively.

## 7.3. Implementation at Repair Depots

The Oklahoma City ALC was the lead demonstration overhaul facility with NADEP -JAX as the secondary demonstration facility. At the beginning of the project, both depots already had operational HVOF systems, although the one at OC-ALC required significant upgrading to make it production-ready. This upgrading was accomplished during the execution of the project such that the system was ready for production coating of GTE components by the Summer of 2004.

OC-ALC manages 19 types of engines (aircraft jet engines, missile engines and helicopter engines). It is designated the source of repair (SOR) for 11 of the 19 and is currently repairing the TF30, TF33, F101, F108, F110 and F118 engines. The center also is the SOR for the Navy F110-400 and TF30-414A engines and manages the J79 engine. Within the Air Force there are approximately 18,500 active engines and in FY2004 OC-ALC expects to overhaul 975 engines.

During overhaul there are a number of components that must be repaired due to wear, gouges, or corrosion pits. For items that can be repaired, EHC plating is often used subsequent to machining of the damaged area. As examples, on the TF33 engine there are 12 separate components and on the F100 there are 41 separate components that are commonly plated with hard chrome. In FY2002, there were approximately 700 TF33 components onto which EHC was applied during repair operations. Approximately 70% of the total GTE hard chrome plating workload at OC-ALC is for TF33 components, so the replacement of EHC on that engine provides the greatest benefit.

OC-ALC currently has one fully operational Sulzer-Metco DJ2700 HVOF thermal spray system and is currently installing a second system. Figure 7-1 shows the spray booth, which is 16 feet wide by 12 feet deep by 10 feet high in which even the largest GTE components that are currently EHC plated can be mounted. Figure 7-2 shows the spray gun mounted to a Fanuc M16i robot with air jets used for cooling of components during coating application. The system also consists of a Sulzer Metco Diamond Jet Controller and a 9MP Powder Feeder. The instantaneous surface temperature of components is measured using an infrared pyrometer as shown in Figure 7-3.

**Figure 7-1 Thermal Spray Booth at OC-ALC**

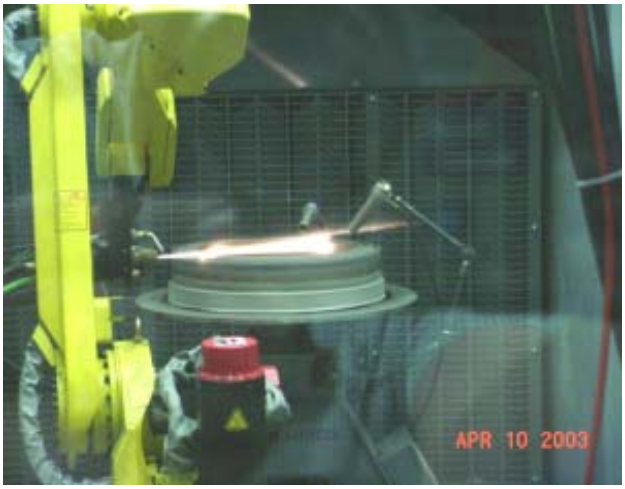


**Figure 7-2 Sulzer-Metco DJ2700 Spray Gun (in operation) Mounted to Fanuc M16i Robot Inside Spray Booth at OC-ALC. Also Shows Air Jet Nozzles for Cooling Components During Spraying**

**Figure 7-3 Infrared Pyrometer for Measuring Surface Temperature of Components During Coating Application.**

OC-ALC, with the assistance of Engelhard Corporation, developed the fixturing for manipulation of the various types of TF33 components and also developed the programming for the seven-axis robot holding the spray gun for application of the coatings. Training of ALC personnel has been performed by Sulzer-Metco and by Engelhard. The Process Engineering Department at OC-ALC has established a quality control methodology which has included the development of process orders to control thermal spray application procedures and acceptance criteria based on analysis of test coupons prior to initiating thermal spray runs. A special skill qualification program has been established to certify thermal spray operators.

NADEP-JAX has two full-production HVOF systems, each containing seven-axis robots for spray gun manipulation. As a result of the successful TF34 accelerated engine test, the Navy issued Manual Change Releases that authorize the application of HVOF coatings to components from this engine.

One of the key end user/OEM issues is the availability of standards and specifications related to the powder used for HVOF coatings, application procedures for the coatings, and grinding procedures for the coatings. The HCAT has worked with the SAE Aerospace Metals Engineering Committee to develop four separate specifications in these areas. Those related to powder, coating deposition and grinding were completed and forwarded to SAE Aerospace Materials Committee B, who has approved them. The following are the designations:

AMS 2448 – "Application of Tungsten Carbide Coatings on Ultra-High-Strength Steels, High-Velocity Oxygen/Fuel Process"

AMS 2449 – "Grinding and Superfinishing of Tungsten Carbide Coatings, High-Velocity Oxygen/Fuel Process"

AMS 7881 – "Tungsten Carbide-Cobalt Powder, Agglomerated and Sintered"

AMS 7882 – “Tungsten Carbide-Cobalt Chromium Powder, Agglomerated and Sintered”

Although AMS 2448 was developed principally for landing gear, the procedures are applicable to other components such as on gas turbine engines. In fact, the parameters defined in AMS 2448 were used for application of WC/Co on the GTE materials specimens. All of these specifications can now be utilized by any manufacturing or overhaul depot and their use will result in consistency between facilities with respect to coating properties.

If other coatings that were evaluated in the GTE materials testing are intended to be used, then additional specifications will have to be developed. This was beyond the scope of this project.

## 7.4. Conclusions

In attempting to qualify and implement a new technology on safety-of-flight components such as rotating parts on GTEs, it is essential to involve the entire stakeholder community from the outset and identify important areas of concern. Contributions from program offices, system support offices, depot engineers, and OEMs were made toward development of the JTP and all results, positive and negative, were presented to them for evaluation and consideration. When an unexpected issue arose it was again important to involve the stakeholder community and obtain their criteria for acceptable performance. There must be flexibility (both programmatic and financial) built into any project of this type so that unplanned testing can be conducted to address unforeseen issues.

The success of the materials testing and the TF33 AMT has resulted in the Air Force proceeding with implementation of HVOF coatings on other gas turbine engines through the Component Improvement Program, with the ultimate goal of eliminating hard chrome plating on all components for which thermal spray is amenable (i.e., where line-of-sight is not an issue). This includes repair of the F100, F101, F110, F118 and T56 engines. In addition, Chromalloy, which is a contractor that overhauls the TF39 for the Air Force, is moving towards implementation of HVOF at its San Antonio repair facility. Their analysis shows a very significant reduction in turnaround time for HVOF repair.

The successful TF34 accelerated engine test and the results of this project have resulted in NADEP-JAX eliminating hard chrome plating from all GTE components with the exception of three J52 components which are expected to be qualified for HVOF in the near future.

This page intentionally left blank.

# 8. References


1 "Hex Cr pel Standard - OSHA's expedited rulemaking", Kathryn McMahon-Lohrer, AESF Jan 2004, AESF Conference, January 2004.

2 “Impact Of Anticipated OSHA Hexavalent Chromium Worker Exposure Standard Navy Manufacturing And Repair Operations”, Navy/Industry Task Group, October 1995.

3 “High Velocity Oxy Fuel Final Results Report,” Final Report issued by Science Applications International Corporation under Government Contract F09603-90-D2215, Oklahoma City Air Logistics Center, Tinker Air Force Base, May 25, 1994

4 Final Report, “Hard Chrome Coatings – Advanced Technology for Waste Elimination”, Grant # NDA 972-93-1-0006, October 1997.

5 Data generated by Jerry Schell, GEAE for HCAT process optimization.

6 Joint Test Protocol, “Validation of Advanced Thermal Spray Coatings as a Replacement for Hard Chrome Plating On Gas Turbine Engines”, March 2002.

7 "Validation of HVOF WC/Co Thermal Spray Coatings as a Replacement for Hard Chrome Plating on Aircraft Landing Gear," by Bruce D. Sartwell et al. Naval Research Laboratory Report NRL/MR/6170-04-8762, 31 March 2004. Available on HCAT web site.

8 “Summary of Discussion on Almen Strips and Temperature Measurement During HVOF Processing and Test Bar Spraying”, J. Sauer, July (2000). Available on HCAT web site.

9 MIL-HDBK-5, “Metallic Materials and Elements for Aerospace Vehicle Structures”, 1998.

10 PH13-8Mo Fatigue Data. Available on HCAT web site.

11 “Corrosion Testing of HVOF and Chrome Plate”, S. Gaydos, HCAT Program Review, Orlando, Feb. 2002. Available on HCAT web site.

12 J.F. Archard: J. Appl.Phys. Vol. 24 (1953), p. 981.